AD NUMBER
AD056235
CLASSIFICATION CHANGES
TO: unclassified
FROM: confidential
LIMITATION CHANGES
TO: Approved for public release, distribution unlimited
FROM: Distribution authorized to U.S. Gov't. agencies and their contractors; Administrative/Operational Use; Dec 1954. Other requests shall be referred to the Office of Naval Research, 800 North Quincy Street, Arlington, VA 22217-5660.
AUTHORITY
15 Feb 1960, ASTIA Tab NO. U-60-1-4; ONR ltr, 13 Sep 1977

UNCLASSIFIED

AD 56235

CLASSIFICATION CHANGED FROM CONFIDENTIAL

TO UNCLASSIFIED AUTHORITY LISTED IN

ASTIA TAB NO. U60-1-4 DATE 15 Feb. 60

Armed Services Technical Information Agency

ARLINGTON HALL STATION; ARLINGTON 12 VIRGINIA

UNCLASSIFIED

CORNELL AERONAUTICAL LABORATORY, INC.

REPORT NO. DD-799-A-1

THEORETICAL STUDIES OF THE PERFORMANCE OF HEAT ENGINES USING PRESSURE WAVES

by
J. G. LOGAN, JR.

Contract NONR-665-(00)
DECEMBER 1954

B U F F A L O   N E W   Y O R K

CORNELL AERONAUTICAL LABORATORY, INC.
BUFFALO, N. Y.

REPORT NO. DD-799-A-1
OFFICE OF NAVAL RESEARCH
CONTRACT NO. NONR-665-(00)

THEORETICAL STUDIES OF THE PERFORMANCE OF HEAT ENGINES USING PRESSURE WAVES

By

J. G. LOGAN, JR.

DECEMBER 1954

ABSTRACT

Theoretical performance investigations have been undertaken for a number of wave-engine configurations using the techniques of the method of characteristics. The use of these nonsteady flow techniques permits a determination of intermittent engine performance parameters such as thrust per unit area, specific fuel consumption, compression efficiency and cycle time which are much more realistic than those obtained by the use of the conventional quasi-steady or steady-flow methods.

Because of the possible use of engines of this nature for a variety of propulsion applications, a somewhat detailed review of the results of the studies is included in this report. Two basic cycles were investigated. In one, part or all of the initial mass of gas was burned during a single combustion period per cycle. In the second, the initial combustion of a small portion of the volume was used to compress the remaining mass of gas to a high pressure and this compressed mass was also burned during the cycle.

From these studies, it has been possible to draw some conclusions as to the optimum engine geometry for maximum performance. For the single combustion cycles, optimum values of specific fuel consumption of the order of $\frac{1.8 \text{ lbs. fuel per hr.}}{\text{lb. thrust}}$ were indicated at $M = 0.65$ for standard conditions. For the modified cycle, with secondary heat addition, optimum theoretical specific fuel consumption values of the order of 1.5 were obtained.

TABLE OF CONTENTS

INDEX OF TABLES AND CHARACTERISTIC CYCLES

INDEX OF TABLES AND CHARACTERISTIC CYCLES
(Cont'd)

INTRODUCTION

The recent development of techniques for the analysis of nonsteady flow phenomena, including the effects of heat addition, has enabled the investigation of a large group of phenomena, hitherto not amenable to theoretical treatment. Of especial interest is the application of these techniques to the study of the wave phenomena occurring in intermittent engines of various kinds. For, from the resulting characteristic cycles or wave diagrams, an estimate of nonsteady engine performance parameters such as thrust per unit area, mass flow, cycle time and specific fuel consumption may be obtained.

These techniques, consequently, are particularly adapted to the study of the wave phenomena occurring in intermittent engines of the type being investigated in this Laboratory[1]. This engine configuration consists, essentially, of two concentric shells, subdivided into a number of equal passages and terminated at either end by a rotating disc valve. It is possible, in any configuration such as this, to employ a relatively large number of different thermodynamic cycles, since the particular cycle would be controlled by the relative combustion chamber volume, the location of the combustion region, the valve phasing, valve geometry and valve timing. This paper attempts to evaluate the possible merits of the simplest of these cycles.

The chief obstacle to the accurate determination of intermittent engine performance is the lack of information concerning the heat addition phenomena and the boundary conditions at the engine inlet and exhaust during outflow and inflow. Basic information with regard to the combustion phenomena occurring under the highly turbulent flow conditions encountered in practice is lacking. Consequently, it has been necessary to employ a somewhat idealized heat addition picture in the cycle calculations. For this purpose, the process of heat addition was represented by the following modes of heat addition:

1. Constant volume combustion

2. Gradual heat addition with heat added at a constant rate

The reasons for making these assumptions and the consequences are discussed in detail in Appendix 2.

Although general methods of construction of the characteristic or wave cycles can be found in a number of recent articles[4,5], details of the method for application to specific problems are not as yet available in print (see Reference 6). For this reason, a brief review of the procedures is given in Appendix B, and a few specific examples are worked in detail.

The following performance parameters were obtained from the wave diagrams:

1. Specific Fuel Consumption $\frac{(\text{lbs. fuel hr.})}{\text{lb. thrust}}$
2. Mass flow per sec/sq.ft. ($^m/A$)
3. Thrust per sq. in. (T/A)
4. Adiabatic compression efficiency
5. Thrust coefficient ($C_T = \frac{T}{AP_o}$)
6. Mass flow coefficient ($C_M = \frac{m}{\rho_o a_o A}$)
7. Over-all efficiency
8. Entropy rise prior to compression
9. Entropy rise due to wave compression
10. Entropy rise due to heat addition
11. Total entropy rise in the cycle
12. Pressure and temperature rise prior to heat addition
13. Pressure and temperature rise due to heat addition
14. Cycle time

The methods used for determining these parameters are described in Appendix 2. Although performance parameters were computed for sea-level conditions, the method by which these results may be extended to other altitude conditions is also given in Appendix 2.

All of the wave engine cycles studied are included in Appendix 1. A summary of the performance for the different configurations studied is given at the beginning of Appendix 1. All of the studies made were for straight-tube configurations. The effect of changes in the following quantities were investigated:

1. Air-fuel ratio
2. Combustion chamber mass and length
3. Cycle time

In Part 1 of this report, the performance of the wave engine is discussed assuming the combustion zone occupies one-fourth of the tube volume. The effect of an increase in the volume of the combustion region to one-half of the tube volume is examined in Part 2. Possible modifications of these cycles are discussed in Part 3, including combustion over the whole tube volume at the same time and at different times (secondary combustion cycles). In each section the details of the cycles are discussed and the performance for each cycle is summarized in Tables.

CHARACTERISTIC STUDIES OF WAVE ENGINE PERFORMANCE

In the first wave engine cycles selected for study and based upon the experimental configuration[1], it was assumed that the optimum performance would be obtained by continuously maintaining a shock wave in the tube, which would be strengthened and reinforced by the heat-addition process, Fig. I. It was believed that the strong shock wave resulting from valve closing and heat

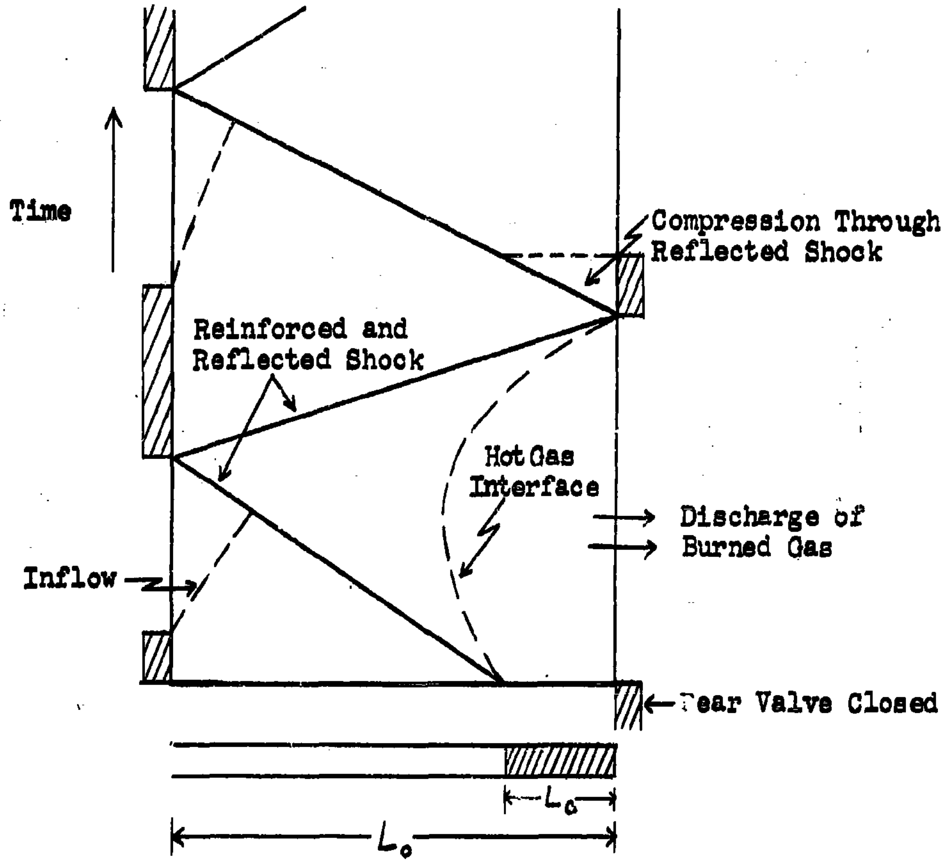

Fig. I

Assumed Characteristic Cycle

addition could be used to obtain efficient compression prior to heat addition if the valve timing and tube length were such that the shock, reflected at the inlet, would arrive at the exit valve upon completion of scavenging. At this instant, the exhaust valve would be closed and the resultant shock reflection would produce relatively high pressures in the combustion region prior to heat addition. For the initial investigation, a combustion region located adjacent to the exhaust valve and occupying approximately one-fourth of the tube volume was assumed. The first heat addition mode, constant volume combustion, was selected primarily because of the simplicity of the calculations. Two different assumptions were made, the first that a constant pressure rise of four atmospheres occurred during the heating process and the second that a constant amount of heat, 520 BTU's per lb. of air, was added per cycle.

The cycles listed in Table 1 were investigated and the performance of the various cycles is summarized in Tables 2, 3 and 4*.

TABLE 1

CONSTANT VOLUME COMBUSTION

Quarter-Length Combustion Chamber

Table	Figures (Appendix)	Mach Number	Heat Addition Assumption	No. Cycles Constructed
2	1A, 1B, 1C	M = 0.65	Constant pressure rise of 4 atmospheres	3
3	2A, 2B, 2C	M = 0.65	Constant air-fuel ratio, 31-1	3
4	3A, 3B	M = 0	Constant pressure rise	2

* In these tables and all subsequent diagrams and tables, performance calculations are for sea-level conditions.

The principle features of the wave cycles are shown in the Appendix, Figures 1A to 3B. The most significant feature of these studies is the rapid increase in entropy observed from cycle to cycle as periodic conditions are approached. A mass of air, initially entering the inlet, was found to require approximately four complete cycles before it propagated through the tube and reached the exhaust valve. Consequently, for three cycles, as can be seen from Figs. 2A to 2C, the air mass would undergo alternate compressions and expansions before heat addition, which resulted in a large increase in entropy due to the passage of the strong shock waves, without an appreciable increase in the pressure level.

In no case in these studies was a completely periodic condition attained as indicated by the fluctuation in specific fuel consumption values, as well as the increase in the total entropy of the air from cycle to cycle, Tables 2 and 3. However, after three cycles, it can be seen that periodic conditions are gradually being approached as all air particles from the third cycle on will have approximately the same history of entropy losses as the air heated during the third cycle.

The performance, wherever possible, is given in a dimensionless form in the tables. The combustion chamber mass is given in terms of the ratio of the mass in the combustion region to the total mass that would occupy the tube under the free-flight flow conditions with the inlet and exit valves open and no heat addition. The definitions of adiabatic compression efficiency, thermal efficiency, propulsive efficiency and overall efficiency are defined in the standard manner. Entropy rise (Δ s) is denoted in dimensionless units, $\frac{\Delta s}{\gamma R}$, where γ is the ratio of specific heats and R the gas constant. Pressures are given in terms of the ratio of the actual pressures encountered to a reference ambient pressure, p_o. Temperatures are also given in terms of a

TABLE 2
CONSTANT VOLUME COMBUSTION, $M_1 = 0.65$

PERFORMANCE BASED ON CHARACTERISTIC CYCLE ANALYSIS	FIRST CYCLE	SECOND CYCLE	THIRD CYCLE	FOURTH CYCLE
Figures (Appendix)	1A	1B	1C	1C
Air-fuel Ratio	45.0	34.4	27.2	20.9
Combustion Chamber Mass	0.450	0.534	0.370	
Specific Fuel Consumption	2.026	2.519	2.665	
Mass Flow per sec./sq. ft.	31.55	42.23	32.58	
Thrust per sq. in.	8.65	12.18	11.24	
Adiabatic Compression Efficiency	0.925	0.642	0.343	0.229
Thrust Coefficient	0.588	0.829	0.765	
Mass Flow Coefficient	0.369	0.494	0.381	
Overall Efficiency	0.086	0.069	0.065	
Entropy Rise Prior to Hammer Comp.	0	0.388	0.924	1.553
Entropy Rise Due to Hammer Comp.	0.044	0.007	0.151	0.165
Entropy Rise Due to Heat Addition	2.475	2.475	2.475	2.475
Total Entropy of Cycle	2.519	2.870	3.550	4.194
Pressure Before Heat Addition	2.334	3.608	3.161	3.362
Pressure After Heat Addition	9.335	14.430	12.643	13.448
Temperature Before Heat Addition	1.296	1.690	2.136	2.811
Temperature After Heat Addition	5.185	6.759	8.543	11.244
Cycle Time	1.218	1.080	0.970	
Combustion Chamber Length	0.25	0.25	0.25	0.25

TABLE 3
CONSTANT VOLUME COMBUSTION, $M_1 = 0.65$

PERFORMANCE BASED ON CHARACTERISTIC CYCLE ANALYSIS	FIRST CYCLE	SECOND CYCLE	THIRD CYCLE	FOURTH CYCLE
Figures (Appendix)	2A	2B	2C	2C
Air-fuel Ratio	31	31	31	31
Combustion Chamber Mass	0.450	0.560	0.342	0.269
Specific Fuel Consumption	2.530	2.083	2.387	
Mass Flow per sec./sq. ft.	35.45	48.58	31.76	
Thrust per sq. in.	11.30	18.80	10.73	
Adiabatic Compression Efficiency	0.91	0.51	0.26	0.19
Thrust Coefficient	0.769	1.279	0.730	
Mass Flow Coefficient	0.415	0.569	0.372	
Overall Efficiency	0.069	0.084	0.073	
Entropy Rise Prior to Hammer Comp.	0	0.539	1.409	1.800
Entropy Rise Due to Hammer Comp.	0.044	0.187	0.213	0.300
Entropy Rise Due to Heat Addition	3.010	2.376	2.191	1.773
Total Entropy of Cycle	3.054	3.086	3.600	3.873
Pressure Before Heat Addition	2.334	4.644	3.849	3.553
Pressure After Heat Addition	12.600	17.416	11.653	9.682
Temperature Before Heat Addition	1.296	2.073	2.811	3.305
Temperature After Heat Addition	6 998	7.775	8.514	9.007
Cycle Time	1.085	0.985	0 920	
Combustion Chamber Length	0.25	0.25	0.25	0.25

TABLE 4
CONSTANT VOLUME COMBUSTION, $M_1 = 0$

PERFORMANCE BASED ON CHARACTERISTIC CYCLE ANALYSIS	FIRST CYCLE	SECOND CYCLE	THIRD CYCLE	FOURTH CYCLE
Figures (Appendix)	3A	3B	3B	
Air-fuel Ratio	58.4	52.8	48.24	
Combustion Chamber Mass	0.250	0.284	0.250	
Specific Fuel Consumption	1.557	1.662		
Mass Flow per sec./sq. ft.	11.86	14.43		
Thrust per sq. in.	3.26	4.11		
Adiabatic Compression Efficiency	1.000	0.629	0.270	
Thrust Coefficient	0.222	0.280		
Mass Flow Coefficient	0.139	0.169		
Overall Efficiency				
Entropy Rise Prior to Hammer Comp.	0	0.083	0.334	
Entropy Rise Due to Hammer Comp.	0	0.005	0.004	
Entropy Rise Due to Heat Addition	2.475	2.475	2.475	
Total Entropy of Cycle	2.475	2.564	2.815	
Pressure Before Heat Addition	1.000	1.256	1.214	
Pressure After Heat Addition	4.000	5.036	4.856	
Temperature Before Heat Addition	1.000	1.107	1.211	
Temperature After Heat Addition	4.000	4.427	4.844	
Cycle Time	1.800	1.680		
Combustion Chamber Length	0.25	0.25	0.25	

ratio, the reference temperature being the ambient temperature, ϑ_o. Cycle time is expressed in the dimensionless form

$$\tau \text{ (cycle time)} = \frac{a_o t}{L}$$

where: L is the overall tube length

a_o is the ambient velocity of sound

t is time, in seconds

Since all systems investigated were straight-tube configurations, the relative combustion chamber volume is expressed in terms of percent of overall tube length, L_c/L_o.

All of the characteristics cycles were constructed in a dimensionless form for a particular Mach number. The specific performance parameters thrust/unit area, specific fuel consumption and mass flow/unit time/unit area for the particular Mach number may therefore be obtained for any altitude by substituting the appropriate values of pressure, density, temperature and sound velocity. The performance parameters given in the Tables and Figures in the Appendix were determined for sea-level conditions. For any other altitude condition, the performance parameters may be determined using the following relations:

$$(\text{S.F.C.})_{alt.} = (\text{S.F.C.})_{S.L.} \frac{(a_o)_{alt.}}{(a_o)_{S.L.}}$$

$$(\text{Thrust/unit area})_{alt.} = (\text{Thrust/unit area})_{S.L.} \frac{(a_o^2 \rho_o)_{alt.}}{(a_o^2 \rho_o)_{S.L.}}$$

$$(\text{Mass flow/sec/unit area})_{alt.} = (\text{Mass flow/sec/unit area})_{S.L.} \frac{(a_o \rho_o)_{alt.}}{(a_o \rho_o)_{S.L.}}$$

where: a_o = ambient velocity of sound

ρ_o = ambient density

S.F.C. = specific fuel consumption (lbs.fuel/sec./lb.thrust)

S.L. = sea-level conditions

alt. = altitude conditions

The compression efficiency, thermal efficiency, propulsive efficiency and overall efficiency obtained for a particular Mach number do not vary with altitude.

The assumption of a constant pressure rise of 4 atmospheres was found to be unsatisfactory. As can be seen from Table 2, as the entropy increased prior to the heat-addition process, more and more fuel was required in succeeding cycles in order to sustain the assumed pressure rise. For example, at M = 0.65, Table 2, the required air-fuel ratio varied from 45 to 20.9. Since periodic conditions were being approached slowly and the entropy rise from cycle to cycle was increasing rapidly, it appeared that a condition could be approached wherein sufficient fuel could not be supplied in order to sustain the assumed pressure rise, assuming a limiting air-fuel ratio of 15-1. Because of the unrealistic nature of this assumption, all subsequent calculations were made with a constant amount of heat added per cycle, as in Table 3.

Although the diagrams were constructed for a particular quantity of heat added per cycle at sea level to yield a constant fuel-air ratio, the resulting temperature ratio can be correlated with a different amount of heat and hence, a different fuel-air ratio at any other altitude, using the relation

$$(f/a)_{alt.} = (f/a)_{S.L.} \frac{(\vartheta_0)_{alt.}}{(\vartheta_0)_{S.L.}} = (f/a)_{S.L.} \frac{(a_0^2)_{alt.}}{(a_0^2)_{S.L.}}$$

where: ϑ_0 = ambient temperature

One unexpected outgrowth of these studies was the observation that the quarter-length cycles would not conform to the original, ideal shock picture. In all the cycles studied, it was found, as periodic conditions were approached, that the shock reflected at the inlet valve would propagate through the burned gas before scavenging could be completed, even under the ideal conditions of instantaneous heat addition. Consequently, the actual compression prior to heat addition occurred through a single shock generated by rapid closure of the exhaust valve, Fig.II.

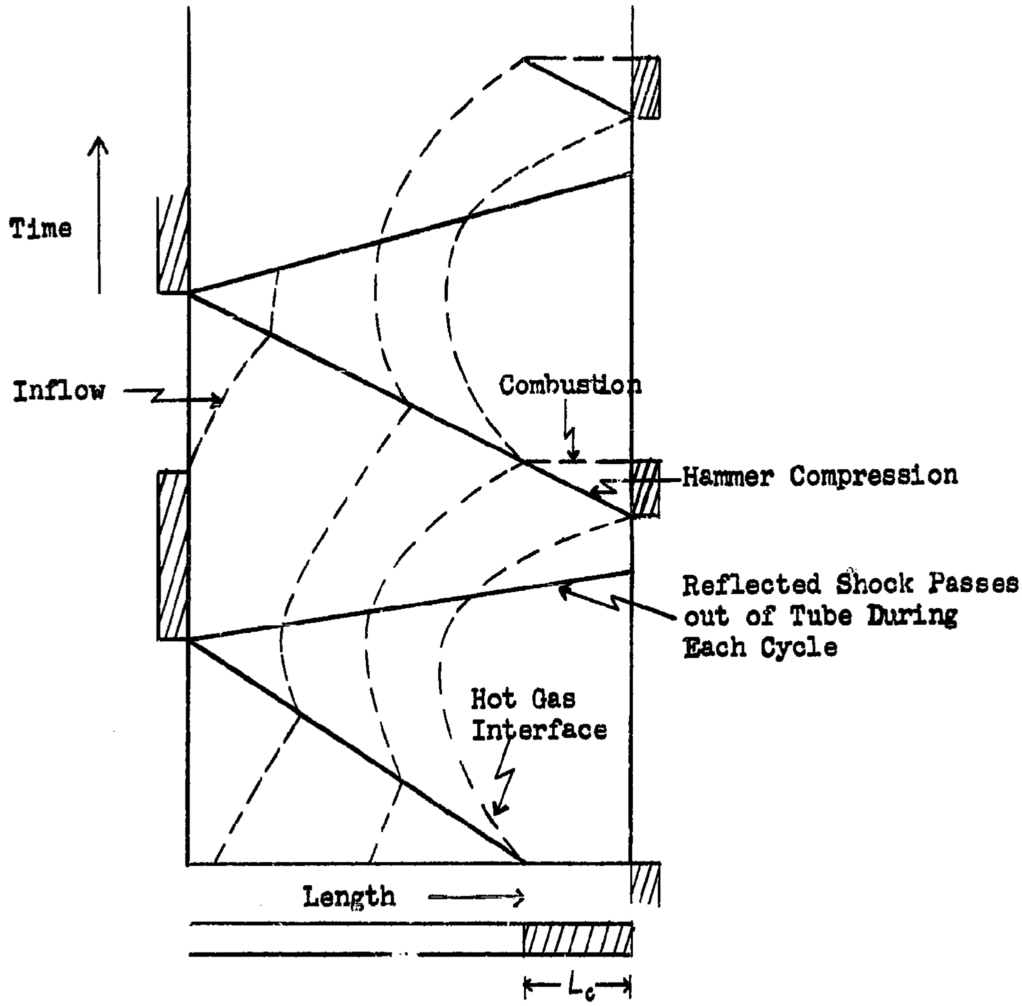

Fig. II

Actual Characteristic Cycle

The optimum compression obtainable, then, would be that of a "hammer" shock created as a result of rapid closure of the exhaust valve. Although this process of compression by a "hammer" shock can be relatively efficient, the characteristic studies indicated that the losses associated with the passage of strong shocks through the unburned gas prior to compression seriously reduced the resultant compression efficiency. For example, at M = 0.65, (Table 3) in the third cycle, the resulting compression efficiency before heat addition was 26 percent. The resultant specific fuel consumption at this Mach number was 2.4 lbs. fuel/hr./lb. thrust. The adiabatic compression efficiency obtained in the next cycle which was not carried to completion was found to be even less. Performance was determined by graphical integration of the resultant pressure and momentum contributions assuming ideal exit flow conditions. The value of specific fuel consumption was based on net thrust, i.e., exit momentum contributions minus the momentum of the incoming air.

Because of the relatively poor resultant performance and the unsatisfactory heat-addition assumption, the study at M = 0 was not carried through the third cycle, since it was observed that similar phenomena would occur.

In order to determine if the constant-volume, instantaneous-heat-addition assumption tended to overemphasize the actual shock losses which would occur, studies were also made assuming a gradual heat-addition process which would be more closely related to the actual physical process. The following cycles listed in Table 5 were investigated.

TABLE 5

GRADUAL HEAT ADDITION

Quarter-Length Combustion Chamber

Table	Figures (Appendix)	Mach Number	No. of Cycles Investigated	Comments
6	4A, 4B, 4C	0.65	3	
7	5A, 5B	0.95	2	Initial conditions based on 3rd cycle condition of Table 6
8	6A, 6B, 6C	0.65	3	Effect of change in closing time of exit valve after scavenging
9	7A	0.65	1	Study of effect of mass removal at the inlet

Typical features of these cycles are shown in the Appendix, Figs. 4A to 7A, and the performance is summarized in Tables 6-9.

Because of the assumption of a fixed period for the heat addition, the resultant pressure rise depended upon the entropy values at the beginning of the heat-addition process. Since the entropy before heat addition increased from cycle to cycle, the resultant pressure rise due to heat addition decreased, at M = 0.65, from 3.1 atmospheres in the first cycle to 1.4 atmospheres in the third cycle. As can be seen from Table 6, for the beginning of the 4th cycle, the total entropy rise before heat addition was somewhat less than in the previous cycle. The performance figure quoted for the third cycle represents, therefore, a performance very near that for the cyclic condition. Since the constant-volume combustion calculations indicated a specific fuel consumption of 2.4 lbs.fuel per hr./lb.thrust, the maximum performance values for this quarter-length combustion cycle would lie in the specific fuel consumption range 2.4 - 2.9.

The relatively low values of specific impulse obtained in the second cycles, Tables 3 and 6, were due to the fact that the compressed gas had not undergone the complete history of losses as in the third cycle and hence, the pressures were achieved at compression efficiencies of about 50 percent as compared to 30 percent in the third cycle.

The fuel consumption values varying between 2.4 and 2.9 were much larger than expected and these results were due primarily to the accumulated entropy losses in the unburned gas prior to compression and heat addition. The pressures of approximately three atmospheres, prior to heat addition, were obtained at the expense of a considerable portion of the available energy of the cycle.

Studies were also made at M = 0.95, Table 7, to determine if improved inflow conditions could be obtained resulting in an increase in the mass of gas

TABLE 6
GRADUAL HEAT ADDITION, $M_1 = 0.65$

PERFORMANCE BASED ON CHARACTERISTIC CYCLE ANALYSIS	FIRST CYCLE	SECOND CYCLE	THIRD CYCLE	FOURTH CYCLE
Figures (Appendix)	4A	4B	4C	4C
Air-fuel Ratio	31	31	31	31
Combustion Chamber Mass	0.450	0.507	0.357	0.333
Specific Fuel Consumption	2.484	2.431	3.043	
Mass Flow per sec./sq. ft.	27.26	33.44	23.27	
Thrust per sq. in.	8.85	11.10	6.17	
Adiabatic Compression Efficiency	0.91	0.54	0.29	0.30
Thrust Coefficient	0.602	0.755	0.420	
Mass Flow Coefficient	0.319	0.391	0.272	
Overall Efficiency	0.070	0.072	0.057	
Entropy Rise Prior to Hammer Comp.	0	0.305	0.870	0.797
Entropy Rise Due to Hammer Comp.	0.044	0.273	0.378	0.303
Entropy Rise Due to Heat Addition	3,170	2.777	2.515	
Total Entropy of Cycle	3.214	3.355	3.763	
Pressure Before Heat Addition	2.334	3.717	3.311	3.000
Pressure After Heat Addition	7.293	6.168	4.611	
Temperature Before Heat Addition	1.296	1.833	2.320	2.250
Temperature After Heat Addition	6.408	6.518	6.901	
Cycle Time	1.410	1.295	1.310	
Combustion Chamber Length	0.25	0.25	0.25	0.25

TABLE 7

GRADUAL HEAT ADDITION, $M_1 = 0.95$

(Initial Conditions from $M_1 = 0.65$)

PERFORMANCE BASED ON CHARACTERISTIC CYCLE ANALYSIS	FIRST CYCLE	SECOND CYCLE
Figure (Appendix)	5A	5B
Air-fuel Ratio	31	31
Combustion Chamber Mass	0.269	0.414
Specific Fuel Consumption	4.311	2.786
Mass Flow per sec./sq. ft.	19.29	28.64
Thrust per sq. in.	3.61	8.29
Adiabatic Compression Efficiency	0.19	0.31
Thrust Coefficient	0.246	0.564
Mass Flow Coefficient	0.226	0.335
Overall Efficiency	0.059	0.091
Entropy Rise Prior to Hammer Compression	1.782	1.096
Entropy Rise Due to Hammer Compression	0.300	0.380
Entropy Rise Due to Heat Addition	2.018	2.166
Total Entropy of Cycle	4.100	3.642
Pressure Before Heat Addition	3.553	4.627
Pressure After Heat Addition	3.955	6.704
Temperature Before Heat Addition	3.305	2.796
Temperature After Heat Addition	7.634	7.392
Cycle Time	1.190	1.235
Total Mass		
Combustion Chamber Length	0.25	0.25

TABLE 8
GRADUAL HEAT ADDITION, $M_1 = 0.65$
Variation of Closing Time of First Cycle of IV

PERFORMANCE BASED ON CHARACTERISTIC CYCLE ANALYSIS	TUBE LEFT OPEN UNTIL $\tau = 1.350$	TUBE LEFT OPEN UNTIL $\tau = 1.560$	TUBE LEFT OPEN UNTIL $\tau = 2.750$	
Figures (Appendix)	6A	6B	6C	
Air-fuel Ratio	31	31	31	
Combustion Chamber Mass	0.450	0.450	0.450	
Specific Fuel Consumption	1.986	1.833	1.833	
Mass Flow per sec./sq. ft.	24.03	20.95	12.61	
Thrust per sq. in.	9.76	9.22	5.55	
Adiabatic Compression Efficiency	0.910	0.910	0.910	
Thrust Coefficient	0.664	0.627	0.378	
Mass Flow Coefficient	0.281	0.245	0.148	
Overall Efficiency	0.088	0.095	0.095	
Entropy Rise Prior to Hammer Comp.	0	0	0	
Entropy Rise Due to Hammer Comp.	0.044	0.044	0.044	
Entropy Rise Due to Heat Addition	3.170	3.170	3.170	
Total Entropy of Cycle	3.214	3.214	3.214	
Pressure Before Heat Addition	2.334	2.334	2.334	
Pressure After Heat Addition	7.293	7.293	7.293	
Temperature Before Heat Addition	1.296	1.296	1.296	
Temperature After Heat Addition	6.408	6.408	6.408	
Cycle Time	1.600	1.835	3.050	
Combustion Chamber Length	0.25	0.25	0.25	

TABLE 9

GRADUAL HEAT ADDITION, $M_1 = 0.65$

Effect of Mass Removal at Inlet

PERFORMANCE BASED ON CHARACTERISTIC CYCLE ANALYSIS	FIRST CYCLE	SECOND CYCLE
Figure (Appendix)	7A	7A
Air-fuel Ratio	31	31
Combustion Chamber Mass	0.450	0.526
Specific Fuel Consumption	2.850	
Mass Flow per sec./sq. ft.	29.74	
Thrust per sq. in.	8.43	
Adiabatic Compression Efficiency	0.91	0.52
Thrust Coefficient	0.573	
Mass Flow Coefficient	0.348	
Overall Efficiency	0.061	
Entropy Rise Prior to Hammer Compression	0	0.140
Entropy Rise Due to Hammer Compression	0.044	0.634
Entropy Rise Due to Heat Addition	3.170	
Total Entropy of Cycle	3.214	
Pressure Before Heat Addition	2.334	4.120
Pressure After Heat Addition	7.293	
Temperature Before Heat Addition	1.296	1.960
Temperature After Heat Addition	6.408	
Cycle Time	1.290	
Total Mass		
Combustion Chamber Length	0.25	0.25

consumed per cycle and a corresponding reduction in the entropy losses due to shock passage in the unburned gas. The wave phenomena was such that, although an improvement in mass flow was evidenced, the number of cycles required for a particle to move completely through the tube remained approximately the same. The mass flow increase resulted only from the increase in density corresponding to the increase in Mach number. The results of calculations assuming gradual heat addition for M = 0.95 are summarized in Table 7 and the details of the wave cycle are shown in Fig. 5. In order to facilitate the calculations, the initial cycle flow conditions were based on the flow conditions obtained in the third cycle calculation for gradual heat addition, M = 0.65.

In all the previous investigations, the cycle studies were initiated by assuming that the tube was completely open and that free-flight flow condition were existing in the tube at the instant of closure of the rear valve. The resultant hammer compression condition was then taken as the initial condition for heat addition. As a result, the performance of the first and second cycles was always superior to the performance of succeeding cycles, since the entropy losses in the unburned gas were not accurately represented. With these initial assumptions, it was always necessary to construct at least three cycles before an accurate estimate of performance could be obtained. Attempts to reduce the calculation time by assuming arbitrary initial conditions to obtain more rapid convergence as in Table 7 were found to be impractical, due to the impossibility of duplicating the entropy distributions in the unburned gas as the periodic condition was approached. This inability to accurately represent the correct entropy distributions could lead to reduced performance, as in the first cycle of Table 9 when the entropy was overestimated, or to exaggerated performance values and high pressures prior to combustion, when as in some of the early unreported investigations, the entropy increase was underestimated. Since the number of cycles required for a particle to pass through the tube was not altered appreciably upon increasing the Mach number from 0.65 to 0.95, these studies were not continued.

It became obvious during these studies that the initial cycle visualized, Fig. 1, in which a shock wave was maintained continuously in the tube would not be a practical configuration. In order to match the time of arrival of the interface and the reflected shock, as indicated in Fig. 1, it would be necessary to further reduce the relative combustion chamber length. This would lead to an increase in the number of shock passages occurring in the unburned gas before the actual process of compression and heat addition and result in a lower overall performance than shown in Tables 2 and 6.

As a result of the necessity for improving the scavenging characteristics, modifications of the quarter-length combustion cycle were investigated. The first modification studied was the effect of discharging a portion of the unburned gas during the cycle upon completion of the scavenging of the burned gas, see Fig. 6. Instead of closing the exit valve upon completion of scavenging of the burned gas, the exit valve was left open and cold air was permitted to escape, Table 8. The exhaust of this high-velocity cold air caused an appreciable increase in the cycle performance, decreasing the specific fuel consumption from 2.5, Table 6, to 2.0, Table 8. The major disadvantage of this modification was the long period required to complete the scavenging of the cold air mass, Figs. 6A, 6B and 6C. If only the portion of unburned gas possessing a high velocity was scavenged, the remaining mass with a low velocity but still possessing a relatively large entropy value would, upon closure of the exit valve, result in a very low compression ratio prior to heat addition. Performance in succeeding cycles would then be poor. As can be seen from Fig. 6C, if the exit valve remained open until all the gas with a high entropy was discharged, the total cycle time would be so long that the cycle would not be a practical one. During the low velocity discharge phase, a shock is created at the exit which propagates upstream, further reducing the discharge velocity and increasing the total cycle time.

The boundary condition applied during the outflow phase was the conventional condition that the pressure was equal to the ambient pressure. This condition, however, is strictly true only for the case of static operation. During exhaust at high flight speeds when the exhaust velocity of the jet is less than that of the surrounding stream, it would be expected that shear forces would be acting, tending to accelerate the flow at the exit. This would occur because the total head of the surrounding stream would be greater than that of the hot exhaust gas during the low velocity phase of discharge. The assumption of ambient pressure conditions would hence be a conservative one for the case of an engine discharging directly to the atmosphere and would tend to cause an over-estimation of the required scavenging time.

Another method proposed by A. Hertzberg, that of mass removal at the intake, was studied. This method involved the removal of a portion of the unburned gas in the tube at the air inlet upon completion of the heat-addition process. This air would be taken into a set of rotating tubes at the inlet and readmitted into the wave tubes at a more favorable time to improve the scavenging, Fig. 7A, Table 9. In this cycle, however, no reflected shock passed through the major portion of the burned gas to its scavenging velocity. As a consequence, the performance of this cycle was much less than the first cycle performance for the original cycle, Table 6. Although this cycle would permit a greater amount of energy to be utilized in the compression process, resulting in a higher pressure prior to heat addition, no improvement in compression efficiency was observed over that of the original cycle, Table 6 and hence, resulting cycles would show no significant improvement.

A conventional pulsejet cycle was also studied, Table 10, Fig. 8A, to determine if a portion of the hot gas exhaust could be utilized for compression. An exhaust valve was located at the exit during the discharge to generate a shock wave that would propagate upstream and compress the unburned gas prior

TABLE 10
GRADUAL HEAT ADDITION, $M_1 = 0$
Pulsejet Cycle

PERFORMANCE BASED ON CHARACTERISTIC CYCLE ANALYSIS	FIRST CYCLE	SECOND CYCLE
Figure (Appendix)	8A	8A
Air-fuel Ratio	31	31
Combustion Chamber Mass	0.15	0.144
Specific Fuel Consumption	2.138	
Mass Flow per sec./sq. ft.	10.34	
Thrust per sq. in.	3.90	
Adiabatic Compression Efficiency	1.00	0.925
Thrust Coefficient	0.265	
Mass Flow Coefficient	0.121	
Overall Efficiency		
Entropy Rise Prior to Hammer Compression	0	0
Entropy Rise Due to Hammer Compression	0	0.028
Entropy Rise Due to Heat Addition	3.685	
Total Entropy of Cycle	3.685	
Pressure Before Heat Addition	1.000	1.485
Pressure After Heat Addition	2.500	
Temperature Before Heat Addition	1.000	1.130
Temperature After Heat Addition	5.671	
Cycle Time	1.24	
Total Mass		
Combustion Chamber Length	0.15	0.11

to heat addition, Fig. 8A. However, the velocity profile during discharge was such that the exit valve could only be inserted in a low-velocity region in order to obtain compression at the inlet at the proper time and hence, the reflected shock did not result in an appreciable increase of pressure prior to heat addition. These studies were therefore not extended.

In these investigations, the most significant improvement in performance of the first cycle at M = 0.65 occurred, Table 8, when the cycle time was increased to permit discharge of a portion of the unburned gas at high exit velocities. The specific fuel consumption value of 2.5, obtained when only the hot gas was discharged during the cycle, dropped to 2.0 when a portion of the high velocity unburned gas was exhausted. In the quarter-length combustion cycle, consequently, a large amount of the available energy of the burned gas was transferred to the unburned gas through the shock wave. This energy, due to the large entropy increase caused by the passage of shock waves, could not be effectively used for compression in succeeding cycles.

Since this quarter-length cycle did not lead to a practical cycle, studies of the effect of increasing the relative combustion chamber volume were initiated. By increasing the combustion chamber volume and length, the reflected shock would pass through the burned gas much earlier and hence, a considerable portion of the available energy would be used in accelerating the burned gas during discharge, Fig. III.

Performance studies of this configuration indicated that an increase in combustion chamber length to approximately one-half of the overall tube length would, in addition, reduce the time of travel of a given air mass through the tube to two cycles. Hence, the entropy loss incurred in the unburned gas would be reduced to that corresponding to two shock waves, Fig. III. However, since the major portion of the energy would be utilized in accelerating the hot gas during discharge, the characteristics studies indicated that a very small amount of the energy

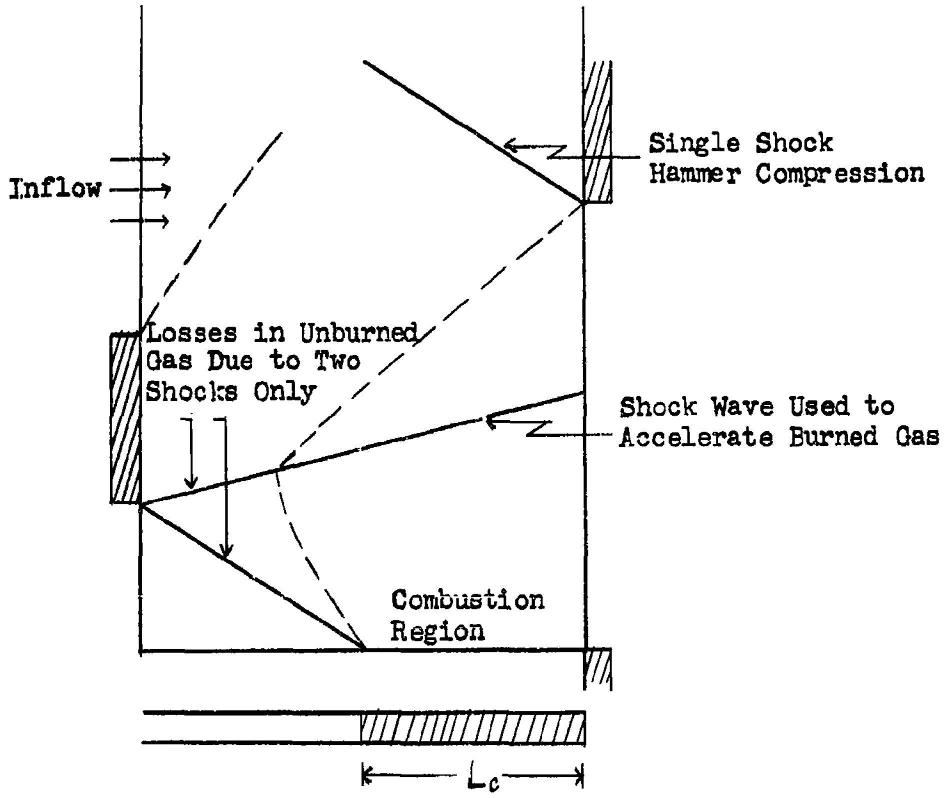

Fig. III

Effect of Change in Combustion Chamber Length
on Wave Engine Cycle

of the heat-addition process would be available for compression in succeeding cycles. In effect, variations in the relative combustion chamber length could be used to control the amount of energy utilized in the compression and expansion processes.

A number of different configurations were studied with the combustion chamber length equal approximately to one-half of the overall tube length. These configurations are tabulated in Table 11, and the cycle diagrams are included in the Appendix, Figs. 9A to 14A.

For these studies, although the initial value of the combustion chamber length was selected as one-half of the total tube length, it was found that the remaining volume of air in the tube which suffered an entropy increase due to

TABLE 11

HALF-LENGTH COMBUSTION CYCLE

a/f = 31/1

Table	Figures (Appendix)	f/a	Mach Number	Combustion Mode	No. Cycles Investigated
12	9A, 9B, 9C	1/31	0.65	Constant volume combustion	3
13	10A,10B,10C	1/31	0.95	Constant volume combustion	3
14	11A,11B,11C	1/31	0.65	Gradual heat addition	3
15	12A,12B,12C	1/31	0.95	Gradual heat addition	3
16	13A,13B,13C	1/31	0.0	Constant volume combustion	3
17	14A	1/31	0.95	Constant volume combustion	3rd Cycle

shock passage occupied a region in the next cycle slightly greater than the original assumed length. In the constant volume calculations, Tables 12 and 13, the fixed combustion chamber length was based on conditions found in the second or third cycles.

As can be seen by comparing third cycle conditions, Tables 3 and 12, even though the initial and final third cycle pressures were greater for the quarter-length cycle than the half-length cycle, Table 12, the overall entropy rise for the quarter-length cycle was also greater. Consequently, the resultant performance of the half-length cycle was substantially improved over that obtained for the quarter-length cycle. This was due primarily to the smaller losses encountered in the unburned gas prior to compression.

Studies were also carried out at M = 0.95 assuming constant volume combustion. The results, Table 13, indicated a slight increase in specific fuel consumption with Mach number.

TABLE 12
CONSTANT VOLUME COMBUSTION, $M_1 = 0.65$

PERFORMANCE BASED ON CHARACTERISTIC CYCLE ANALYSIS	FIRST CYCLE	SECOND CYCLE	THIRD CYCLE	FOURTH CYCLE
Figures (Appendix)	9A	9B	9C	9C
Air-fuel Ratio	31	31	31	31
Combustion Chamber Mass	0.900	0.633	0.723	
Specific Fuel Consumption	1.754	2.173	1.934	
Mass Flow per sec./sq. ft.	38.93	24.98	30.81	
Thrust per sq. in.	17.90	9.27	12.84	
Adiabatic Compression Efficiency	0.91	0.31	0.53	0.34
Thrust Coefficient	1.218	0.631	0.873	
Mass Flow Coefficient	0.456	0.292	0.361	
Overall Efficiency	0.099	0.080	0.090	
Entropy Rise Prior to Hammer Comp.	0	0.541	0.238	0.491
Entropy Rise Due to Hammer Comp.	0.044	0.113	0.115	0.108
Entropy Rise Due to Heat Addition	3.010	2.793	2.917	2.826
Total Entropy of Cycle	3.054	3.447	3.279	3.425
Pressure Before Heat Addition	2.334	1.694	1.856	1 699
Pressure After Heat Addition	12.596	8.090	9.564	8.227
Temperature Before Heat Addition	1.296	1.510	1.378	1.484
Temperature After Heat Addition	6.997	7.215	7.080	7.186
Cycle Time	1.975	2.164	2.005	
Combustion Chamber Length	0.50	0.565	0.535	0.535

TABLE 13
CONSTANT VOLUME COMBUSTION, $M_1 = 0.95$

PERFORMANCE BASED ON CHARACTERISTIC CYCLE ANALYSIS	FIRST CYCLE	SECOND CYCLE	THIRD CYCLE	FOURTH CYCLE
Figures (Appendix)	10A	10B	10C	10C
Air-fuel Ratio	31	31	31	31
Combustion Chamber Mass	1.116	0.674	0.862	0.762
Specific Fuel Consumption	2.086	2.200	2.065	
Mass Flow per sec./sq. ft.	50.17	29.82	40.80	
Thrust per sq. in.	19.40	10.93	15.93	
Adiabatic Compression Efficiency	0.85	0.339	0.567	0.426
Thrust Coefficient	1.320	0.744	1.084	
Mass Flow Coefficient	0.587	0.349	0.478	
Overall Efficiency	0.122	0.116	0.123	
Entropy Rise Prior to Hammer Comp.	0	0.718	0.287	0.450
Entropy Rise Due to Hammer Comp.	0.119	0.094	0.100	0.175
Entropy Rise Due to Heat Addition	2.826	2.608	2.803	2.687
Total Entropy of Cycle	2.945	3.420	3.190	3.312
Pressure Before Heat Addition	3.290	2.148	2.394	2.297
Pressure After Heat Addition	16.018	9.264	11.501	10.337
Temperature Before Heat Addition	1.474	1.721	1.499	1.629
Temperature After Heat Addition	7.176	7.423	7.201	7.331
Cycle Time	1.900	1.930	1.805	
Combustion Chamber Length	0.500	0.540	0.540	0.540

Cycles were also constructed assuming gradual heat addition, Tables 14 and 15 For the study at M = 0.65, it was assumed that the exit was slightly constricted in the initial cycle before heat addition. This assumption resulted in a reduced pressure and flow condition prior to heat addition which led to a more rapid cyclic condition. Since the combustion chamber length was selected as 0.60 in succeeding cycles, a mixture of fresh gas and air that had previously incurred an entropy penalty due to shock passage was obtained in the combustion chamber. Carrying out the usual averaging process to obtain the new cycle conditions resulted in a lower overall entropy rise and a resultant higher compression efficiency. This yielded a specific fuel consumption value of 1.8 as opposed to 1.93 for the case of constant volume combustion. The heat-addition assumption, for the low initial entropy level, resulted in pressure increases during the heat-addition process of the same order of magnitude achieved for the constant volume combustion picture, 5-6 atmospheres.

The performance study at M = 0.95, assuming gradual heat addition was carried out assuming that only air from the previous cycle was included in the combustion region for the succeeding cycle, Fig. 12, Table 15. For this case, also, the resultant specific fuel consumption value, 2.0, was slightly larger than the specific fuel consumption for M = 0.65.

It may be concluded that the optimum performance for this cycle at M = 0.65 lies between the specific fuel consumption limits 1.8 and 1.9, and, because of the reduced shock losses, indicates an appreciable gain in performance over that of the quarter-length cycle.

It was observed during these studies that the amount of fresh air admitted into the combustion region with the air that had previously incurred an entropy penalty due to shock passage could appreciably alter the cycle results. The calculations for the third cycle Table 13 were repeated, including only the air that had undergone the shock passage, Fig. 14A, Table 17. The specific fuel consumption in the approximately cyclic condition increased from 2.1, Table 13 to 2.3, Table 17.

TABLE 14

GRADUAL HEAT ADDITION, M_1=0.65
Initial Constriction at Exit = 0.70
Exit Completely Open in Succeeding Cycles

PERFORMANCE BASED ON CHARACTERISTIC CYCLE ANALYSIS	FIRST CYCLE	SECOND CYCLE	THIRD CYCLE	FOURTH CYCLE
Figures (Appendix)	11A	11B	11C	11C
Air-fuel Ratio	31	31	31	31
Combustion Chamber Mass	0.988	0.937	0.986	0.969
Specific Fuel Consumption	1.881	1.855	1.807	
Mass Flow per sec./sq. ft.	33.63	29.53	32.40	
Thrust per sq. in.	14.42	12.84	14.46	
Adiabatic Compression Efficiency	0.98	0.78	0.75	0.81
Thrust Coefficient	0.981	0.873	0.984	
Mass Flow Coefficient	0.394	0.346	0.379	
Overall Efficiency	0.093	0.094	0.096	
Entropy Rise Prior to Hammer Comp.	0	0.667	0.107	0.083
Entropy Rise Due to Hammer Comp.	0.010	0.055	0.050	0.026
Entropy Rise Due to Heat Addition	3.274	3.108	3.017	
Total Entropy of Cycle	3.284	3.230	3.173	
Pressure Before Heat Addition	2.021	1.998	2.189	2.082
Pressure After Heat Addition	11.991	11.486	12.185	
Temperature Before Heat Addition	1.228	1.280	1.332	1.289
Temperature After Heat Addition	7.256	7.312	7.268	
Cycle Time	2.510	2.710	2.60	
Combustion Chamber Length	0.60	0.60	0.60	0.60

TABLE 15
GRADUAL HEAT ADDITION, M_1=0.95

PERFORMANCE BASED ON CHARACTERISTIC CYCLE ANALYSIS	FIRST CYCLE	SECOND CYCLE	THIRD CYCLE	FOURTH CYCLE
Figures (Appendix)	12A	12B	12C	12C
Air-fuel Ratio	31	31	31	31
Combustion Chamber Mass	1.116	0.816	0.828	0.772
Specific Fuel Consumption	1.932	1.892	1.983	
Mass Flow per sec./sq. ft.	51.13	39.96	39.40	
Thrust per sq. in.	21.34	17.03	16.02	
Adiabatic Compression Efficiency	0.855	0.478	0.568	0.548
Thrust Coefficient	1.452	1.159	1.090	
Mass Flow Coefficient	0.599	0.468	0.461	
Overall Efficiency	0.132	0.135	0.128	
Entropy Rise Prior to Hammer Comp.	0	0.376	0.220	0.205
Entropy Rise Due to Hammer Comp.	0.119	0.150	0.170	0.197
Entropy Rise Due to Heat Addition	2.910	2.767	2.932	
Total Entropy of Cycle	3.029	3.293	3.222	
Pressure Before Heat Addition	3.290	2.331	2.419	2.304
Pressure After Heat Addition	13.857	11.131	11.405	
Temperature Before Heat Addition	1.474	1.572	1.505	1.491
Temperature After Heat Addition	7.118	7.431	7.274	
Cycle Time	1.865	1.745	1.795	
Combustion Chamber Length	0.50	0.55	0.515	0.50

TABLE 16
CONSTANT VOLUME COMBUSTION, $M_1 = 0$

PERFORMANCE BASED ON CHARACTERISTIC CYCLE ANALYSIS	FIRST CYCLE	SECOND CYCLE	THIRD CYCLE	FOURTH CYCLE
Figures (Appendix)	13A	13B	13C	13C
Air-fuel Ratio	31	31	31	31
Combustion Chamber Mass	0.500	0.477	0.557	0.441
Specific Fuel Consumption	1.872	1.949	1.673	
Mass Flow per sec./sq. ft.	17.94	28.20	24.24	
Thrust per sq. in.	7.73	11.67	11.69	
Adiabatic Compression Efficiency	1.000	0.516	0.298	0.115
Thrust Coefficient	0.526	0.794	0.795	
Mass Flow Coefficient	0.210	0.330	0.284	
Overall Efficiency				
Entropy Rise Prior to Hammer Comp.	0	0.248	0.399	0.849
Entropy Rise Due to Hammer Comp.	0	0	0.377	0.042
Entropy Rise Due to Heat Addition	3.392	3.072	2.696	2.785
Total Entropy of Cycle	3.392	3.320	3.[illegible]71	3.676
Pressure Before Heat Addition	1.000	1.514	1.796	1.222
Pressure After Heat Addition	6.682	8.453	8.126	5.811
Temperature Before Heat Addition	1.000	1.244	1.612	1.512
Temperature After Heat Addition	6.682	6.946	7.294	7.194
Cycle Time	2.380	1.445	1.962	
Combustion Chamber Length	0.500	0.392	0.500	0.546

TABLE 17
CONSTANT VOLUME COMBUSTION, $M_1 = 0.95$

PERFORMANCE BASED ON CHARACTERISTIC CYCLE ANALYSIS	FIRST CYCLE	SECOND CYCLE	THIRD CYCLE	FOURTH CYCLE
Figures (Appendix)	10A	10B	14A	
Air-fuel Ratio	31	31	31	31
Combustion Chamber Mass	1.116	0.674	0.732	0.872
Specific Fuel Consumption	2.086	2.200	2.303	
Mass Flow per sec./sq. ft.	50.17	31.29	36.46	
Thrust per sq. in.	19.40	10.93	12.77	
Adiabatic Compression Efficiency	0.85	0.339	0.533	0.439
Thrust Coefficient	1.320	0.744	0.869	
Mass Flow Coefficient	0.587	0.349	0.427	
Overall Efficiency	0.122	0.116	0.111	
Entropy Rise Prior to Hammer Comp.	0	0.718	0.326	0.445
Entropy Rise Due to Hammer Comp.	0.119	0.094	0.107	0.143
Entropy Rise Due to Heat Addition	2.826	2.608	2.797	2.708
Total Entropy of Cycle	2.945	3.420	3.230	3.296
Pressure Before Heat Addition	3.290	2.148	2.334	2.346
Pressure After Heat Addition	16.018	9.264	11.120	10.563
Temperature Before Heat Addition	1.474	1.721	1.514	1.628
Temperature After Heat Addition	7.176	7.423	7.216	7.330
Cycle Time	1.900	1.840	1.715	
Combustion Chamber Length	0.50	0.540	0.475	0.605

Studies were also carried out at M = 0 assuming constant volume combustion, Table 16, Figs. 13A to 13C. Periodic conditions were approached much more slowly in this cycle as the degree of scavenging varied greatly from cycle to cycle. Although a specific fuel consumption value of 1.7 was obtained in the third cycle, the initial and fourth cycle conditions indicated that the resultant performance would be much less than that obtained in either of the first three cycles, since complete scavenging of the burned gas could not be obtained in a single cycle.

For this configuration with the half-length combustion chamber, the final compression level prior to the heat-addition process was intermediate between the ideal ram pressure recovery level and the ideal hammer recovery pressure level. Although the cycle time for the half-length combustion cycle was in general of the order of twice the length of the quarter cycle, the indicated thrust, in lbs./sq.in., was much larger for the half-length cycles, as shown in Table 18.

TABLE 18

VARIATION IN SPECIFIC THRUST WITH COMBUSTION CHAMBER VOLUME

Cycle	Mach Number	Thrust Lbs./Sq.In.	Heat Addition Mode	Cycle
Quarter-length	0.65	11.24	Constant volume	3
Half-length	0.65	12.84	Constant volume	3
Quarter-length	0.65	6.17	Gradual heat addition	3
Half-length	0.65	14.46	Gradual heat addition	3

In order to determine the effect of change in fuel-air ratio, the following cycles were investigated for air-fuel ratios of 56 to 1:

TABLE 19

HALF-LENGTH COMBUSTION CHAMBER

Table	Figures (Appendix)	f/a	Mach Number	Combustion Mode	No. Cycles Investigated
20	15A,15B,15C	1/56	0.65	Constant volume	3
21	16A,16B,16C	1/56	0.95	Constant volume	3
22	17A,17B,17C	1/56	0.65	Gradual heat addition	3

It was observed that when the combustion chamber length was held fixed, the resultant specific fuel consumption values were slightly lower than those obtained for the air-fuel ratio 31 to 1. These results are, however, not of great significance, since for lean air-fuel ratios, the pressure rise during the combustion process, as well as the amount of fresh gas included in the combustion chamber in succeeding cycles, varies. To determine the effect of change in air-fuel ratio alone, the 3rd cycle, M = 0.65, Table 20, was reconstructed, including only the air from the previous cycle that had suffered an entropy penalty. This resulted, Table 23, in a reduction in the combustion chamber length and an increase in specific fuel consumption for the 3rd cycle from 1.8 to 2.6, Fig. 18A. It is apparent from this study that the relative combustion chamber length is much more important a factor in determining the overall performance than the air-fuel ratio.

Since the compression ratio prior to the heat-addition process for the half-length combustion cycle was found to be nearly equal to that for hammer compression at the corresponding Mach number, the resultant performance should approach that for the hammer compression engine suggested by R. Weatherston of this Laboratory[3]. In the hammer compression cycle, the complete tube volume is assumed to be burned at constant volume and completely scavenged in one cycle. The maximum compression is assumed to be that of hammer compression at the corresponding Mach number. Since the study at M = 0 for the half-length cycle, Fig. 13, indicated that complete scavenging of one-half the tube could not be obtained at M = 0, this engine would not operate in the static condition. The calculation of a hammer compression cycle at M = 0.65, f/a = 1/31, Fig. 19A indicated that complete scavenging could be achieved and that hammer compression equivalent to that occurring at the corresponding flight Mach number could be obtained. The first cycle condition, Table 24, with an adiabatic compression efficiency of 0.91 and a specific fuel consumption of 1.8, consequently corresponded to the periodic condition. This specific fuel consumption value is somewhat better than that obtained for the corresponding half-tube combustion configuration, 2.0, Table 12. The gradual heat addition assumption

TABLE 20
CONSTANT VOLUME COMBUSTION, $M_1 = 0.65$

PERFORMANCE BASED ON CHARACTERISTIC CYCLE ANALYSIS	FIRST CYCLE	SECOND CYCLE	THIRD CYCLE	FOURTH CYCLE
Figures (Appendix)	15A	15B	15C	15C
Air-fuel Ratio	56	56	56	56
Combustion Chamber Mass	0.900	0.732	0.824	0.805
Specific Fuel Consumption	1.638	2.184	1.763	
Mass Flow per sec./sq. ft.	35.73	26.76	29.38	
Thrust per sq. in.	9.74	5.47	7.44	
Adiabatic Compression Efficiency	0.927	0.445	0.630	0.581
Thrust Coefficient	0.663	0.372	0.506	
Mass Flow Coefficient	0.418	0.313	0.344	
Overall Efficiency	0.106	0.080	0.099	
Entropy Rise Prior to Hammer Comp.	0	0.301	0.153	0.191
Entropy Rise Due to Hammer Comp.	0.043	0.115	0.070	0.077
Entropy Rise Due to Heat Addition	2.190	2.112	2.187	2.168
Total Entropy of Cycle	2.233	2.528	2.410	2.436
Pressure Before Heat Addition	2.333	1.731	1.830	1.816
Pressure After Heat Addition	7.973	5.646	6.232	6.116
Temperature Before Heat Addition	1.296	1.382	1.299	1.320
Temperature After Heat Addition	4.420	4.507	4.424	4.445
Cycle Time	2.152	2.335	2.395	
Combustion Chamber Length	0.500	0.585	0.535	0.585

TABLE 21
CONSTANT VOLUME COMBUSTION, $M_1 = 0.95$

PERFORMANCE BASED ON CHARACTERISTIC CYCLE ANALYSIS	FIRST CYCLE	SECOND CYCLE	THIRD CYCLE	FOURTH CYCLE
Figures (Appendix)	16A	16B	16C	16C
Air-fuel Ratio	56	56	56	56
Combustion Chamber Mass	1.116	0.854	0.958	0.924
Specific Fuel Consumption	1.781	1.975	1.909	
Mass Flow per sec./sq. ft.	48.52	34.91	40.83	
Thrust per sq. in.	12.16	7.89	9.55	
Adiabatic Compression Efficiency	0.855	0.462	0.613	0.583
Thrust Coefficient	0.827	0.537	0.650	
Mass Flow Coefficient	0.568	0.409	0.478	
Overall Efficiency	0.143	0.129	0.133	
Entropy Rise Prior to Hammer Comp.	0	0.450	0.192	0.225
Entropy Rise Due to Hammer Comp.	0.119	0.105	0.135	0.131
Entropy Rise Due to Heat Addition	2.038	1.943	2.040	2.038
Total Entropy of Cycle	2.157	2.498	2.368	2.394
Pressure Before Heat Addition	3.290	2.315	2.397	2.314
Pressure After Heat Addition	10.299	6.875	7.518	7.249
Temperature Before Heat Addition	1.474	1.587	1.463	1.465
Temperature After Heat Addition	4.614	4.712	4.588	4.589
Cycle Time	1.965	2.090	2.005	
Combustion Chamber Length	0.500	0.585	0.585	0.585

TABLE 22

GRADUAL HEAT ADDITION, M_1=0.65

PERFORMANCE BASED ON CHARACTERISTIC CYCLE ANALYSIS	FIRST CYCLE	SECOND CYCLE	THIRD CYCLE	FOURTH CYCLE
Figures (Appendix)	17A	17B	17C	17C
Air-fuel Ratio	56	56	56	56
Combustion Chamber Mass	0.900	0.746	0.577	0.849
Specific Fuel Consumption	1.568	1.818	2.130	
Mass Flow per sec./sq. ft.	39.34	32.26	27.00	
Thrust per sq. in.	11.20	7.92	5.66	
Adiabatic Compression Efficiency	0.93	0.54	0.53	0.48
Thrust Coefficient	0.762	0.539	0.385	
Mass Flow Coefficient	0.461	0.378	0.316	
Overall Efficiency	0.111	0.096	0.082	
Entropy Rise Prior to Hammer Comp.	0	0.128	0.112	0.155
Entropy Rise Due to Hammer Comp.	0.044	0.178	0.163	0.290
Entropy Rise Due to Heat Addition	2.261	2.193	2.229	
Total Entropy of Cycle	2.305	2.499	2.504	
Pressure Before Heat Addition	2.330	1.796	1.651	1.990
Pressure After Heat Addition	7.863	6.896	6.052	
Temperature Before Heat Addition	1.295	1.335	1.288	1.454
Temperature After Heat Addition	4.533	4.718	4.554	
Cycle Time	1.955	1.975	1.825	
Combustion Chamber Length	0.500	0.555	0.450	0.620

TABLE 23

CONSTANT VOLUME COMBUSTION, $M_1=0.65$

PERFORMANCE BASED ON CHARACTERISTIC CYCLE ANALYSIS	FIRST CYCLE	SECOND CYCLE	THIRD CYCLE	FOURTH CYCLE
Figures (Appendix)	15A	15B	18A	
Air-fuel Ratio	56	56	56	56
Combustion Chamber Mass	0.900	0.732	0.584	0.767
Specific Fuel Consumption	1.638	2.184	2.582	
Mass Flow per sec./sq. ft.	35.73	29.09	26.74	
Thrust per sq. in.	9.74	5.47	4.62	
Adiabatic Compression Efficiency	0.927	0.445	0.506	0.400
Thrust Coefficient	0.663	0.372	0.314	
Mass Flow Coefficient	0.418	0.313	0.313	
Overall Efficiency	0.106	0.080	0.067	
Entropy Rise Prior to Hammer Comp.	0	0.301	0.226	0.275
Entropy Rise Due to Hammer Comp.	0.043	0.115	0.090	0.242
Entropy Rise Due to Heat Addition	2.190	2.112	2.171	2.050
Total Entropy of Cycle	2.233	2.528	2.488	2.567
Pressure Before Heat Addition	2.333	1.731	1.683	1.791
Pressure After Heat Addition	7.973	5.646	5.677	5.644
Temperature Before Heat Addition	1.296	1.382	1.317	1.452
Temperature After Heat Addition	4.420	4.507	4.442	4.578
Cycle Time	2.152	2.150	1.865	
Combustion Chamber Length	0.50	0.585	0.457	0.622

TABLE 24

CONSTANT VOLUME COMBUSTION, M_1=0.65

PERFORMANCE BASED ON CHARACTERISTIC CYCLE ANALYSIS	FIRST CYCLE	SECOND CYCLE
Figure (Appendix)	19A	19A
Air-fuel Ratio	31	31
Combustion Chamber Mass	1.800	1.800
Specific Fuel Consumption	1.807	
Mass Flow per sec./sq. ft.	40.45	
Thrust per sq. in.	18.05	
Adiabatic Compression Efficiency	0.91	0.91
Thrust Coefficient	1.228	
Mass Flow Coefficient	0.474	
Overall Efficiency	0.096	
Entropy Rise Prior to Hammer Compression	0	0.006
Entropy Rise Due to Hammer Compression	0.044	0.044
Entropy Rise Due to Heat Addition	3.010	3.010
Total Entropy of Cycle	3.054	3.054
Pressure Before Heat Addition	2.334	2.334
Pressure After Heat Addition	12.588	12.588
Temperature Before Heat Addition	1.296	1.296
Temperature After Heat Addition	6.996	6.996
Cycle Time	3.800	
Total Mass		
Combustion Chamber Length	1.00	1.00

for the half-tube cycle, however, yields approximately the same performance as the hammer cycle, Table 12. The major objections to the use of the hammer cycle may be in the actual achievement of rapid volume combustion and the relative long period of time required for complete scavenging. The total cycle time is approximately twice that of the corresponding half-tube cycle and four times that of the corresponding quarter-tube cycle.

During the characteristic studies, it was observed that a very high pressure region was created upon reflection of the reinforced hammer shock at the inlet valve, Fig.IV. For example, from Table 2, Fig. 1A, with an initial pressure of 2.33 atmospheres before heat addition and a 4 atmosphere pressure rise during combustion, a pressure of 10 atmospheres was obtained after the shock reflection at the inlet valve. This pressure was obtained with a compression efficiency of 78 percent. H.R. Lawrence and J. G. Logan of this Laboratory suggested that heat addition at this point might lead to improved performance, since a portion of the air in the tube would be burned at relatively high pressures and that the compression would occur with reasonable efficiency. The basic characteristics of this cycle are indicated in Fig. IV.

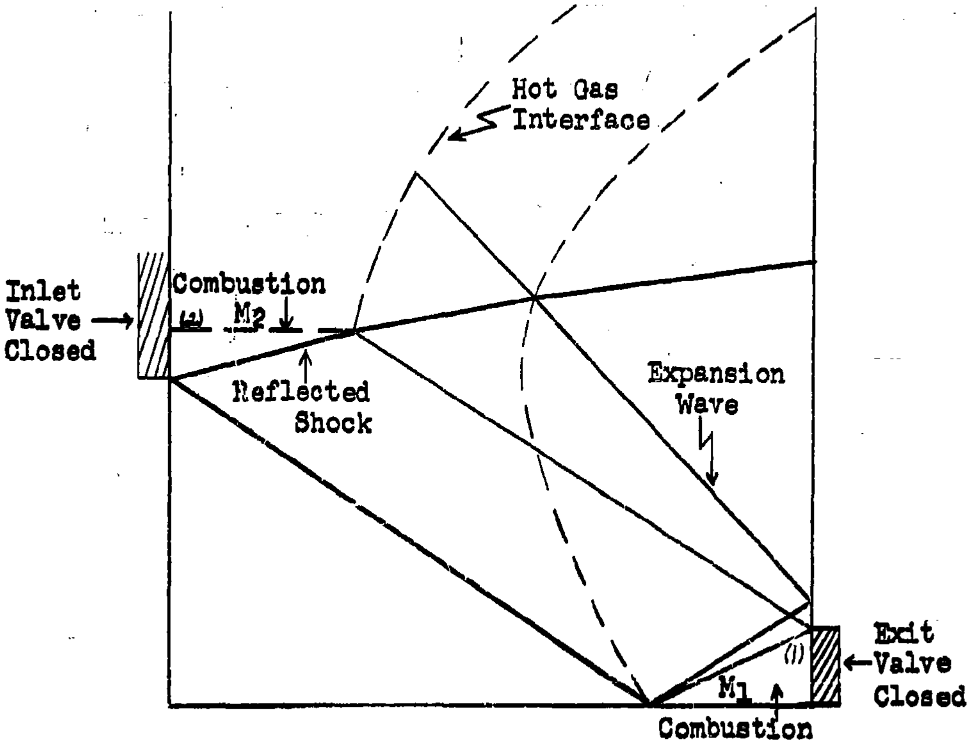

Fig. IV
Typical Cycle Configuration with Secondary Combustion

After completion of the combustion at (1) the exit valve, fuel would be injected at a point adjacent to the inlet valve (2) after the shock reflection. The various configurations studied are summarized in Table 25.

TABLE 25

SECONDARY COMBUSTION CYCLES

M = 0.65

Table	Figures (Appendix)	f / a		% Mass in Tube Burned		Total	Combustion Model
		(1)	(2)	(1)	(2)		
26	20A	1/31	1/31	38	61	100	Constant volume combustion
27	21A	1/31	1/31	29	29	58	Constant volume combustion
28	22A	1/31	1/31	31	31	62	Gradual heat addition
29	23A	1/56	1/56	55	45	100	Gradual heat addition
30	24A	1/56	1/56	55	45	100	Constant volume combustion
31	25A	1/56	1/56	23	77	100	Constant volume combustion
32	26A	1/14	1/56	24	76	100	Constant volume combustion

During the calculation of the cycles, it was observed that the expansion waves generated at the exit due to the opening of the rear valve could exert an appreciable effect upon the pressures obtained at the inlet with respect to both the duration of the pressure level and the magnitude. For example, during the gradual heat addition calculation, Table 28, Fig. 22A, the pressure dropped from 10 atmospheres before heat addition to 6 atmospheres after heat addition. Even so, the resulting specific fuel consumption value of 1.6 was superior to the value 1.8 obtained with the half-tube cycle, Table 14. This may have been due, however, to the presence of unburned cold air in the tube which was exhausted at a high velocity leading to a form of augmentation.

TABLE 26

CONSTANT VOLUME COMBUSTION, M

Double Burning

PERFORMANCE BASED ON CHARACTERISTIC CYCLE ANALYSIS	FIRST COMBUSTION I	SECOND COMBUSTION II
Figure (Appendix)	20A	20A
Air-fuel Ratio	31	31
Combustion Chamber Mass	0.630	0.996
Specific Fuel Consumption	2.111	
Mass Flow per sec./sq. ft.	43.47	
Thrust per sq. in.	16.60	
Adiabatic Compression Efficiency	0.910	0.676
Thrust Coefficient	1.129	
Mass Flow Coefficient	0.509	
Overall Efficiency	0.083	
Entropy Rise Prior to Hammer Compression	0	0.495
Entropy Rise Due to Hammer Compression	0.043	0.067
Entropy Rise Due to Heat Addition	3.011	2.059
Total Entropy of Cycle	3.054	2.621
Pressure Before Heat Addition	2.330	13.443
Pressure After Heat Addition	12.594	42.578
Temperature Before Heat Addition	1.295	2.631
Temperature After Heat Addition	6.996	8.332
Cycle Time	3.195	
Total Mass	1.626	
Combustion Chamber Length	0.350	0.195

TABLE 27

CONSTANT VOLUME COMBUSTION, $M_1 = 0.65$

Double Burning

PERFORMANCE BASED ON CHARACTERISTIC CYCLE ANALYSIS	FIRST COMBUSTION I	SECOND COMBUSTION II
Figure (Appendix)	21A	21A
Air-fuel Ratio	31	31
Combustion Chamber Mass	0.450	0.450
Specific Fuel Consumption	1.625	
Mass Flow per sec./sq. ft.	26.19	
Thrust per sq. in.	13.00	
Adiabatic Compression Efficiency	0.910	0.678
Thrust Coefficient	0.884	
Mass Flow Coefficient	0.307	
Overall Efficiency	0.107	
Entropy Rise Prior to Hammer Compression	0	0.495
Entropy Rise Due to Hammer Compression	0.044	0.070
Entropy Rise Due to Heat Addition	3.010	2.037
Total Entropy of Cycle	3.054	2.602
Pressure Before Heat Addition	2.334	14.266
Pressure After Heat Addition	12.600	44.630
Temperature Before Heat Addition	1.295	2.679
Temperature After Heat Addition	6.996	8.381
Cycle Time	2.935	
Total Mass	1.575	
Combustion Chamber Length	0.250	0.085

TABLE 28

CONSTANT VOLUME COMBUSTION, M_1 - 0.65

Double Burning

PERFORMANCE BASED ON CHARACTERISTIC CYCLE ANALYSIS	FIRST COMBUSTION I	SECOND COMBUSTION II
Figure (Appendix)	22A	22A
Air-fuel Ratio	31	31
Combustion Chamber Mass	0.450	0.450
Specific Fuel Consumption	1.601	
Mass Flow per sec./sq. ft.	23.48	
Thrust per sq. in.	11.83	
Adiabatic Compression Efficiency	0.910	0.761
Thrust Coefficient	0.805	
Mass Flow Coefficient	0.275	
Overall Efficiency	0.109	
Entropy Rise Prior to Hammer Compression	0	0.306
Entropy Rise Due to Hammer Compression	0.044	0.052
Entropy Rise Due to Heat Addition	3.170	2.742
Total Entropy of Cycle	3.214	3.100
Pressure Before Heat Addition	2.334	10.548
Pressure After Heat Addition	7.293	5.858
Temperature Before Heat Addition	1.298	2.262
Temperature After Heat Addition	6.408	5.726
Cycle Time	3.275	
Total Mass	1.450	
Combustion Chamber Length	0.250	0.100

TABLE 29
Gradual Heat Addition , $M_1 = 0.65$
Double Burning

PERFORMANCE BASED ON CHARACTERISTIC CYCLE ANALYSIS	FIRST COMBUSTION I	SECOND COMBUSTION II
Figure (Appendix)	23A	23A
Air-fuel Ratio	56	56
Combustion Chamber Mass	0.900	0.751
Specific Fuel Consumption	1.681	
Mass Flow per sec./sq. ft.	39.08	
Thrust per sq. in.	10.38	
Adiabatic Compression Efficiency	0.930	0.855
Thrust Coefficient	0.706	
Mass Flow Coefficient	0.457	
Overall Efficiency	0.104	
Entropy Rise Prior to Hammer Compression	0	0.115
Entropy Rise Due to Hammer Compression	0.044	0.013
Entropy Rise Due to Heat Addition	2.261	2.003
Total Entropy of Cycle	2.305	2.131
Pressure Before Heat Addition	2.330	9.630
Pressure After Heat Addition	7.863	5.830
Temperature Before Heat Addition	1.295	2.065
Temperature After Heat Addition	4.533	3.881
Cycle Time	3.610	
Total Mass	1.651	
Combustion Chamber Length	0.500	0.160

Studies of the constant volume cycle were made with all of the gas mass being burned during the cycle in the first and second burning periods, and with only a part of the total mass being consumed. As the heat addition process in the second region occurred in each case at approximately the same pressures, a direct comparison of the augmentation effect could be obtained. The results for the cycle with exhaust of cold air indicated a lower specific fuel consumption, 1.63, Table 27, Fig. 21A, than for the case of combustion of all the enclosed air mass, 1.98, Table 26, Fig. 20A. It is interesting to note that the specific fuel consumption for the hammer cycle 1.8, Table 24, was somewhat less than the specific fuel consumption value obtained in Table 26. The presence of the strong shocks due to the constant volume combustion assumption may have contributed to the somewhat higher specific fuel consumption value obtained. It can be seen from Fig. 20A that the strong shock generated during the second combustion period as a result of the assumed constant volume combustion mode results in an appreciable entropy rise of the gas through which it passes before reaching the exit valve. The entropy of the gas encountering the shock was increased from 3.054 to 3.281. It is this gas mass that generates the major portion of the impulse. On the other hand, because of slow build-up of the shock with the gradual-heat-addition assumption, Table 29, no significant entropy rise occurred, Fig. 23A, as a result of the shock passage. Since the pressure before heat addition of 9 atmospheres was obtained at a compression efficiency of 86 percent, and since the gradual buildup in shock strength probably more nearly corresponds to the actual phenomena, future investigations of the cycle may lead to much improved performance. This is also partially confirmed by the results of constant volume calculations assuming an air-fuel ratio of 56 to 1, for which case considerably reduced pressures after heat addition were obtained. The use of the relatively lean mixtures, Table 25, Figs. 23A to 26A, indicated that somewhat reduced specific fuel consumption values could be obtained if all the gas was burned at the same air-fuel ratio, the specific fuel consumption values varying between 1.51 and 1.61 for the combustion of different relative volumes, Tables 30 and 31, Figs. 24A and 25A. When a rich initial mixture was employed, Table 32, Fig. 26A, in order to increase the initial pressure, no performance improvement was obtained. The specific fuel consumption value actually increased from 1.51 to 1.95.

Since the cycle time for these cycles varied from 2.9 to 4.0, this engine configuration would be subject to the same objection as the constant volume hammer cycle, an impractically long cycle time. In order to obtain an adequate basis for comparison of this double-burning cycle with the constant volume hammer cycle, it would be necessary to extend the hammer jet investigation to air-fuel ratios of 56-1. The only case available for comparison for the air-fuel ratio 31-1 indicates that the addition of heat at different periods to take advantage of the possible higher compression ratios, Table 28, yields a lower specific fuel consumption value than the addition of heat uniformly in a tube, Table 24.

TABLE 30
CONSTANT VOLUME COMBUSTION, $M_1 = 0.65$
Double Burning

PERFORMANCE BASED ON CHARACTERISTIC CYCLE ANALYSIS	FIRST COMBUSTION I	SECOND COMBUSTION II
Figure (Appendix)	24A	24A
Air-fuel Ratio	56	56
Combustion Chamber Mass	0.900	0.726
Specific Fuel Consumption	1.513	
Mass Flow per sec./sq. ft.	38.00	
Thrust per sq. in.	11.21	
Adiabatic Compression Efficiency	0.910	0.790
Thrust Coefficient	0.763	
Mass Flow Coefficient	0.445	
Overall Efficiency	0.115	
Entropy Rise Prior to Hammer Compression	0	0.276
Entropy Rise Due to Hammer Compression	0.044	0.025
Entropy Rise Due to Heat Addition	2.189	1.594
Total Entropy of Cycle	2.233	1.895
Pressure Before Heat Addition	2.334	9.830
Pressure After Heat Addition	7.973	24.006
Temperature Before Heat Addition	1.295	2.167
Temperature After Heat Addition	4.418	5.292
Cycle Time	3.655	
Total Mass	1.626	
Combustion Chamber Length	0.500	0.160

TABLE 31
CONSTANT VOLUME COMBUSTION, $M_1 = 0.65$

Double Burning

PERFORMANCE BASED ON CHARACTERISTIC CYCLE ANALYSIS	FIRST COMBUSTION I	SECOND COMBUSTION II
Figure (Appendix)	25A	25A
Air-fuel Ratio	56	56
Combustion Chamber Mass	0.360	1.212
Specific Fuel Consumption	1.611	
Mass Flow per sec./sq. ft.	33.18	
Thrust per sq. in.	9.19	
Adiabatic Compression Efficiency	0.910	0.701
Thrust Coefficient	0.625	
Mass Flow Coefficient	0.388	
Overall Efficiency	0.108	
Entropy Rise Prior to Hammer Compression	0	0.276
Entropy Rise Due to Hammer Compression	0.044	0.028
Entropy Rise Due to Heat Addition	2.189	1.919
Total Entropy of Cycle	2.233	2.223
Pressure Before Heat Addition	2.334	3.539
Pressure After Heat Addition	7.973	10.364
Temperature Before Heat Addition	1.295	1.620
Temperature After Heat Addition	4.418	4.745
Cycle Time	4.050	
Total Mass	1.572	
Combustion Chamber Length	0.200	0.555

TABLE 32
CONSTANT VOLUME COMBUSTION, $M_1 = 0.65$
Double Burning

PERFORMANCE BASED ON CHARACTERISTIC CYCLE ANALYSIS	FIRST COMBUSTION I	SECOND COMBUSTION II
Figure (Appendix)	26A	26A
Air-fuel Ratio	14	56
Combustion Chamber Mass	0.360	1.147
Specific Fuel Consumption	1.951	
Mass Flow per sec./sq. ft.	44.03	
Thrust per sq. in.	17 32	
Adiabatic Compression Efficiency	0.910	0.500
Thrust Coefficient	1.178	
Mass Flow Coefficient	0.515	
Overall Efficiency	0.089	
Entropy Rise Prior to Hammer Compression	0	0.950
Entropy Rise Due to Hammer Compression	0.044	0.140
Entropy Rise Due to Heat Addition	4.223	1.250
Total Entropy of Cycle	4.267	2.340
Pressure Before Heat Addition	2.334	11.187
Pressure After Heat Addition	24.834	22.525
Temperature Before Heat Addition	1.296	3.084
Temperature After Heat Addition	13.796	6.208
Cycle Time	2.925	
Total Mass	1.507	
Combustion Chamber Length	0.200	0.315

SUMMARY AND CONCLUSIONS

This series of characteristic studies was undertaken to obtain some information as to the scavenging and compression processes occurring in intermittent engines. All the studies were of straight-tube wave engine configurations and the wave phenomena established by valve action was based on the assumption of instantaneous valve opening and closing. The results consequently are not immediately applicable to practical configurations wherein some variation in tube geometry occurs as well as a gradual valve action as opposed to the instantaneous assumption employed. Nevertheless, the results of the studies should have some influence upon the nature of the experimental work to be undertaken in order to develop intermittent engines for specific applications.

The characteristic investigations of cycles with a single combustion process occurring in each cycle led to the somewhat unexpected conclusion that high values of compression prior to heat addition cannot be efficiently achieved because of the large shock losses that would be encountered. It should be stressed that this is only true of the straight-tube configurations studied in this investigation. It may be possible that some method of avoiding the shock losses in the unburned gas prior to heat addition can be developed. For the simple configuration initially visualized, however, the use of shock waves continually reinforced and reflected in the tube, as an agent for compression, would result in very poor cyclic performance.

The performance estimates obtained from the characteristic cycles indicate that the resultant specific fuel consumption values decrease as the relative volume of gas burned per cycle is increased. In these intermittent engines, it appears to be more efficient to utilize the energy of the heat-addition process to accelerate the flow to produce thrust rather than high pressures. Optimum performance occurs when all compression is obtained as a result of hammer or ram pressure.

The studies also indicated that scavenging difficulties may be encountered in the static operating condition if the relative combustion chamber volume is larger than 50 percent. This would apply both to the constant volume hammer cycle as well as to the cycles that were modified by introducing a secondary combustion zone in the cycle in order to take advantage of the existence of regions of relatively efficient, high-pressure compression.

Although insufficient studies were undertaken to determine the relative merits of cycles with secondary heat-addition regions, such studies may lead to efficient high-pressure intermittent engines of relatively simple geometry. The major objection, the relatively long periods required for the completion of scavenging, may only be due to the application of the ambient pressure boundary condition. It is to be expected that during the non-steady discharge when the total head and velocity of the jet are appreciably less than for the surrounding stream, an appreciable acceleration of the jet would occur, due to shear forces which would alter the present length of the theoretical cycle.

As a result of these studies, it is concluded that the characteristics of the wave engine cycle prevent the attainment of performance equivalent to that of present-day turbojet engines. The theoretical studies show that this engine, in any of the forms studied in this paper, will occupy a position intermediate between that of the ramjet and turbojet.

REFERENCES

1. Hertzberg, A. and Logan, J.: A New Form of Heat Engine Utilizing Pressure Waves Project Squid Technical Memo No. CAL-35 15 August 1951 (Confidential).
2. Foa, J.: Single Flow Jet Engines - A Generalized Treatment Journal of the American Rocket Society September 1951.
3. Project Squid Quarterly Progress Report 1 October 1950 page 6.
4. Kahane, A. and Lees L.: Unsteady One-Dimensional Flow, with Heat Addition or Entropy Gradients Project Squid Technical Memo No. PR-2 November 1947.
5. Kantrowitz, A.: Heat Engines Based on Wave Processes Cornell University Presented at Annual ASME Meeting November 1948.
6. Rudinger, G.: Wave Diagrams for Nonsteady Flow in Ducts D. Von Nostrand New York (To be published).

APPENDIX 1

The detailed analysis of the wave phenomena for the intermittent engine configurations was performed by means of the numerical method of characteristics. This method, including details for the representation of the effects of heat addition, has been described elsewhere[4,5,6]. All of the cycles described in the report have been included in the Appendix for reference. For convenience, these cycles are summarized on pages 58 and 59.

The abscissa and ordinate of the wave diagrams are given in terms of the usual dimensionaless parameters L and τ, where

$L = l/l_o$

$\tau = a_o t/l_o$

l_o = tube length

t = time

a_o = reference sound velocity

The encircled values on the wave diagrams denote the entropy value at that point, with the ambient condition taken as the zero reference level. This entropy is represented in the dimensionless form

$s = \mathcal{s}/\gamma R$

where:

s = dimensionless entropy factor

$\mathcal{s}$ = entropy

R = gas constant

γ = ratio of specific heats

Heavy lines are usually employed to represent the shock waves. The interface between hot and unburned gas is denoted by the dashed lines. Local entropy discontinuities and particle paths are indicated by the finely dotted lines. The only values of pressure, flow velocity and velocity of sound included, are for the inlet and exit conditions. These values are also given in a dimensionless form, the quantities being rendered dimensionless by division by the related ambient quantity.

$P = p/p_o$

$U = u/a_o$

$A = a/a_o$

$\theta = \vartheta/\vartheta_o$

The conditions before and after heat addition are based on the average conditions of entropy and temperature obtained. For the case of gradual heat addition and for all conditions before heat addition, small variations in entropy and temperature occurred. To simplify the heat-addition calculations, average values were determined so that uniform conditions were obtained throughout the combustion chamber region.

In the calculations, the effect of temperature on the ratio of specific heats was represented as follows:

(a) during compression and expansion $\gamma = 1.4$

(b) during combustion $\gamma = 1.36$ $(c_v = 0.19)$

All performance values given are for sea-level conditions with

ambient air temperature,	$\vartheta = 518^oR$
ambient air density	$\rho_o = 0.76$ lbs./cu.ft.
total heat added	$q = H\, n_{(comb)}\, f/a$
combustion efficiency	$n_{(comb)} = 0.9$
fuel heating value	$H = 19{,}200$ btu's/lb.
fuel-air ratio = f/a	

For any other altitude condition, at the same Mach number, the fuel-air ratio, thrust/unit area, specific fuel consumption and mass flow/sec/unit area may be obtained using the following relations:

$$(f/a)_{alt.} = (f/a)_{S.L.} \frac{(a_o^2)_{alt.}}{(a_o^2)_{S.L.}}$$

$$(S.F.C.)_{alt.} = (S.F.C.)_{S.L.} \frac{(a_o)_{alt.}}{(a_o)_{S.L.}}$$

$$(\text{Thrust/Unit Area})_{alt.} = (\text{Thrust/Unit Area})_{S.L.} \frac{(a_o^2 \ \rho_o)_{alt.}}{(a_o^2 \ \rho_o)_{S.L.}}$$

$$(\text{Mass Flow/Sec/Unit Area})_{alt.} = (\text{Mass Flow/Sec/Unit Area})_{S.L.} \frac{(a_o \ \rho_o)_{alt.}}{(a_o \ \rho_o)_{S.L.}}$$

SUMMARY TABLE OF PERFORMANCE

FIGURE (APPENDIX)	CYCLE	TABLE	FLIGHT MACH NUMBER	COMBUSTION CHAMBER LENGTH	FUEL-AIR RATIO f/a	MODE OF* ADDITION	** S.F.C.	*** T/A	PAGE
1A	1	2	0.65	0.25	1/45	C.V.C.	2.026	8.65	61
1B	2	2		0.25	1/34.4		2.519	12.18	63
1C	3	2		0.25	1/27.2		2.665	11.24	65
2A	1	3	0.65	0.25	1/31	C.V.C.	2.530	11.30	67
2B	2	3		0.25			2.083	18.80	69
2C	3	3		0.25			2.387	10.73	71
3A	1	4	0	0.25	1/58.4	C.V.C.	1.557	3.76	73
3B	2	4		0.25	1/52.8		1.662	4.11	75
4A	1	6	0.65	0.25	1/31	G.H.A.	2.484	8.85	77
4B	2	6		0.25			2.431	11.10	79
4C	3	6		0.25			3.043	6.17	81
5A	1	7	0.95	0.25	1/31	G.H.A.	4.311	3.61	83
5B	2	7		0.25			2.786	8.29	85
6A	1	8	0.65	0.25	1/31	G.H.A.	1.986	9.76	87
6B	1	8		0.25			1.833	9.22	89
6C	1	8		0.25			1.833	5.55	91
7A	1	9	0.65	0.25	1/31	G.H.A.	2.850	8.43	93
8A	1	10	0	0.15	1/31	G.H.A.	2.138	3.90	95
9A	1	12	0.65	0.50	1/31	C.V.C.	1.754	17.90	97
9B	2	12		0.565			2.173	9.27	99
9C	3	12		0.535			1.934	12.84	101
10A	1	13	0.95	0.50	1/31	C.V.C.	2.086	19.40	103
10B	2	13		0.54			2.200	10.93	105
10C	3	13		0.54			2.065	15.73	107
11A	1	14	0.65	0.60	1/31	G.H.A.	1.881	14.42	109
11B	2	14		0.60			1.855	12.84	111
11C	3	14		0.60			1.807	14.46	113
12A	1	15	0.95	0.50	1/31	G.H.A.	1.932	21.34	115
12B	2	15		0.550			1.892	17.03	117
12C	3	15		0.515			1.983	16.02	119
13A	1	16	0	0.500	1/33	C.V.C.	1.872	7.73	121
13B	2	16		0.392			1.949	11.67	123
13C	3	16		0.500			1.673	11.69	125
14A	3	17	0.95	0.475	1/31	C.V.C.	2.303	12.77	127
15A	1	20	0.65	0.500	1/56	C.V.C.	1.638	9.74	129
15B	2	20		0.585			2.184	5.47	131
15C	3	20		0.585			1.763	7.44	133

SUMMARY TABLE OF PERFORMANCE (Cont)

FIGURE (APPENDIX)	CYCLE	TABLE	FLIGHT MACH NUMBER	COMBUSTION CHAMBER LENGTH	FUEL-AIR RATIO f/a	MODE OF* ADDITION	** S.F.C.	*** T/A	PAGE
16A	1	21	0.95	0.500	1/56	C.V.C.	1.781	12.16	135
16B	2	21		0.585			1.975	7.89	137
16C	3	21		0.585			1.909	9.55	139
17A	1	22	0.65	0.500	1/56	G.H.A.	1.568	11.20	141
17B	2	22		0.555			1.818	7.92	143
17C	3	22		0.450			2.130	5.66	145
18A	3	23	0.65	0.457	1/56	G.V.C.	2.582	4.62	147
19A	1	24	0.65	1.000	1/31	C.V.C.	1.807	18.05	149
20A	1	26	0.65	L_1=0.350 L_2=0.195	1.31	C.V.C.	2.111	16.60	151
21A	1	27	0.65	L_1=0.25 L_2=0.085	1/31	C.V.C.	1.625	13.00	153
22A	1	28	0.65	L_1=0.25 L_2=0.100	1/31	G.H.A.	1.601	11.83	155
23A	1	29	0.65	L_1=0.500 L_2=0.160	1/56	G.H.A.	1.681	10.38	157
24A	1	30	0.65	L_1=0.500 L_2=0.160	1/56	C.V.C.	1.513	11.21	159
25A	1	31	0.65	L_1=0.200 L_2=0.555	1/56	C.V.C.	1.611	9.19	161
26A	1	32	0.65	L_1=0.200 L_2=0.315	$(f/a)_1$=1.15 $(f/a)_2$=1.60	C.V.C.	1.951	17.32	163

* C.V.C. = Constant volume combustion
G.H.A. = Gradual heat addition

** S.F.C. in $\frac{\text{lbs.fuel/hr.}}{\text{lbs.thrust}}$

*** T/A in $\frac{\text{lbs.}}{\text{sq.in.}}$

CONFIDENTIAL

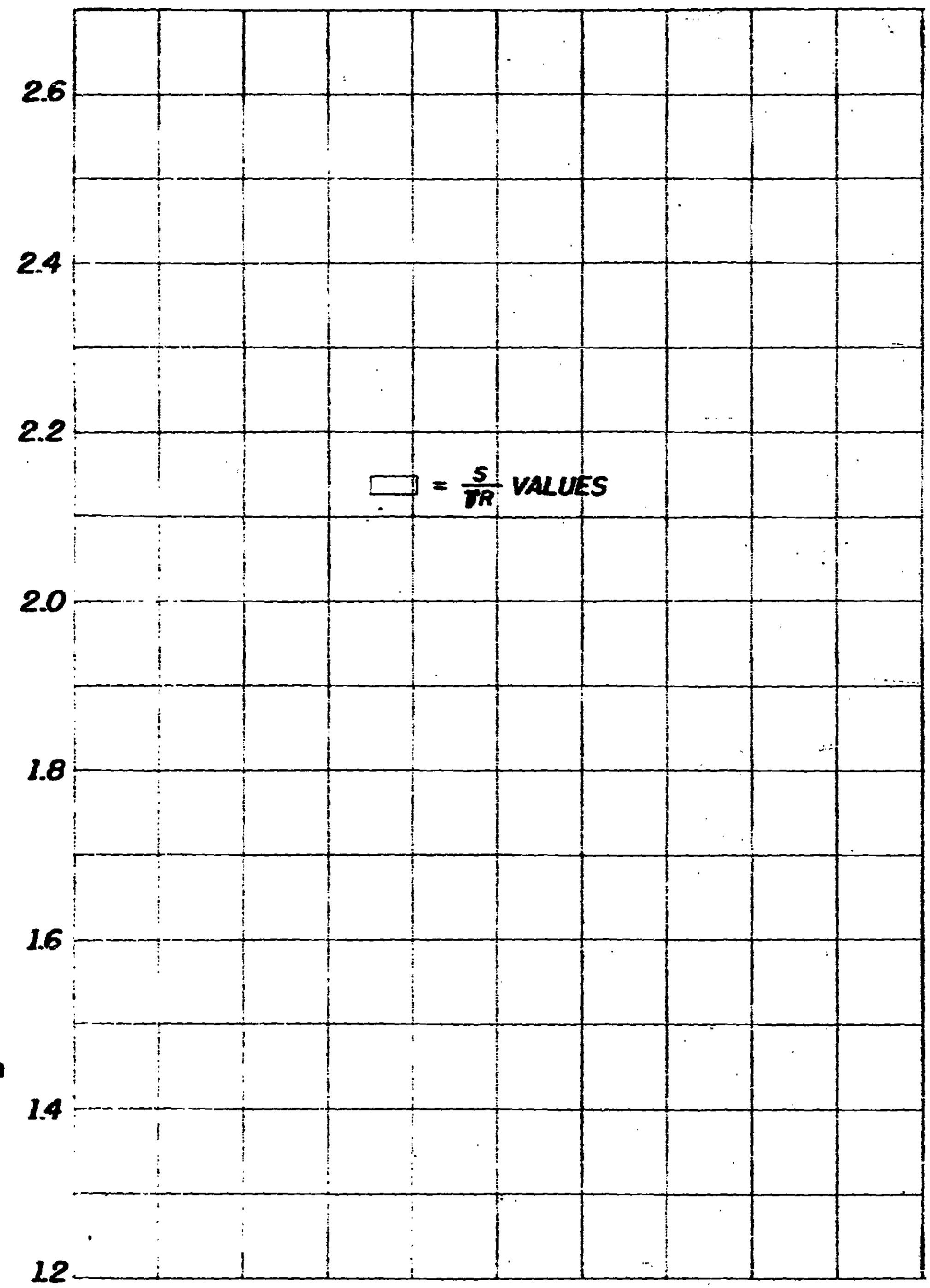

INLET AND EXIT CONDITIONS

POINT	P	u	a
EXIT			
1	2.605	1.898	1.898
2	1.000	1.470	1.655
3	1.000	0.990	1.655
4	1.000	0.735	1.655
5	1.000	0.490	1.655
6	1.000	0.660	1.655
7	2.243	0	1.210
8	2.243	0	1.210
9	6.012	0	1.398
10	3.590	0	1.299
INLET			
11	1.000	0.650	1.000
12	9.990	0	1.477
13	2.417	0	1.286
14	1.924	0	1.168
15	1.328	0	1.108
16	1.272	0.245	1.035
17			
18			
19			
20			

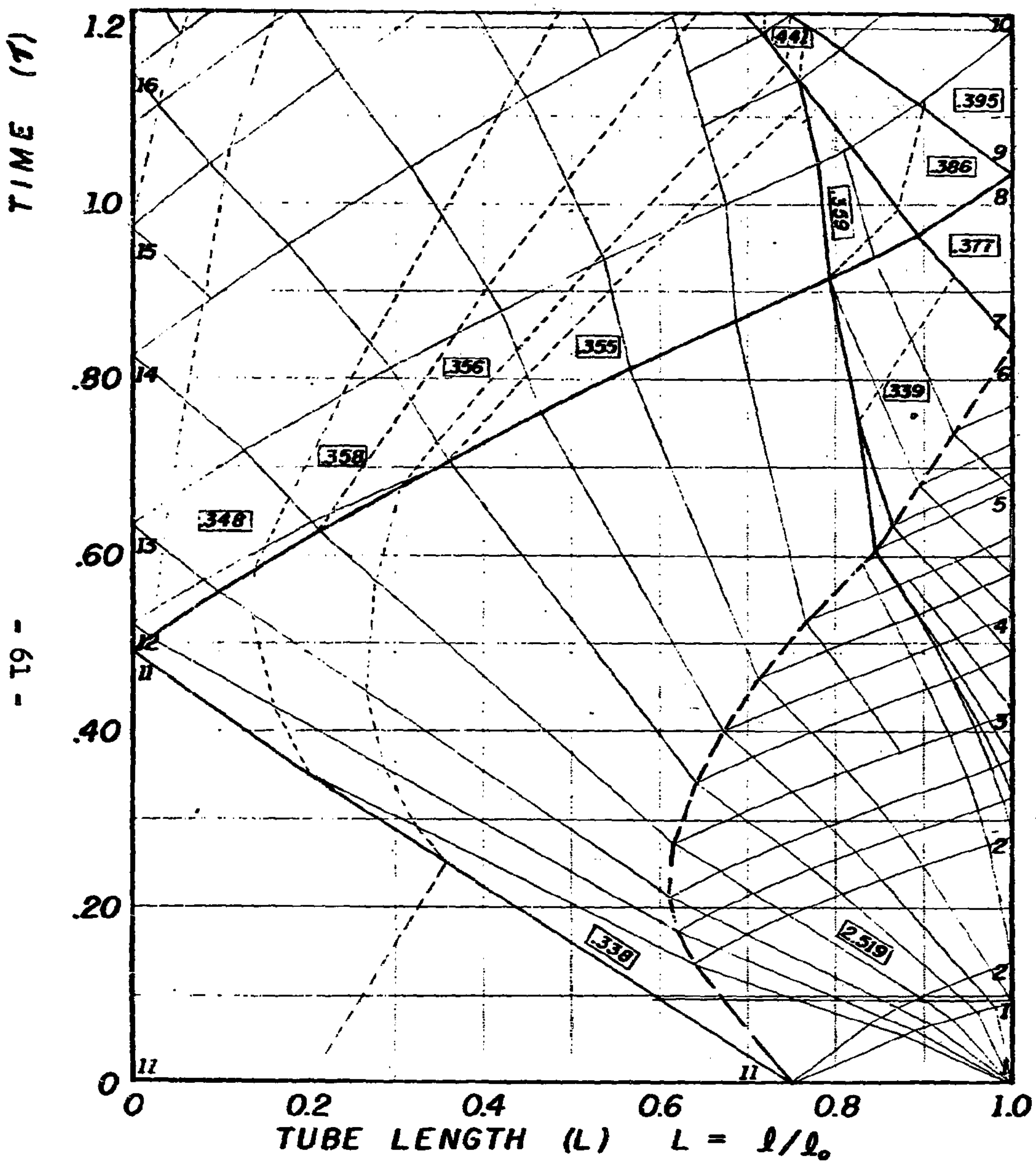

AVERAGE CONDITIONS BEFORE AND AFTER HEAT ADDITION

	BEFORE	AFTER
P =	2.334	9.335
θ =	1.296	5.185
S =	0.044	2.519

CHARACTERISTIC CYCLE PERFORMANCE

SFC $\left(\frac{\text{LBS. FUEL/HR}}{\text{LBS. THRUST}}\right) = 2.026$, $T/A\left(\frac{\text{LBS.}}{\text{SQ. IN.}}\right) = 8.65$

$\eta_c = 0.920$ $\eta_o = 0.086$

COMBUSTION CHAMBER MASS $(m/m_o) = 0.450$

FUEL-AIR RATIO - 1/45

CYCLE 1

MACH NUMBER = 0.65

WAVE ENGINE CYCLE

HEAT ADDITION MODE: CONSTANT VOLUME COMBUSTION

Fig. 1A

CONFIDENTIAL

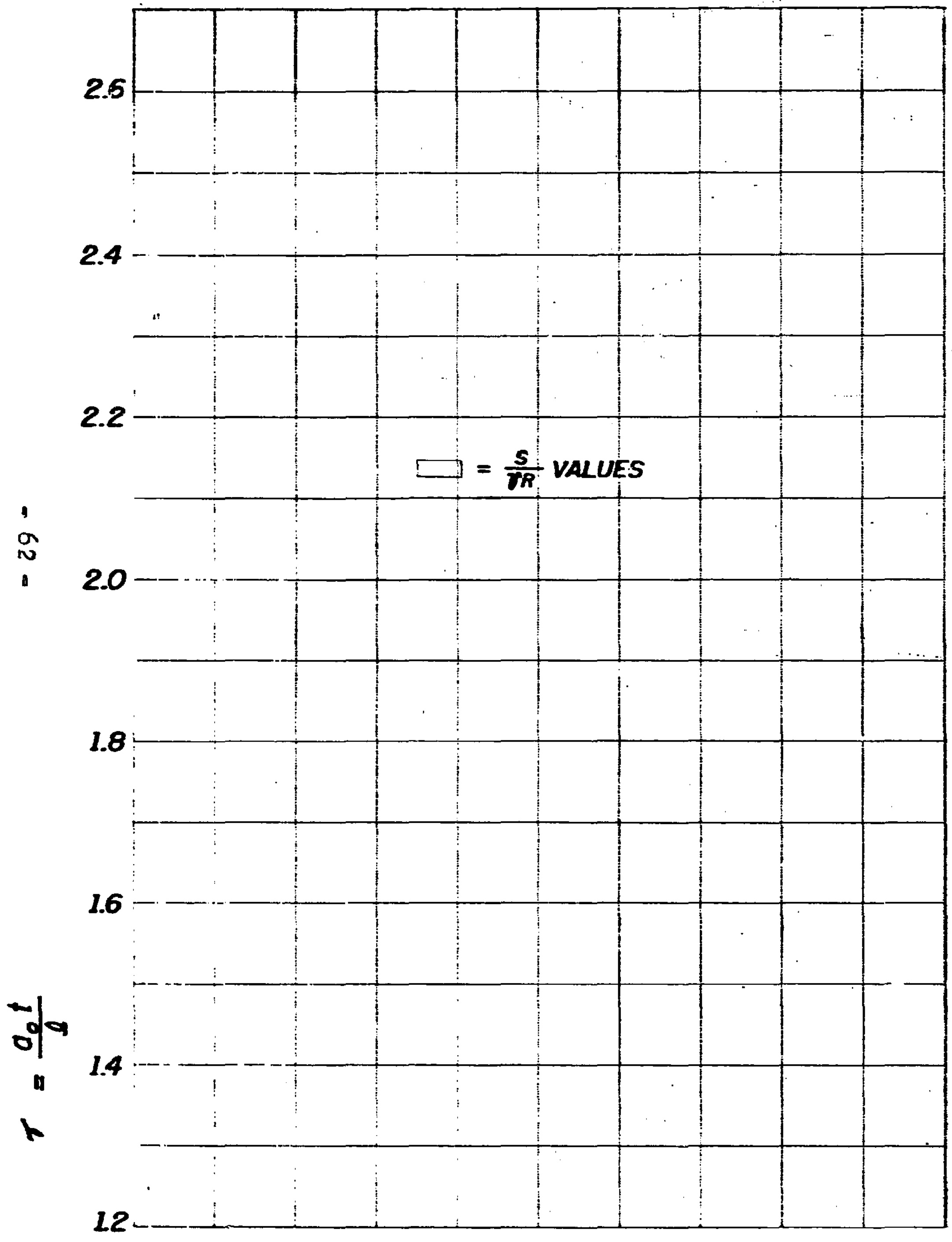

INLET AND EXIT CONDITIONS

POINT	P	u	a
EXIT			
1	3.906	2.158	2.158
2	1.026	1.782	1.782
3	1.000	1.240	1.776
4	1.000	0.560	1.776
5	1.000	0.560	1.776
6	1.659	1.921	1.921
7	1.052	1.801	1.801
8	6.433	0	1.604
9	4.824	0	1.539
10	3.560	0	1.474
INLET			
11	1.230	0.340	1.030
12	1.133	0.490	1.018
13	1.125	0.495	1.017
14	17.482	0	1.643
15	8.344	0	1.477
16	7.042	0	1.442
17	3.292	0	1.294
18	1.328	0	1.136
19	1.298	0.162	1.038
20	1.264	0.280	1.034

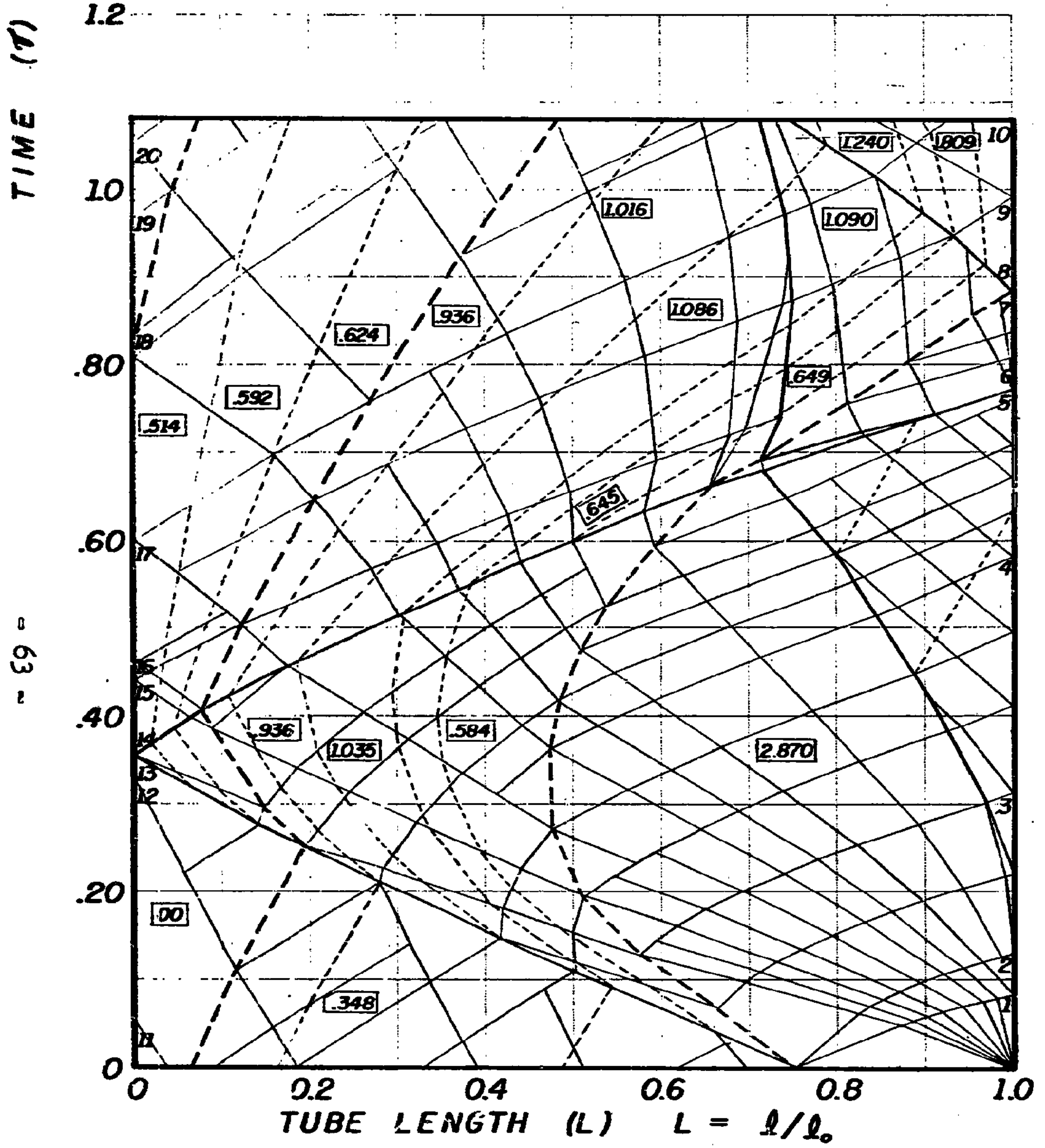

AVERAGE CONDITIONS BEFORE AND AFTER HEAT ADDITION

	BEFORE	AFTER
P =	3.608	14.430
θ =	1.690	6.759
S =	0.395	2.879

CHARACTERISTIC CYCLE PERFORMANCE

$SFC\left(\frac{\text{LBS. FUEL/HR}}{\text{LBS. THRUST}}\right) = 2.519, \; T/A\left(\frac{\text{LBS.}}{\text{SQ. IN.}}\right) = 12.18$

$\eta_c = 0.640 \qquad \eta_o = 0.069$

COMBUSTION CHAMBER MASS $(m/m_o) = 0.534$

FUEL-AIR RATIO – $1/34.4$

CYCLE 2

MACH NUMBER = 0.65

WAVE ENGINE CYCLE

HEAT ADDITION MODE: CONSTANT VOLUME COMBUSTION

Fig. I B

CONFIDENTIAL

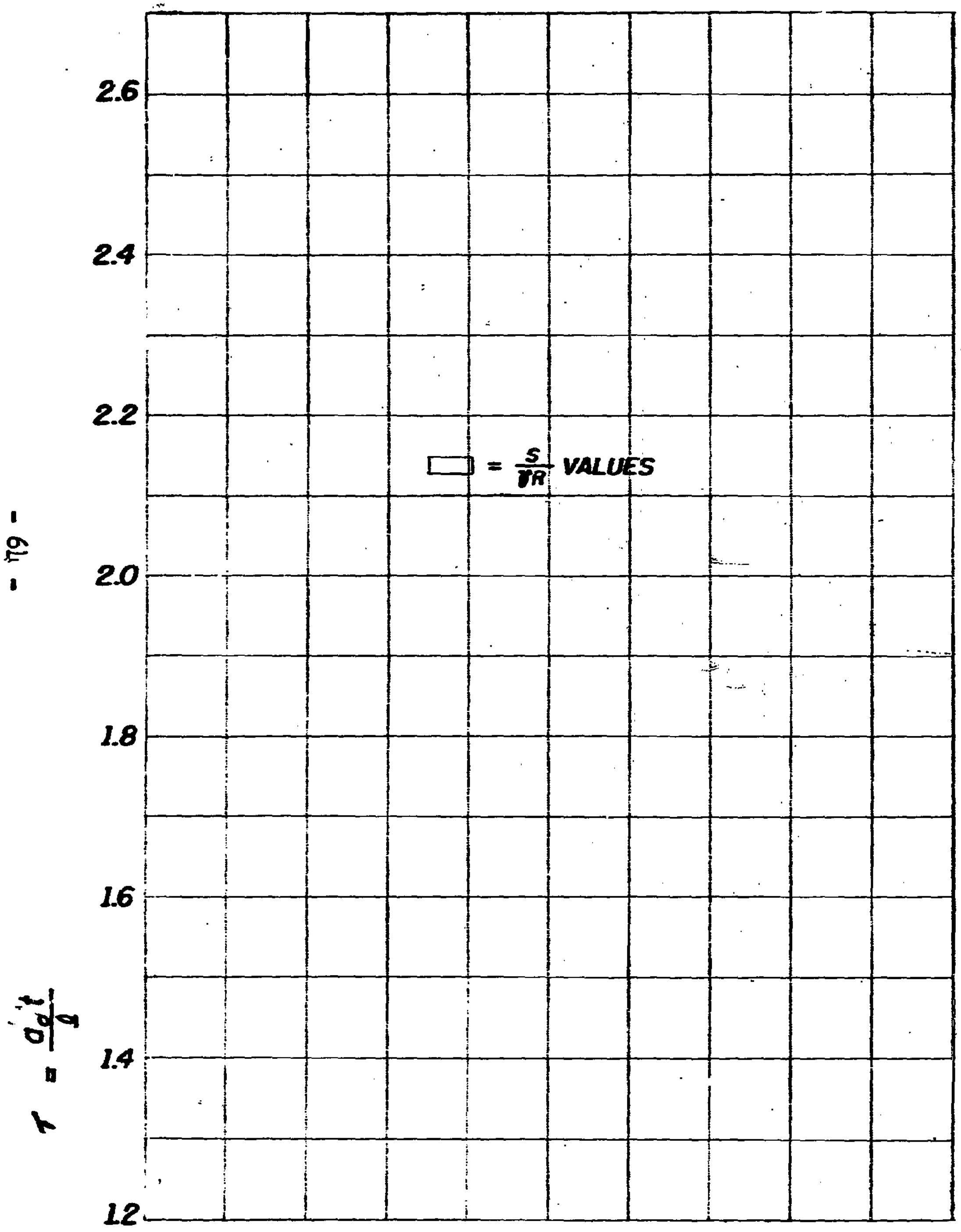

INLET AND EXIT CONDITIONS

POINT	P	u	a
EXIT			
1	3.109	2.392	2.392
2	1.000	1.912	2.034
3	1.000	1.490	2.034
4	1.000	0.800	2.034
5	1.000	0.880	2.034
6	1.538	2.172	2.172
7	1.076	2.064	2.064
8	6.061	0	1.909
9	4.230	0	1.814
10	3.464	0	1.762
INLET			
11	1.222	0.350	1.029
12	1.181	0.420	1.024
13	1.121	0.502	1.016
14	16.215	0	1.615
15	9.227	0	1.490
16	3.503	0	1.298
17	2.195	0	1.214
18	1.328	0	1.130
19	1.277	0.238	1.036
20	1.230	0.345	1.030

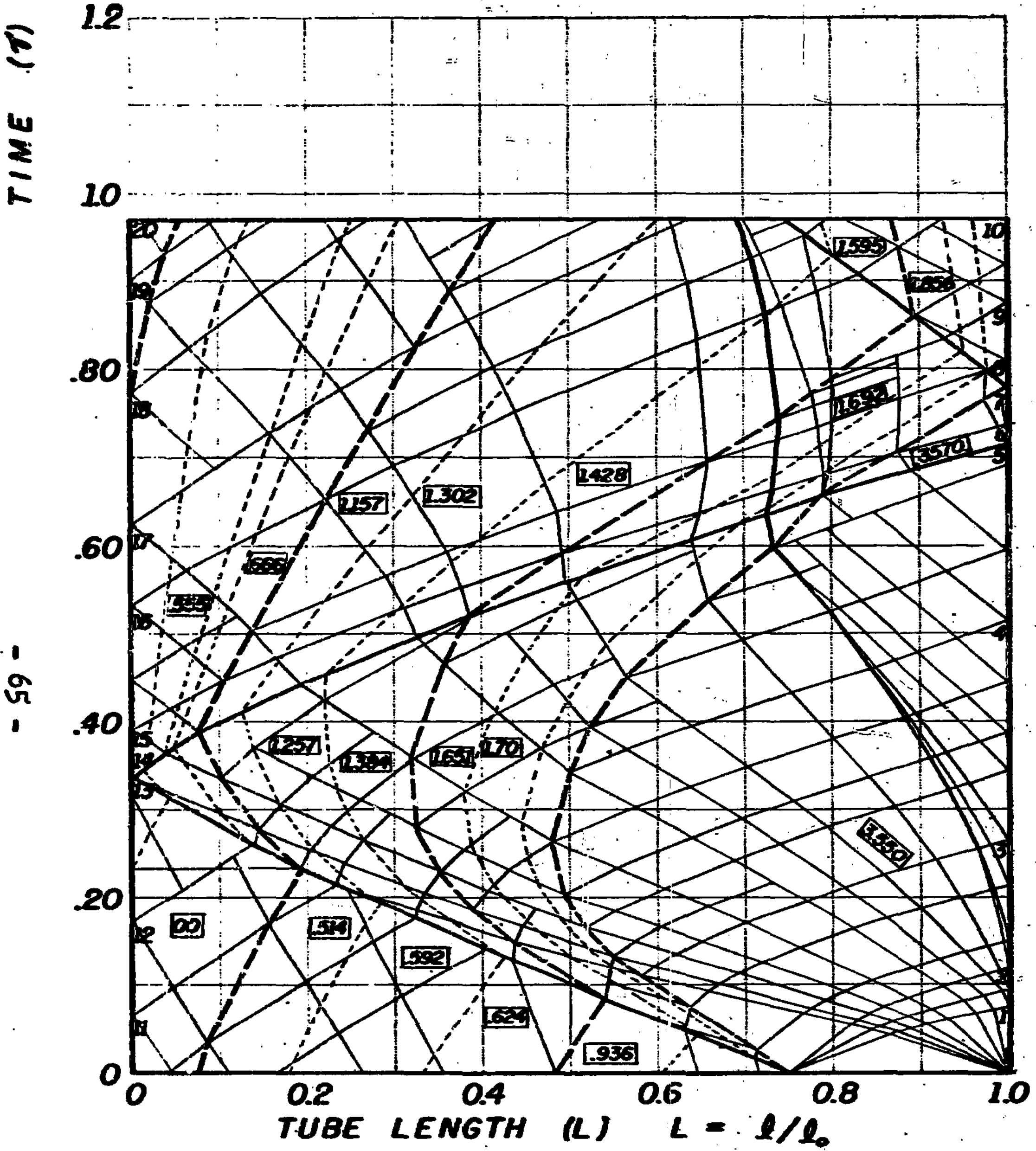

AVERAGE CONDITIONS BEFORE AND AFTER HEAT ADDITION

	BEFORE	AFTER
P =	3.161	12.643
θ =	2.136	8.543
S =	1.075	3.550

CHARACTERISTIC CYCLE PERFORMANCE

$SFC\left(\frac{\text{LBS. FUEL/HR}}{\text{LBS. THRUST}}\right) = 2.665$, $T/A\left(\frac{\text{LBS.}}{\text{SQ. IN.}}\right) = 11.24$

$\eta_c = 0.34$, $\eta_o = .065$

COMBUSTION CHAMBER MASS $(m/m_o) = 0.370$

FUEL-AIR RATIO - $1/27.2$

CYCLE 3

MACH NUMBER = 0.65

WAVE ENGINE CYCLE

HEAT ADDITION MODE: CONSTANT VOLUME COMBUSTION

Fig. 1 C

CONFIDENTIAL

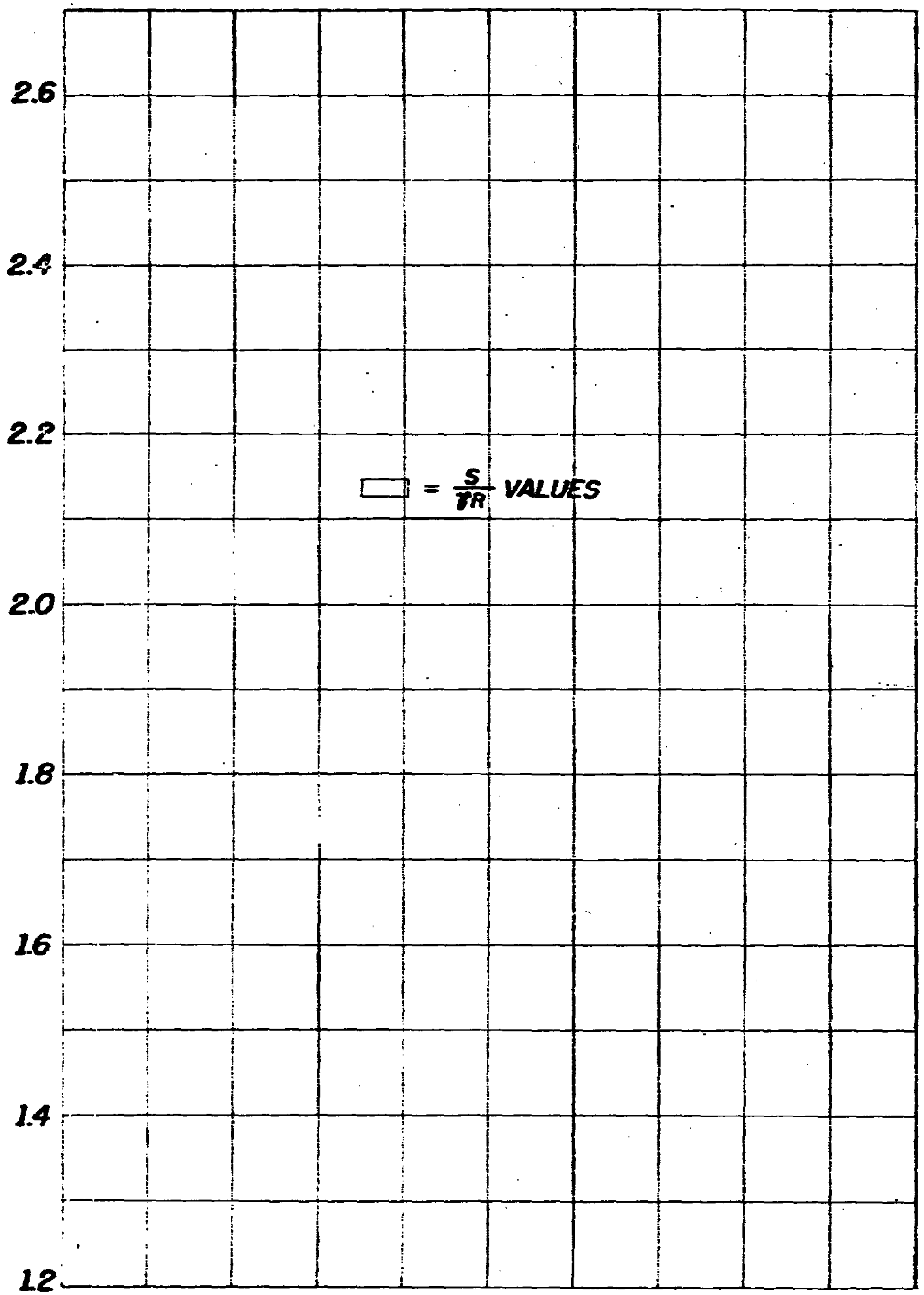

$\tau = \frac{a_0 t}{D}$

INLET AND EXIT CONDITIONS

POINT	P	u	a
EXIT			
1	3.517	2.204	2.204
2	1.016	1.846	1.846
3	1.000	1.360	1.842
4	1.000	1.040	1.842
5	1.000	0.840	1.842
6	1.000	0.630	1.842
7	1.000	0.713	1.842
8	1.000	0.697	1.842
9	8.520	0	1.567
10	4.668	0	1.436
INLET			
11	1.000	0.650	1.000
12	13.707	0	1.581
13	8.230	0	1.470
14	4.539	0	1.350
15	2.575	0	1.245
16	1.542	0	1.157
17	1.328	0	1.133
18	1.272	0.180	1.035
19			
20			

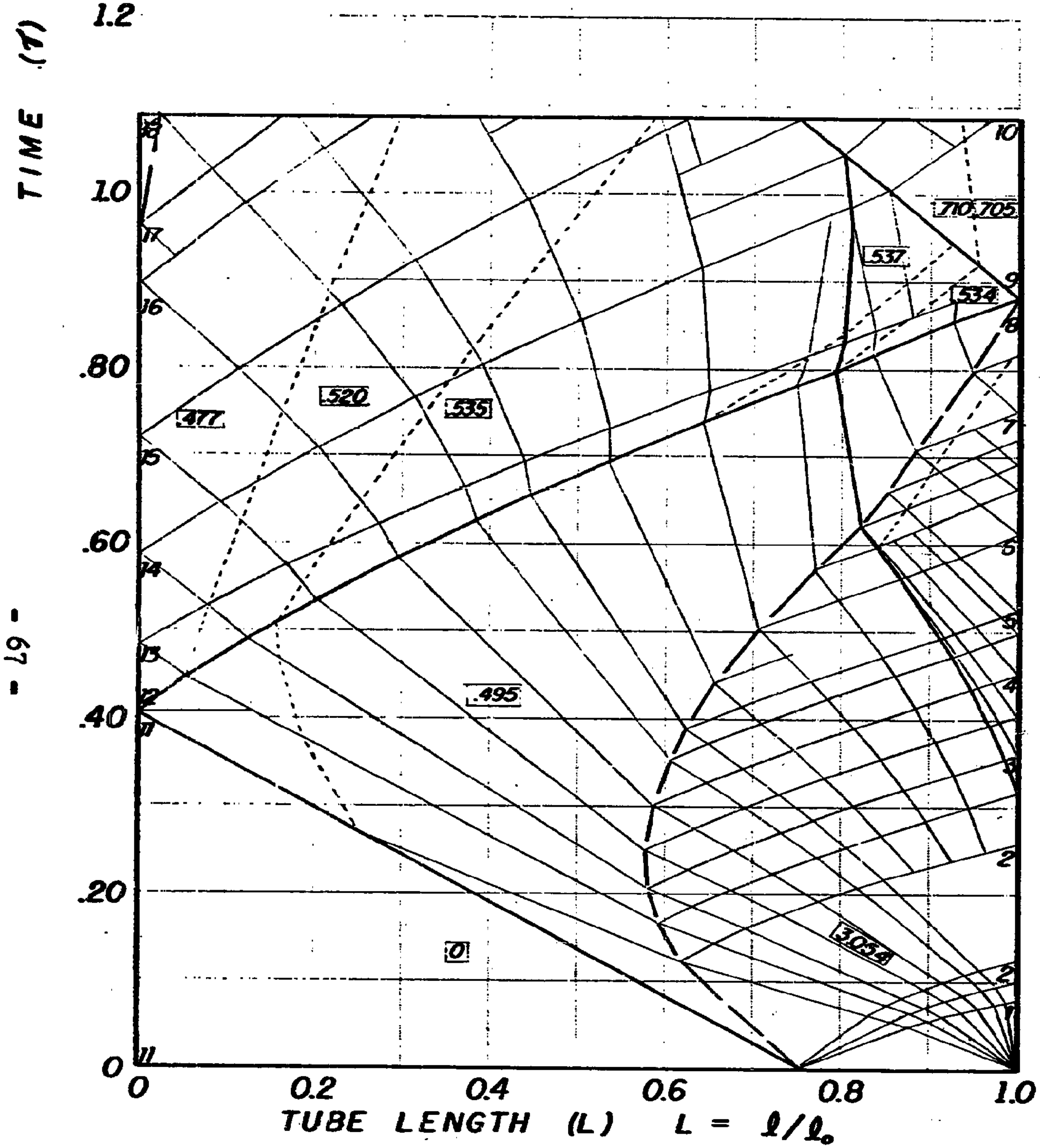

AVERAGE CONDITIONS BEFORE AND AFTER HEAT ADDITION

	BEFORE	AFTER
P =	2.334	12.600
θ =	1.296	6.998
S =	0.044	3.054

CHARACTERISTIC CYCLE PERFORMANCE

$SFC\left(\frac{\text{LBS. FUEL/HR}}{\text{LBS. THRUST}}\right) = 2.530$, $T/A\left(\frac{\text{LBS.}}{\text{SQ. IN.}}\right) = 11.30$

$\eta_c = 0.91$ $\eta_o = .069$

COMBUSTION CHAMBER MASS $(m/m_o) = 0.450$

FUEL-AIR RATIO - 1/31

CYCLE 1

MACH NUMBER = 0.65

WAVE ENGINE CYCLE

HEAT ADDITION MODE: CONSTANT VOLUME COMBUSTION

Fig. 2 A

CONFIDENTIAL

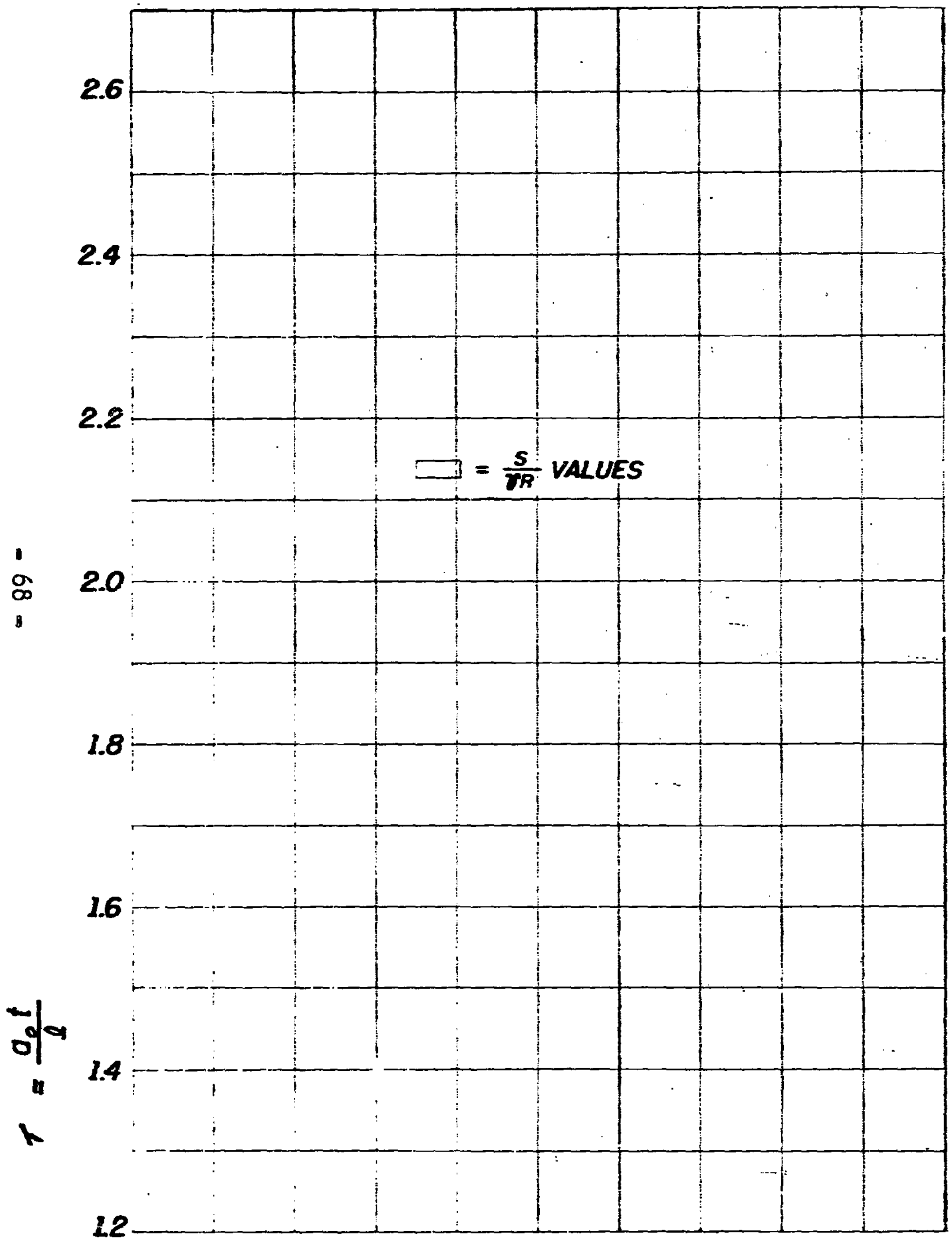

INLET AND EXIT CONDITIONS

EXIT			
POINT	P	u	a
1	4.321	2.285	2.285
2	1.159	1.893	1.893
3	1.000	1.120	1.854
4	1.000	0.830	1.854
5	2.326	2.033	2.109
6	1.800	2.037	2.037
7	1.333	1.951	1.951
8	6.979	0	1.870
9	4.536	0	1.758
10	3.861	0	1.718
INLET			
11	1.255	0.291	1.033
12	1.205	0.387	1.027
13	1.181	0.420	1.024
14	23.495	0	1.748
15	15.416	0	1.646
16	6.826	0	1.465
17	3.752	0	1.345
18	1.791	0	1.210
19	1.328	0	1.159
20	1.281	0.222	1.036

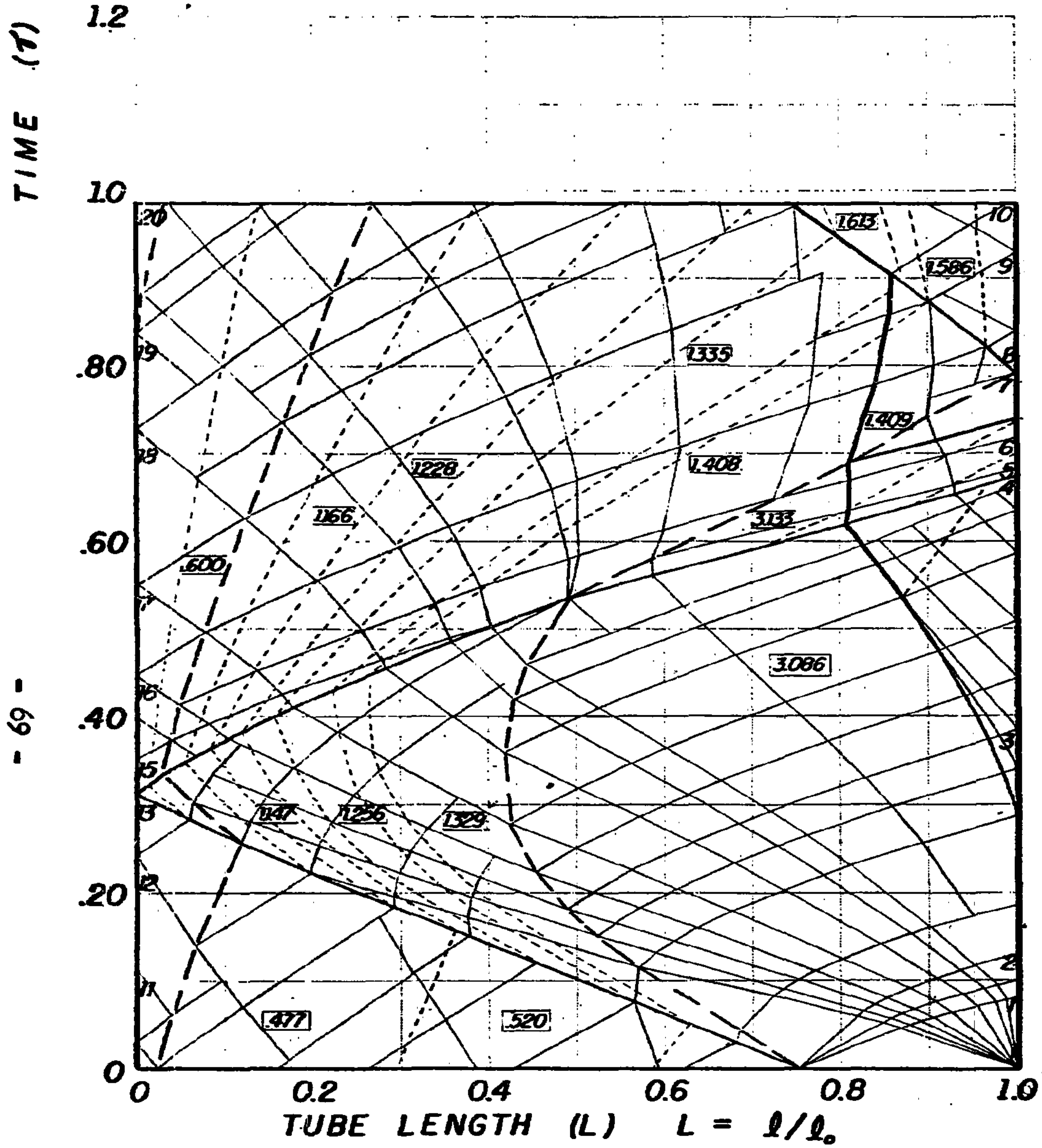

AVERAGE CONDITIONS BEFORE AND AFTER HEAT ADDITION

	BEFORE	AFTER
P =	4.644	17.416
θ =	2.073	7.775
S =	0.726	3.086

CHARACTERISTIC CYCLE PERFORMANCE

SFC $\left(\frac{\text{LBS. FUEL/HR}}{\text{LBS. THRUST}}\right) = 2.083$, $T/A\left(\frac{\text{LBS.}}{\text{SQ. IN.}}\right) = 18.80$

$\eta_c = 0.51$ $\eta_o \doteq 0.084$

COMBUSTION CHAMBER MASS $(m/m_o) = 0.560$

FUEL-AIR RATIO – 1/31

CYCLE 2

MACH NUMBER = 0.65

WAVE ENGINE CYCLE

HEAT ADDITION MODE: CONSTANT VOLUME COMBUSTION

Fig. 2B

CONFIDENTIAL

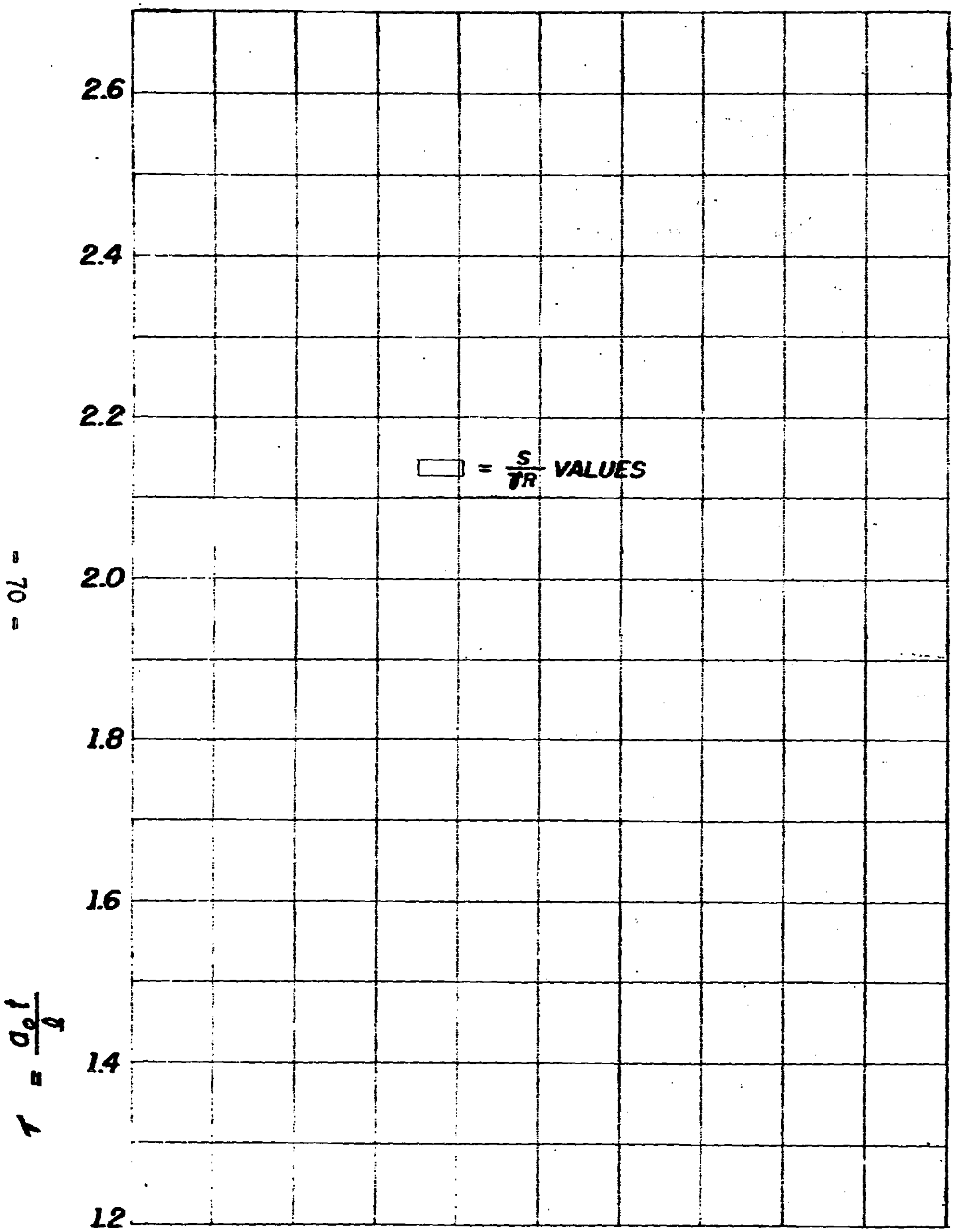

INLET AND EXIT CONDITIONS

POINT	P	u	a
EXIT			
1	2.910	2.393	2.393
2	1.000	1.947	2.055
3	1.000	1.187	2.055
4	1.000	0.805	2.055
5	1.000	0.915	2.055
6	1.564	2.198	2.198
7	1.225	2.124	2.124
8	6.258	0	2.061
9	5.013	0	1.996
10	3.586	0	1.903
INLET			
11	1.264	0.278	1.034
12	1.197	0.392	1.026
13	1.141	0.480	1.019
14	14.927	0	1.584
15	7.816	0	1.444
16	4.844	0	1.348
17	2.815	0	1.248
18	2.152	0	1.201
19	1.328	0	1.120
20	1.264	0.278	1.034

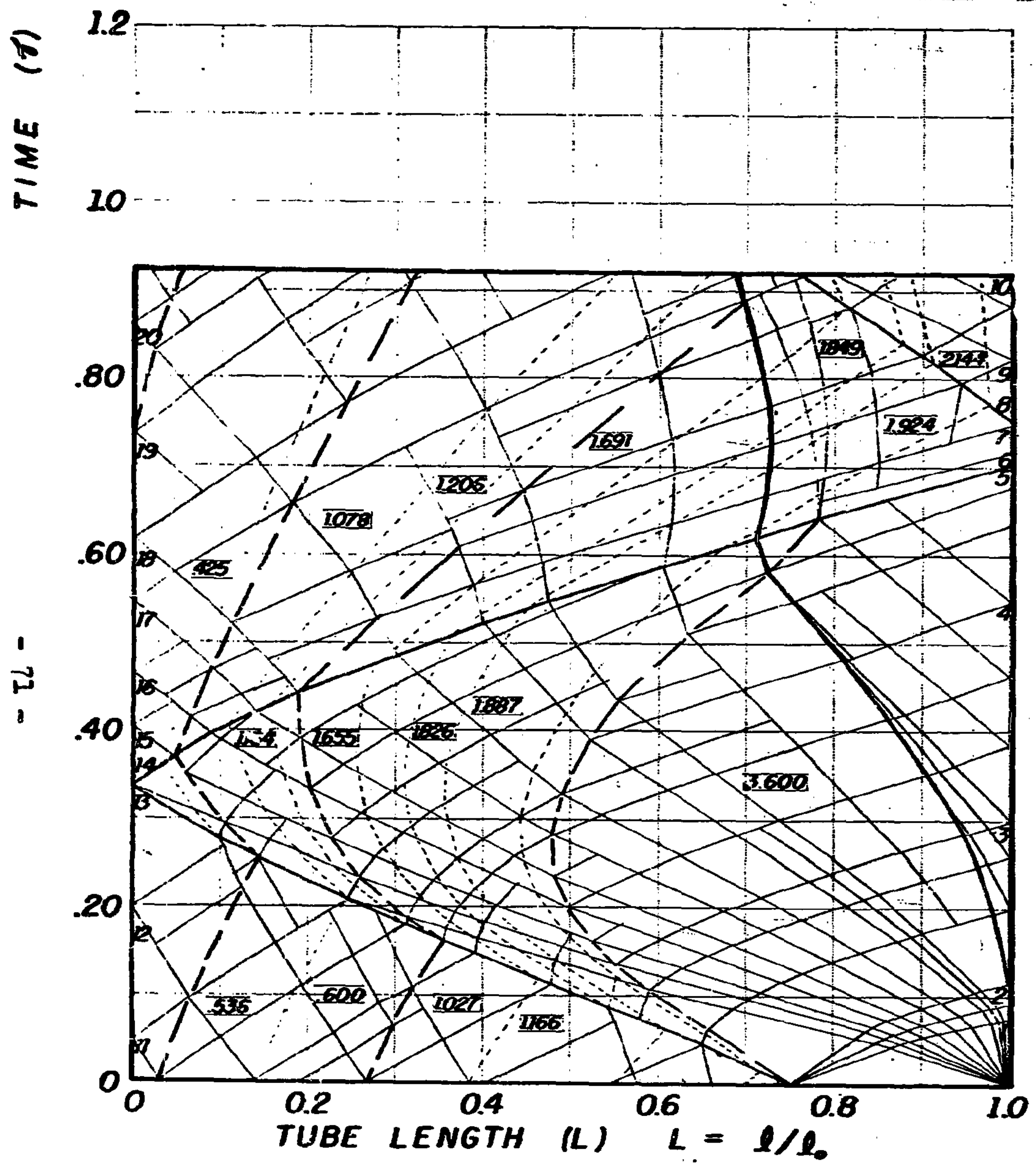

AVERAGE CONDITIONS BEFORE AND AFTER HEAT ADDITION

	BEFORE	AFTER
P =	3.849	11.653
θ =	2.811	8.514
S =	1.622	3.600

CHARACTERISTIC CYCLE PERFORMANCE

$SFC\left(\frac{\text{LBS. FUEL/HR}}{\text{LBS. THRUST}}\right) = 2.387, \; T/A\left(\frac{\text{LBS.}}{\text{SQ. IN.}}\right) = 10.73$

$\eta_c = 0.26 \qquad \eta_o = 0.073$

COMBUSTION CHAMBER MASS $(m/m_o) = 0.342$

FUEL-AIR RATIO - $1/31$

CYCLE 3

MACH NUMBER = 0.65

WAVE ENGINE CYCLE

HEAT ADDITION MODE: CONSTANT VOLUME COMBUSTION

Fig. 2C

CONFIDENTIAL

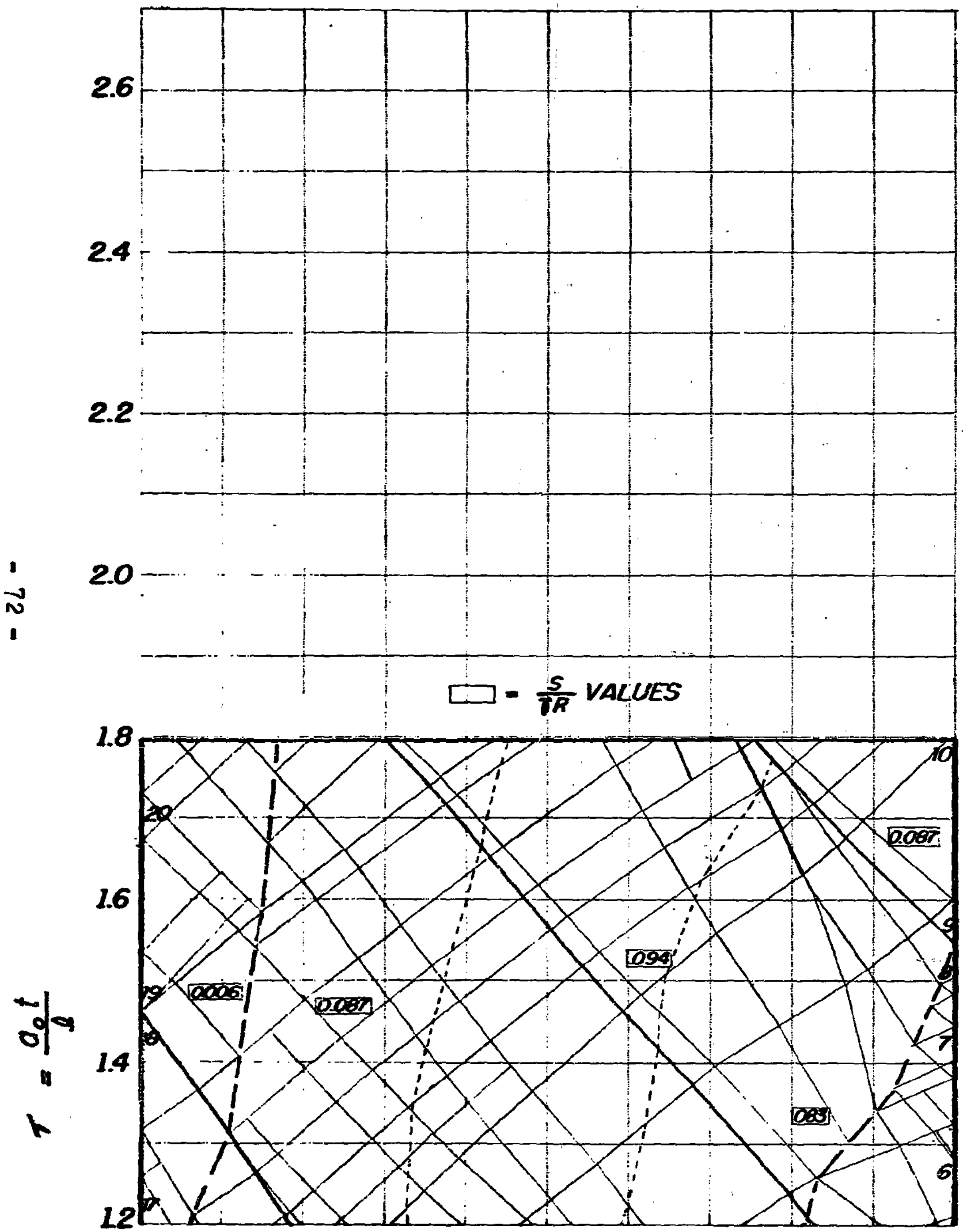

INLET AND EXIT CONDITIONS

POINT	P	u	a
EXIT			
1	1.118	1.667	1.667
2	1.000	0.425	1.641
3	1.000	0	1.641
4	1.000	-0.034	1.000
5	1.050	1.007	1.007
6	1.000	0.955	1.641
7	1.000	0.517	1.641
8	1.000	0.290	1.641
9	1.480	0	1.076
10	0.984	0	1.015
INLET			
11	1.000	0	1.000
12	5.339	0	1.292
13	2.210	0	1.139
14	1.345	0	1.061
15	1.000	0	1.017
16	0.951	0.255	0.993
17	0.918	0.350	0.988
18	0.855	0.464	0.978
19	0.992	-0.040	1.000
20	0.992	0.044	1.000

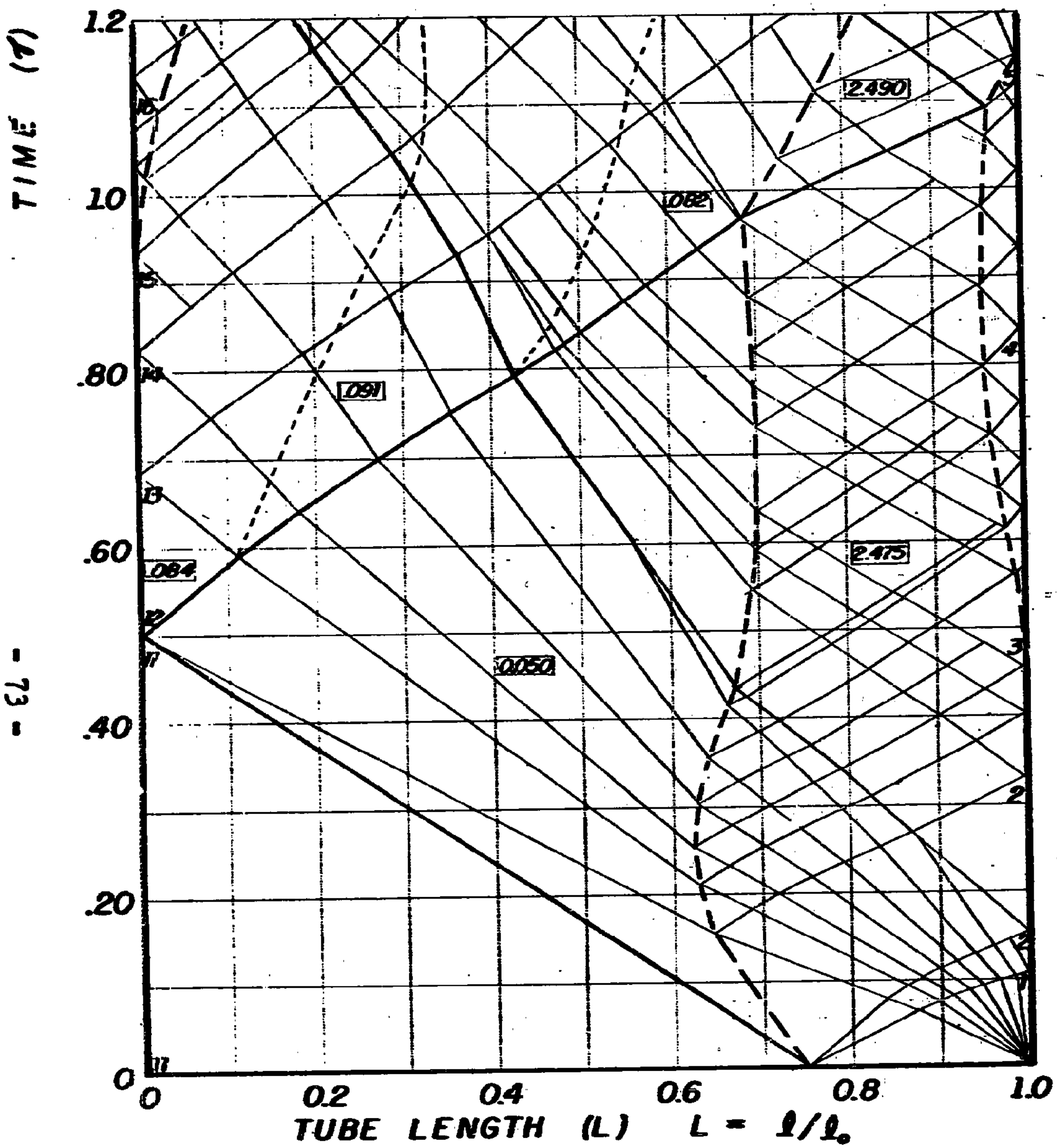

AVERAGE CONDITIONS BEFORE AND AFTER HEAT ADDITION

	BEFORE	AFTER
P =	1.000	4.000
θ =	1.000	4.000
S =	0.0	2.475

CHARACTERISTIC CYCLE PERFORMANCE

SFC $\left(\frac{\text{LBS. FUEL/HR.}}{\text{LBS. THRUST}}\right) = 1.557$, $T/A\left(\frac{\text{LBS.}}{\text{SQ. IN.}}\right) = 3.26$

$\eta_c = 1.00$ $\eta_o =$ —

COMBUSTION CHAMBER MASS $(m/m_o) = 0.250$

FUEL-AIR RATIO – $1/58.4$

CYCLE 1

MACH NUMBER = 0

WAVE ENGINE CYCLE

HEAT ADDITION MODE: CONSTANT VOLUME COMBUSTION

Fig. 3A

CONFIDENTIAL

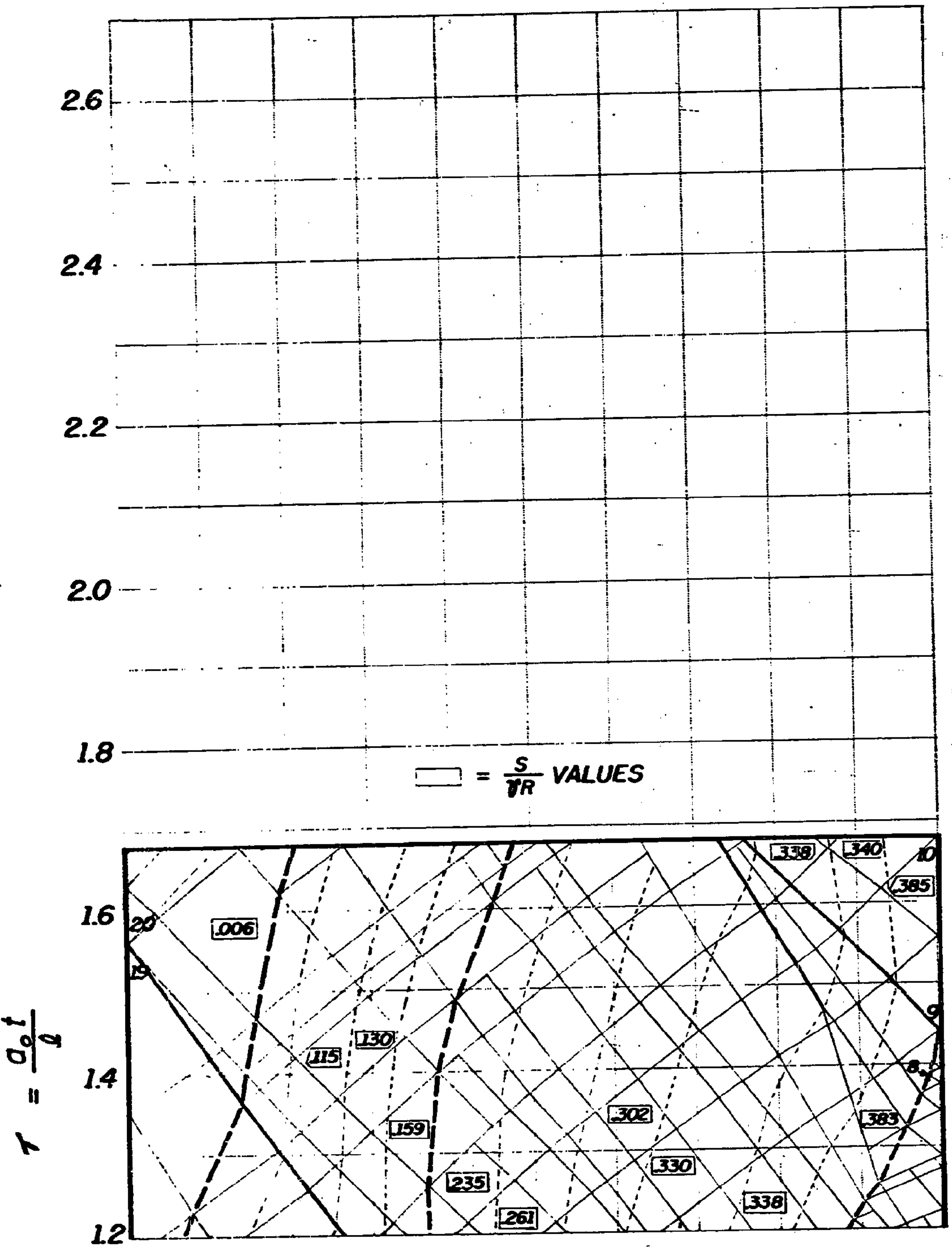

INLET AND EXIT CONDITIONS

POINT	P	u	a
EXIT			
1	1.404	1.753	1.753
2	1.000	0.730	1.670
3	1.000	0	1.670
4	0.972	-0.210	0.996
5	1.000	0.285	1.000
6	1.000	0.200	1.670
7	1.000	1.247	1.673
8	1.000	0.233	1.673
9	1.338	0	1.134
10	1.220	0	1.115
INLET			
11	0.964	0.212	0.996
12	0.992	-0.030	1.000
13	0.978	0.155	0.998
14	5.221	0	1.291
15	3.080	0	1.198
16	1.703	0	1.100
17	1.000	0	1.020
18	0.951	0.265	0.993
19	0.841	0.490	0.976
20	0.992	-0.043	1.000

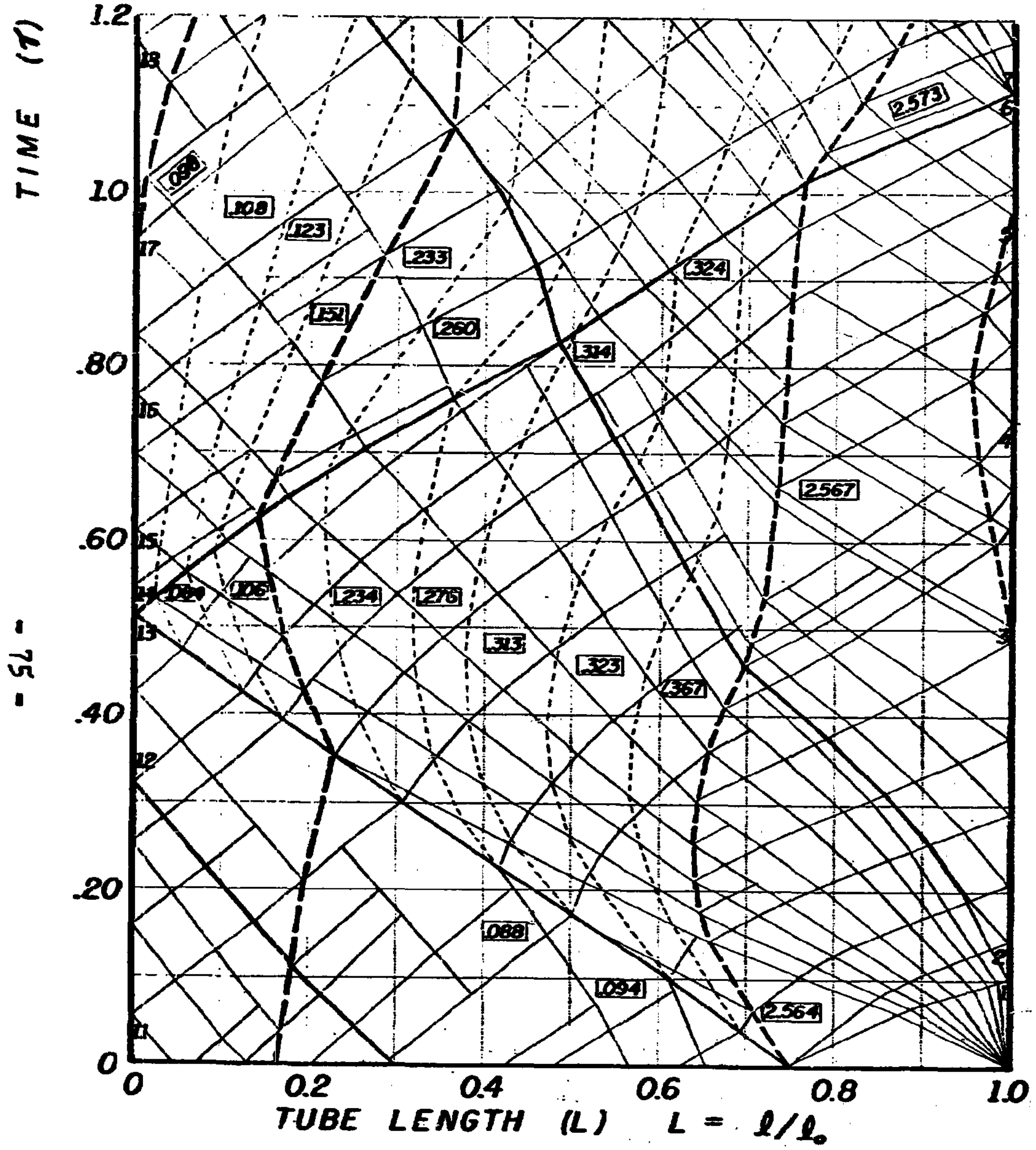

AVERAGE CONDITIONS BEFORE AND AFTER HEAT ADDITION

	BEFORE	AFTER
P =	1.256	5.036
θ =	1.107	4.427
S =	0.087	2.564

CHARACTERISTIC CYCLE PERFORMANCE

SFC $\left(\frac{\text{LBS. FUEL/HR.}}{\text{LBS. THRUST}}\right) = 1.662$, $T/A \left(\frac{\text{LBS.}}{\text{SQ. IN.}}\right) = 4.11$

$\eta_c = 0.66$ $\eta_o =$ ——

COMBUSTION CHAMBER MASS $(m/m_o) = 0.284$

FUEL-AIR RATIO - $1/52.8$

CYCLE 2

MACH NUMBER = 0

WAVE ENGINE CYCLE

HEAT ADDITION MODE: CONSTANT VOLUME COMBUSTION

Fig. 3B

CONFIDENTIAL

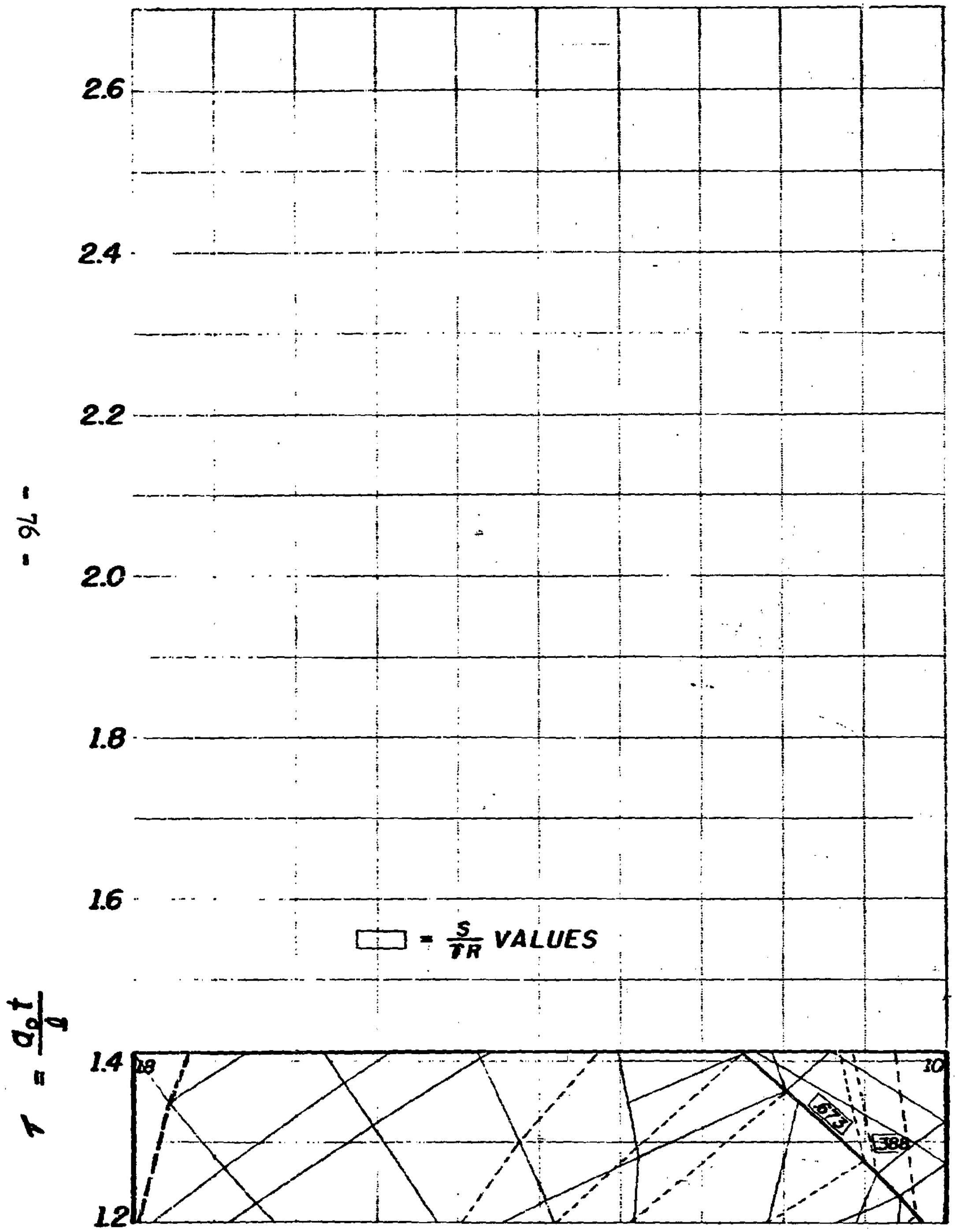

INLET AND EXIT CONDITIONS

POINT	P	u	a
	EXIT		
1	2.334	0	1.138
2	7.293	0	2.526
3	2.034	2.105	2.105
4	1.000	1.814	1.902
5	1.000	1.497	1.902
6	1.000	0.574	1.961
7	1.305	2.045	2.045
8	1.000	1.787	1.971
9	7.109	0	1.494
10	4.005	0	1.377
	INLET		
11	1.000	0.650	1.000
12	11.763	0	1.529
13	9.703	0	1.487
14	5.412	0	1.368
15	3.004	0	1.258
16	1.587	0	1.148
17	1.328	0	1.120
18	1.247	0.298	1.032
19			
20			

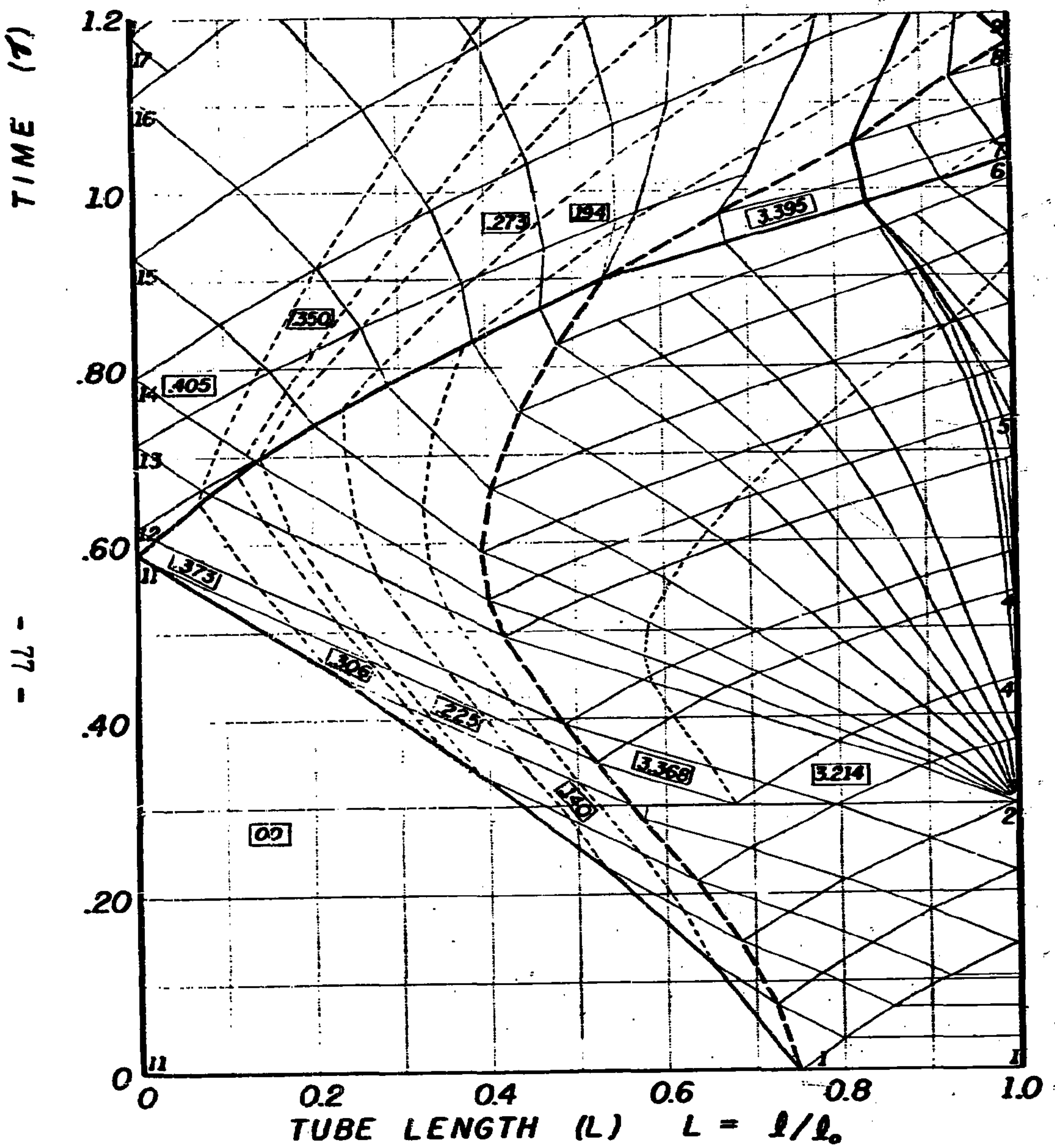

AVERAGE CONDITIONS BEFORE AND AFTER HEAT ADDITION

	BEFORE	AFTER
P =	2.334	7.2930
θ =	1.296	6.408
S =	0.044	3.214

CHARACTERISTIC CYCLE PERFORMANCE

$SFC\left(\frac{\text{LBS. FUEL/HR.}}{\text{LBS. THRUST}}\right) = 2.484$, $T/A\left(\frac{\text{LBS.}}{\text{SQ. IN.}}\right) = 8.85$

$\eta_c = 0.91$ $\eta_o = .070$

COMBUSTION CHAMBER MASS $(m/m_o) = 0.450$

FUEL-AIR RATIO – 1/31

CYCLE I

MACH NUMBER = 0.65

WAVE ENGINE CYCLE

HEAT ADDITION MODE: GRADUAL HEAT ADDITION

Fig. 4A

CONFIDENTIAL

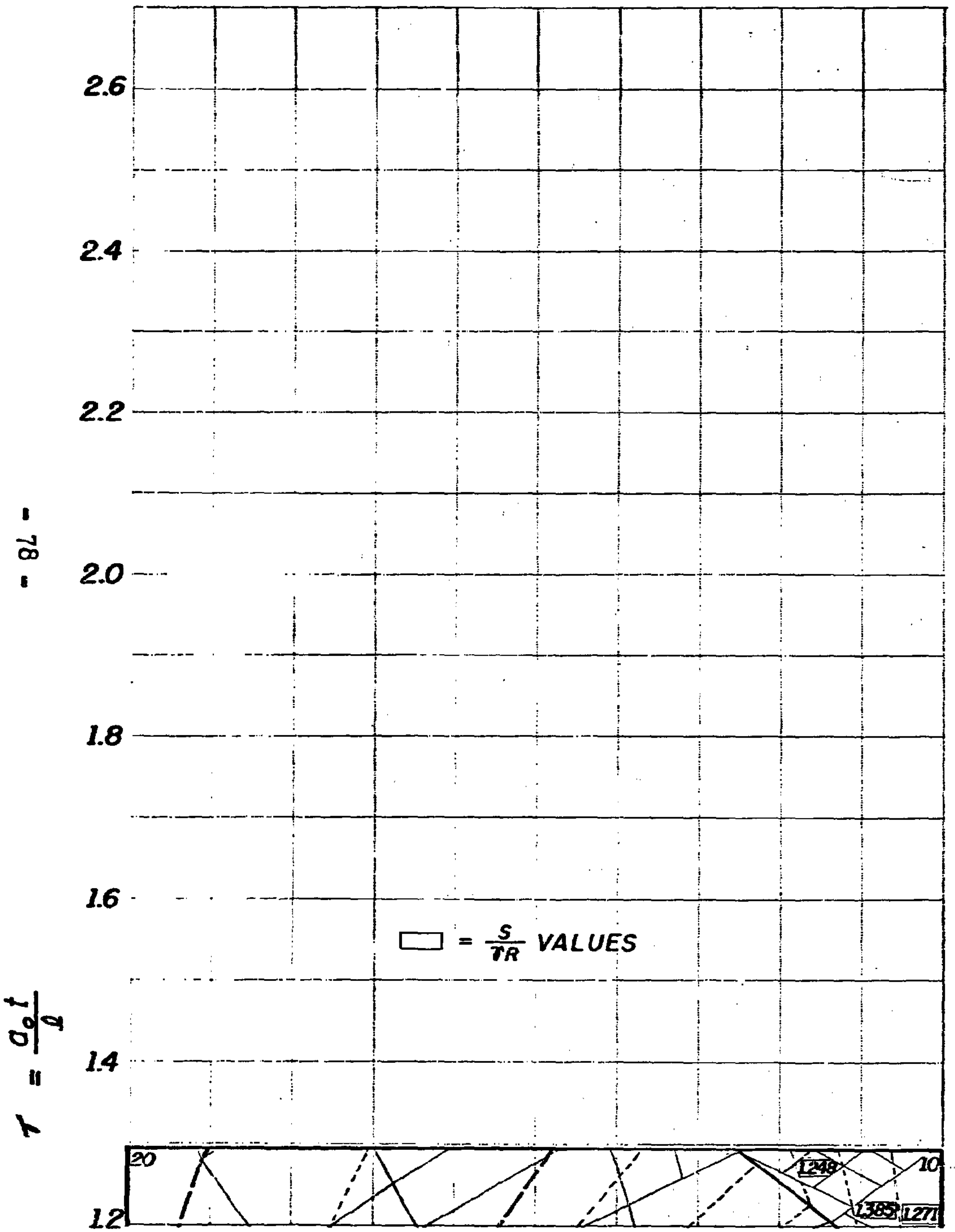

INLET AND EXIT CONDITIONS

POINT	P	u	a
EXIT			
1	3.717	0	1.354
2	6.168	0	2.537
3	1.721	2.114	2.114
4	1.000	1.505	1.956
5	1.000	1.582	1.977
6	1.889	2.612	2.193
7	1.525	2.136	2.136
8	1.000	1.960	2.025
9	6.983	0	1.650
10	3.359	0	1.486
INLET			
11	1.247	0.298	1.032
12	1.149	0.455	1.020
13	1.080	0.555	1.011
14	14.444	0	1.583
15	15.565	0	1.600
16	13.155	0	1.562
17	7.635	0	1.445
18	2.220	0	1.211
19	1.328	0	1.125
20	1.205	0.296	1.027

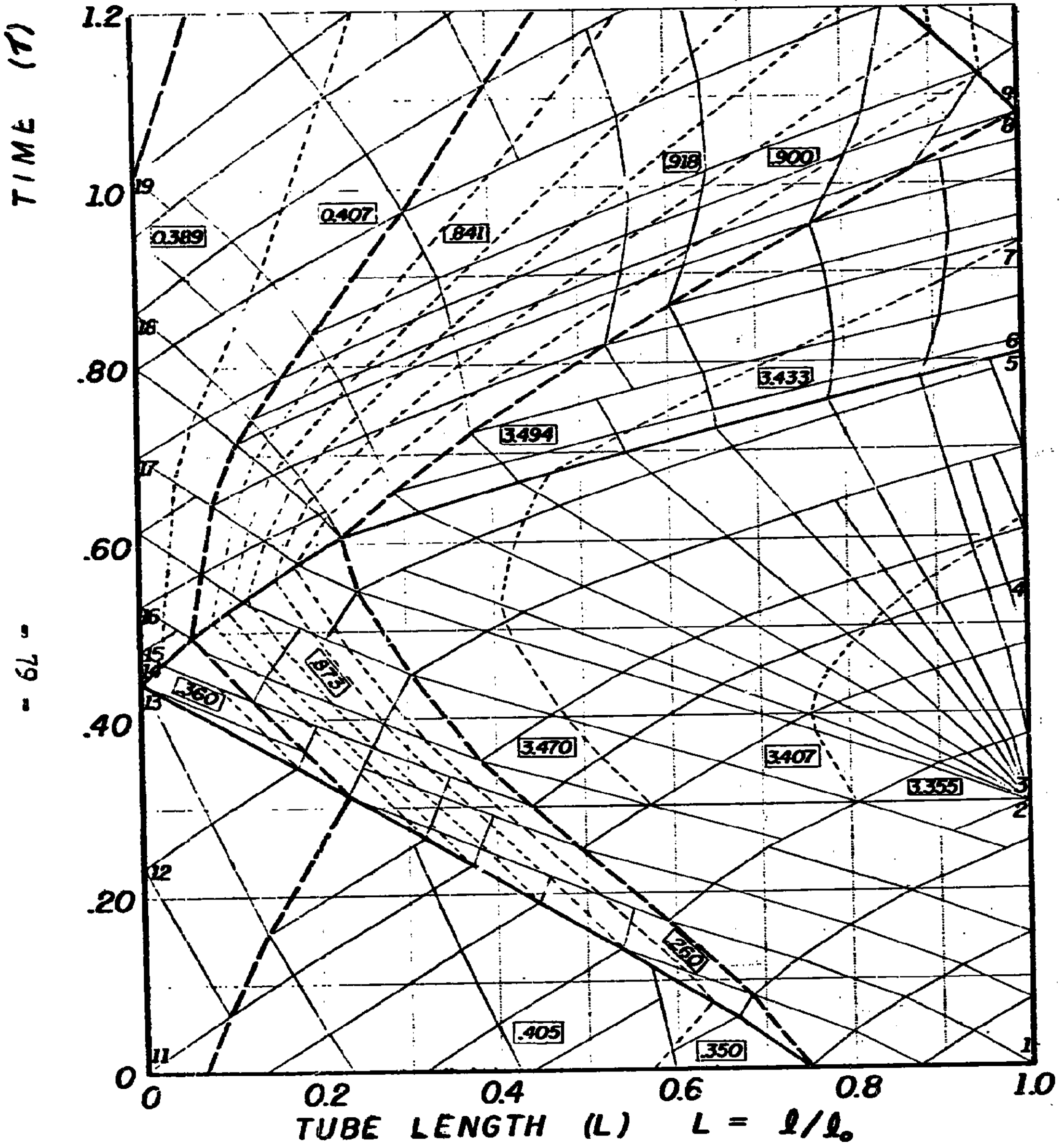

AVERAGE CONDITIONS BEFORE AND AFTER HEAT ADDITION

	BEFORE	AFTER
P =	3.717	6.168
θ =	1.833	6518
S =	0.578	3.355

CHARACTERISTIC CYCLE PERFORMANCE

$SFC\left(\frac{\text{LBS. FUEL/HR.}}{\text{LBS. THRUST}}\right) = 2.431,\ T/A\left(\frac{\text{LBS.}}{\text{SQ. IN.}}\right) = 11.10$

$\eta_c = 0.54 \qquad \eta_o = .072$

COMBUSTION CHAMBER MASS $(m/m_o) = 0.507$

FUEL-AIR RATIO – $1/31$

CYCLE 2

MACH NUMBER = 0.65

WAVE ENGINE CYCLE

HEAT ADDITION MODE: GRADUAL HEAT ADDITION

Fig. 4B

CONFIDENTIAL

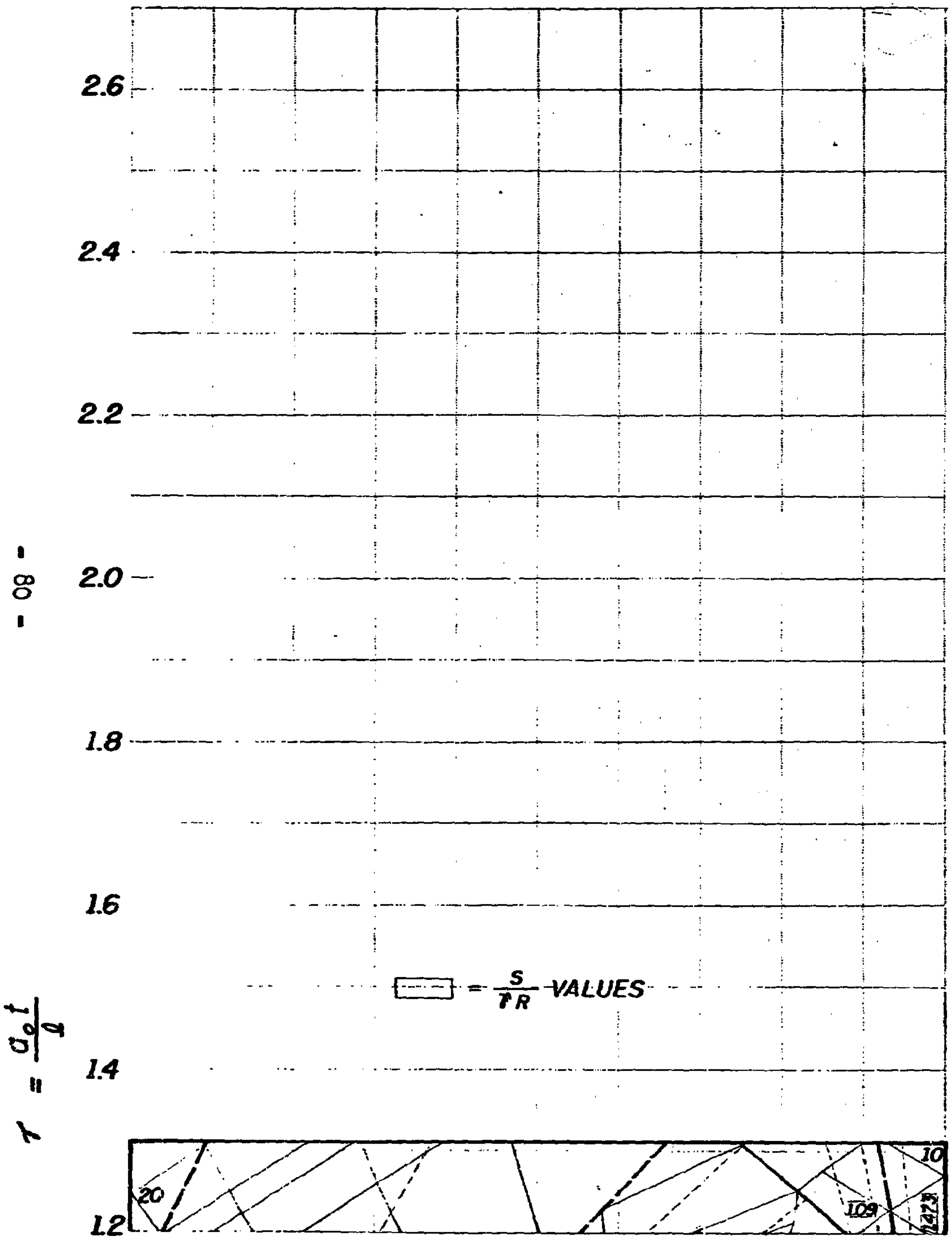

INLET AND EXIT CONDITIONS

POINT	P	u	a
EXIT			
1	3.311	0	1.523
2	4.611	0	2.618
3	1.148	2.146	2.146
4	1.000	1.558	2.109
5	1.000	1.178	2.122
6	1.749	2.062	2.304
7	1.000	2.082	2.142
8	1.000	1.720	2.150
9	4.872	0	1.711
10	3.169	0	1.608
INLET			
11	1.149	0.455	1.020
12	1.072	0.560	1.010
13	1.054	0.588	1.008
14	11.542	0	1.513
15	7.580	0	1.425
16	5.450	0	1.359
17	2.651	0	1.226
18	1.328	0	1.111
19	1.281	0.232	1.036
20	1.238	0.325	1.031

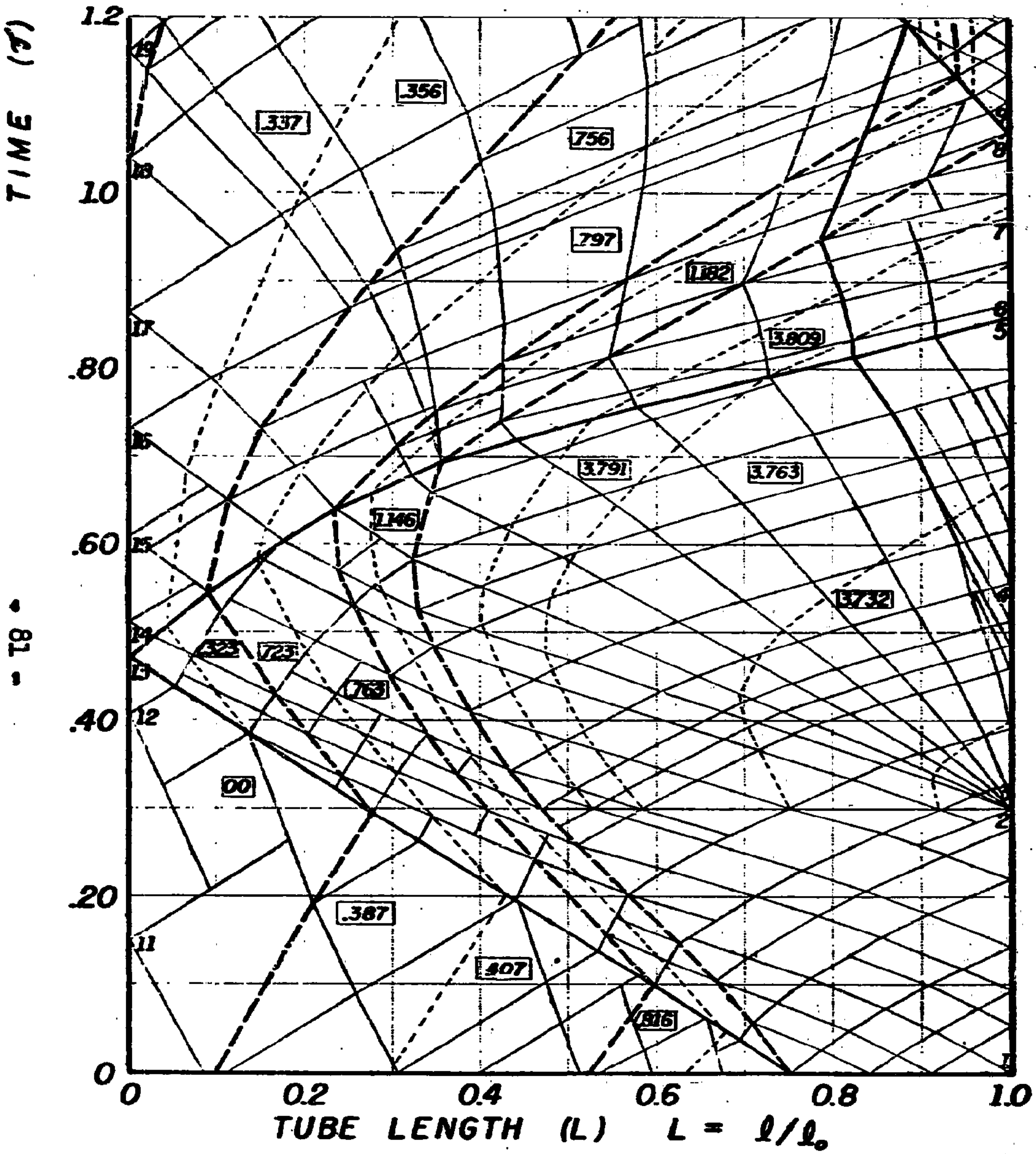

AVERAGE CONDITIONS BEFORE AND AFTER HEAT ADDITION

	BEFORE	AFTER
P =	3.311	4.611
θ =	2.320	6.901
S =	1.248	3.763

CHARACTERISTIC CYCLE PERFORMANCE

SFC $\left(\frac{\text{LBS. FUEL/HR.}}{\text{LBS. THRUST}}\right) = 3.043$, $T/A\left(\frac{\text{LBS.}}{\text{SQ. IN.}}\right) = 6.17$

$\eta_c = 0.29$ $\eta_o = 0.057$

COMBUSTION CHAMBER MASS $(m/m_o) = 0.357$

FUEL-AIR RATIO – $1/31$

CYCLE 3

MACH NUMBER = 0.65

WAVE ENGINE CYCLE

HEAT ADDITION MODE: GRADUAL HEAT ADDITION

Fig. 4C

CONFIDENTIAL

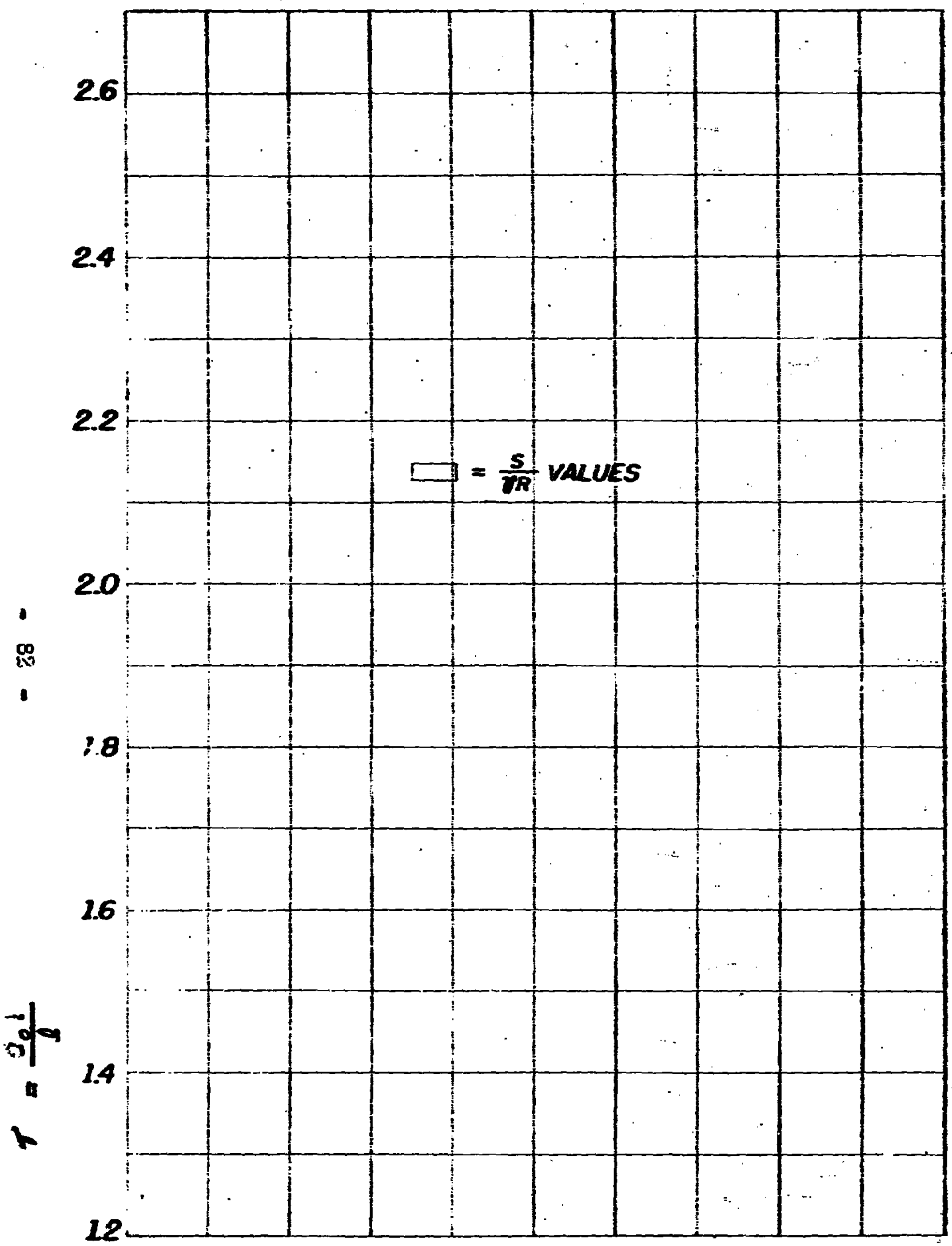

INLET AND EXIT CONDITIONS

POINT	P	u	a
EXIT			
1	3.553	0	1.818
2	3.955	0	2.763
3	1.000	2.244	2.270
4	1.000	1.949	2.276
5	1.000	1.164	2.276
6	1.000	1.110	2.280
7	7.067	0	1.868
8	4.838	0	1.772
9	4.430	0	1.750
10	4.699	0	1.765
INLET			
11	1.445	0.590	1.054
12	1.370	0.652	1.046
13	1.325	0.695	1.041
14	9.124	0	1.429
15	6.485	0	1.361
16	5.519	0	1.330
17	4.466	0	1.290
18	3.244	0	1.233
19	1.787	0	1.132
20	1.692	0.295	1.078

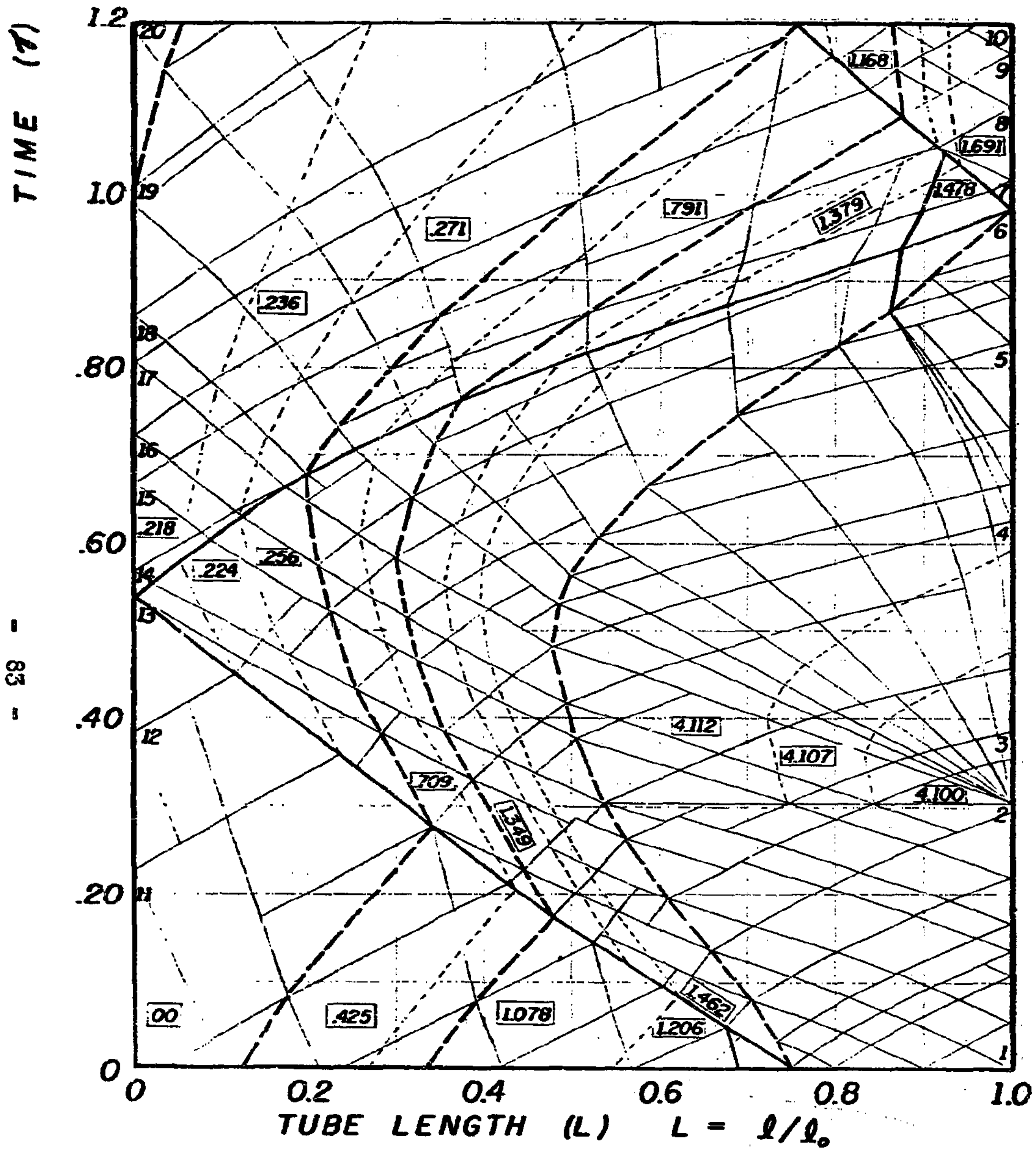

AVERAGE CONDITIONS BEFORE AND AFTER HEAT ADDITION

	BEFORE	AFTER
P =	3.553	3.955
θ =	3.305	7.634
S =	2.082	4.100

CHARACTERISTIC CYCLE PERFORMANCE

$SFC\left(\frac{\text{LBS. FUEL/HR.}}{\text{LBS. THRUST}}\right) = 4.311$, $T/A\left(\frac{\text{LBS.}}{\text{SQ. IN.}}\right) = 3.61$

$\eta_c = 0.19$ $\eta_o = 0.059$

COMBUSTION CHAMBER MASS $(m/m_o) = 0.269$

FUEL-AIR RATIO - $1/31$

CYCLE I

MACH NUMBER = 0.95

WAVE ENGINE CYCLE

HEAT ADDITION MODE: GRADUAL HEAT ADDITION

Fig. 5A

CONFIDENTIAL

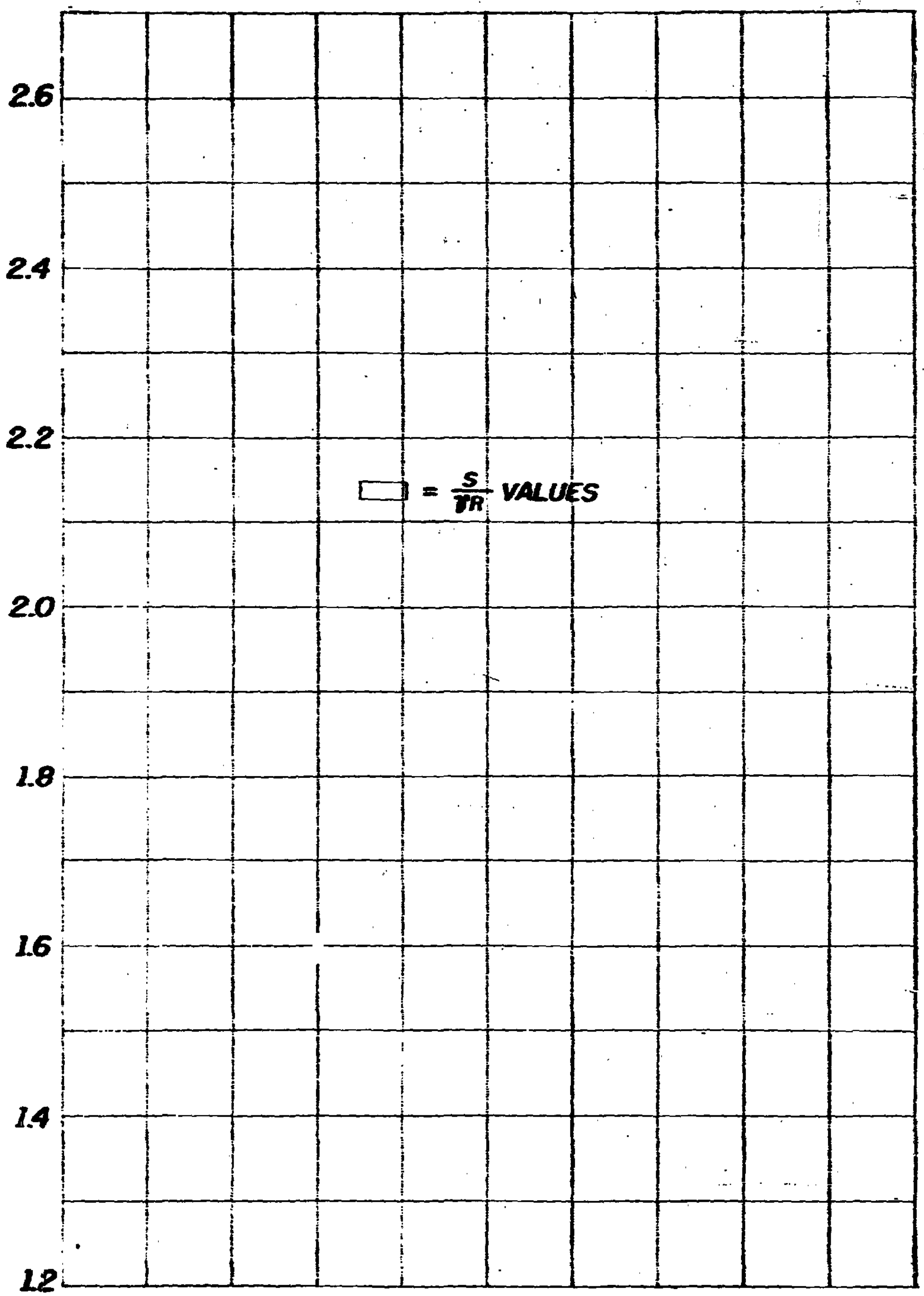

INLET AND EXIT CONDITIONS

POINT	P	u	a
EXIT			
1	4.627	0	1.672
2	6.704	0	2.719
3	1.871	2.266	2.266
4	1.068	2.091	2.091
5	1.011	2.088	2.088
6	1.000	1.792	2.085
7	1.000	1.340	2.085
8	1.800	2.263	2.273
9	1.114	2.148	2.148
10	8.651	0	1.736
INLET			
11	1.692	0.295	1.078
12	1.574	0.460	1.067
13	1.464	0.565	1.056
14	1.398	0.632	1.049
15	16.167	0	1.593
16	10.809	0	1.505
17	8.306	0	1.450
18	3.097	0	1.259
19	1.787	0	1.164
20			

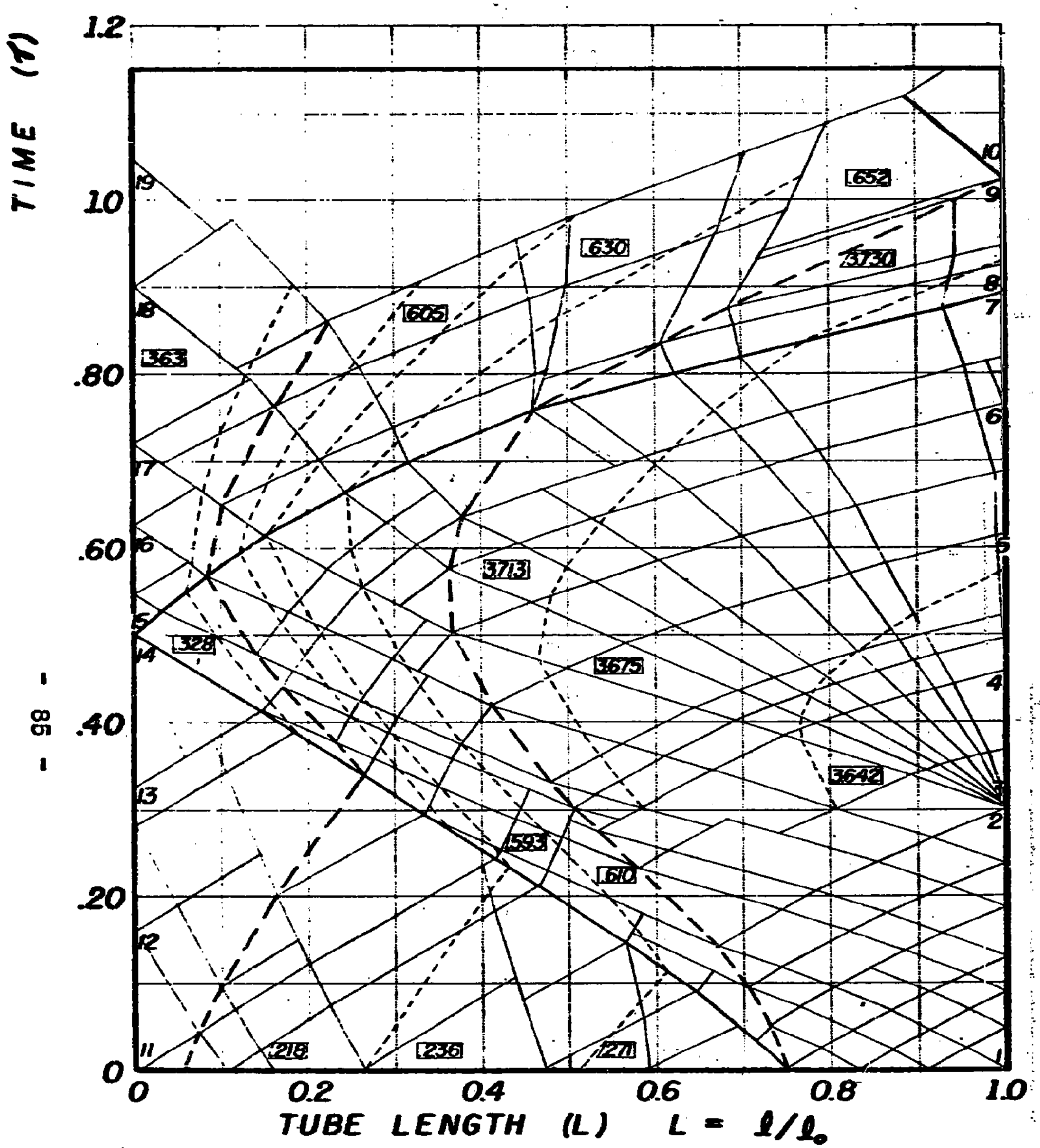

AVERAGE CONDITIONS BEFORE AND AFTER HEAT ADDITION

	BEFORE	AFTER
P =	4.627	6.704
θ =	2.796	7.392
S =	1.476	3.642

CHARACTERISTIC CYCLE PERFORMANCE

$SFC\left(\frac{LBS.\ FUEL/HR.}{LBS.\ THRUST}\right) = 2.786,\ T/A\left(\frac{LBS.}{SQ.\ IN.}\right) = 8.29$

$\eta_c = 0.31, \quad \eta_o = 0.091$

COMBUSTION CHAMBER MASS $(m/m_o) = 0.414$

FUEL-AIR RATIO – 1/31

CYCLE 2

MACH NUMBER = 0.95

WAVE ENGINE CYCLE

HEAT ADDITION MODE: GRADUAL HEAT ADDITION

Fig. 5B

CONFIDENTIAL

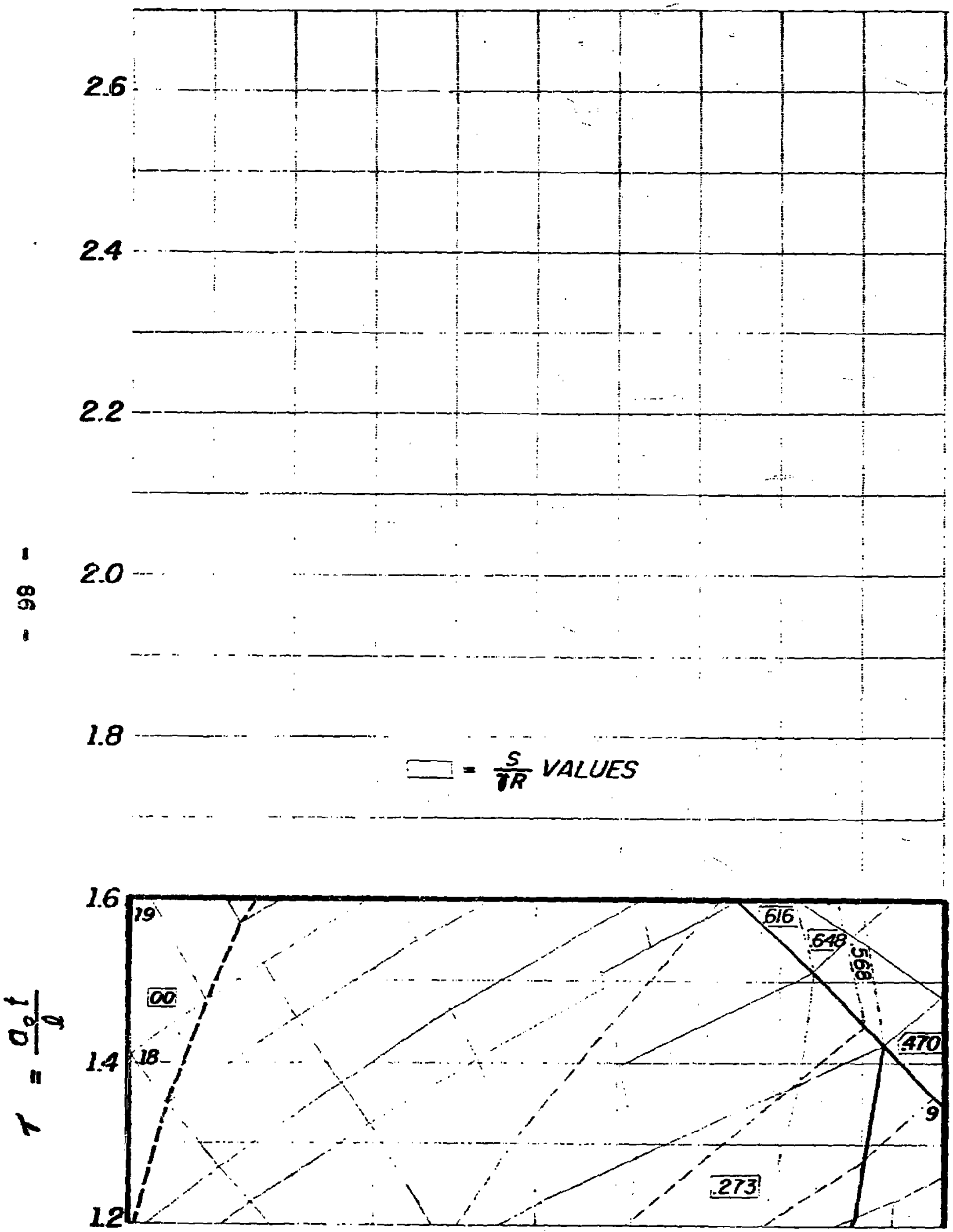

INLET AND EXIT CONDITIONS

POINT	P	u	a
EXIT			
1	2.334	0	1.138
2	7.293	0	2.526
3	2.034	2.105	2.105
4	1.000	1.814	1.902
5	1.000	1.497	1.902
6	1.000	0.574	1.961
7	1.305	2.045	2.045
8	1.000	1.787	1.023
9	1.194	1.067	1.067
10	4.265	0	1.310
INLET			
11	1.000	0.650	1.000
12	11.763	0	1.529
13	9.703	0	1.487
14	5.412	0	1.368
15	3.004	0	1.258
16	1.587	0	1.148
17	1.328	0	1.120
18	1.251	0.298	1.032
19	1.152	0.458	1.020
20			

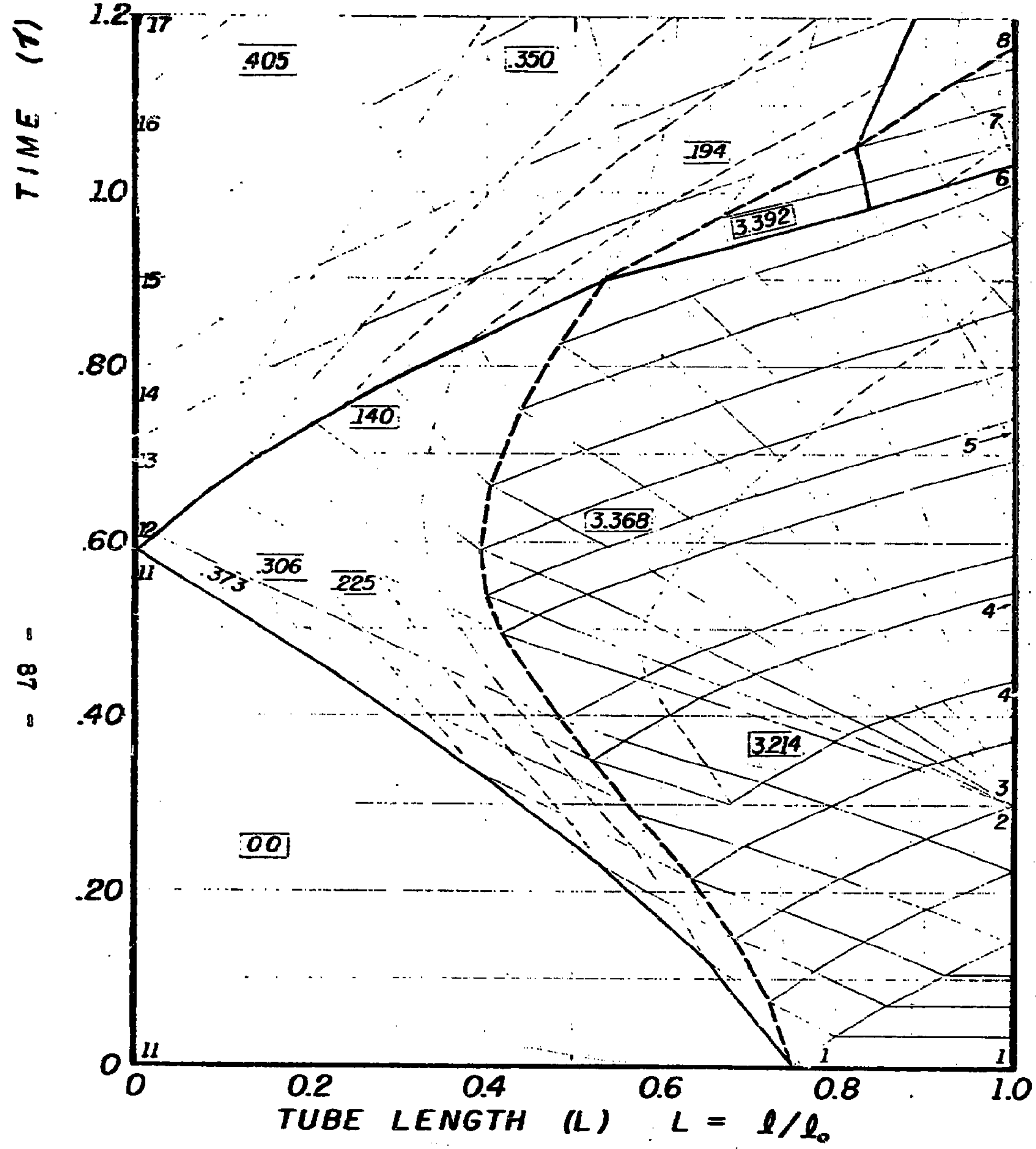

AVERAGE CONDITIONS BEFORE AND AFTER HEAT ADDITION

	BEFORE	AFTER
P =	2.334	7.293
θ =	1.296	6.408
S =	0.044	3.214

CHARACTERISTIC CYCLE PERFORMANCE

$SFC\left(\frac{\text{LBS. FUEL/HR.}}{\text{LBS. THRUST}}\right) = 1.986,\ T/A\left(\frac{\text{LBS.}}{\text{SQ. IN.}}\right) = 9.76$

$\eta_c = 0.91$ $\eta_o = .088$

COMBUSTION CHAMBER MASS $(m/m_o) = 0.450$

FUEL-AIR RATIO – 1/31

CYCLE 1

MACH NUMBER = 0.65

WAVE ENGINE CYCLE

HEAT ADDITION MODE: GRADUAL HEAT ADDITION

Fig. 6A

CONFIDENTIAL

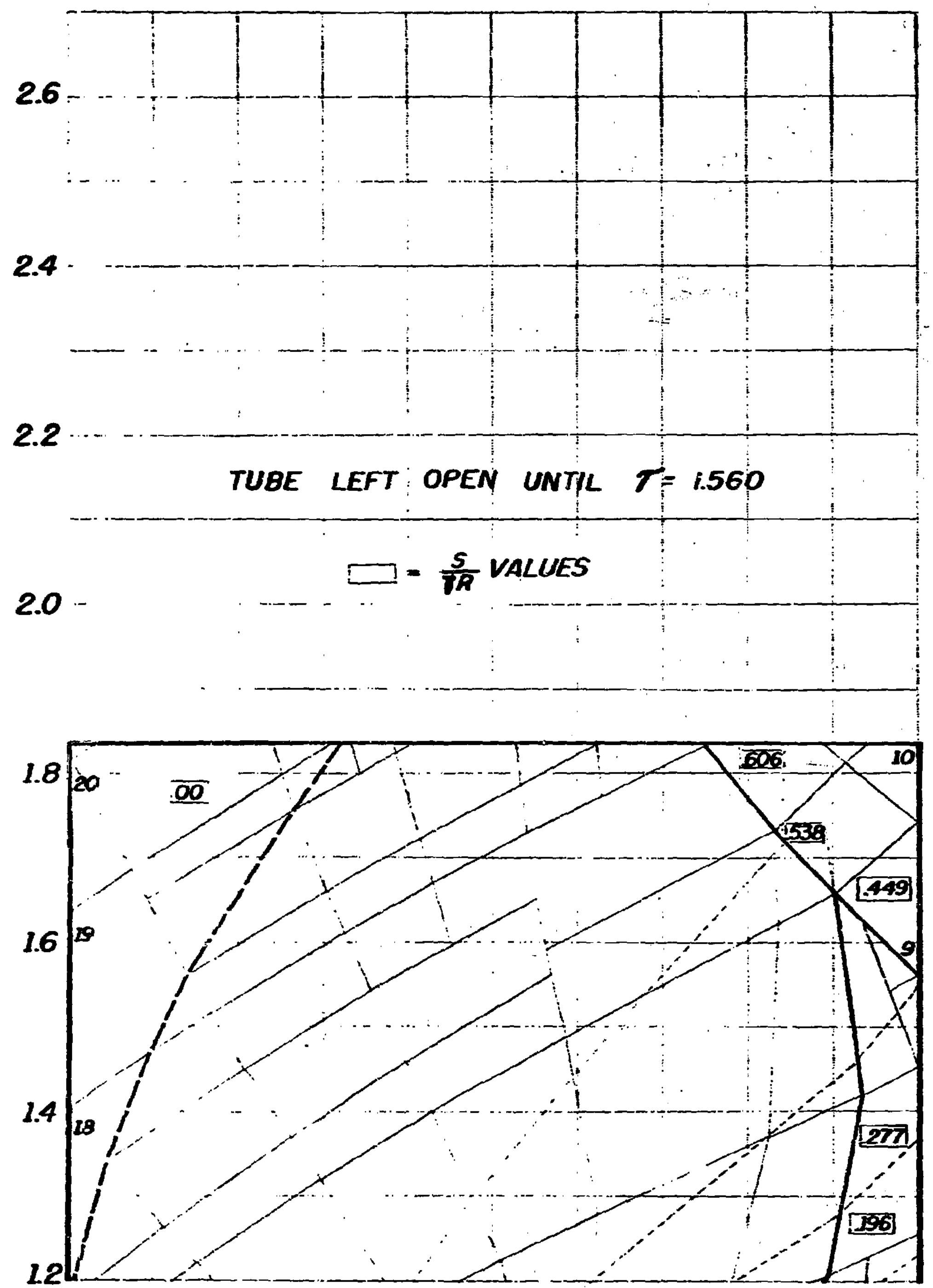

INLET AND EXIT CONDITIONS

POINT	P	u	a
EXIT			
1	2.334	0	1.138
2	7.293	0	2.526
3	2.034	2.105	2.105
4	1.000	1.814	1.902
5	1.000	1.497	1.902
6	1.000	0.574	1.961
7	1.305	2.045	2.045
8	1.000	1.787	1.023
9	2.329	0	1.222
10	1.422	0	1.139
INLET			
11	1.000	0.650	1.000
12	11.763	0	1.529
13	9.703	0	1.487
14	5.412	0	1.368
15	3.004	0	1.258
16	1.587	0	1.148
17	1.328	0	1.120
18	1.247	0.298	1.032
19	1.149	0.458	1.020
20	1.127	0.496	1.018

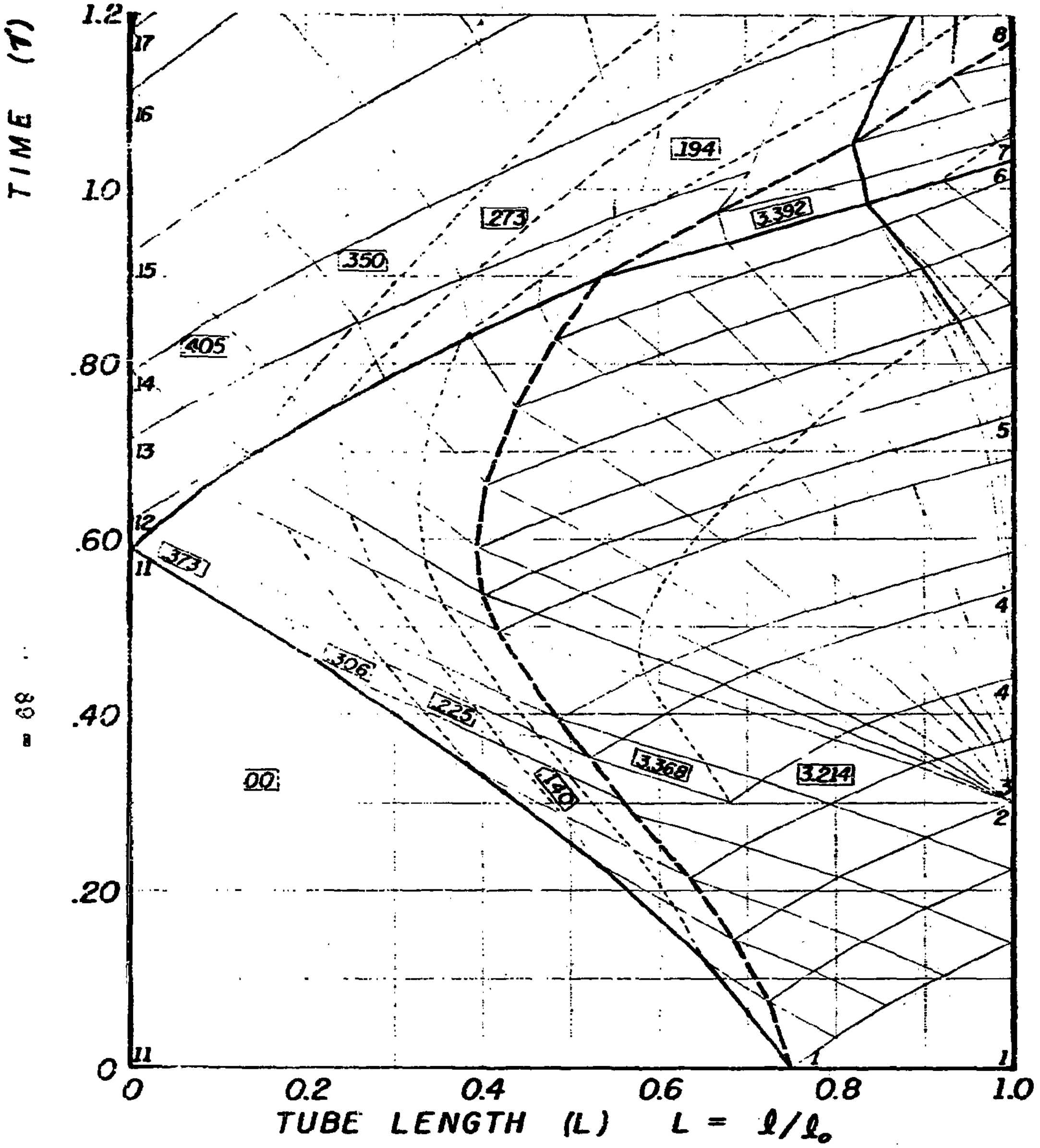

AVERAGE CONDITIONS BEFORE AND AFTER HEAT ADDITION

	BEFORE	AFTER
P =	2.334	7.293
θ =	1.296	6.408
S =	0.044	3.214

CHARACTERISTIC CYCLE PERFORMANCE

$SFC\left(\frac{\text{LBS. FUEL/HR.}}{\text{LBS. THRUST}}\right) = 1.833$, $T/A\left(\frac{\text{LBS.}}{\text{SQ. IN.}}\right) = 9.22$

$\eta_c = 0.91$ $\eta_o = 0.095$

COMBUSTION CHAMBER MASS $(m/m_o) = 0.450$

FUEL-AIR RATIO – $1/31$

CYCLE 1

MACH NUMBER = 0.65

WAVE ENGINE CYCLE
HEAT ADDITION MODE: GRADUAL HEAT ADDITION

Fig. 6B

CONFIDENTIAL

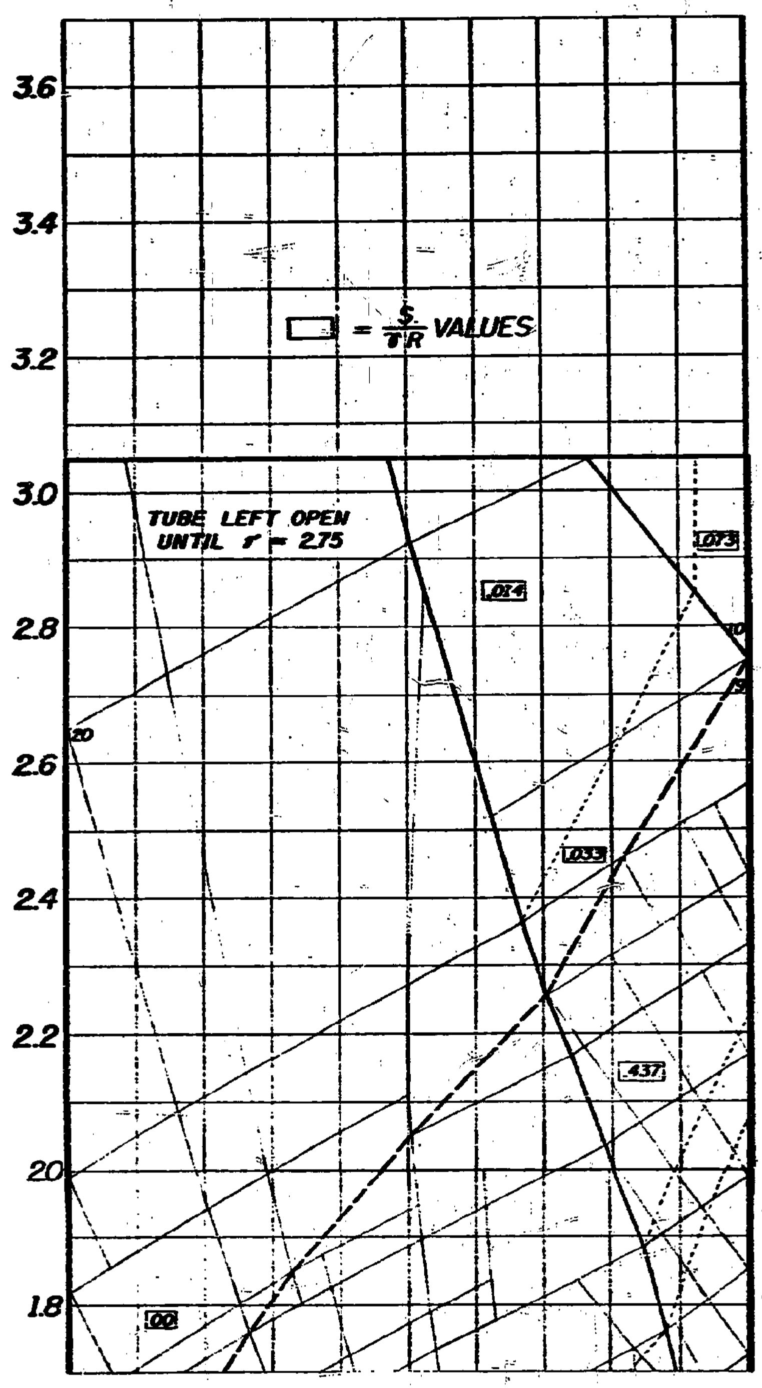

INLET AND EXIT CONDITIONS

POINT	P	u	a
	EXIT		
1	2.334	0	1.138
2	7.293	0	2.526
3	2.034	2.105	2.105
4	1.000	1.814	1.902
5	1.000	1.497	1.902
6	1.000	0.574	1.961
7	1.305	2.045	2.045
8	1.000	1.787	1.023
9	1.000	0.632	1.082
10	2.274	0	1.140
	INLET		
11	1.000	0.650	1.000
12	11.763	0	1.529
13	9.703	0	1.487
14	5.412	0	1.368
15	3.004	0	1.258
16	1.587	0	1.148
17	1.328	0	1.120
18	1.247	0.298	1.032
19	1.146	0.458	1.020
20	0.931	0.719	0.990

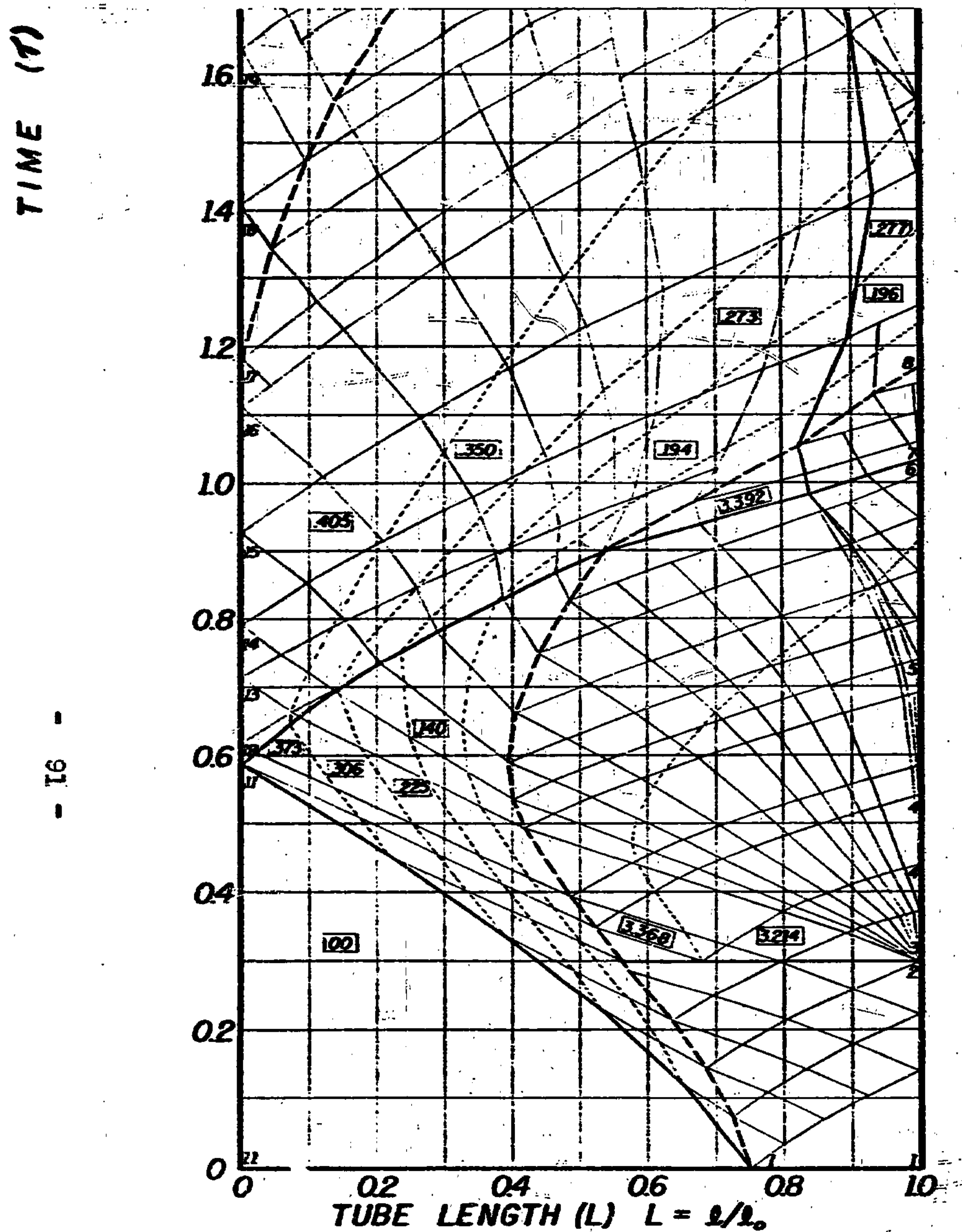

AVERAGE CONDITIONS BEFORE AND AFTER HEAT ADDITION

	BEFORE	AFTER
P =	2.334	7.293
θ =	1.296	6.408
S =	0.044	3.214

CHARACTERISTIC CYCLE PERFORMANCE

$SFC\left(\frac{\text{LBS. FUEL/HR.}}{\text{LBS. THRUST}}\right) = 1.833$, $T/A\left(\frac{\text{LBS.}}{\text{SQ. IN.}}\right) = 5.55$

$\eta_c = 0.91$ $\eta_o = 0.095$

COMBUSTION CHAMBER MASS $(m/m_o) = 0.450$

FUEL-AIR RATIO – 1/31

CYCLE 1

MACH NUMBER = 0.65

WAVE ENGINE CYCLE

HEAT ADDITION MODE: GRADUAL HEAT ADDITION

Fig. 6C

CONFIDENTIAL

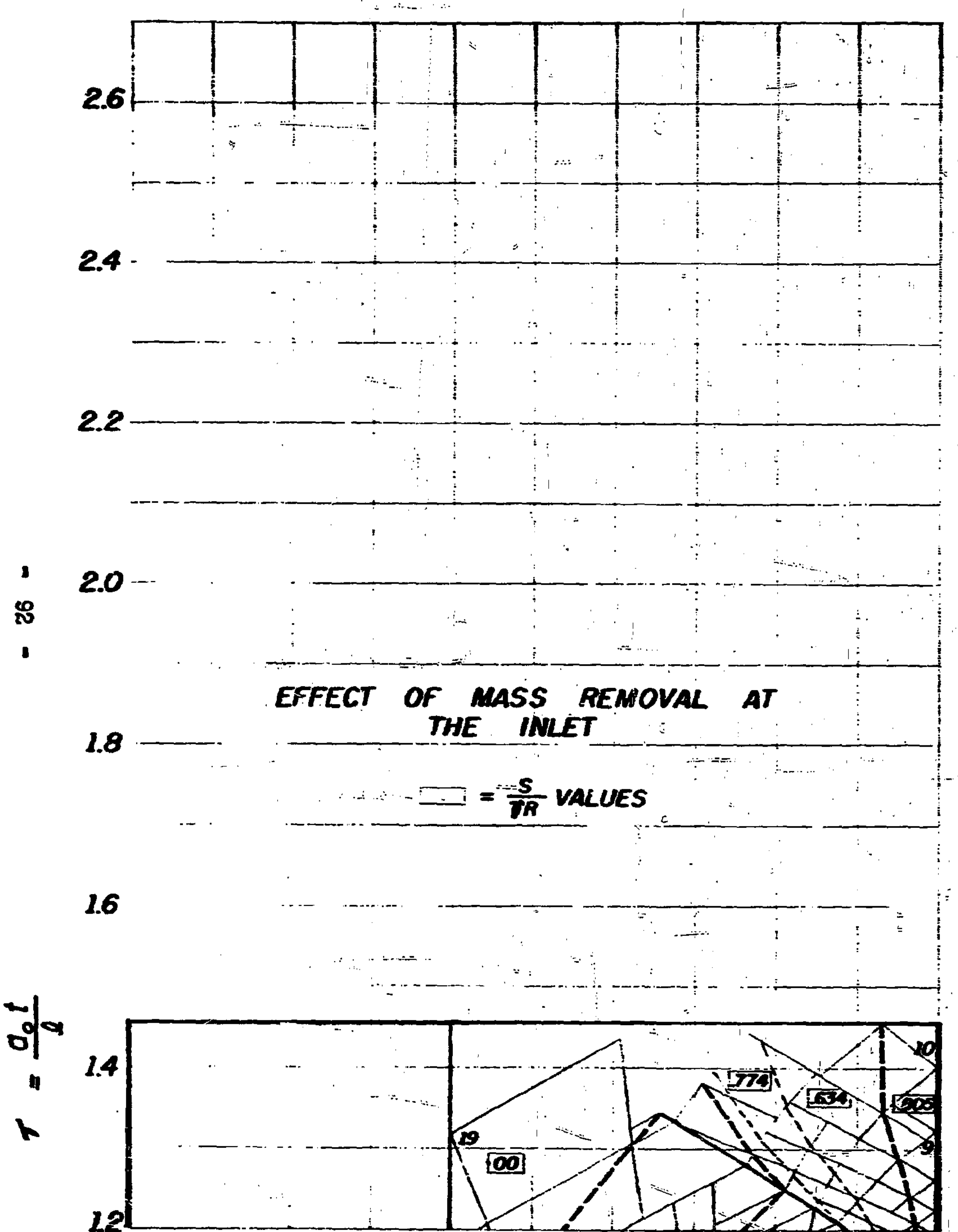

INLET AND EXIT CONDITIONS

POINT	P	u	a
EXIT			
1	2.334	0	1.138
2	7.293	0	2.526
3	1.794	2.105	2.105
4	1.081	1.958	1.958
5	1.000	1.394	1.960
6	1.000	0.188	1.960
7	1.260	2.034	2.034
8	10.248	0	1.584
9	3.107	0	1.331
10	1.630	0	1.218
INLET			
11	1.000	0.650	1.000
12	5.540	-0.786	1.326
13	2.173	0.023	1.149
14	0.925	0	1.017
15	3.364	1.164	1.223
16	3.349	1.182	1.234
17	1.157	0.450	1.021
18	1.102	0.524	1.014
19	1.050	0.592	1.007
20			

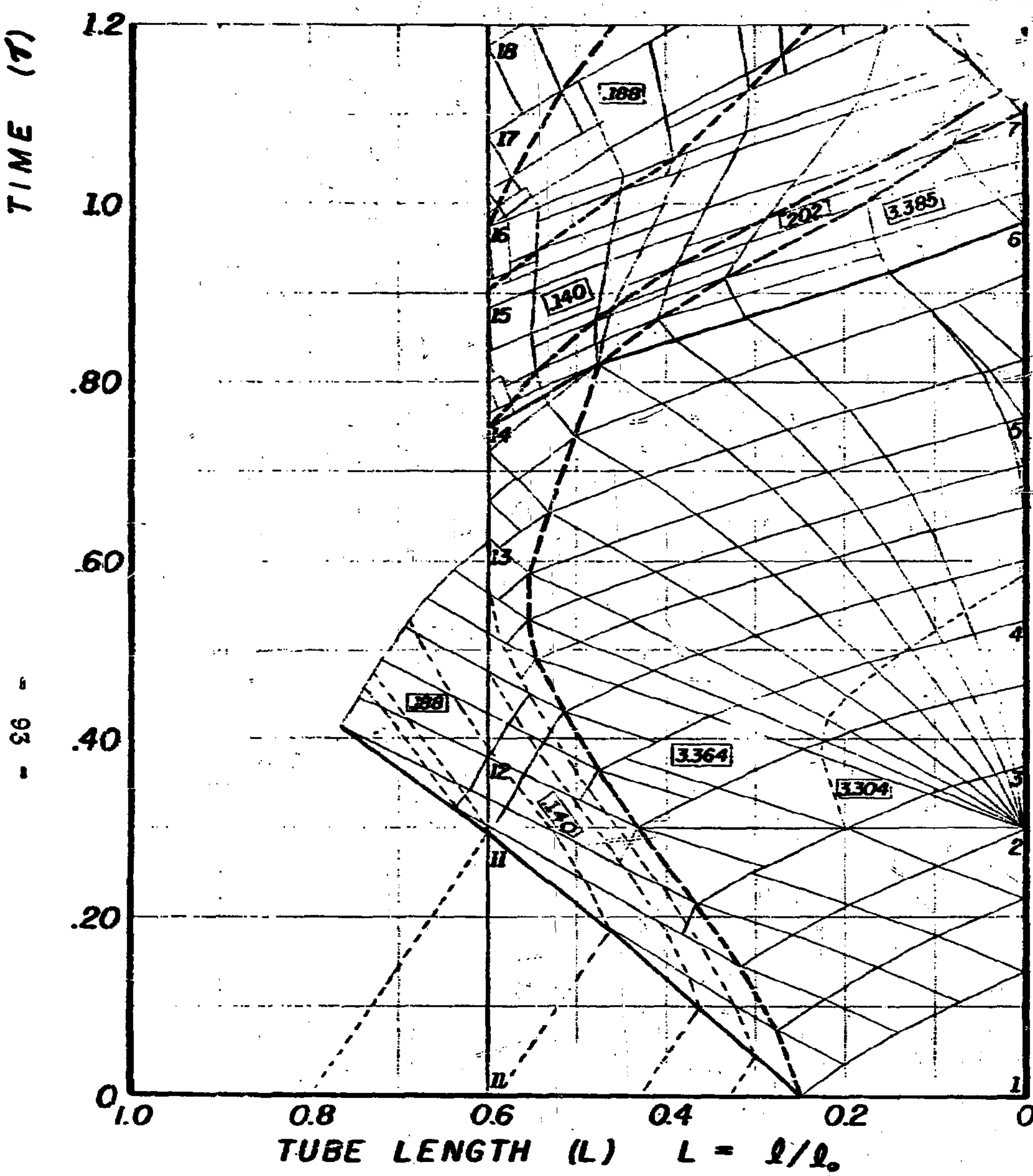

AVERAGE CONDITIONS BEFORE AND AFTER HEAT ADDITION

	BEFORE	AFTER
P =	2.334	7.293
θ =	1.296	6.408
S =	0.044	3.214

CHARACTERISTIC CYCLE PERFORMANCE

$SFC\left(\frac{LBS.\ FUEL/HR.}{LBS.\ THRUST}\right) = 2.850$, $T/A\left(\frac{LBS.}{SQ.\ IN.}\right) = 8.43$

$\eta_{ic} = 0.91$ $\eta_o = 0.061$

COMBUSTION CHAMBER MASS $(m/m_o) = 0.450$

FUEL-AIR RATIO - 1/31

CYCLE I

MACH NUMBER = 0.65

WAVE ENGINE CYCLE

HEAT ADDITION MODE: GRADUAL HEAT ADDITION

Fig. 7A

CONFIDENTIAL

CONFIDENTIAL

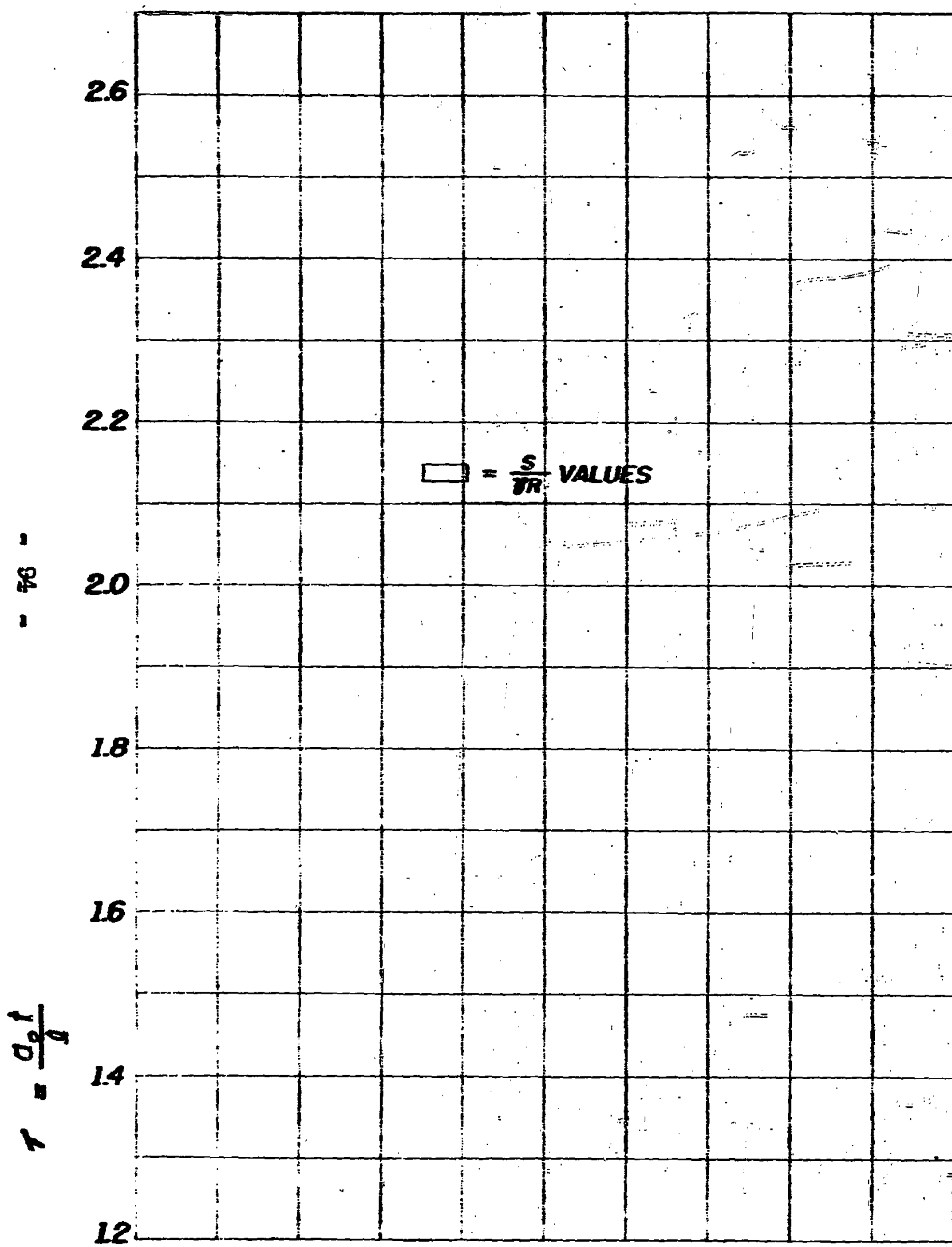

INLET AND EXIT CONDITIONS

POINT	P	u	a
EXIT			
1	1.000	0	2.146
2	1.000	1.328	2.148
3	1.000	1.991	2.148
4	1.000	1.750	2.146
5	1.000	1.470	2.146
6	1.000	1.217	2.146
7	2.108	0	2.402
8	1.437	0	2.274
9	1.135	0	2.199
10	0.988	0	2.156
INLET			
11	1.000	0	1.000
12	3.092	0	1.752
13	2.500	0	2.381
14	1.660	0	2.246
15	1.000	0	2.089
16	0.898	0.395	0.985
17	0.829	0.512	0.974
18			
19			
20			

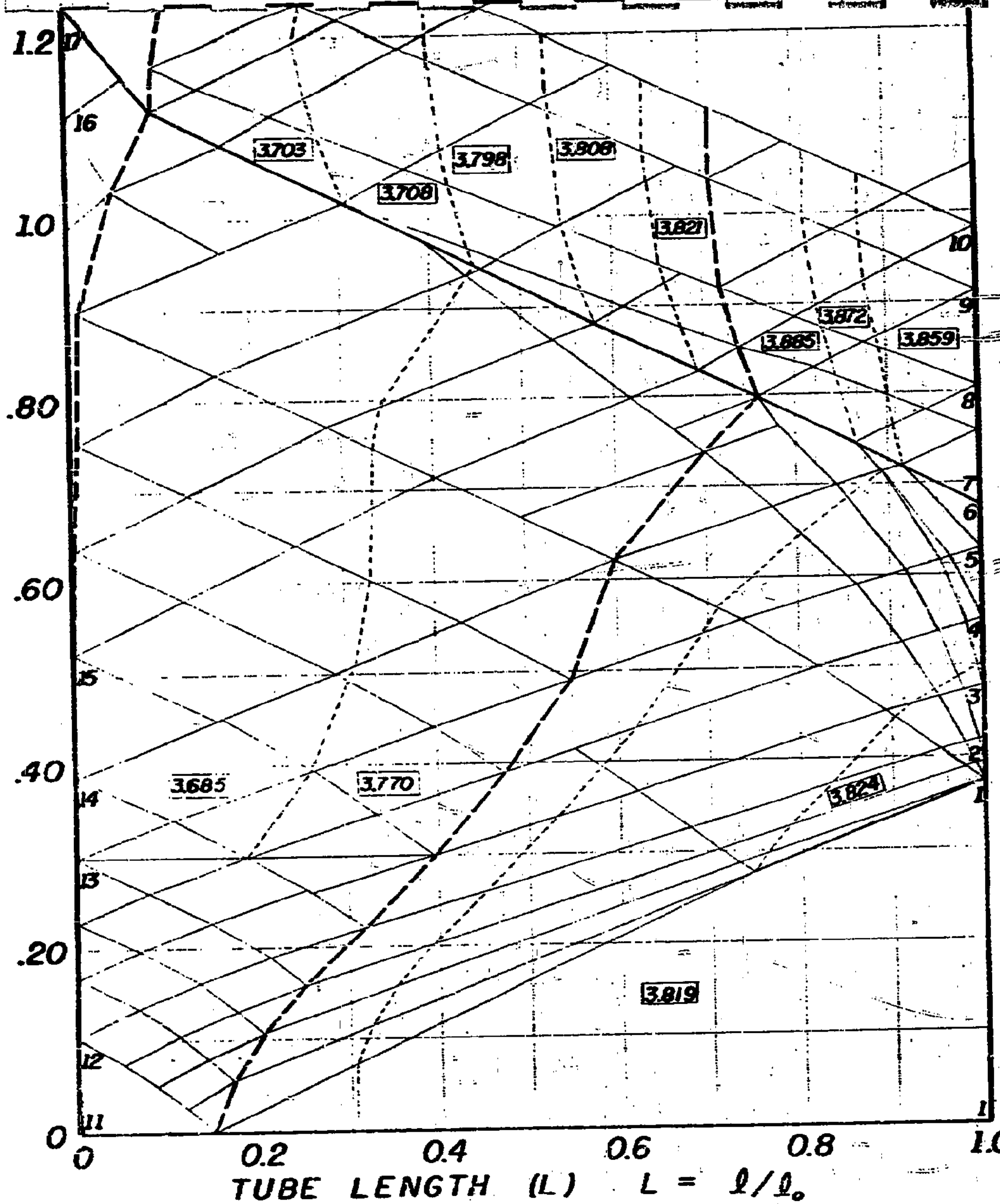

AVERAGE CONDITIONS BEFORE AND AFTER HEAT ADDITION

	BEFORE	AFTER
P =	1.000	2.500
θ =	1.000	5.671
S =	0.0	3.685

CHARACTERISTIC CYCLE PERFORMANCE

$SFC\left(\frac{\text{LBS. FUEL/HR.}}{\text{LBS. THRUST}}\right) = 2.138$, $T/A\left(\frac{\text{LBS.}}{\text{SQ. IN.}}\right) = 3.90$

$\eta_c = 1.00$. $\eta_o =$ ——

COMBUSTION CHAMBER MASS $(m/m_o) = 0.150$

FUEL-AIR RATIO - $1/31$

CYCLE 1

MACH NUMBER = 0

WAVE ENGINE CYCLE

HEAT ADDITION MODE: GRADUAL HEAT ADDITION

Fig. 8A

CONFIDENTIAL

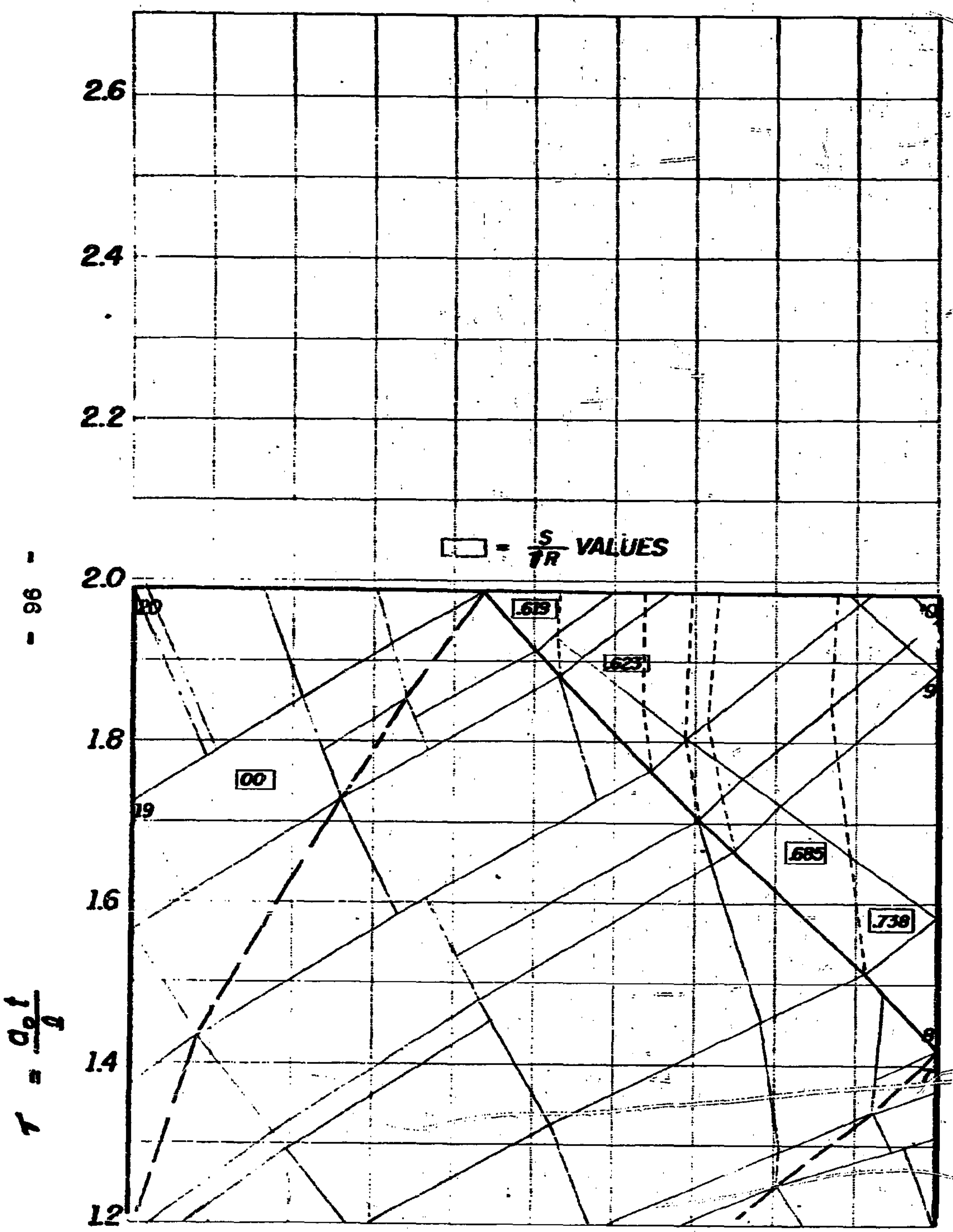

INLET AND EXIT CONDITIONS

POINT	P	u	a
EXIT			
1	12.596	0	2.645
2	4.562	0	2.288
3	1.273	1.907	1.907
4	1.016	1.846	1.846
5	2.617	3.200	2.139
6	1.585	1.979	1.979
7	1.000	1.040	1.852
8	3.231	0	1.347
9	1.298	0	1.183
10	1.448	0	1.202
INLET			
11	1.000	0.650	1.000
12	18.012	0	1.685
13	11.475	0	1.579
14	6.988	0	1.471
15	4.677	0	1.389
16	3.618	0	1.339
17	1.328	0	1.160
18	1.328	0	1.041
19	1.148	0.475	1.020
20	1.072	0.570	1.010

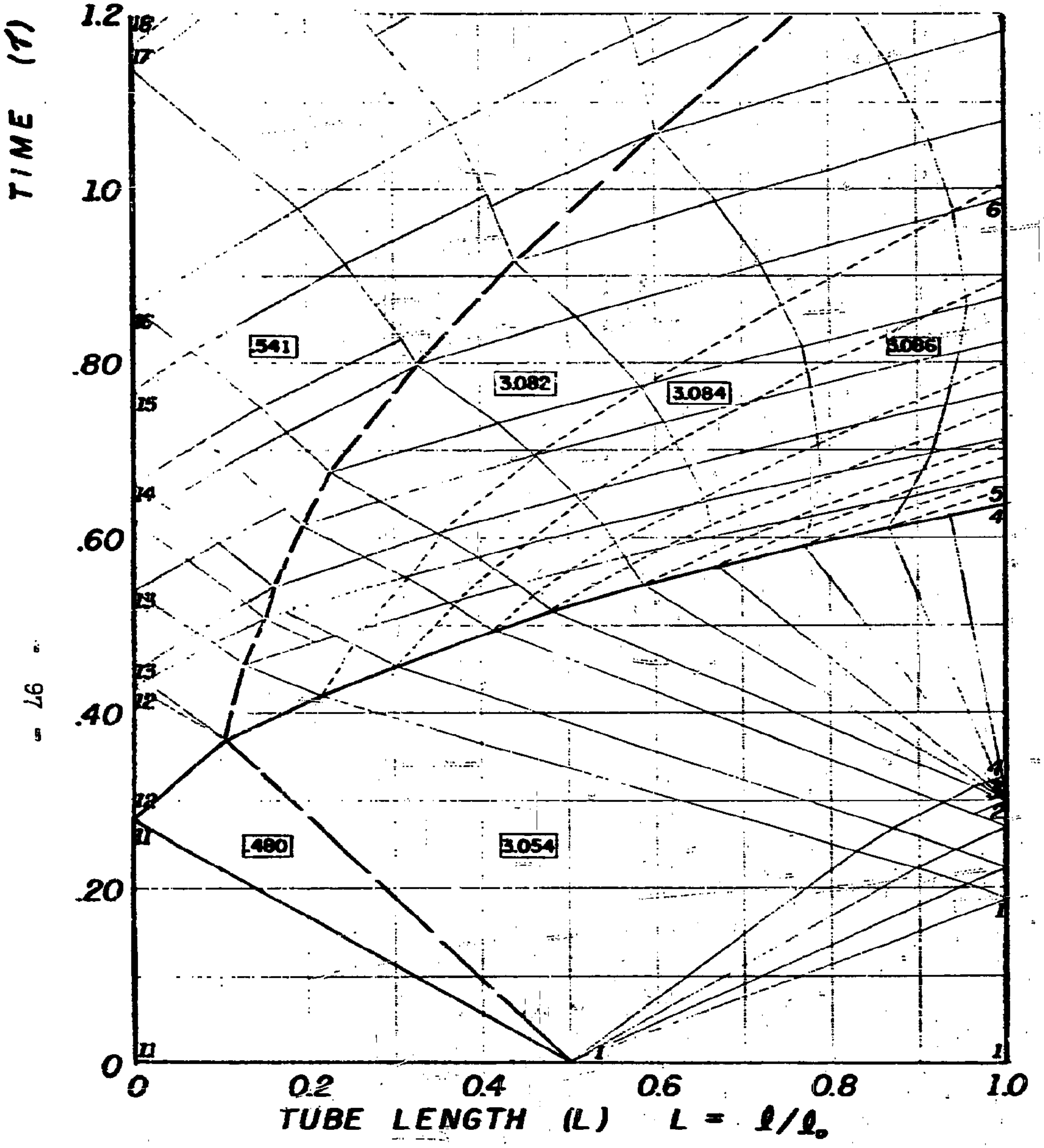

AVERAGE CONDITIONS BEFORE AND AFTER HEAT ADDITION

	BEFORE	AFTER
P =	2.334	12.596
θ =	1.296	6.997
S =	0.044	3.054

CHARACTERISTIC CYCLE PERFORMANCE

$SFC\left(\frac{\text{LBS. FUEL/HR.}}{\text{LBS. THRUST}}\right) = 1.754$, $T/A\left(\frac{\text{LBS.}}{\text{SQ. IN.}}\right) = 17.90$

$\eta_c = 0.91$ $\eta_o = 0.099$

COMBUSTION CHAMBER MASS $(m/m_o) = 0.90$

FUEL-AIR RATIO – 1/31

CYCLE 1

MACH NUMBER = 0.65

WAVE ENGINE CYCLE

HEAT ADDITION MODE: CONSTANT VOLUME COMBUSTION

Fig. 9A

CONFIDENTIAL

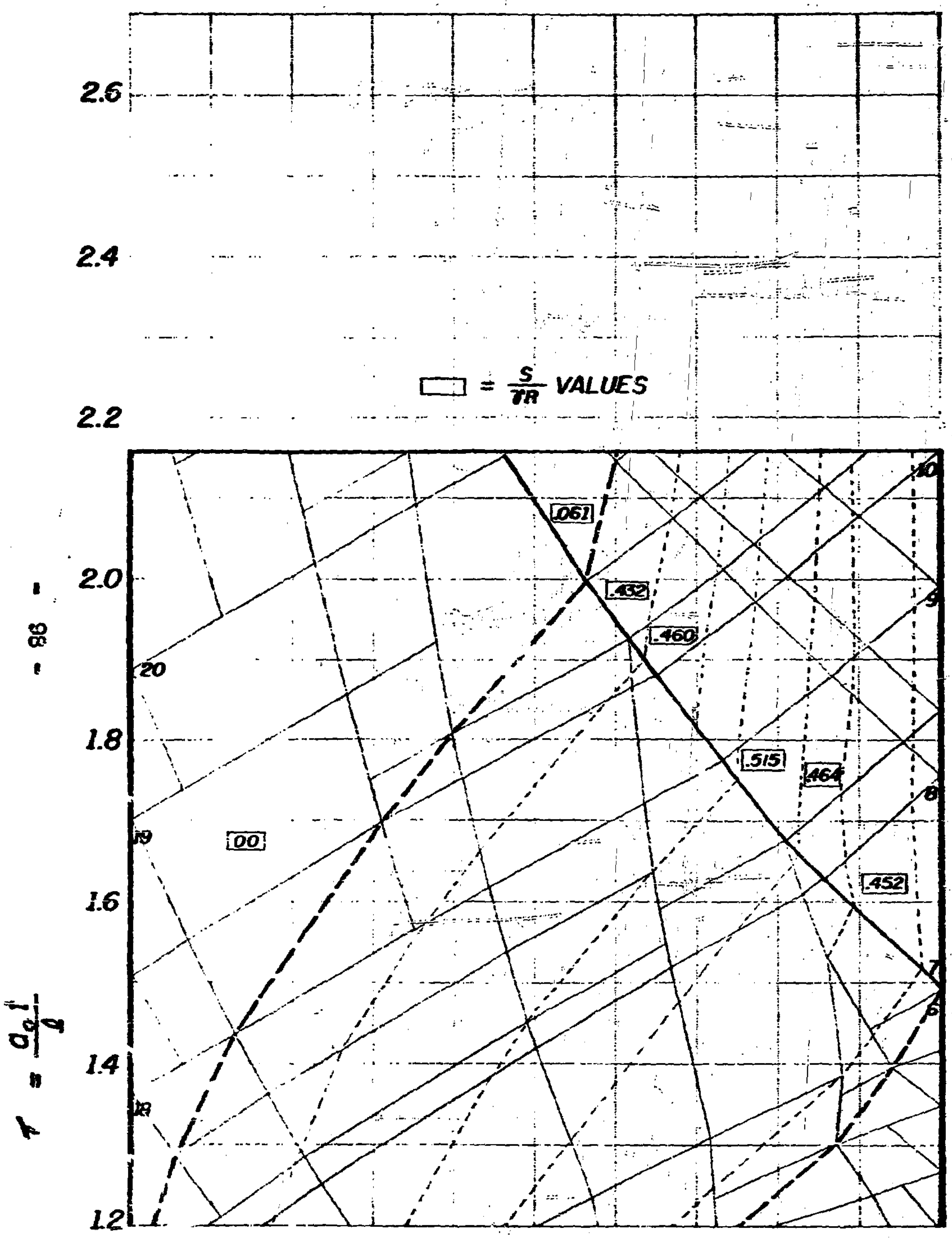

INLET AND EXIT CONDITIONS

POINT	P	u	a
EXIT			
1	8.090	0	2.686
2	1.000	1.787	1.993
3	1.000	1.870	1.993
4	2.007	2.918	2.212
5	1.193	2.048	2.048
6	1.000	0.627	1.997
7	2.120	0	1.231
8	1.285	0	1.146
9	1.792	0	1.202
10	1.904	0	1.213
INLET			
11	1.072	0.570	1.010
12	1.021	0.628	1.003
13	11.565	0	1.520
14	11.109	0	1.511
15	4.797	0	1.340
16	2.390	0	1.213
17	1.328	0	1.116
18	1.221	0.355	1.029
19	1.087	0.545	1.012
20	1.041	0.604	1.006

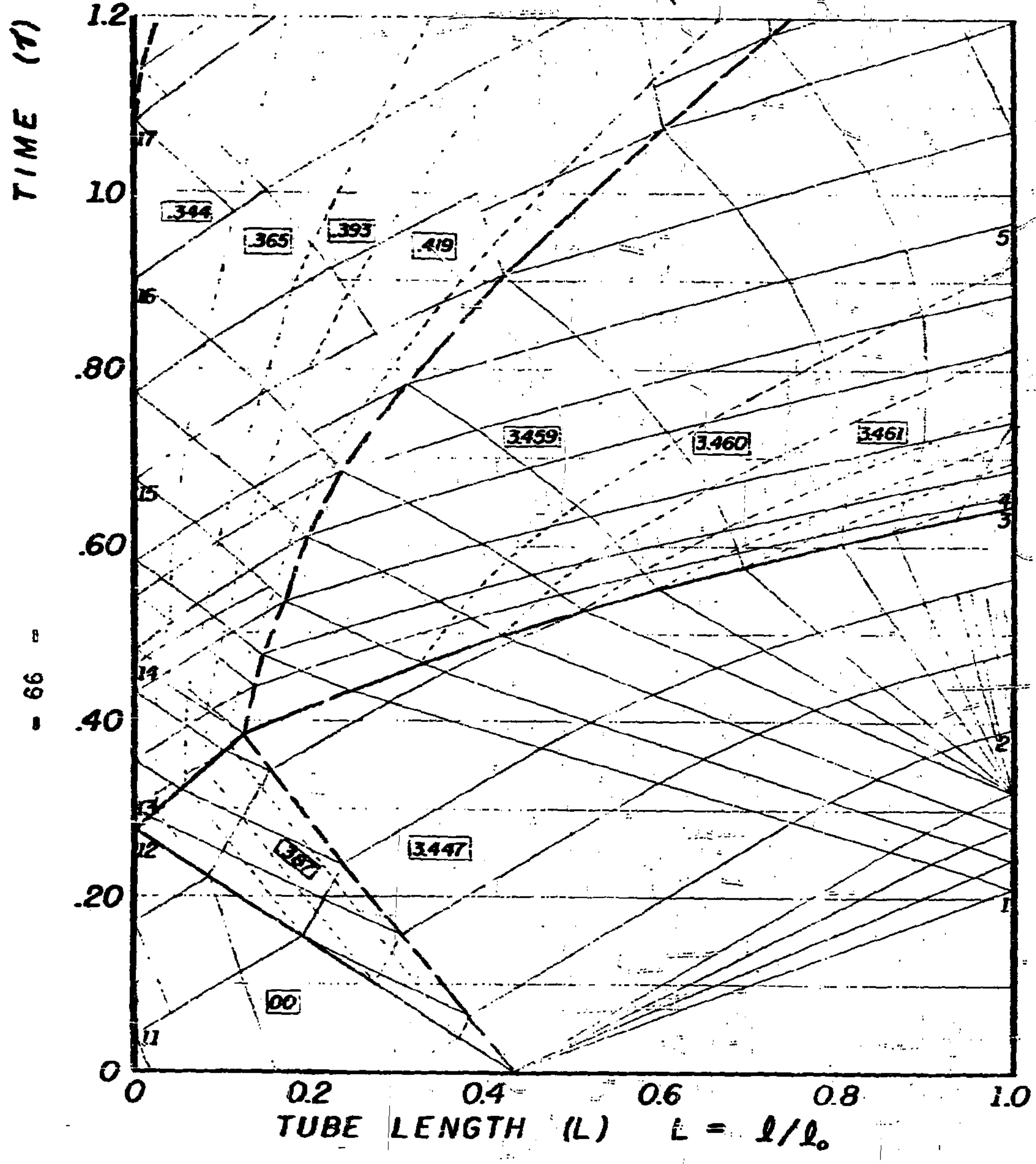

AVERAGE CONDITIONS BEFORE AND AFTER HEAT ADDITION

	BEFORE	AFTER
P =	1.694	8.090
θ =	1.510	7.214
S =	0.654	3.447

CHARACTERISTIC CYCLE PERFORMANCE

$SFC\left(\frac{\text{LBS. FUEL/ HR.}}{\text{LBS. THRUST}}\right) = 2.173$, $T/A\left(\frac{\text{LBS.}}{\text{SQ. IN.}}\right) = 9.27$

$\eta_c = 0.31$, $\eta_o = 0.080$

COMBUSTION CHAMBER MASS $(m/m_o) = 0.633$

FUEL-AIR RATIO - 1/31

CYCLE 2

MACH NUMBER = 0.65

WAVE ENGINE CYCLE

HEAT ADDITION MODE: CONSTANT VOLUME COMBUSTION

Fig. 9B

CONFIDENTIAL

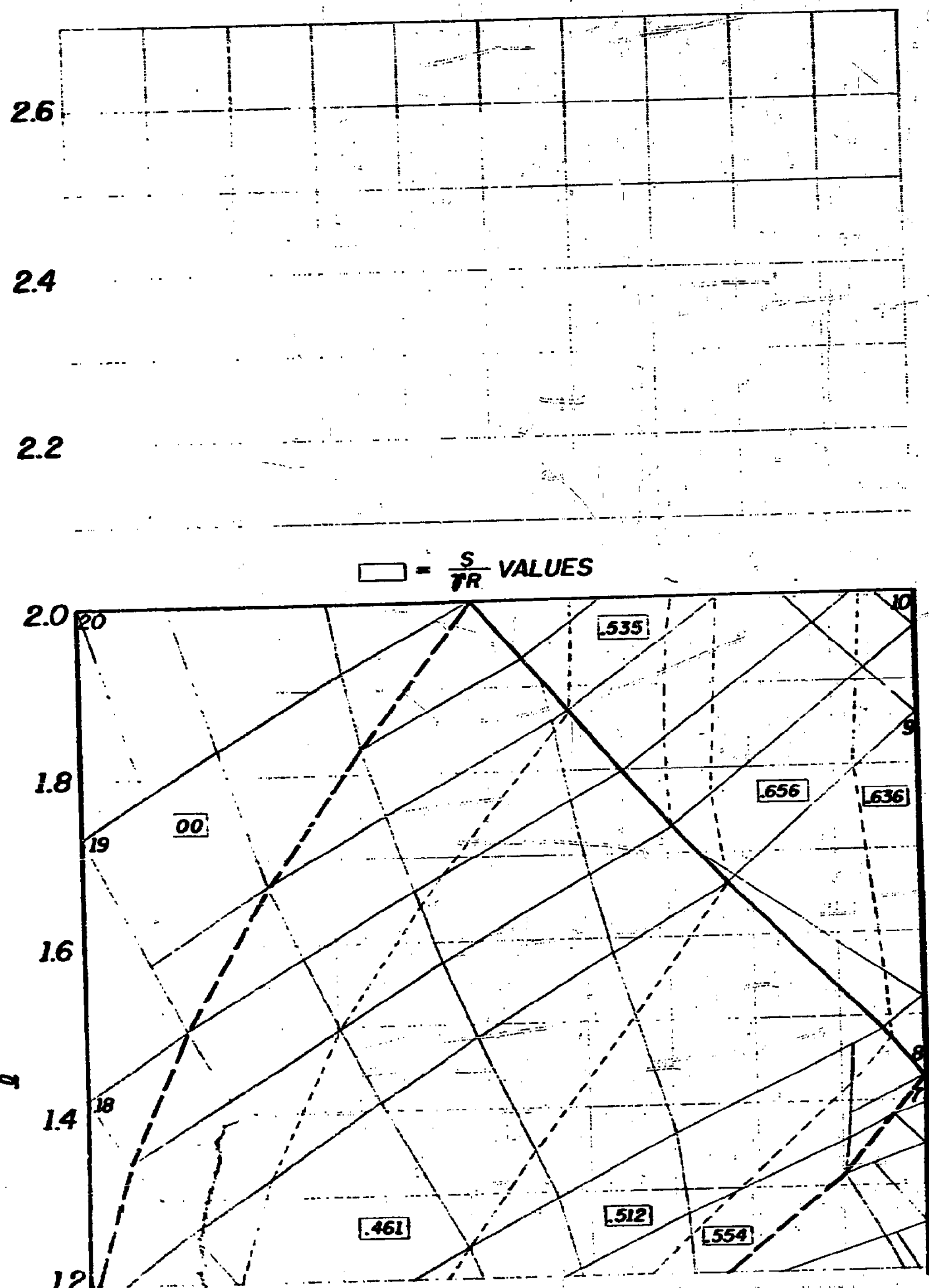

INLET AND EXIT CONDITIONS

POINT	P	u	a
	EXIT		
1	9.564	0	2.660
2	3.211	0	2.276
3	1.000	1.747	1.927
4	1.000	1.897	1.927
5	2.216	3.068	2.173
6	1.148	1.971	1.971
7	1.000	0.860	1.932
8	2.682	0	1.307
9	1.277	0	1.176
10	1.614	0	1.216
	INLET		
11	0.965	0.691	0.995
12	0.945	0.713	0.992
13	12.960	0	1.574
14	14.163	0	1.593
15	6.027	0	1.410
16	2.923	0	1.272
17	1.328	0	1.136
18	1.230	0.340	1.030
19	1.117	0.510	1.016
20	1.050	0.587	1.007

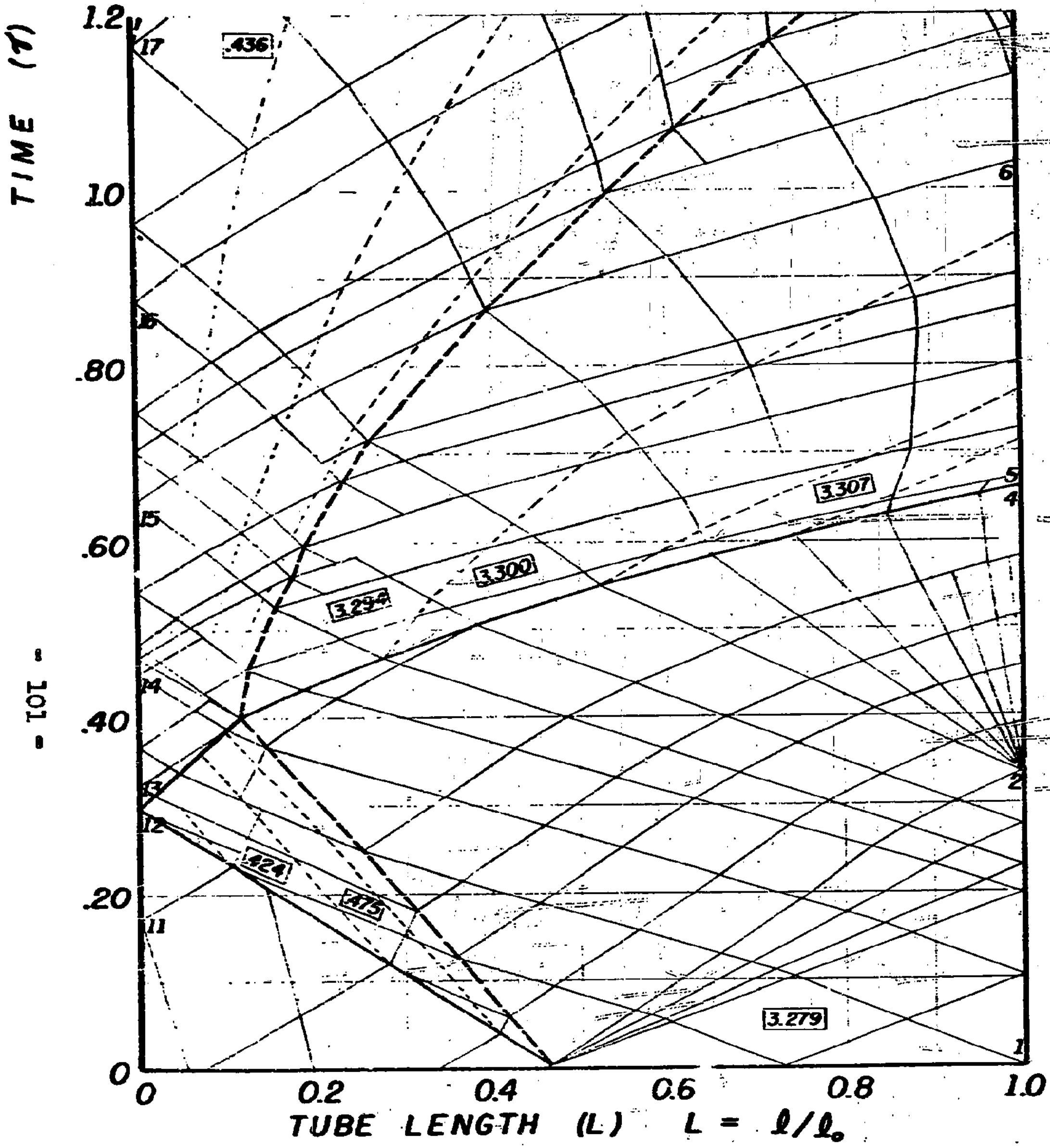

AVERAGE CONDITIONS BEFORE AND AFTER HEAT ADDITION

	BEFORE	AFTER
P =	1.858	9.564
θ =	1.375	7.077
S =	0.353	3.279

CHARACTERISTIC CYCLE PERFORMANCE

$SFC\left(\frac{LBS.FUEL/HR.}{LBS.THRUST}\right) = 1.934,\ T/A\left(\frac{LBS.}{SQ.IN.}\right) = 12.84$

$\eta_c = 0.53, \quad \eta_o = .090$

COMBUSTION CHAMBER MASS $(m/m_o) = 0.723$

FUEL-AIR RATIO - 1/31

CYCLE 3

MACH NUMBER = 0.65

WAVE ENGINE CYCLE

HEAT ADDITION MODE: CONSTANT-VOLUME COMBUSTION

Fig. 9C

CONFIDENTIAL

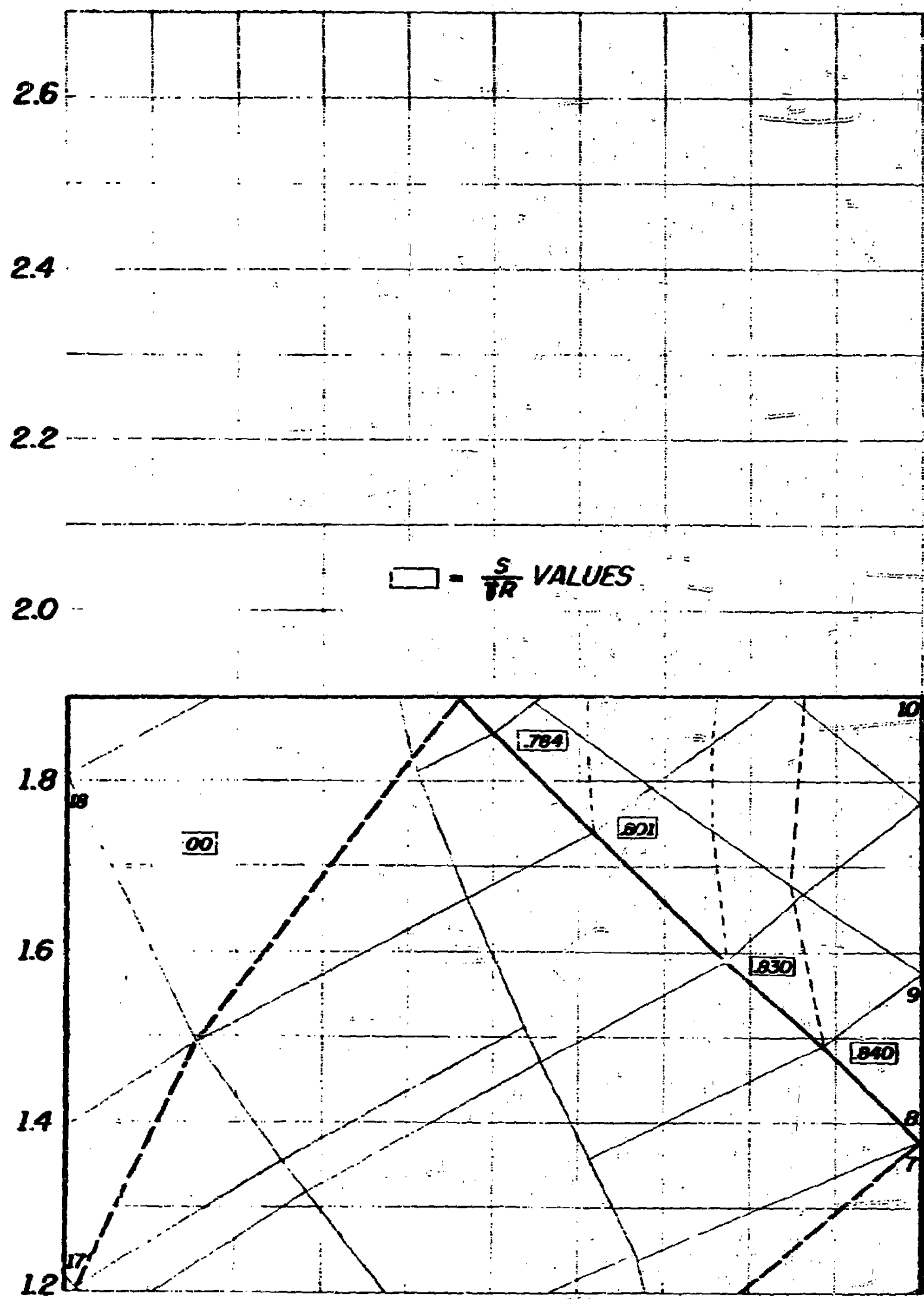

INLET AND EXIT CONDITIONS

POINT	P	u	a
	EXIT		
1	16.018	0	2.679
2	4.711	0	2.249
3	1.314	1.874	1.874
4	3.252	3.195	2.156
5	2.921	2.556	2.116
6	1.813	1.973	1.973
7	1.000	1.173	1.812
8	3.519	0	1.421
9	2.549	0	1.356
10	1.949	0	1.306
	INLET		
11	1.000	0.950	1.000
12	21.803	0	1.793
13	14.955	0	1.699
14	7.938	0	1.552
15	3.725	0	1.393
16	1.787	0	1.254
17	1.759	0.168	1.084
18	1.464	0.575	1.056
19			
20			

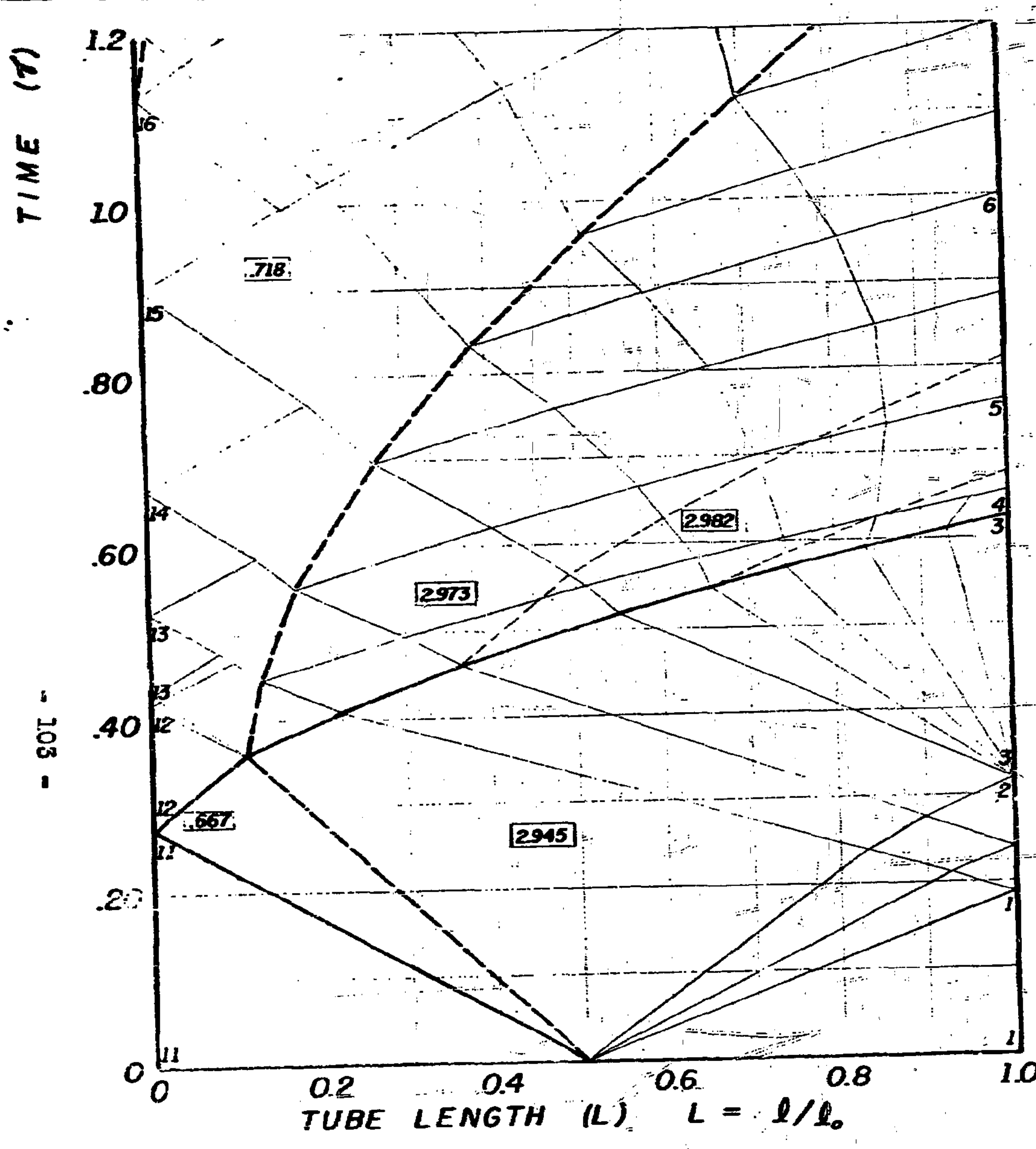

AVERAGE CONDITIONS BEFORE AND AFTER HEAT ADDITION

	BEFORE	AFTER
P =	3.290	16.018
θ =	1.474	7.176
S =	0.119	2.945

CHARACTERISTIC CYCLE PERFORMANCE

$SFC \left(\frac{\text{LBS. FUEL/HR.}}{\text{LBS. THRUST}}\right) = 2.086 \quad T/A\left(\frac{\text{LBS.}}{\text{SQ. IN.}}\right) = 19.40$

$\eta_c = 0.85 \qquad \eta_o = 0.122$

COMBUSTION CHAMBER MASS $(m/m_0) = 1.116$

FUEL-AIR RATIO – 1/31

CYCLE I

MACH NUMBER = 0.95

WAVE ENGINE CYCLE

HEAT ADDITION MODE: CONSTANT VOLUME COMBUSTION

Fig. 10A

CONFIDENTIAL

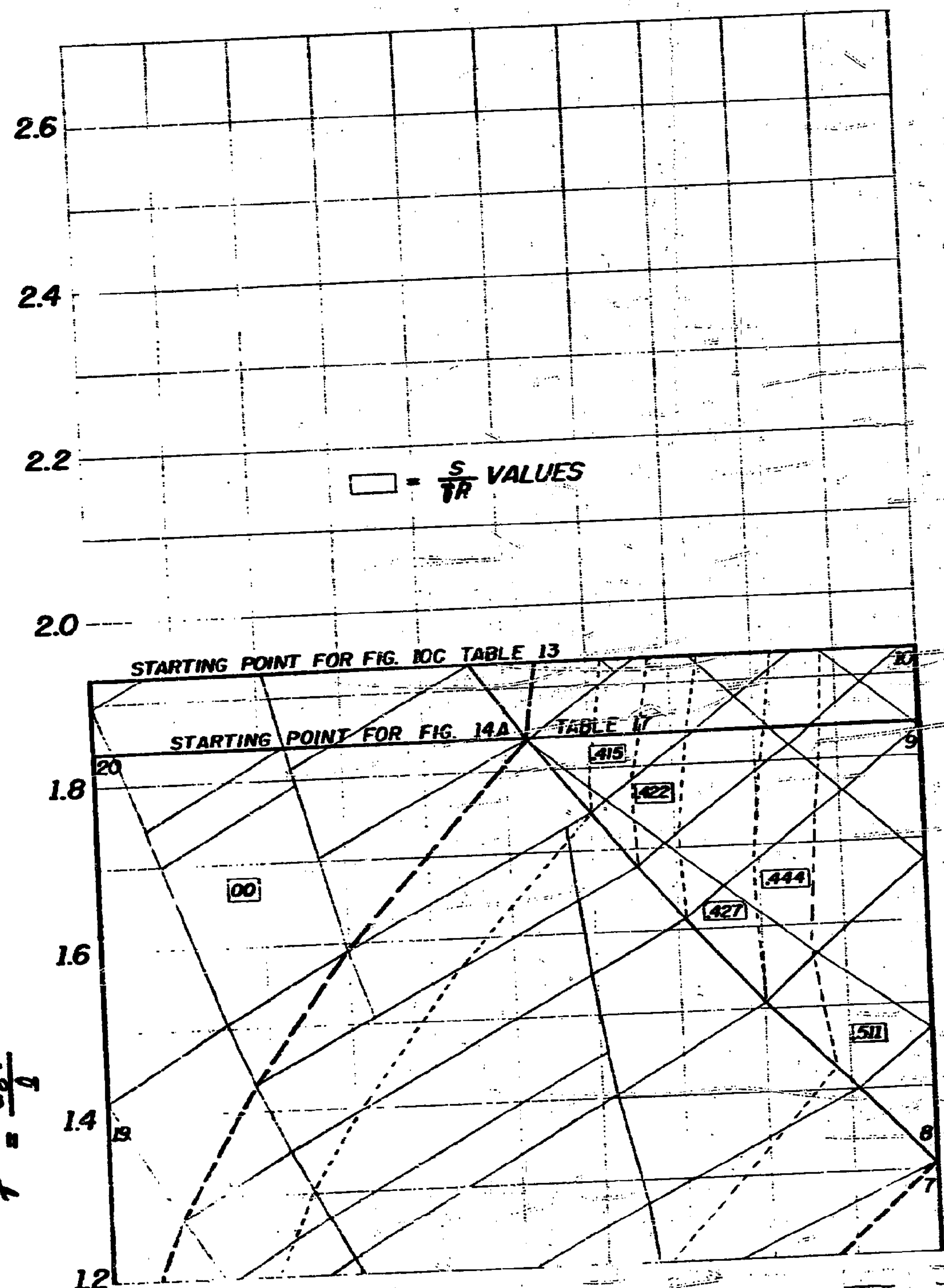

INLET AND EXIT CONDITIONS

POINT	P	u	a
EXIT			
1	9.264	0	2.724
2	3.862	0	2.404
3	1.077	2.003	2.003
4	1.200	2.034	2.034
5	2.224	2.970	2.229
6	1.132	2.022	2.022
7	1.000	1.065	1.985
8	3.388	0	1.331
9	2.322	0	1.261
10	2.440	0	1.270
INLET			
11	1.426	0.600	1.052
12	1.352	0.667	1.044
13	12.793	0	1.524
14	12.389	0	1.517
15	8.314	0	1.433
16	4.754	0	1.323
17	2.589	0	1.213
18	1.787	0	1.150
19	1.564	0.472	1.066
20	1.352	0.668	1.044

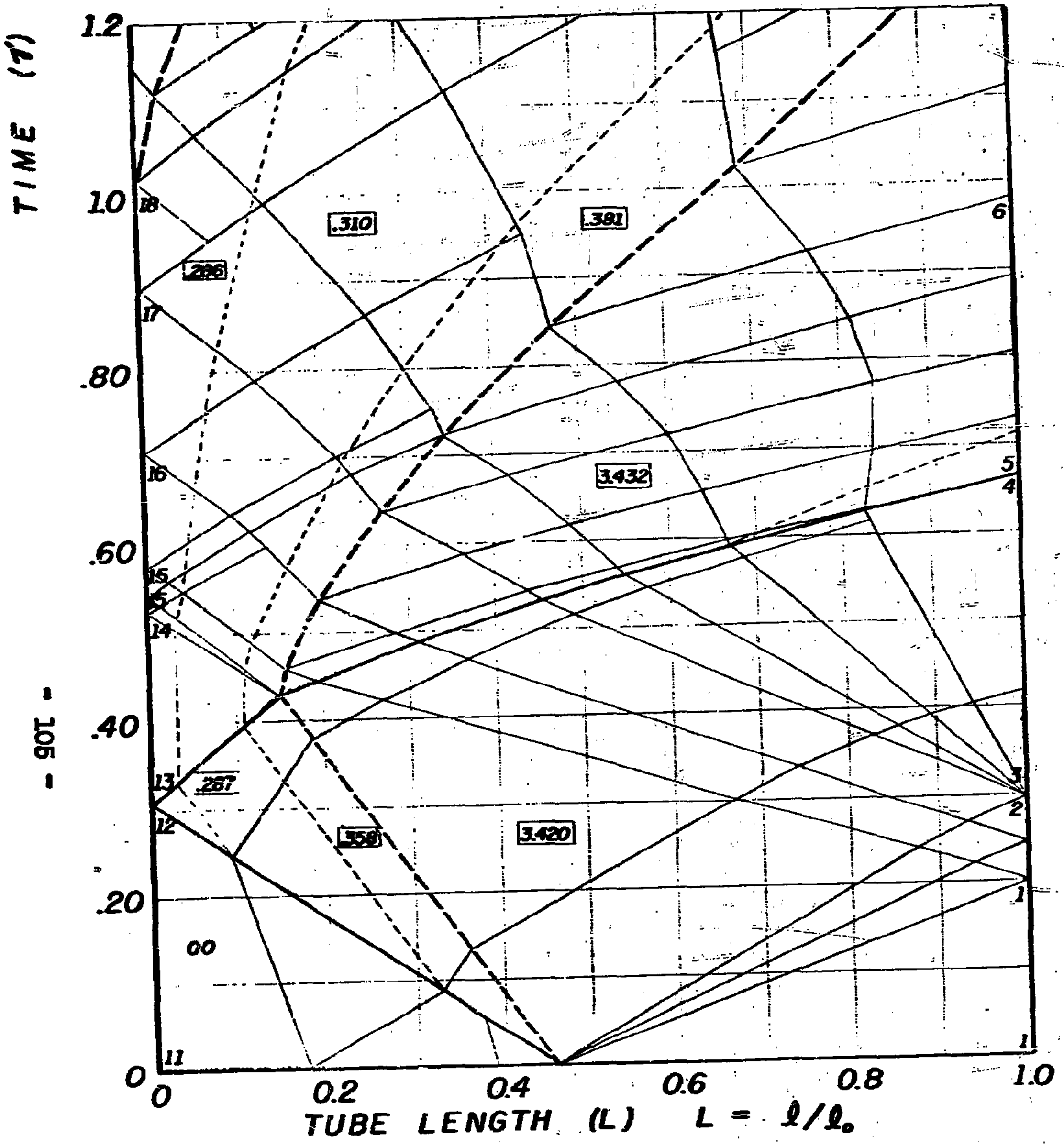

AVERAGE CONDITIONS BEFORE AND AFTER HEAT ADDITION

	BEFORE	AFTER
P =	2.148	9.264
θ =	1.721	7.423
S =	0.812	3.420

CHARACTERISTIC CYCLE PERFORMANCE

SFC $\left(\frac{\text{LBS. FUEL/HR.}}{\text{LBS. THRUST}}\right)$ = 2.200 $T/A\left(\frac{\text{LBS.}}{\text{SQ. IN.}}\right)$ = 10.93

$\eta_c = 0.34$ $\eta_o = .116$

COMBUSTION CHAMBER MASS (m/m_o) = 0.674

FUEL-AIR RATIO - 1/31

CYCLE 2

MACH NUMBER = 0.95

WAVE ENGINE CYCLE

HEAT ADDITION MODE: CONSTANT VOLUME COMBUSTION

Fig. 10B

CONFIDENTIAL

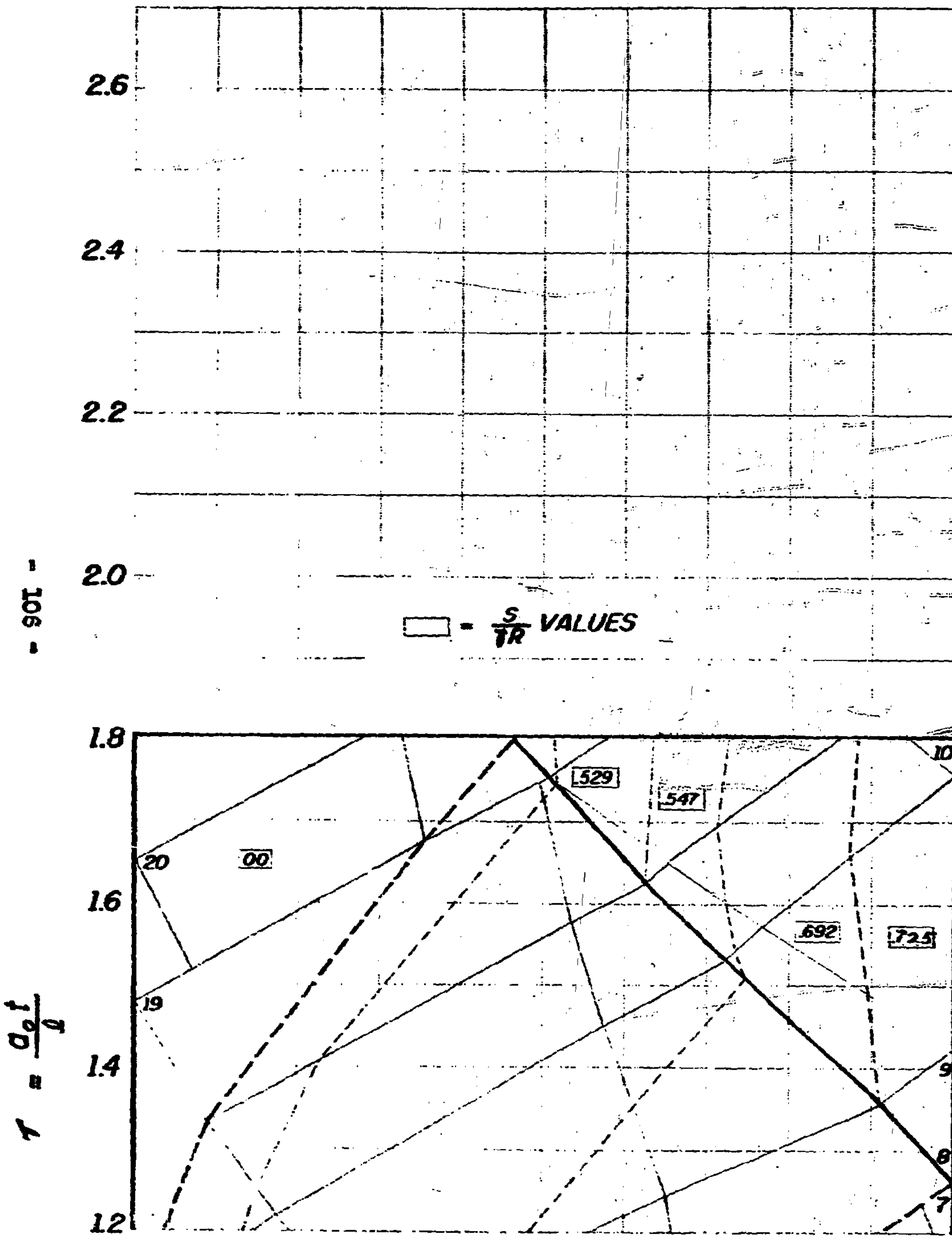

INLET AND EXIT CONDITIONS

POINT	P	u	a
EXIT			
1	11.501	0	2.683
2	4.169	0	2.321
3	1.163	1.934	1.934
4	1.249	1.954	1.954
5	2.573	3.013	2.178
6	2.016	2.272	2.111
7	1.000	1.319	1.898
8	4.169	0	1.431
9	3.011	0	1.366
10	7.848	0	1.274
INLET			
11	1.298	0.714	1.038
12	1.281	0.734	1.036
13	15.969	0	1.608
14	15.286	0	1.598
15	10.426	0	1.513
16	5.615	0	1.385
17	3.198	0	1.278
18	1.787	0	1.176
19	1.564	0.470	1.066
20	1.484	0.550	1.058

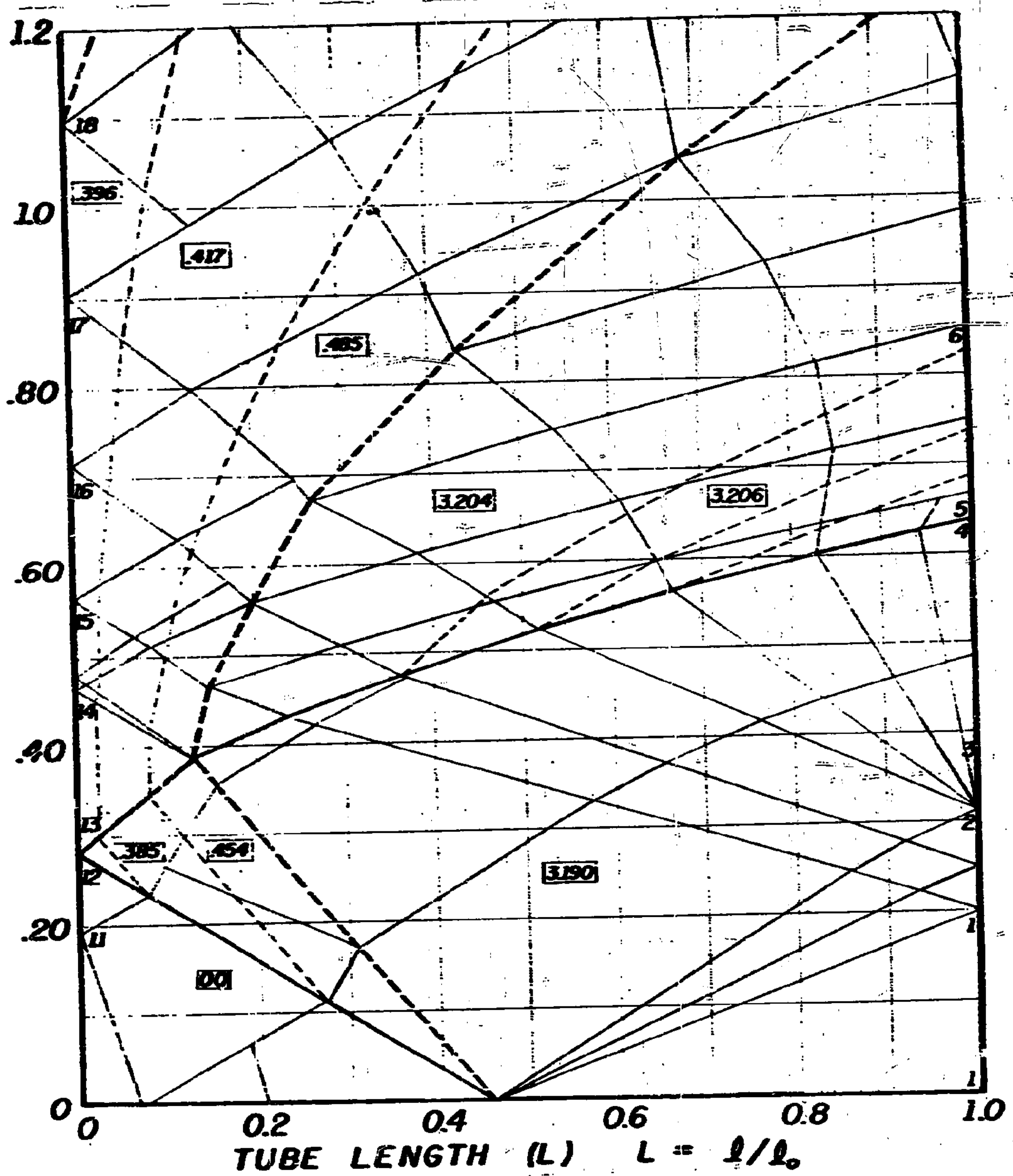

AVERAGE CONDITIONS BEFORE AND AFTER HEAT ADDITION

	BEFORE	AFTER
P =	2.394	11.501
θ =	1.499	7.201
S =	0.387	3.190

CHARACTERISTIC CYCLE PERFORMANCE

$SFC\left(\frac{LBS.\ FUEL/HR}{LBS.\ THRUST}\right) = 2.065,\ T/A\left(\frac{LBS.}{SQ.\ IN.}\right) = 15.93$

$\eta_c = 0.567 \qquad \eta_o = .123$

COMBUSTION CHAMBER MASS $(m/m_o) = 0.862$

FUEL-AIR RATIO - 1/31

CYCLE 3

MACH NUMBER = 0.95

WAVE ENGINE CYCLE
HEAT ADDITION MODE: CONSTANT VOLUME COMBUSTION

Fig. 10 C

CONFIDENTIAL

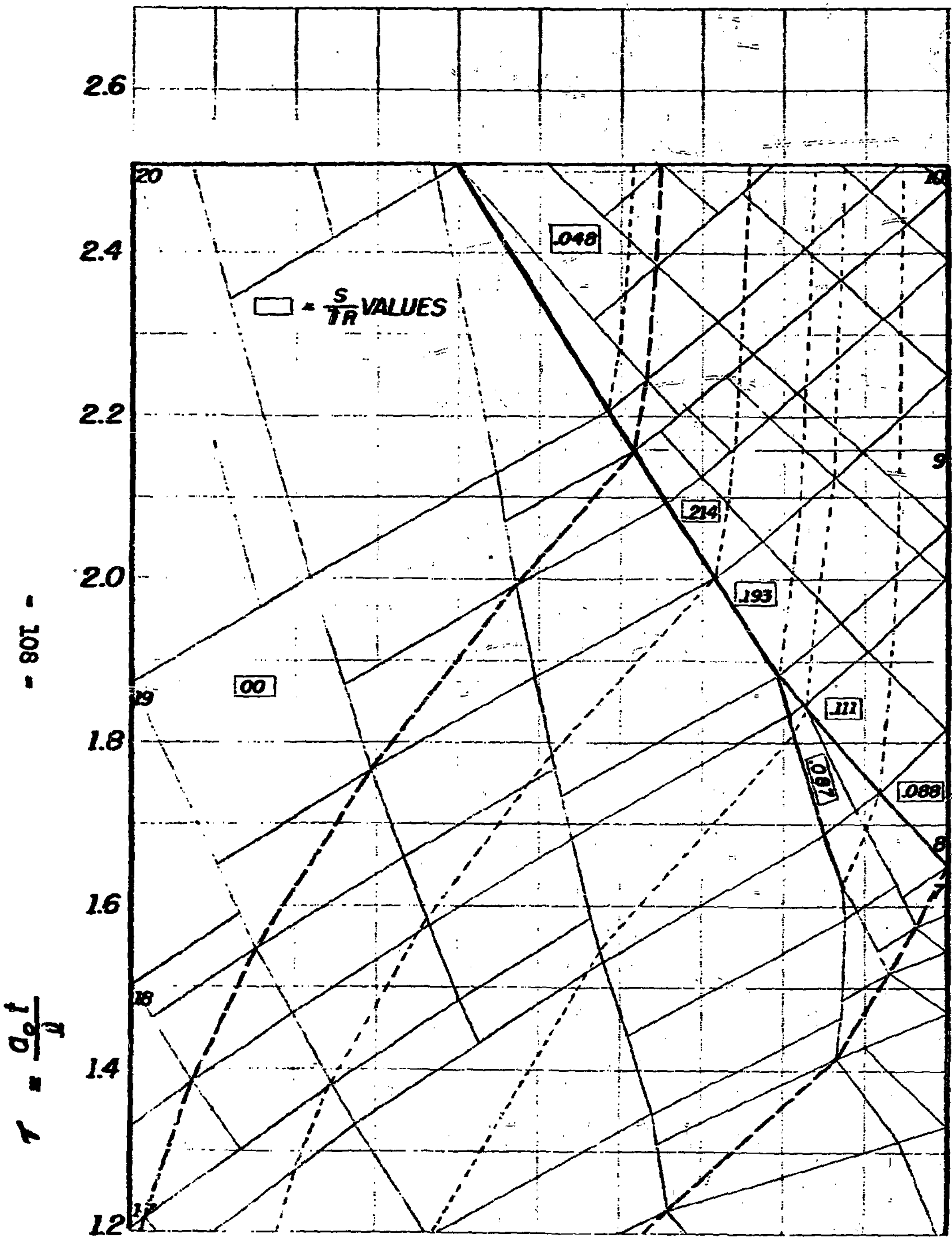

INLET AND EXIT CONDITIONS

POINT	P	u	d
	EXIT		
1	2.021	0	1.108
2	11.991	0	2.694
3	3.347	2.245	2.245
4	1.000	1.820	1.904
5	2.272	3.010	2.158
6	1.000	1.752	1.958
7	1.000	0.473	1.989
8	1.874	0	1.106
9	1.886	0	1.107
10	2.151	0	1.128
	INLET		
11	1.196	0.400	1.026
12	7.427	0	1.370
13	15.099	0	1.516
14	6.317	0	1.338
15	2.121	0	1.145
16	1.328	0	1.071
17	1.290	0.189	1.037
18	1.205	0.380	1.027
19	1.087	0.543	1.012
20	0.993	0.659	0.999

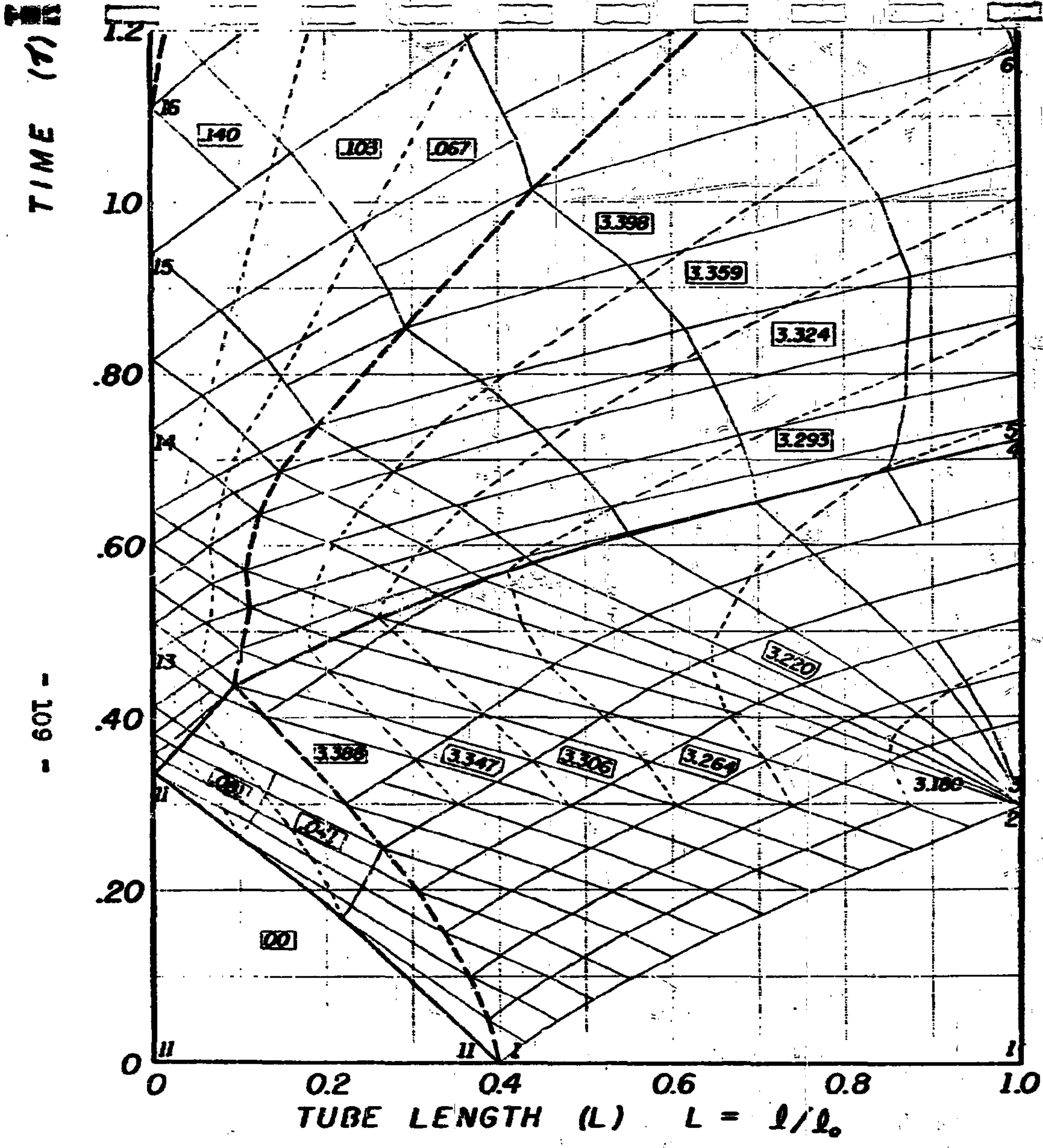

AVERAGE CONDITIONS BEFORE AND AFTER HEAT ADDITION

	BEFORE	AFTER
P =	2.021	11.991
θ =	1.278	7.256
S =	0.010	3.284

CHARACTERISTIC CYCLE PERFORMANCE

$SFC\left(\frac{\text{LBS. FUEL/HR.}}{\text{LBS. THRUST}}\right) = 1.881$, $T/A\left(\frac{\text{LBS.}}{\text{SQ. IN.}}\right) = 14.42$

$\eta_c = 0.98$ $\eta_o = .093$

COMBUSTION CHAMBER MASS $(m/m_o) = 0.988$

FUEL-AIR RATIO - $1/31$

CYCLE I

MACH NUMBER = 0.65

WAVE ENGINE CYCLE
HEAT ADDITION MODE: GRADUAL HEAT ADDITION

Fig. 11A

CONFIDENTIAL

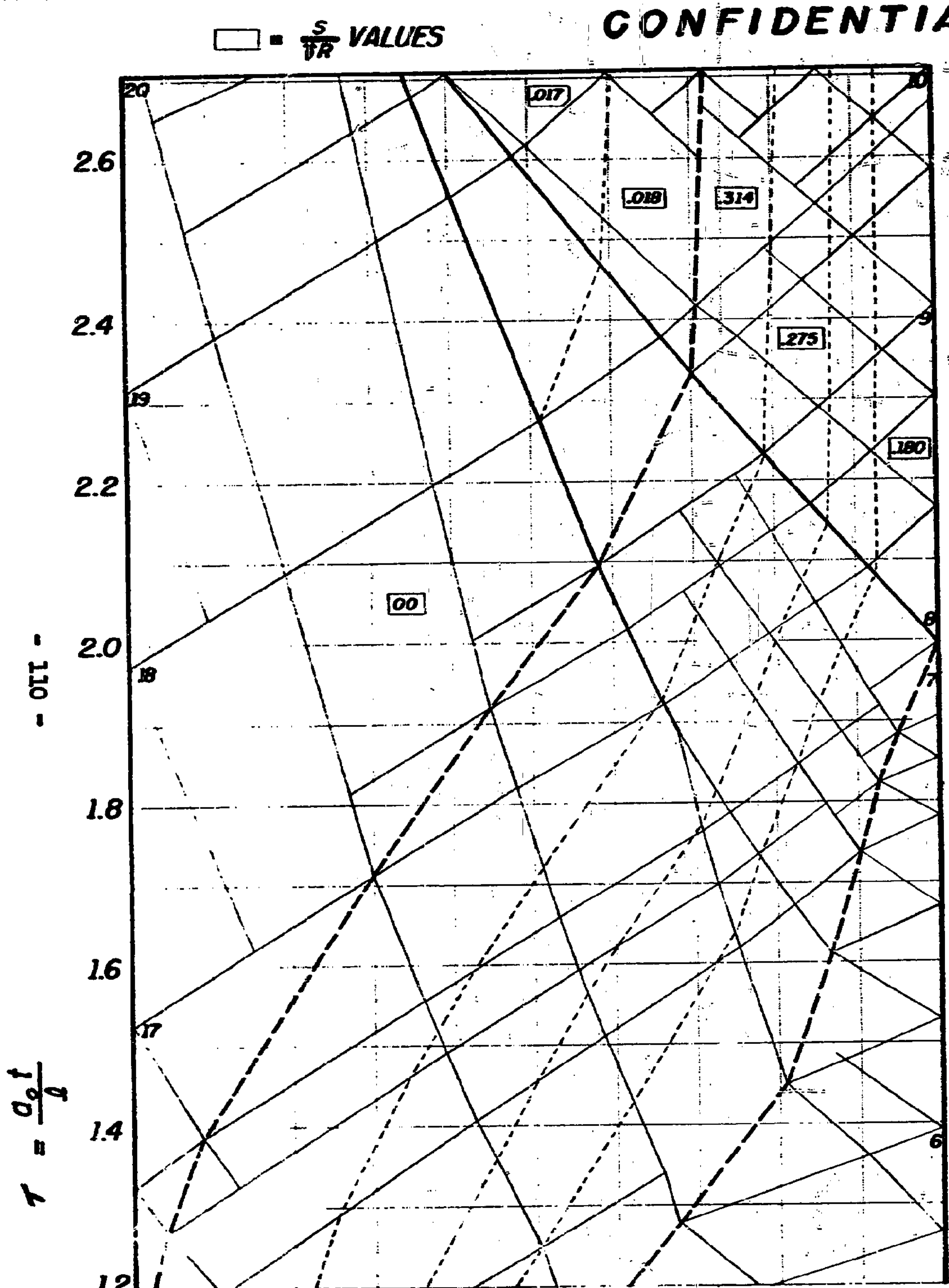

INLET AND EXIT CONDITIONS

POINT	P	u	a
EXIT			
1	1.998	0	1.131
2	11.486	0	2.704
3	3.204	2.253	2.253
4	1.004	1.933	1.933
5	2.167	3.071	2.172
6	1.000	0.752	1.970
7	1.000	0.444	2.004
8	1.776	0	1.111
9	2.065	0	1.135
10	2.256	0	1.150
INLET			
11	0.952	0.699	0.993
12	0.939	0.713	0.991
13	8.747	0	1.447
14	15.075	0	1.564
15	5.097	0	1.339
16	1.328	0	1.105
17	1.181	0.418	1.024
18	1.052	0.580	1.008
19	0.993	0.654	0.999
20	0.932	0.726	0.990

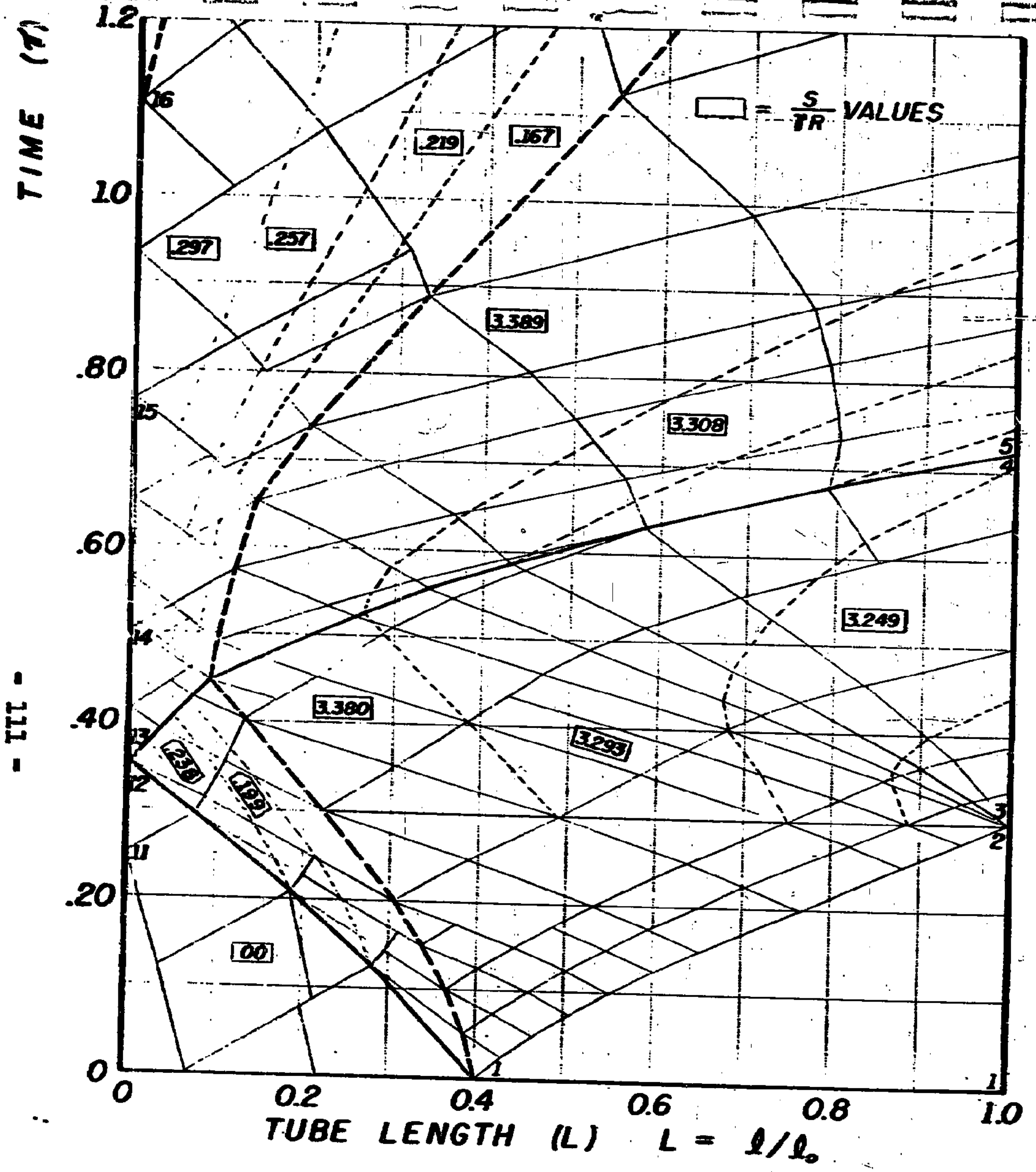

AVERAGE CONDITIONS BEFORE AND AFTER HEAT ADDITION

	BEFORE	AFTER
P =	1.998	11.486
θ =	1.280	7.312
S =	0.122	3.230

CHARACTERISTIC CYCLE PERFORMANCE

SFC $\left(\frac{\text{LBS. FUEL/HR.}}{\text{LBS. THRUST}}\right) = 1.855$, $T/A\left(\frac{\text{LBS.}}{\text{SQ. IN.}}\right) = 12.84$

$\eta_c = 0.78$ $\eta_o = 0.094$

COMBUSTION CHAMBER MASS $(m/m_o) = 0.937$

FUEL-AIR RATIO — 1/31

CYCLE 2

MACH NUMBER = 0.65

WAVE ENGINE CYCLE

HEAT ADDITION MODE: GRADUAL HEAT ADDITION

Fig. 11B

CONFIDENTIAL

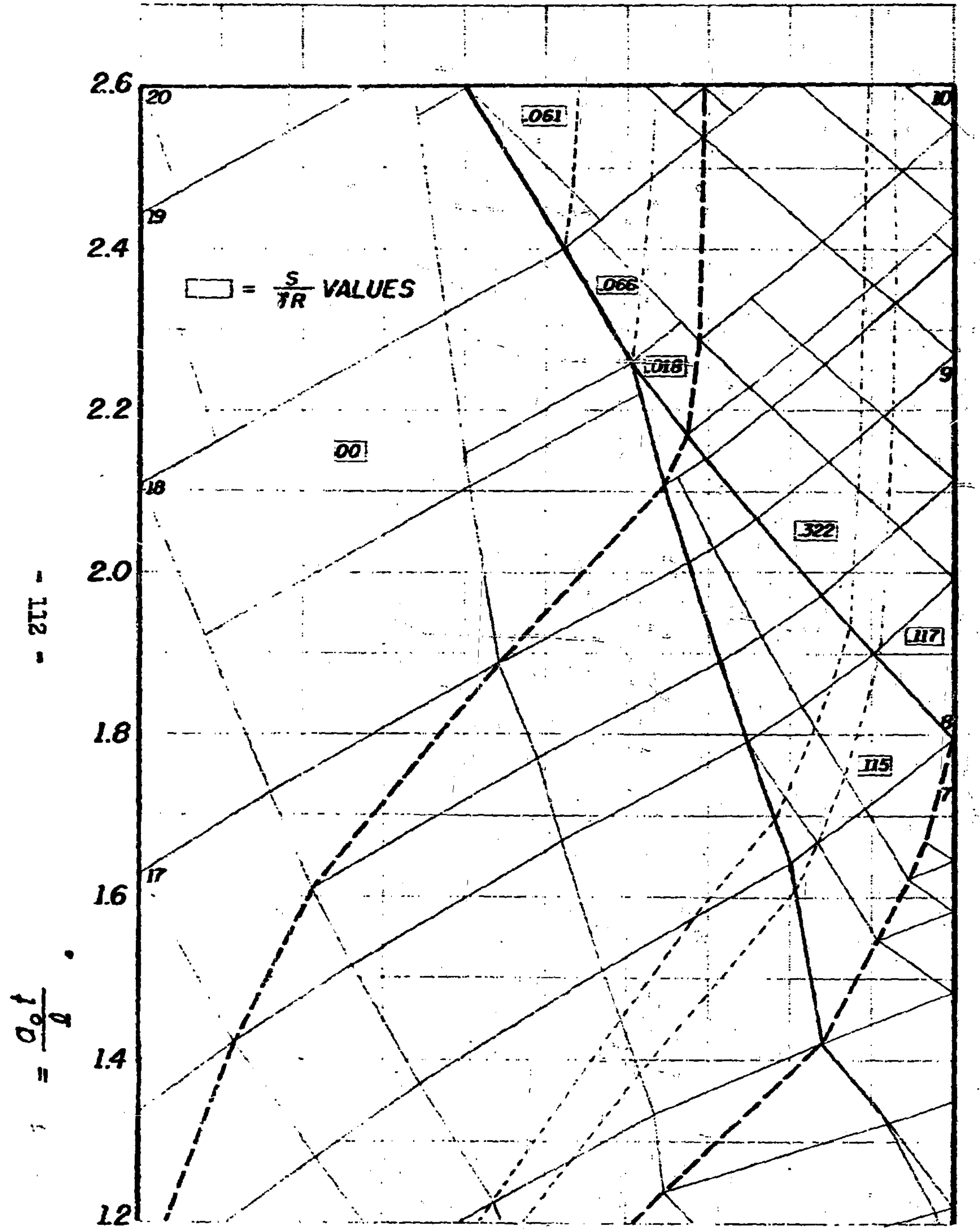

INLET AND EXIT CONDITIONS

POINT	P	u	a
EXIT			
1	2.189	0	1.154
2	12.185	0	2.696
3	3.404	2.247	2.247
4	1.038	1.927	1.927
5	2.128	2.960	2.146
6	1.000	1.775	1.983
7	1.000	0.224	1.983
8	1.356	0	1.055
9	1.978	0	1.113
10	2.159	0	1.127
INLET			
11	0.932	0.726	0.990
12	0.912	0.743	0.987
13	8.720	0	1.450
14	15.508	0	1.574
15	4.993	0	1.339
16	1.328	0	1.108
17	1.148	0.480	1.020
18	1.043	0.604	1.006
19	0.979	0.670	0.997
20	0.958	0.697	0.994

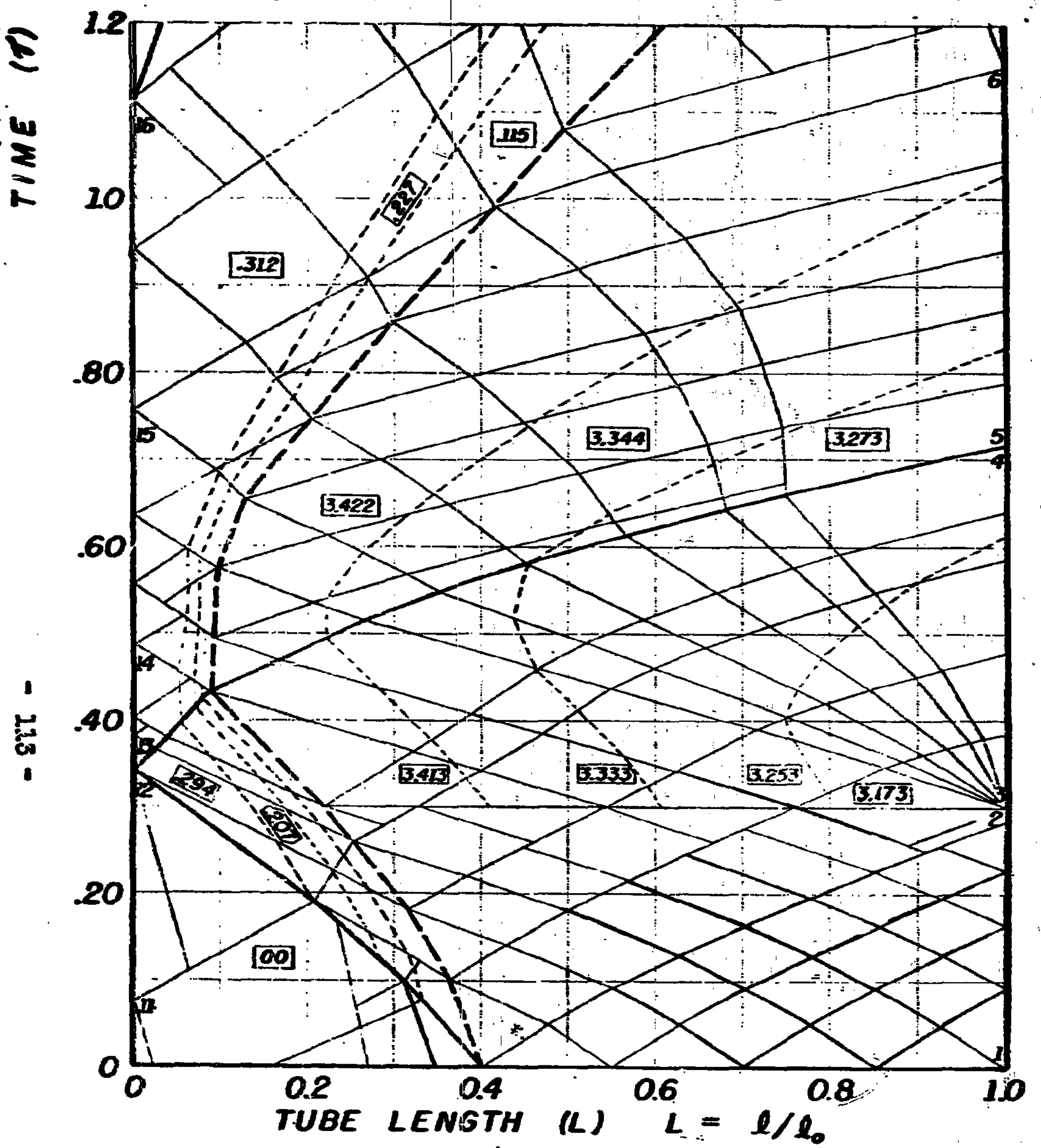

AVERAGE CONDITIONS BEFORE AND AFTER HEAT ADDITION

	BEFORE	AFTER
P =	2.189	12.185
θ =	1.332	7.268
S =	0.156	3.173

CHARACTERISTIC CYCLE PERFORMANCE

SFC $\left(\frac{\text{LBS. FUEL/HR.}}{\text{LBS. THRUST}}\right) = 1.807$, $T/A\left(\frac{\text{LBS.}}{\text{SQ. IN.}}\right) = 14.46$

$\eta_c = 0.75$ $\eta_o = 0.093$

COMBUSTION CHAMBER MASS $(m/m_o) = 0.986$

FUEL-AIR RATIO - 1/31

CYCLE 3

MACH NUMBER = 0.65

WAVE ENGINE CYCLE

HEAT ADDITION MODE: GRADUAL HEAT ADDITION

Fig. 11C

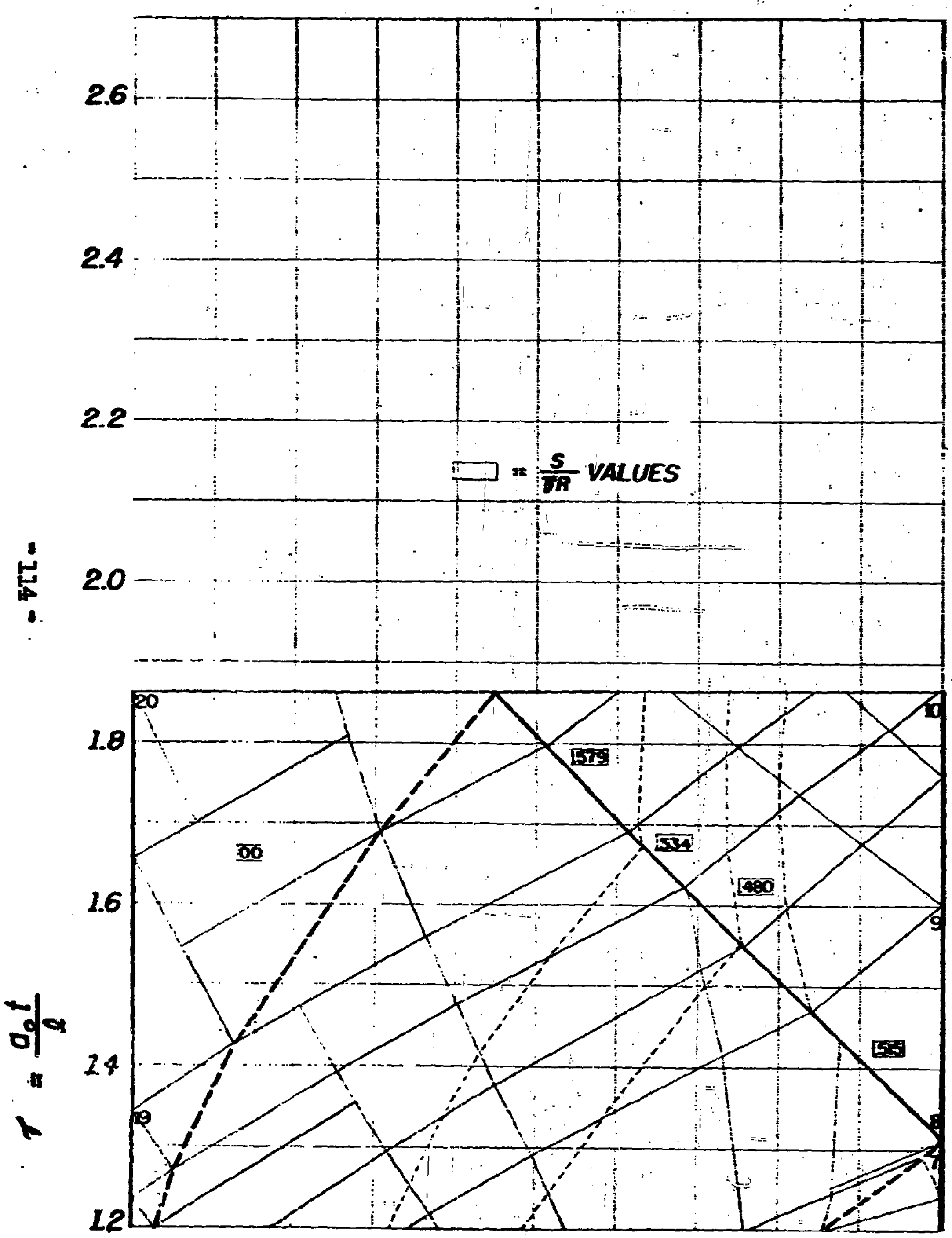

INLET AND EXIT CONDITIONS

POINT	P	u	a
EXIT			
1	3.290	0	1.214
2	13.857	0	2.668
3	3.863	2.223	2.223
4	1.538	1.949	1.949
5	1.367	1.943	1.943
6	2.925	3.070	2.180
7	1.000	1.270	1.917
8	4.410	0	1.334
9	2.250	0	1.211
10	2.237	0	1.210
INLET			
11	1.000	0.950	1.000
12	13.298	0	1.594
13	19.858	0	1.688
14	24.756	0	1.742
15	12.391	0	1.578
16	4.537	0	1.367
17	2.331	0	1.243
18	1.787	0	1.197
19	1.653	0.556	1.074
20	1.436	0.603	1.053

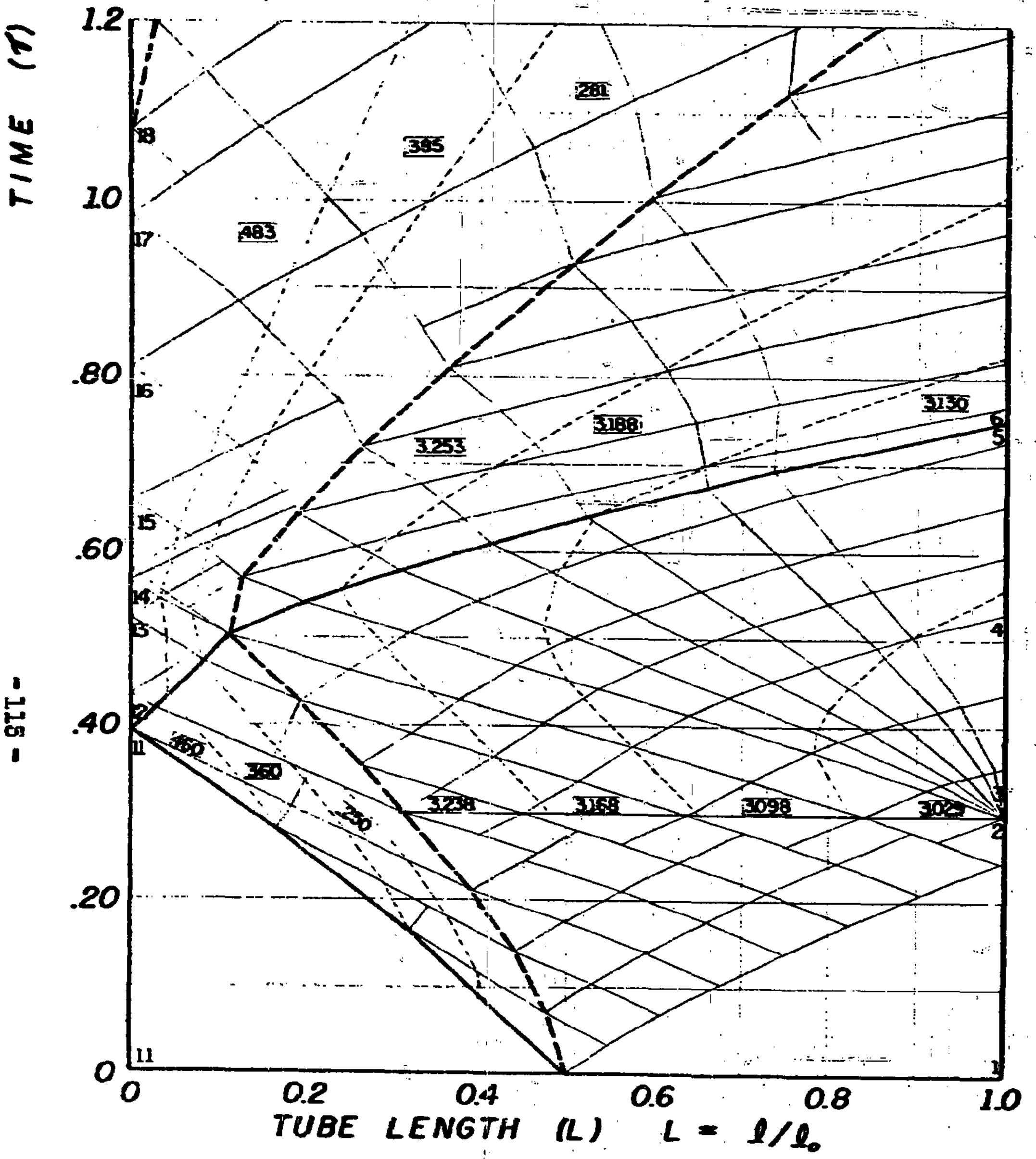

AVERAGE CONDITIONS BEFORE AND AFTER HEAT ADDITION

	BEFORE	AFTER
P =	3.290	13.857
θ =	1.474	7.118
S =	0.119	3.029

CHARACTERISTIC CYCLE PERFORMANCE

SFC $\left(\frac{\text{LBS. FUEL/HR.}}{\text{LBS. THRUST}}\right) = 1.932$, $T/A\left(\frac{\text{LBS.}}{\text{SQ. IN.}}\right) = 21.34$

$\eta_c = 0.855$, $\eta_o = .132$

COMBUSTION CHAMBER MASS $(m/m_o) = 1.116$

FUEL-AIR RATIO – $1/31$

CYCLE I

MACH NUMBER = 0.95

WAVE ENGINE CYCLE

HEAT ADDITION MODE: GRADUAL HEAT ADDITION

Fig. 12A

CONFIDENTIAL

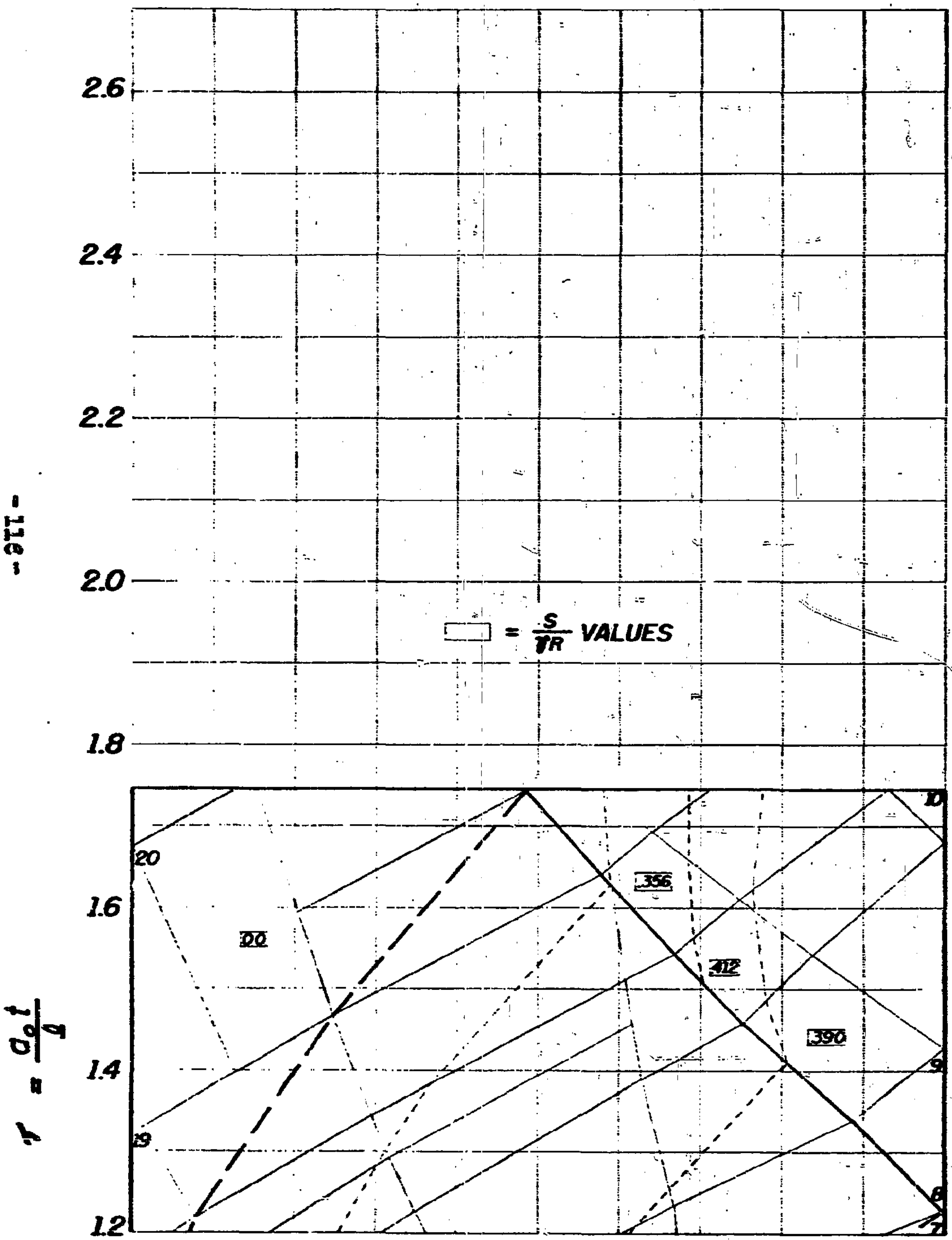

INLET AND EXIT CONDITIONS

POINT	P	u	a
EXIT			
1	2.331	0	1.254
2	11.131	0	2.726
3	3.110	2.272	2.272
4	1.384	2.064	2.064
5	2.280	2.820	2.220
6	1.646	2.159	2.159
7	1.000	1.446	2.010
8	5.336	0	1.370
9	2.825	0	1.251
10	2.050	0	1.195
INLET			
11	1.436	0.603	1.053
12	1.325	0.692	1.041
13	8.718	0	1.417
14	18.932	0	1.583
15	13.108	0	1.502
16	2.971	0	1.215
17	1.787	0	1.130
18	1.670	0.338	1.076
19	1.574	0.461	1.067
20	1.431	0.604	1.052

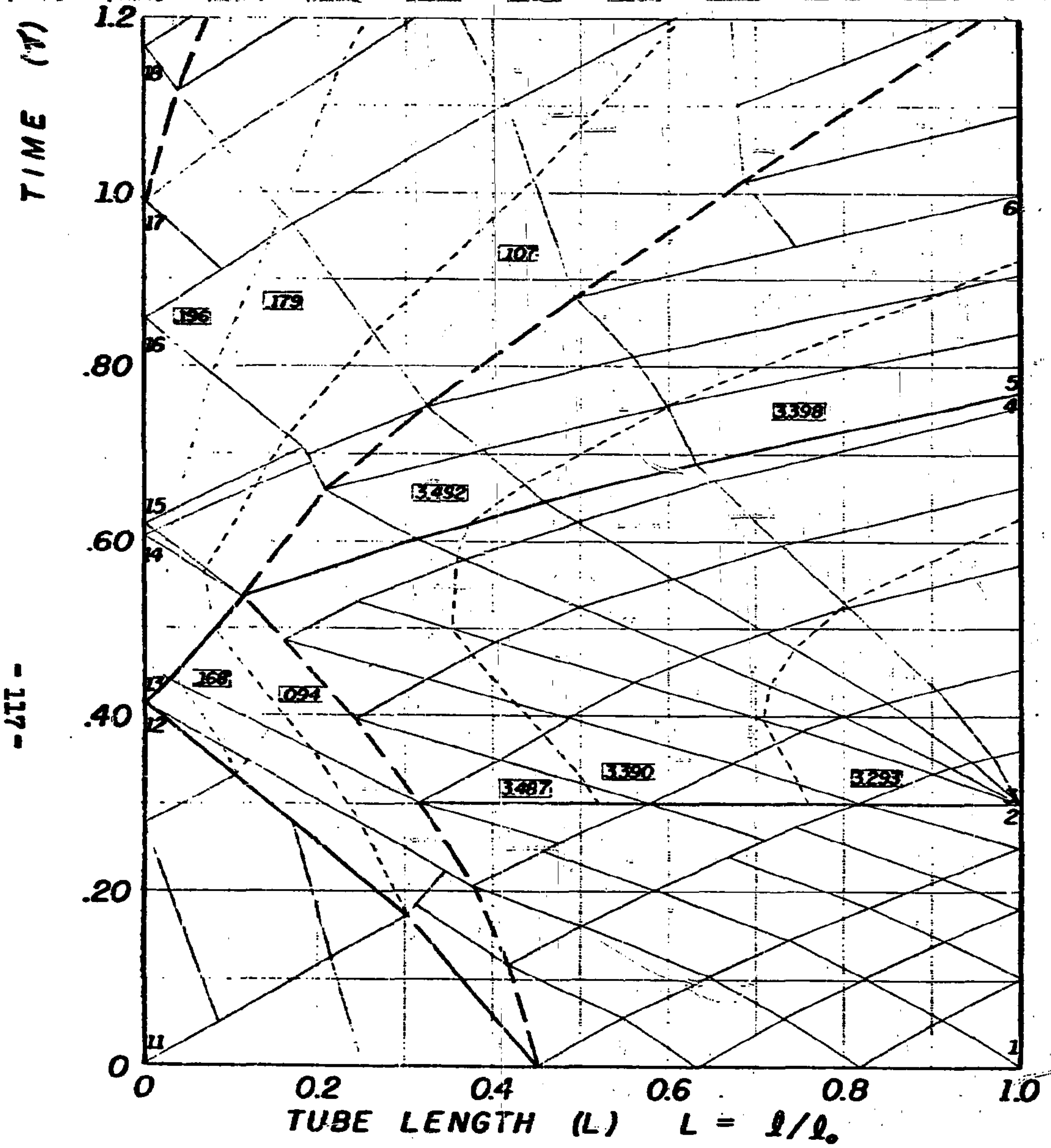

AVERAGE CONDITIONS BEFORE AND AFTER HEAT ADDITION

	BEFORE	AFTER
P =	2.331	11.131
θ =	1.572	7.431
S =	0.526	3.293

CHARACTERISTIC CYCLE PERFORMANCE

$SFC\left(\frac{LBS.\ FUEL/HR.}{LBS.\ THRUST}\right) = 1.892$, $T/A\left(\frac{LBS.}{SQ.\ IN.}\right) = 17.03$

$\eta_c = 0.478$ $\eta_o = 0.135$

COMBUSTION CHAMBER MASS $(m/m_o) = 0.816$

FUEL-AIR RATIO – $1/31$

CYCLE 2

MACH NUMBER = 0.95

WAVE ENGINE CYCLE

HEAT ADDITION MODE: GRADUAL HEAT ADDITION

Fig. 12B

CONFIDENTIAL

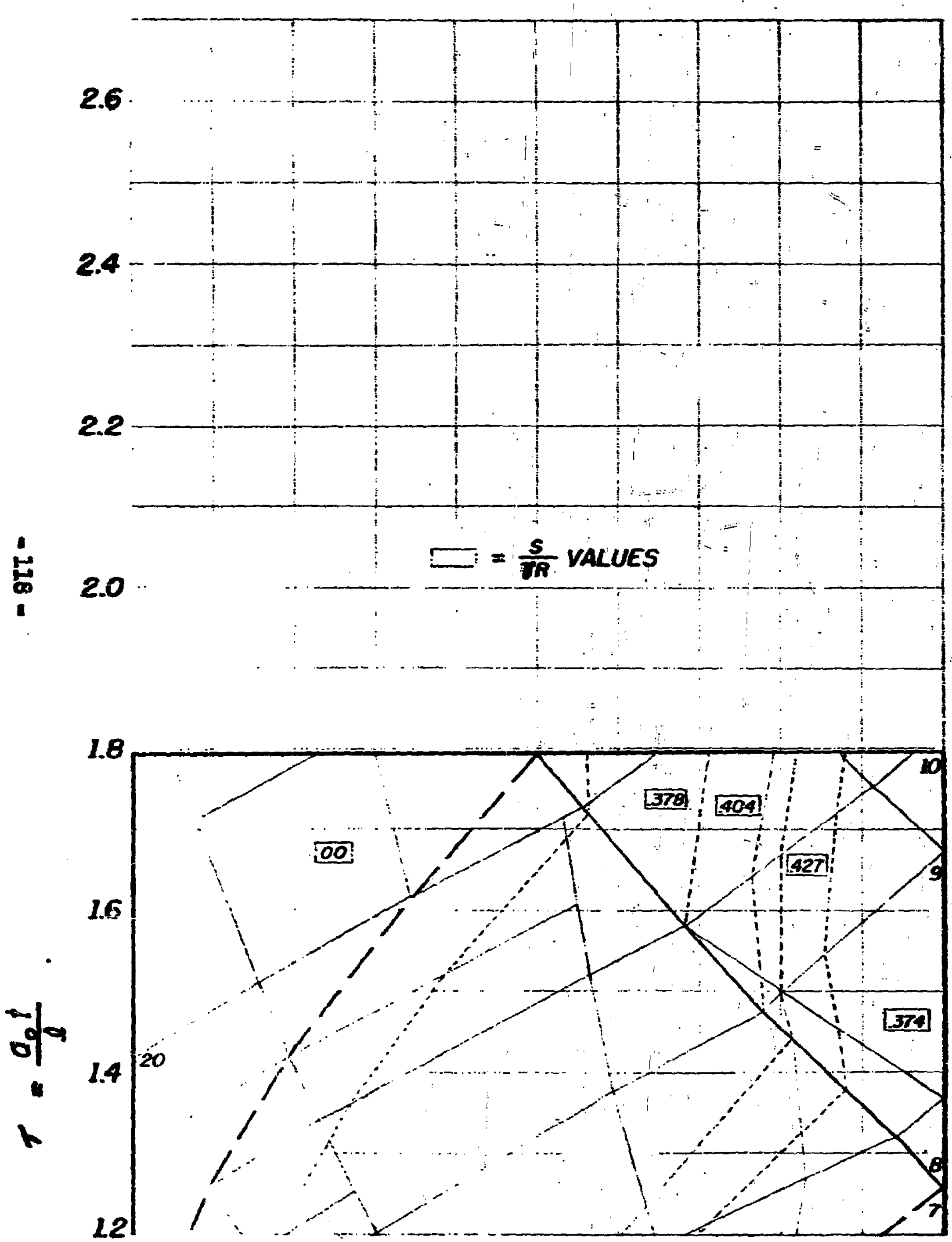

INLET AND EXIT CONDITIONS

POINT	P	u	a
EXIT			
1	2.419	0	1.227
2	11.406	0	2.697
3	3.188	2.248	2.248
4	1.308	2.023	2.023
5	2.318	2.890	2.201
6	1.501	2.112	2.112
7	1.000	1.291	1.992
8	4.586	0	1.326
9	1.692	0	1.150
10	2.201	0	1.194
INLET			
11	1.334	0.687	1.042
12	1.298	0.714	1.038
13	10.751	0	1.478
14	16.482	0	1.571
15	16.189	0	1.567
16	10.803	0	1.479
17	3.254	0	1.246
18	1.787	0	1.144
19	1.703	0.272	1.079
20	1.544	0.485	1.064

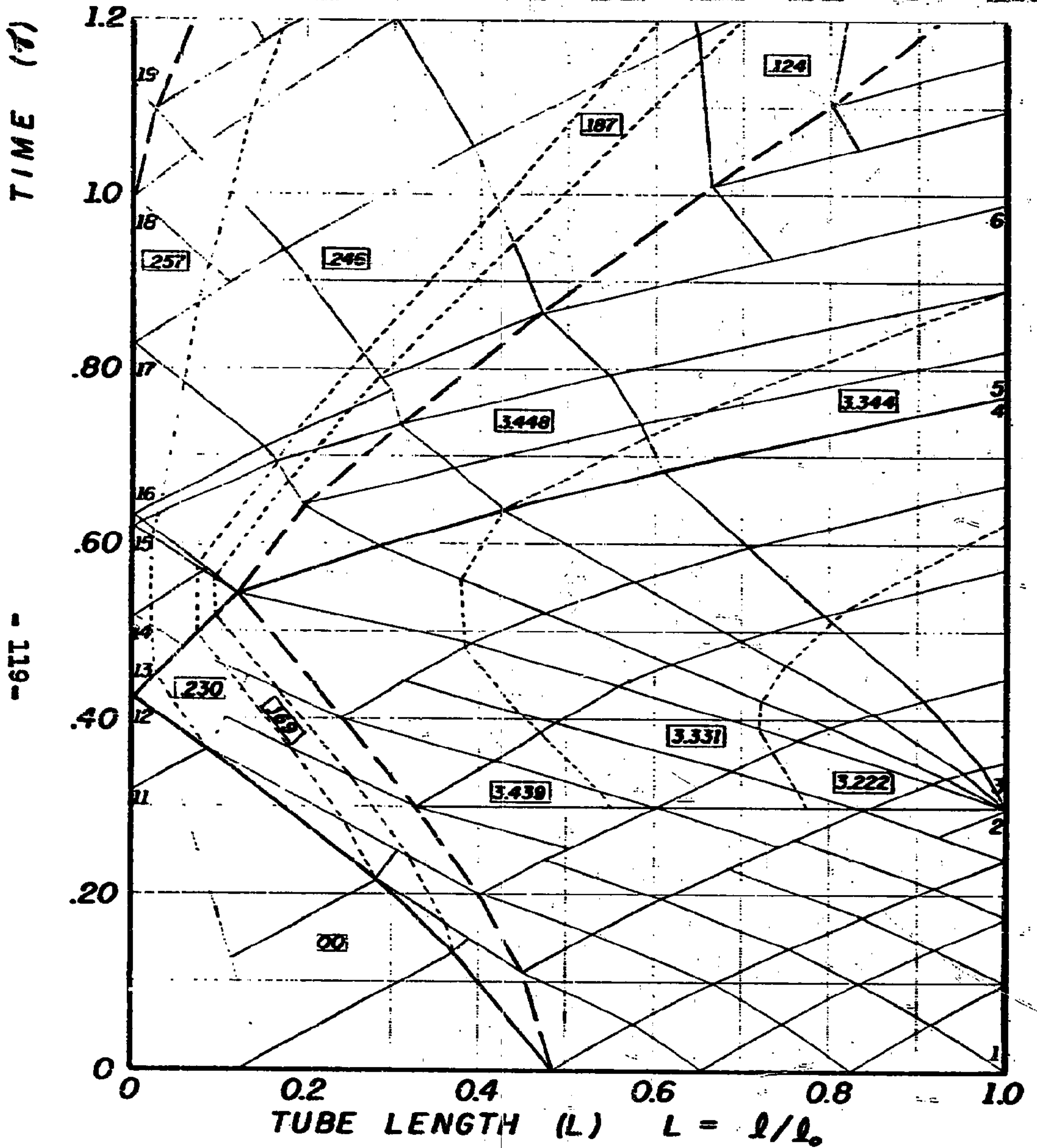

AVERAGE CONDITIONS BEFORE AND AFTER HEAT ADDITION

	BEFORE	AFTER
P =	2.419	11.406
θ =	1.505	7.274
S =	0.390	3.222

CHARACTERISTIC CYCLE PERFORMANCE

SFC $\left(\frac{\text{LBS. FUEL/HR.}}{\text{LBS. THRUST}}\right) = 1.983$, $T/A\left(\frac{\text{LBS.}}{\text{SQ. IN.}}\right) = 16.02$

$\eta_c = 0.568$ $\eta_o = .128$

COMBUSTION CHAMBER MASS $(m/m_o) = 0.828$

FUEL-AIR RATIO – 1/31

CYCLE 3

MACH NUMBER = 0.95

WAVE ENGINE CYCLE

HEAT ADDITION MODE: GRADUAL HEAT ADDITION

Fig. 12C

CONFIDENTIAL

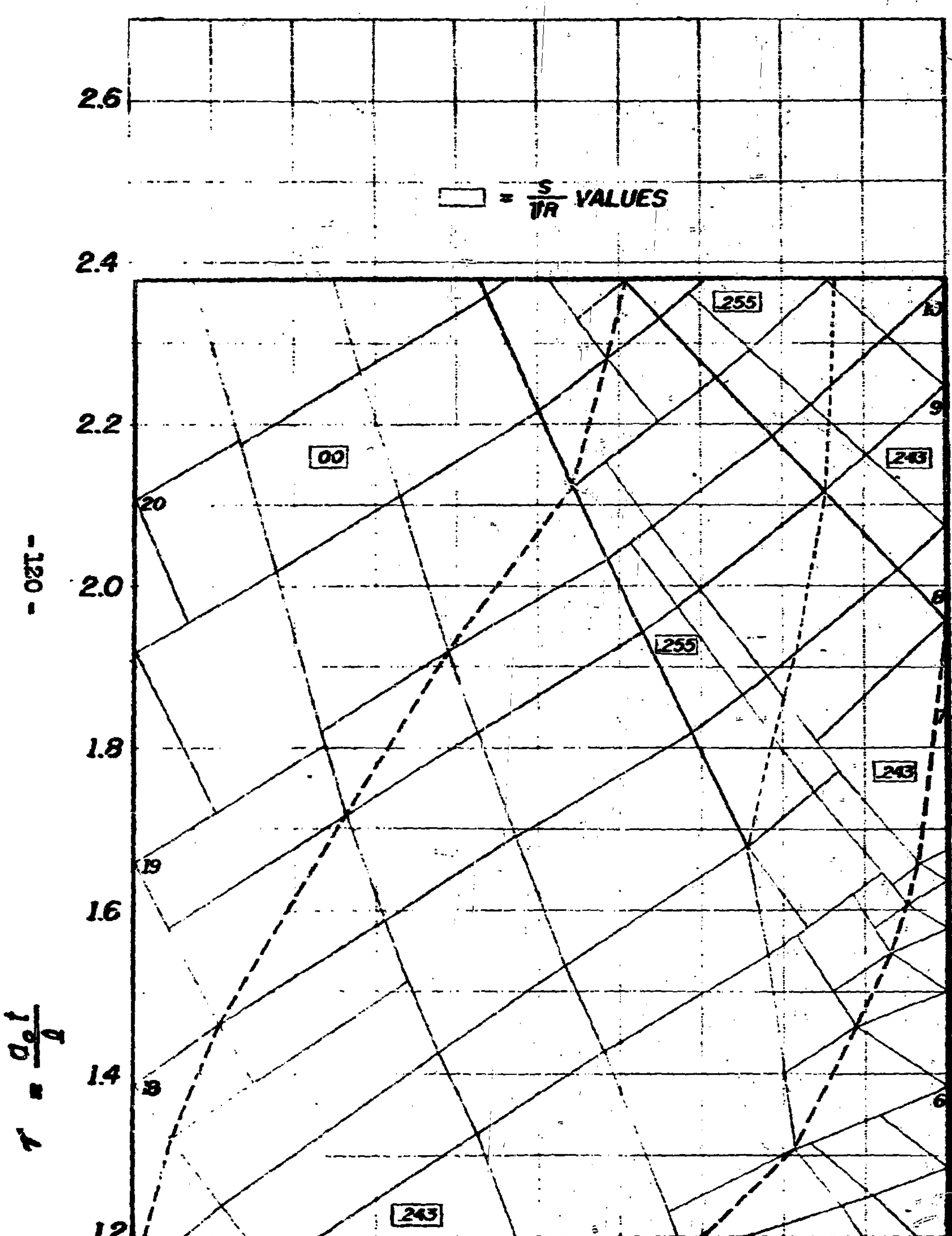

INLET AND EXIT CONDITIONS

POINT	P	u	a
EXIT			
1	6.682	0	2.585
2	1.9190	0	2.163
3	1.000	0.962	1.971
4	2.456	2.330	2.264
5	1.155	2.025	2.025
6	1.000	0.414	1.984
7	1.000	0.077	1.984
8	1.106	0	1.065
9	1.478	0	1.110
10	1.544	0	1.117
INLET.			
11	1.000	0	1.000
12	10.815	0	1.475
13	5.669	0	1.345
14	3.033	0	1.230
15	2.816	0	1.217
16	1.344	0	1.095
17	1.000	0	1.050
18	0.938	0.306	0.991
19	0.862	0.452	0.980
20	0.784	0.570	0.966

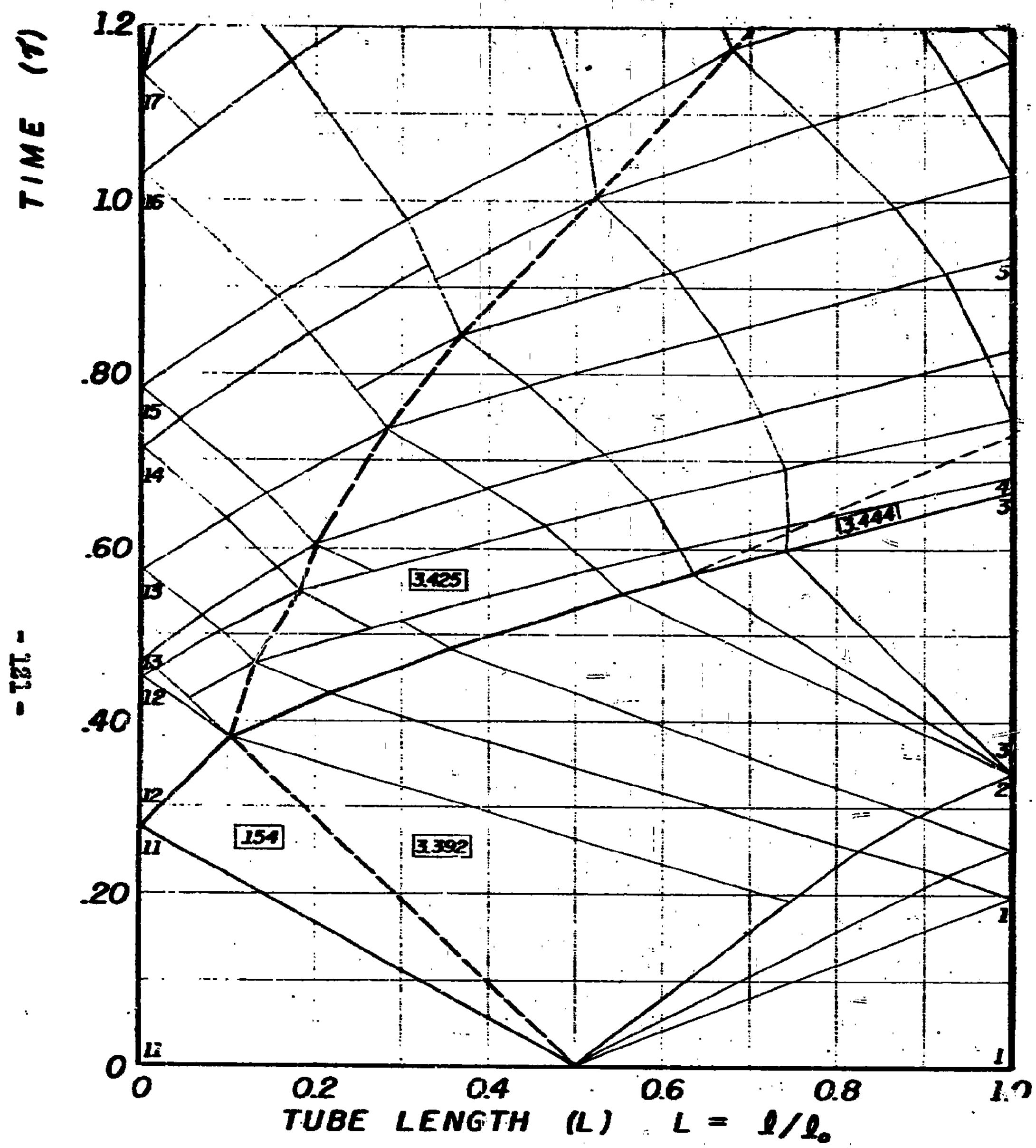

AVERAGE CONDITIONS BEFORE AND AFTER HEAT ADDITION

	BEFORE	AFTER
P =	1.000	6.682
θ =	1.000	6.682
S =	0	3.392

CHARACTERISTIC CYCLE PERFORMANCE

SFC $\left(\frac{\text{LBS. FUEL/HR}}{\text{LBS. THRUST}}\right) = 1.872$, $T/A\left(\frac{\text{LBS.}}{\text{SQ. IN.}}\right) = 7.73$

$\eta_c = 1.00$ $\eta_o =$ ——

COMBUSTION CHAMBER MASS $(m/m_0) = 0.500$

FUEL-AIR RATIO - 1/31

CYCLE 1

MACH NUMBER = 0

WAVE ENGINE CYCLE

HEAT ADDITION MODE: CONSTANT VOLUME COMBUSTION

Fig. 13A

CONFIDENTIAL

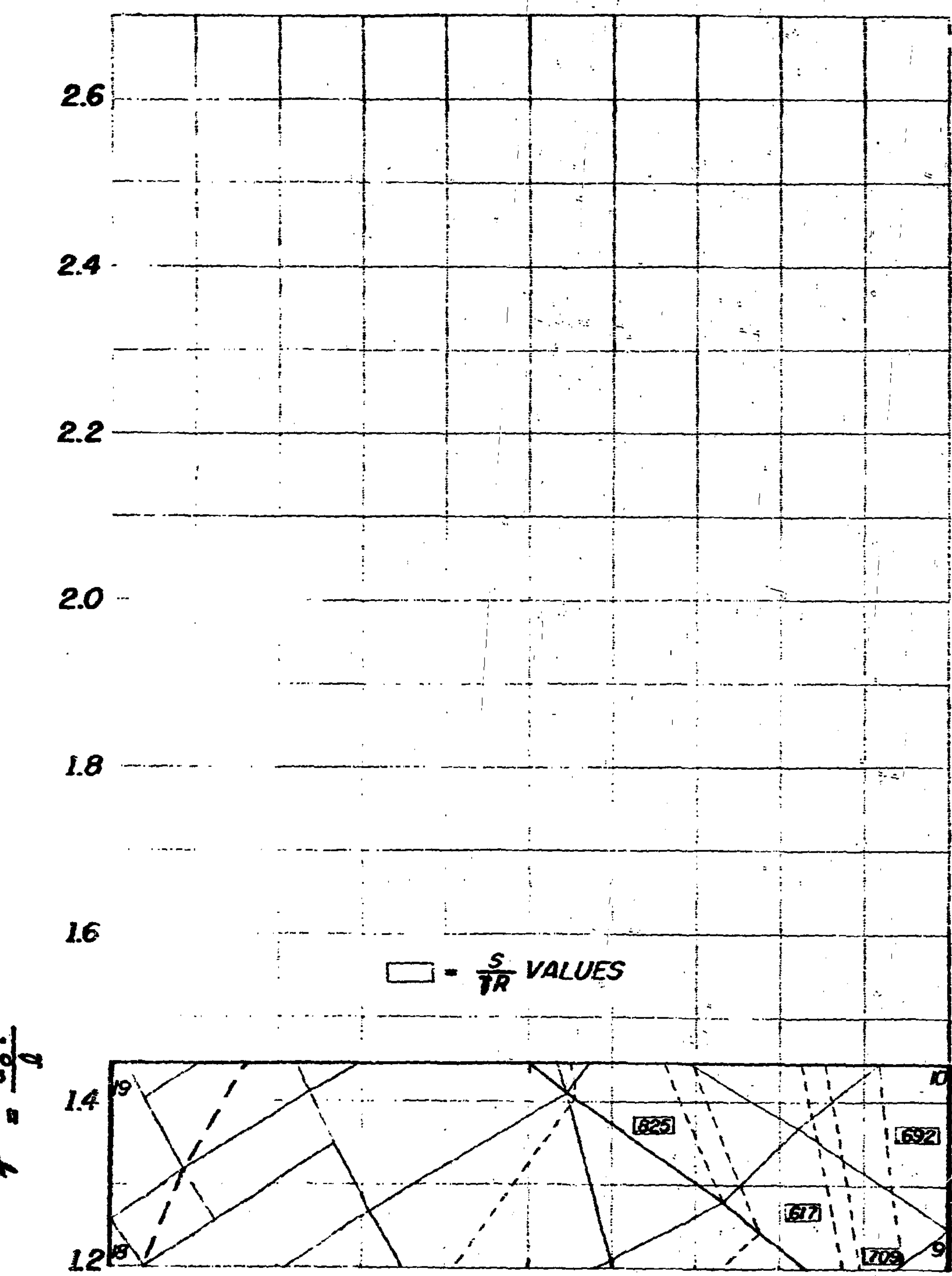

INLET AND EXIT CONDITIONS

POINT	P	u	a
EXIT			
1	8.453	0	2.635
2	2.798	0	2.250
3	1.000	1.536	1.943
4	1.000	1.562	1.943
5	1.000	1.260	1.943
6	1.522	2.066	2.066
7	1.000	1.684	1.953
8	6.188	0	1.490
9	2.736	0	1.326
10	1.841	0	1.253
INLET			
11	0.708	0.684	0.952
12	12.092	0	1.588
13	12.525	0	1.596
14	5.261	0	1.410
15	2.932	0	1.297
16	1.692	0	1.199
17	1.000	0	1.112
18	0.938	0.295	0.991
19	0.862	0.440	0.980
20			

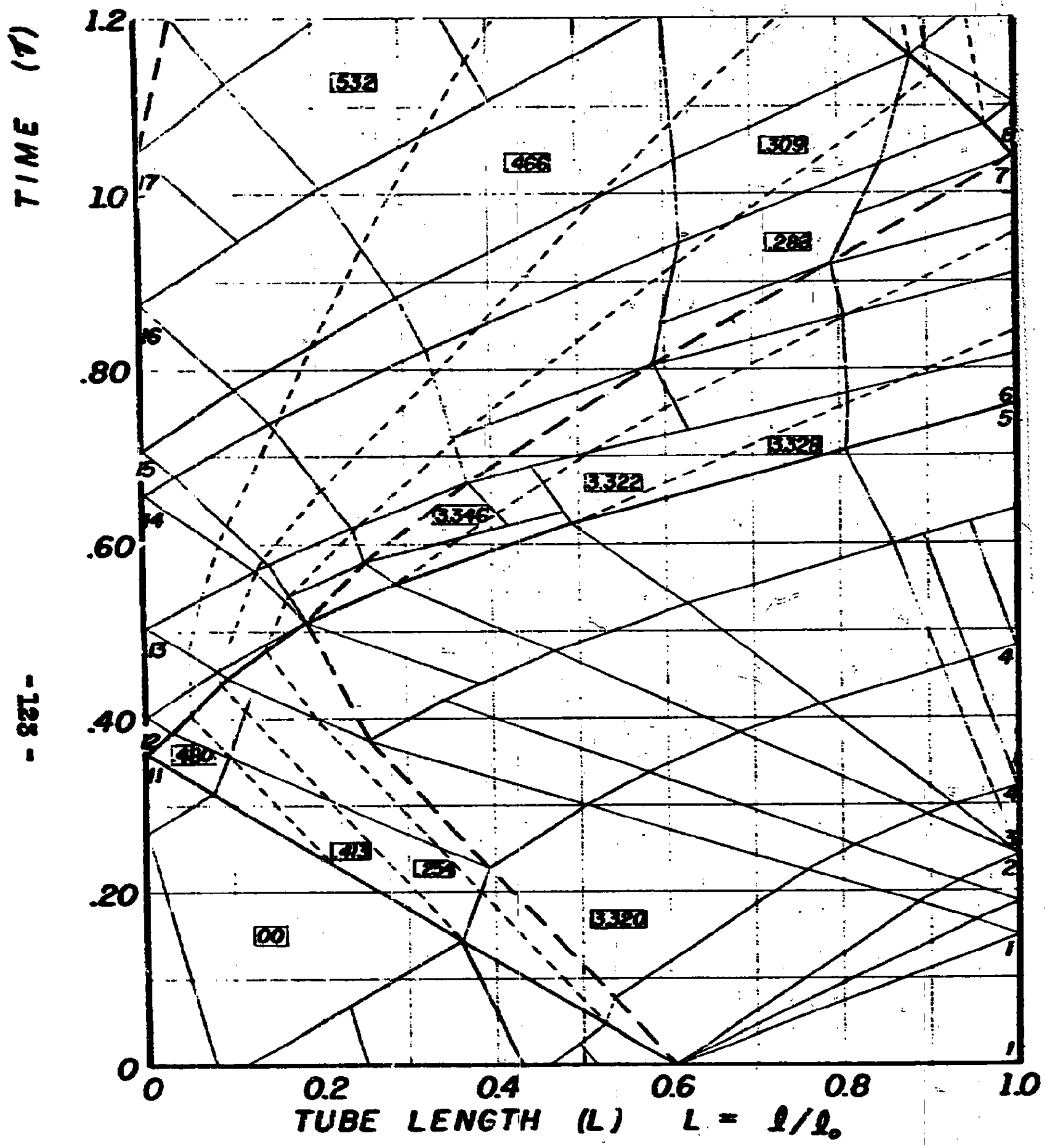

AVERAGE CONDITIONS BEFORE AND AFTER HEAT ADDITION

	BEFORE	AFTER
P =	1.514	8.453
θ =	1.244	6.946
S =	0.248	3.320

CHARACTERISTIC CYCLE PERFORMANCE

$SFC\left(\frac{\text{LBS. FUEL/HR.}}{\text{LBS. THRUST}}\right) = 1.949$, $T/A\left(\frac{\text{LBS.}}{\text{SQ. IN.}}\right) = 11.67$

$\eta_c = 0.516$ $\eta_o =$ —

COMBUSTION CHAMBER MASS $(m/m_o) = 0.477$

FUEL-AIR RATIO - 1/31

CYCLE 2

MACH NUMBER = 0

WAVE ENGINE CYCLE
HEAT ADDITION MODE: CONSTANT VOLUME COMBUSTION

Fig. 13B

CONFIDENTIAL

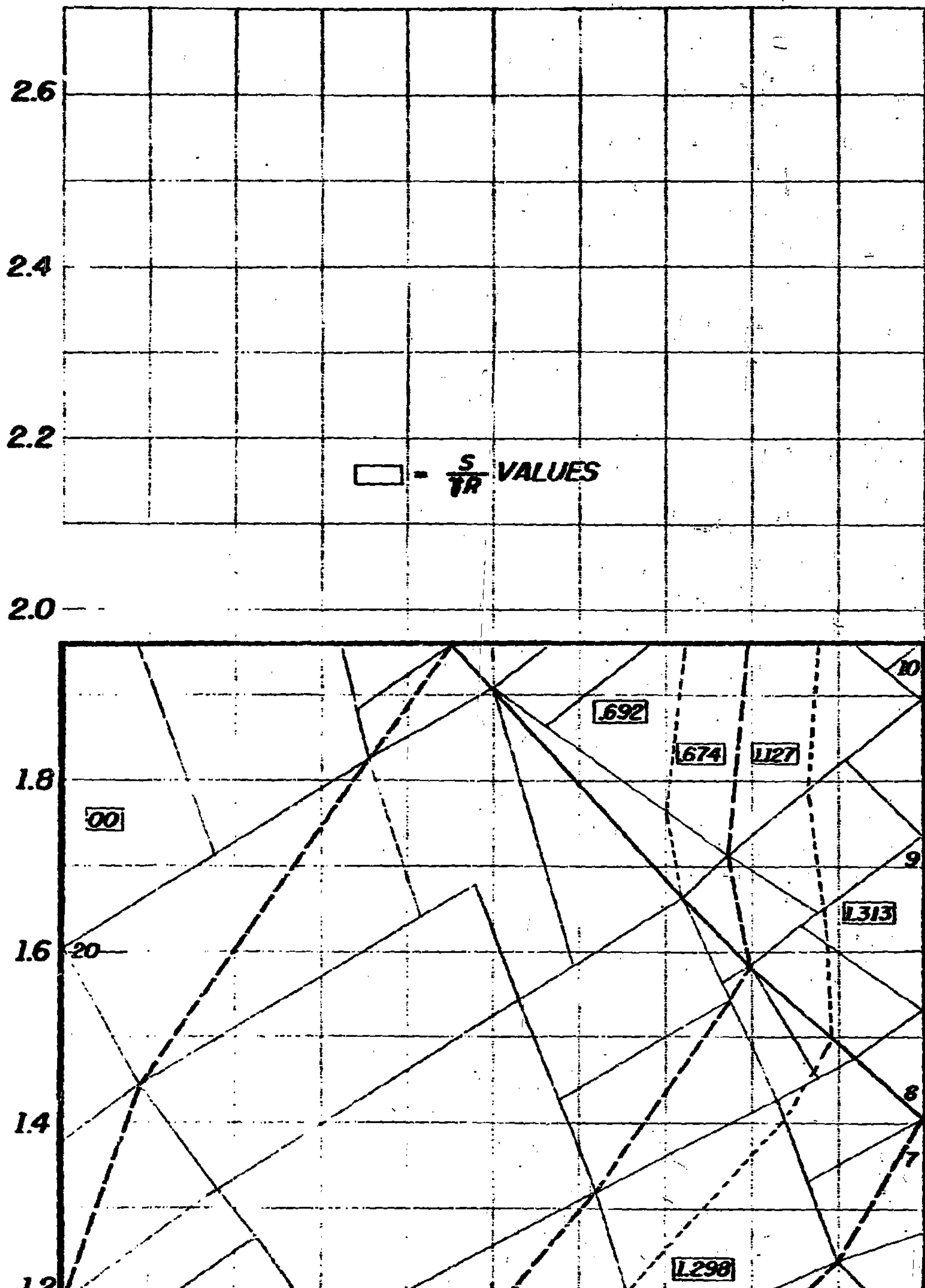

INLET AND EXIT CONDITIONS

POINT	P	u	a
EXIT			
1	8.126	0	2.701
2	1.756	0	2.170
3	1.000	0.840	2.002
4	1.000	1.397	2.002
5	2.490	2.816	2.306
6	1.176	2.054	2.054
7	1.000	0.576	2.013
8	1.798	0	1.414
9	1.314	0	1.352
10	1.025	0	1.305
INLET			
11	0.881	0.422	0.982
12	0.808	0.545	0.970
13	13.434	0	1.643
14	13.959	0	1.652
15	10.586	0	1.588
16	6.778	0	1.490
17	4.606	0	1.410
18	2.581	0	1.298
19	1.000	0	1.134
20	0.873	0.438	0.981

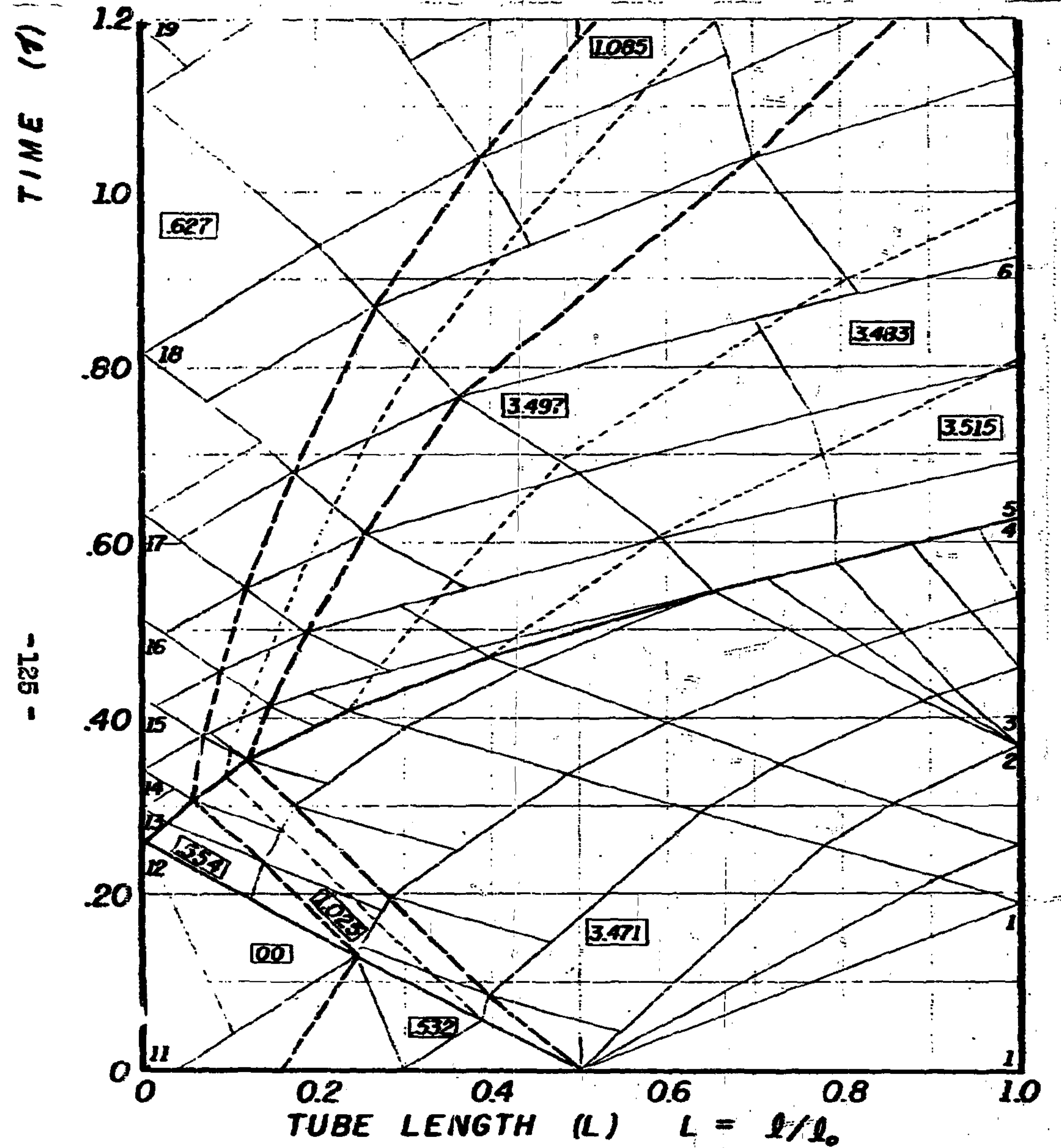

AVERAGE CONDITIONS BEFORE AND AFTER HEAT ADDITION

	BEFORE	AFTER
P =	1.796	8.126
θ =	1.612	7.294
S =	0.776	3.471

CHARACTERISTIC CYCLE PERFORMANCE

$SFC\left(\frac{LBS.\ FUEL/HR.}{LBS.\ THRUST}\right) = 1.673$, $T/A\left(\frac{LBS.}{SQ.\ IN.}\right) = 11.69$

$\eta_c = 0.298$ $\eta_o =$ ——

COMBUSTION CHAMBER MASS $(m/m_o) = 0.557$

FUEL-AIR RATIO - $1/31$

CYCLE 3

MACH NUMBER = 0

WAVE ENGINE CYCLE

HEAT ADDITION MODE: CONSTANT VOLUME COMBUSTION

Fig. 13C

CONFIDENTIAL

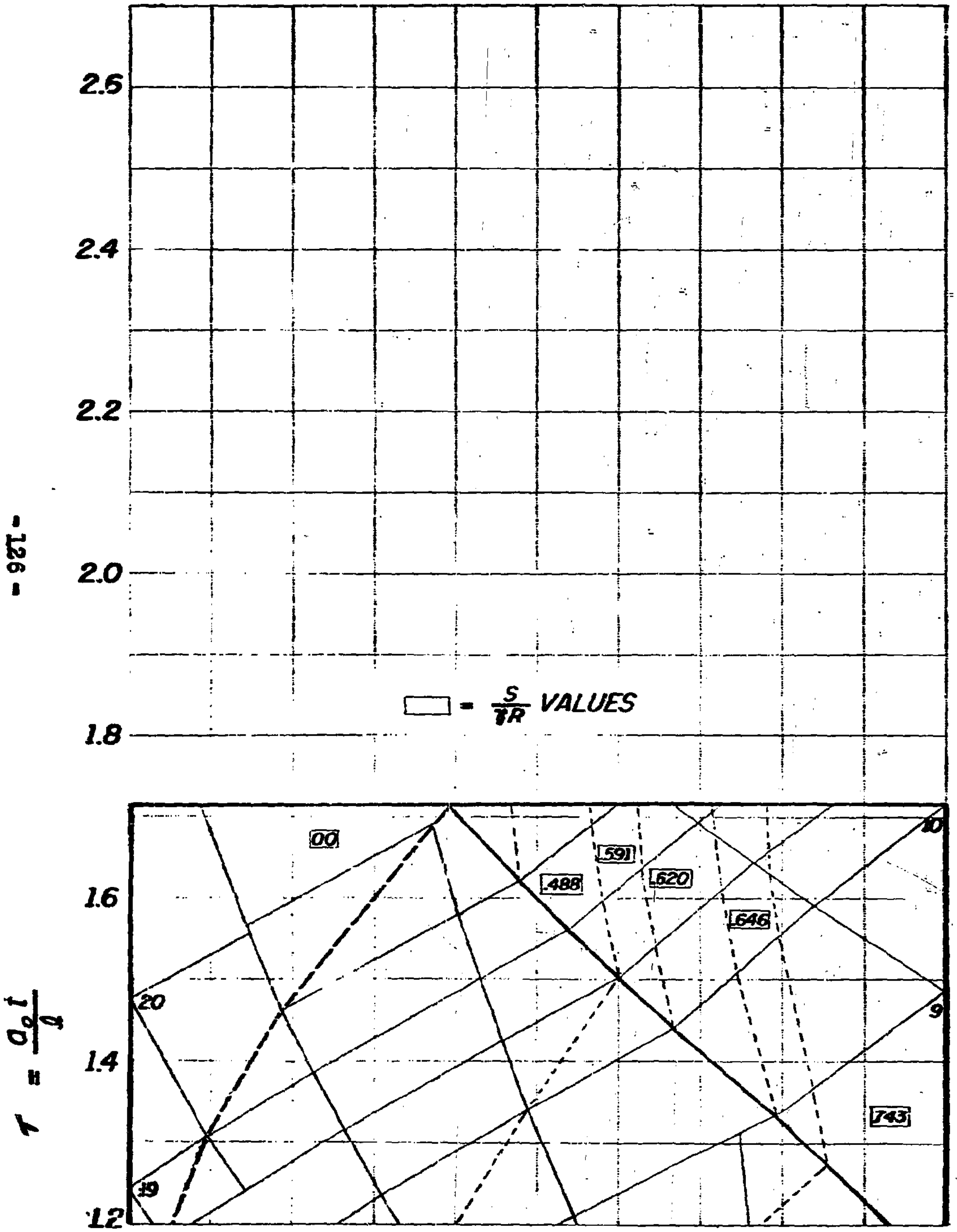

INLET AND EXIT CONDITIONS

POINT	P	u	a
EXIT			
1	11.120	0	2.686
2	4.038	0	2.324
3	1.127	1.937	1.937
4	1.213	1.958	1.958
5	2.307	2.925	2.159
6	1.712	2.198	2.066
7	1.000	1.452	1.912
8	4.676	0	1.476
9	2.556	0	1.354
10	1.744	0	1.282
INLET			
11	1.356	0.668	1.044
12	1.290	0.720	1.037
13	15.241	0	1.590
14	15.107	0	1.588
15	11.451	0	1.526
16	5.158	0	1.562
17	2.675	0	1.240
18	1.787	0	1.171
19	1.664	0.342	1.076
20	1.534	0.505	1.063

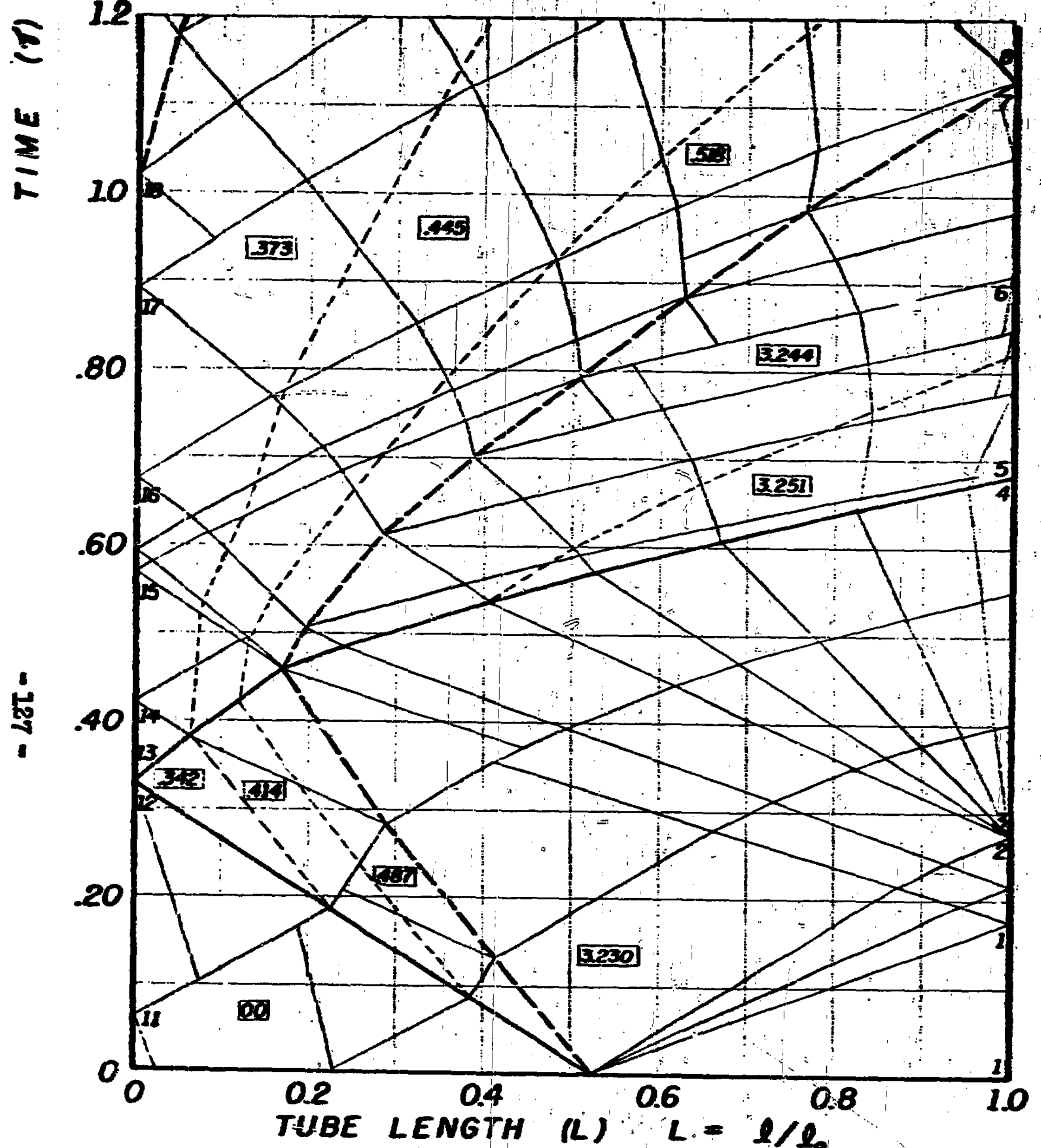

AVERAGE CONDITIONS BEFORE AND AFTER HEAT ADDITION

	BEFORE	AFTER
P =	2.334	11.120
θ =	1.514	7.216
S =	0.433	3.230

CHARACTERISTIC CYCLE PERFORMANCE

SFC $\left(\frac{\text{LBS. FUEL/HR.}}{\text{LBS. THRUST}}\right) = 2.303$, $T/A \left(\frac{\text{LBS.}}{\text{SQ. IN.}}\right) = 12.77$

$\eta_c = 0.532$ $\eta_o = 0.111$

COMBUSTION CHAMBER MASS $(m/m_o) = 0.732$

FUEL-AIR RATIO - 1/31

CYCLE 3

MACH NUMBER = 0.95

WAVE ENGINE CYCLE

HEAT ADDITION MODE: CONSTANT VOLUME COMBUSTION

Fig. 14A

CONFIDENTIAL

CONFIDENTIAL

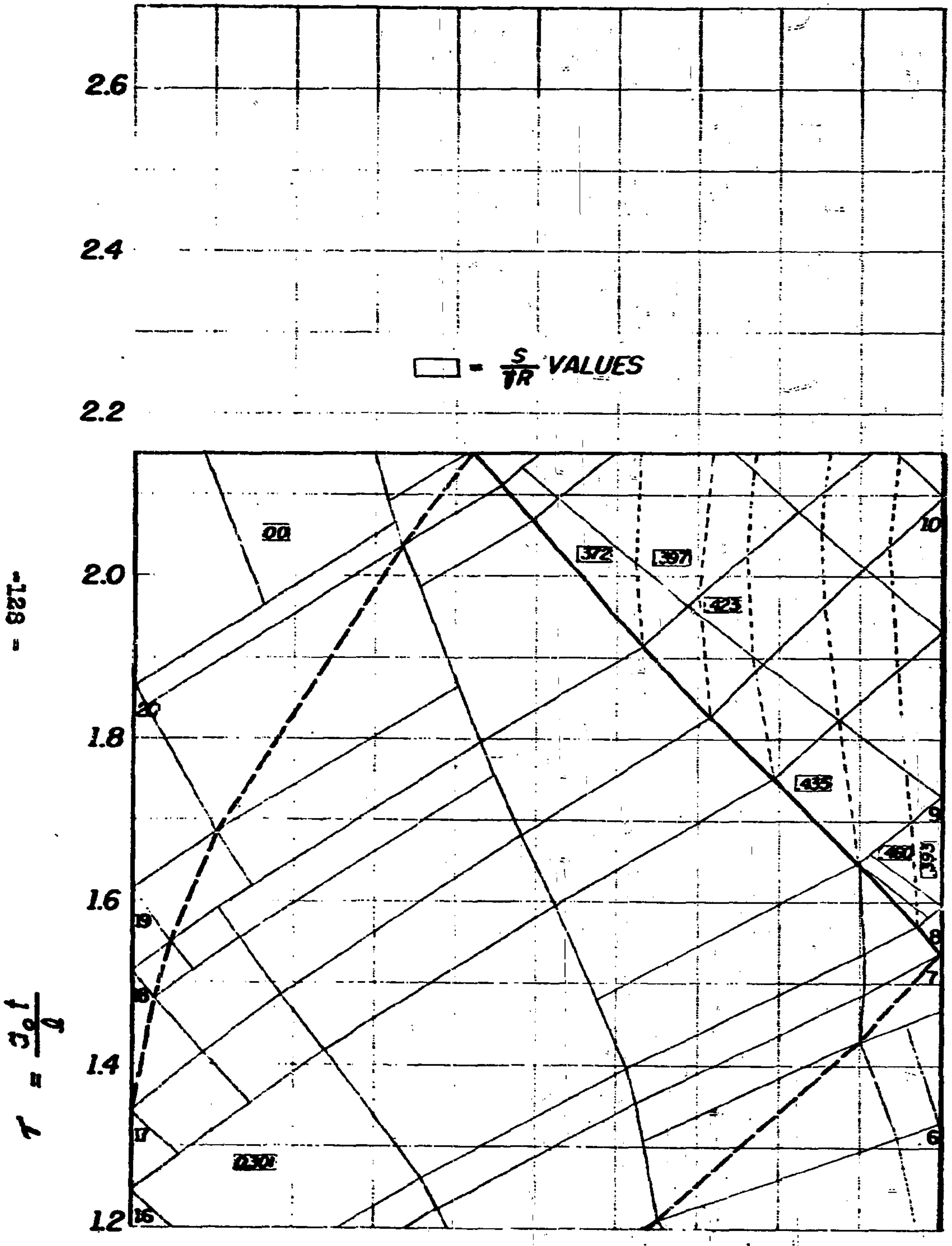

INLET AND EXIT CONDITIONS

POINT	P	u	a
	EXIT		
1	7.973	0	2.102
2	2.956	0	1.824
3	1.000	1.305	1.563
4	2.000	2.127	1.734
5	1.524	1.799	1.668
6	1.000	1.358	1.570
7	1.000	0.917	1.570
8	3.023	0	1.267
9	2.165	0	1.208
10	1.299	0	1.123
	INLET		
11	1.000	0.650	1.000
12	9.832	0	1.824
13	7.642	0	1.420
14	4.276	0	1.307
15	3.095	0	1.248
16	1.632	0	1.139
17	1.328	0	1.106
18	1.281	0.222	1.036
19	1.238	0.320	1.031
20	1.157	0.456	1.021

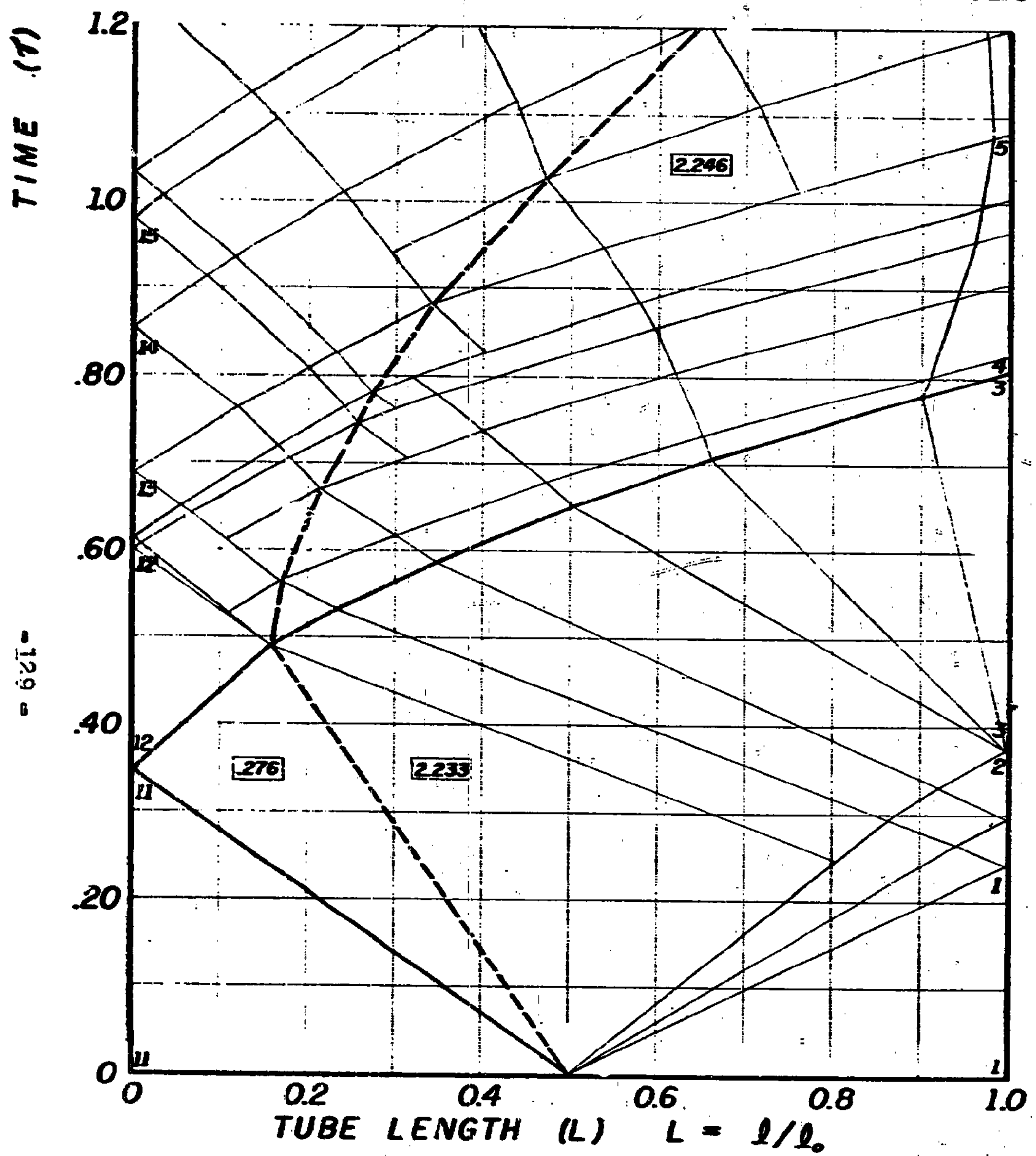

AVERAGE CONDITIONS BEFORE AND AFTER HEAT ADDITION

	BEFORE	AFTER
P =	2.333	7.973
θ =	1.296	4.420
S =	0.043	2.233

CHARACTERISTIC CYCLE PERFORMANCE

SFC $\left(\frac{\text{LBS. FUEL/HR.}}{\text{LBS. THRUST}}\right) = 1.638$, $T/A\left(\frac{\text{LBS.}}{\text{SQ. IN.}}\right) = 9.74$

$\eta_c = 0.93$ $\eta_o = 0.106$

COMBUSTION CHAMBER MASS $(m/m_o) = 0.90$

FUEL-AIR RATIO - $1/56$

CYCLE 1

MACH NUMBER 0.65

WAVE ENGINE CYCLE

HEAT ADDITION MODE: CONSTANT VOLUME COMBUSTION

Fig. 15A

CONFIDENTIAL

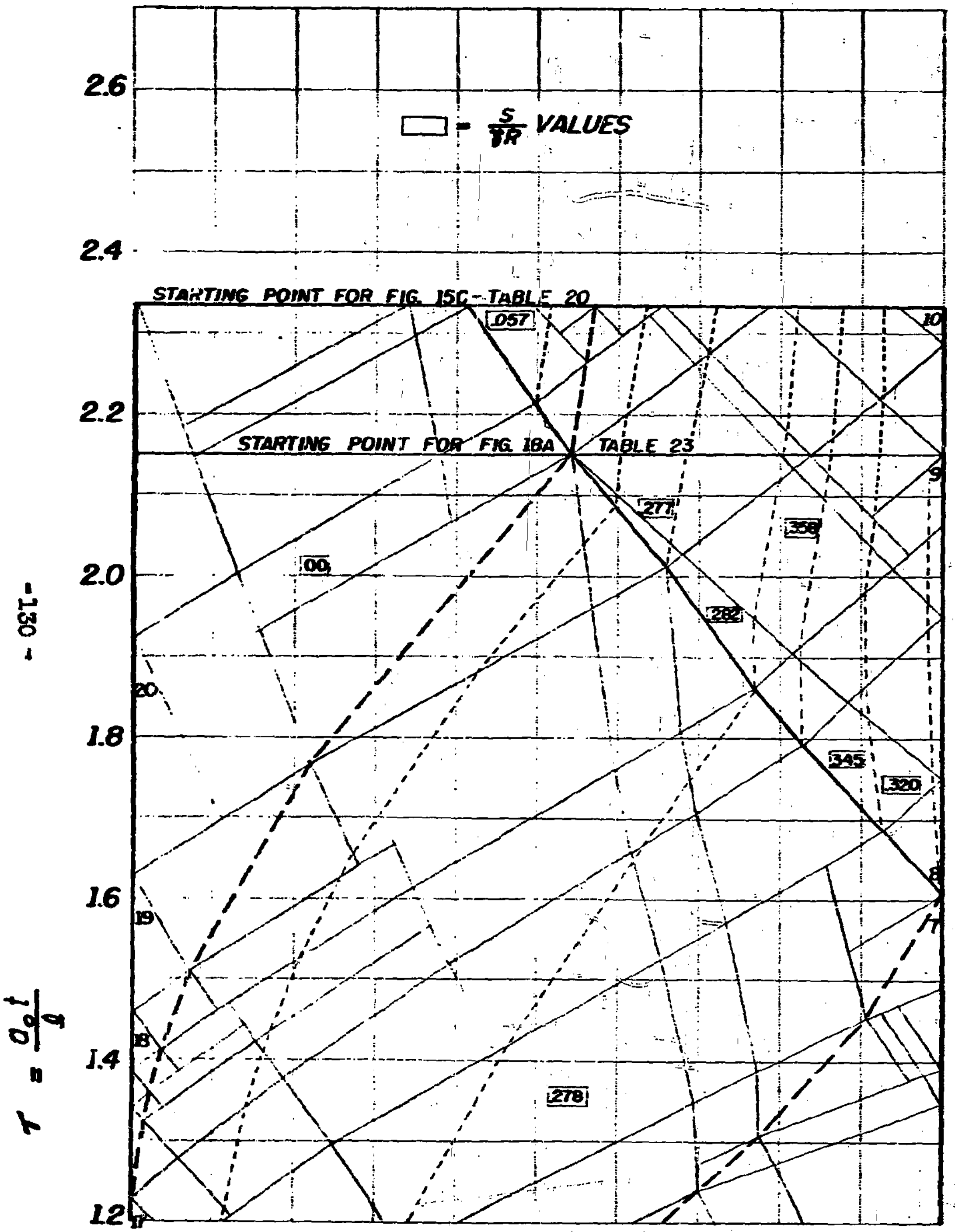

INLET AND EXIT CONDITIONS

POINT	P	u	a
EXIT			
1	5.646	0	2.123
2	2.465	0	1.886
3	1.000	1.139	1.658
4	1.000	1.306	1.658
5	1.345	1.671	1.731
6	1.055	1.672	1.672
7	1.000	0.607	1.659
8	2.129	0	1.185
9	1.653	0	1.143
10	1.970	0	1.172
INLET			
11	1.028	0.614	1.004
12	7.056	0	1.374
13	6.774	0	1.366
14	5.329	0	1.320
15	2.799	0	1.204
16	1.698	0	1.121
17	1.328	0	1.082
18	1.255	0.288	1.033
19	1.181	0.416	1.024
20	1.102	0.529	1.014

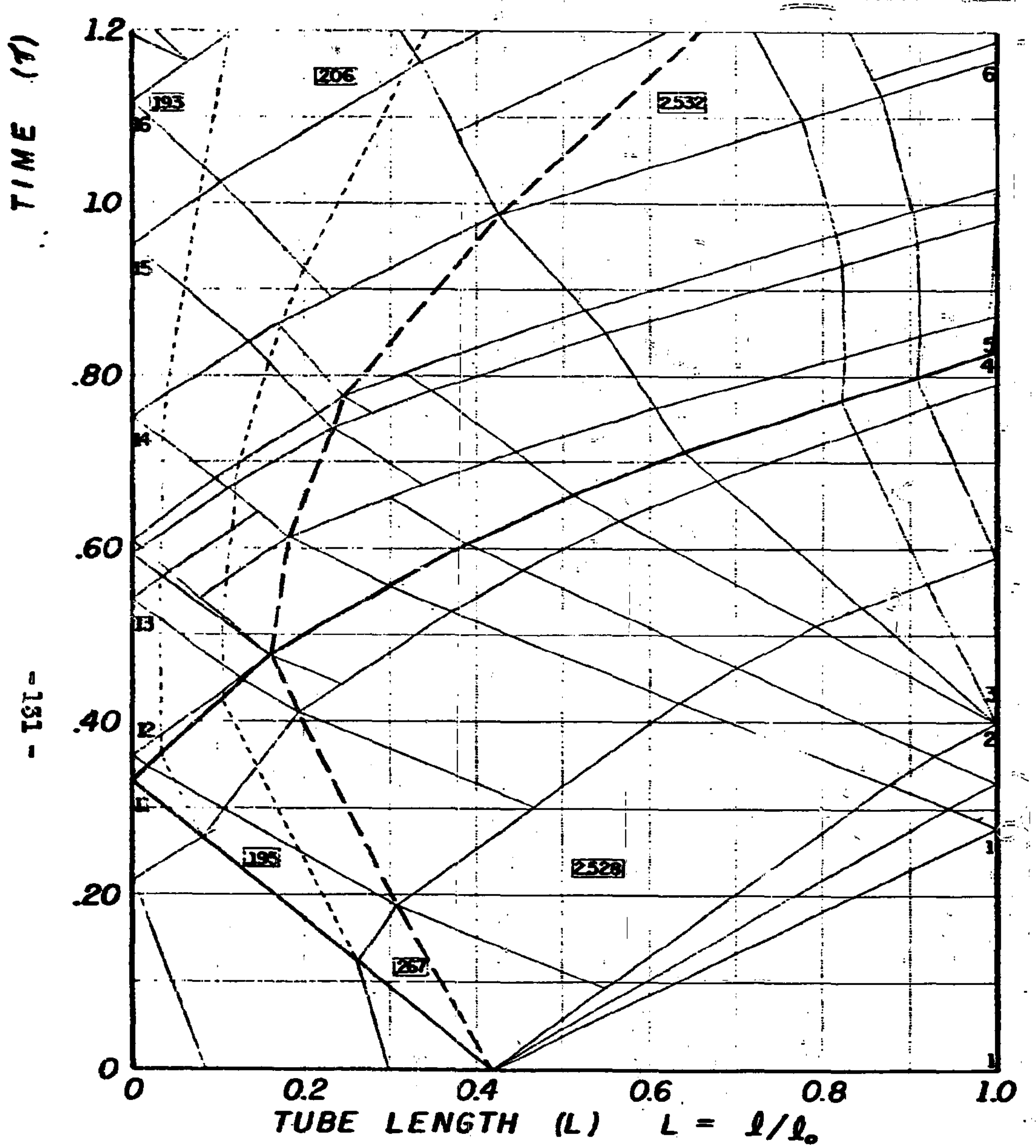

AVERAGE CONDITIONS BEFORE AND AFTER HEAT ADDITION

	BEFORE	AFTER
P =	1.731	5.646
θ =	1.362	4.507
S =	0.416	2.528

CHARACTERISTIC CYCLE PERFORMANCE

SFC $\left(\frac{\text{LBS. FUEL/HR.}}{\text{LBS. THRUST}}\right) = 2.184$, $T/A\left(\frac{\text{LBS.}}{\text{SQ. IN.}}\right) = 5.47$

$\eta_c = 0.44$ $\eta_o = .080$

COMBUSTION CHAMBER MASS $(m/m_o) = 0.732$

FUEL-AIR RATIO - 1/56

CYCLE 2

MACH NUMBER = 0.65

WAVE ENGINE CYCLE

HEAT ADDITION MODE: CONSTANT VOLUME COMBUSTION

Fig. 15B

CONFIDENTIAL

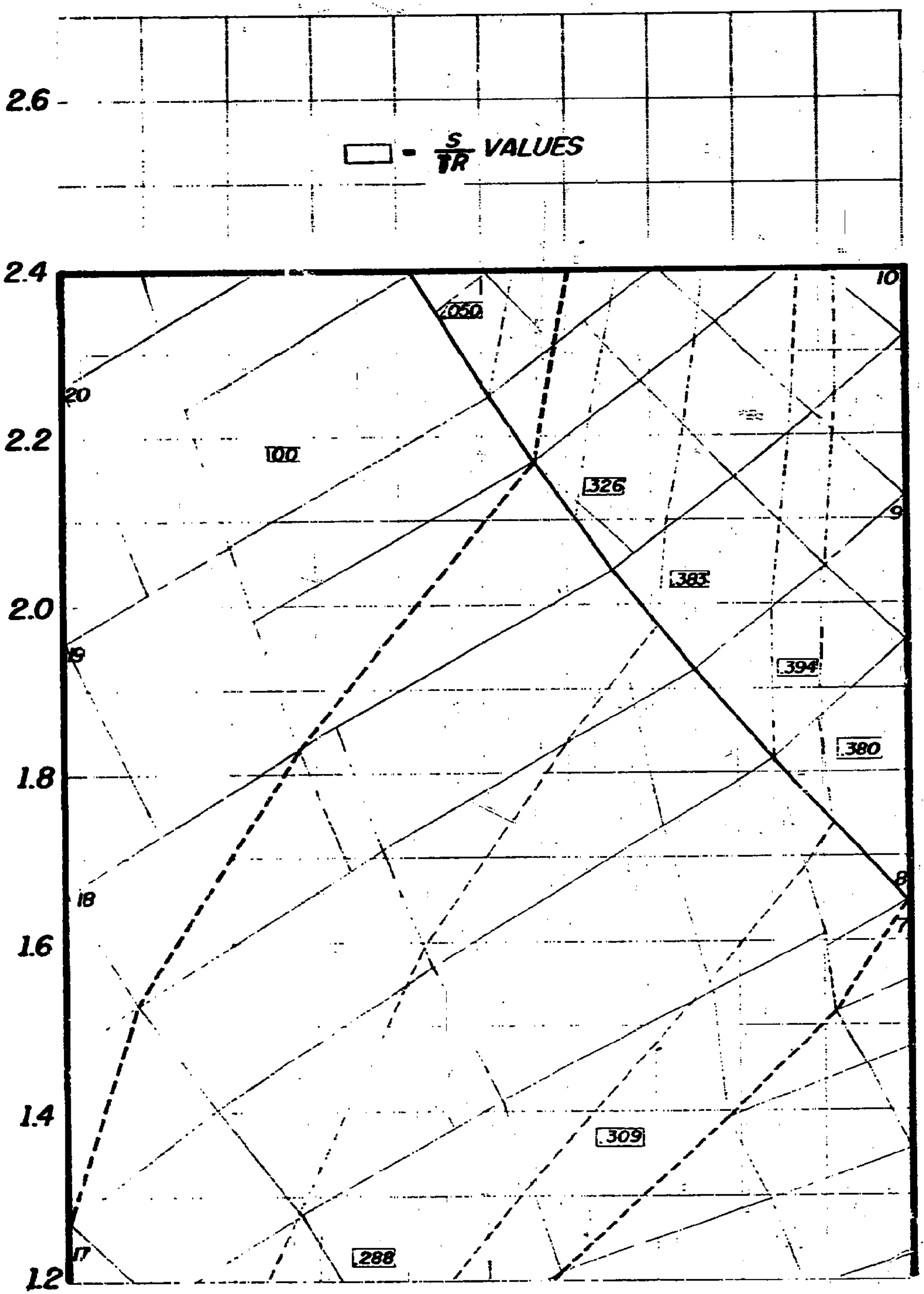

INLET AND EXIT CONDITIONS

POINT	P	u	a
EXIT			
1	6.232	0	2.103
2	2.696	0	1.866
3	1.000	1.232	1.620
4	1.000	1.316	1.620
5	1.736	1.983	1.756
6	1.332	1.689	1.689
7	1.000	0.656	1.621
8	2.234	0	1.209
9	1.554	0	1.148
10	1.964	0	1.187
INLET			
11	1.014	0.633	1.002
12	0.965	0.691	0.995
13	7.534	0	1.400
14	7.496	0	1.399
15	6.182	0	1.361
16	2.197	0	1.174
17	1.328	0	1.093
18	1.189	0.410	1.025
19	1.102	0.530	1.014
20	1.050	0.625	1.007

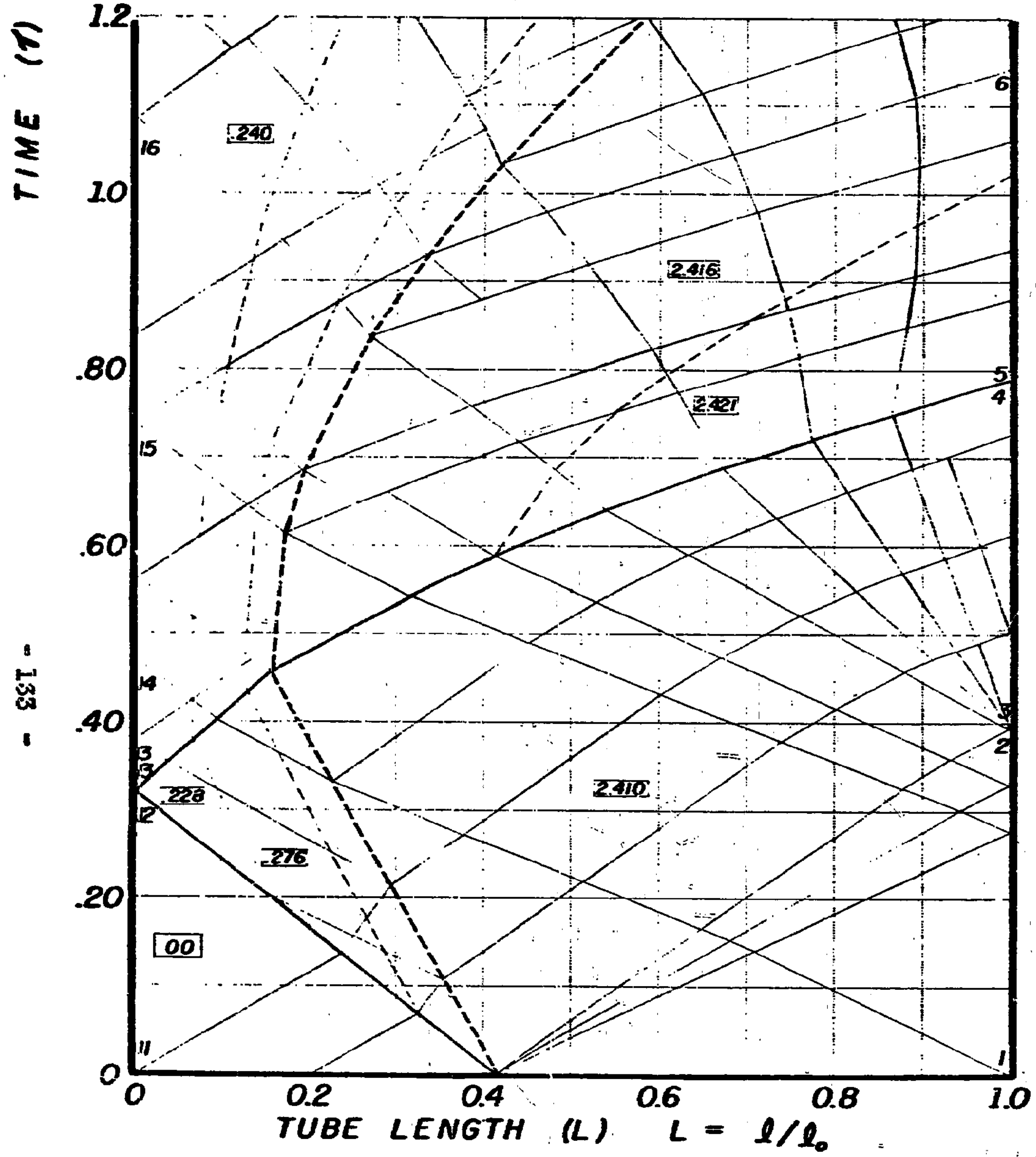

AVERAGE CONDITIONS BEFORE AND AFTER HEAT ADDITION

	BEFORE	AFTER
P =	1.830	6.232
θ =	1.299	4.424
S =	0.223	2.410

CHARACTERISTIC CYCLE PERFORMANCE

SFC $\left(\frac{\text{LBS. FUEL/HR.}}{\text{LBS. THRUST}}\right)$ = 1.763, $T/A\left(\frac{\text{LBS.}}{\text{SQ. IN.}}\right)$ = 7.44

η_c = 0.630 η_o = .099

COMBUSTION CHAMBER MASS (m/m_o) = 0.824

FUEL-AIR RATIO - 1/56

CYCLE 3

MACH NUMBER = 0.65

WAVE ENGINE CYCLE

HEAT ADDITION MODE: CONSTANT VOLUME COMBUSTION

Fig. 15C

CONFIDENTIAL

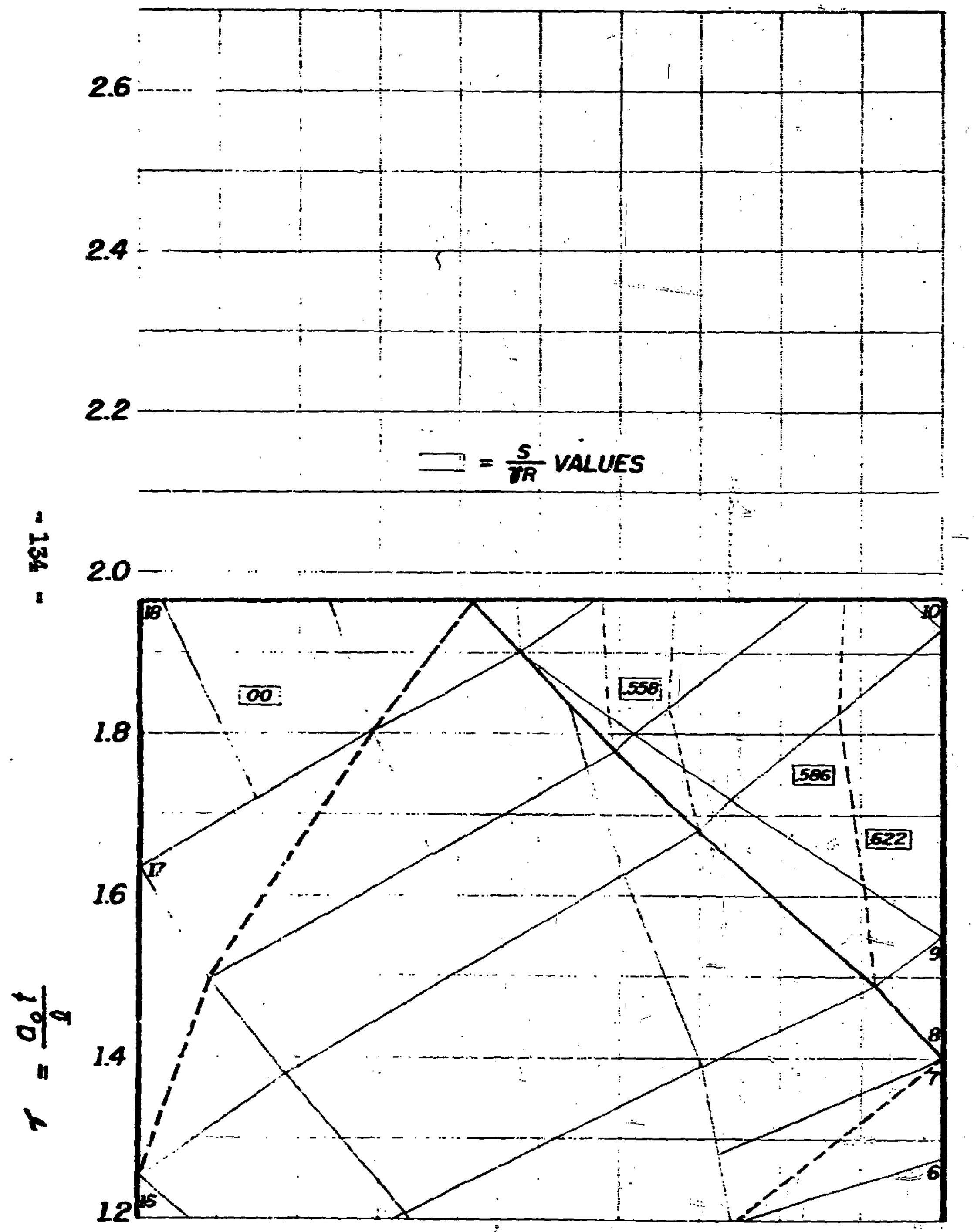

INLET AND EXIT CONDITIONS

POINT	P	u	a
	EXIT		
1	10.299	0	2.148
2	3.948	0	1.873
3	1.102	1.561	1.561
4	2.192	2.372	1.730
5	2.016	1.953	1.706
6	1.068	1.558	1.558
7	1.000	1.287	1.543
8	4.174	0	1.397
9	3.234	0	1.347
10	1.832	0	1.242
	INLET		
11	1.000	0.950	1.000
12	12.356	0	1.567
13	9.938	0	1.519
14	5.756	0	1.405
15	3.324	0	1.299
16	1.787	0	1.189
17	1.590	0.440	1.068
18	1.445	0.587	1.054
19			
20			

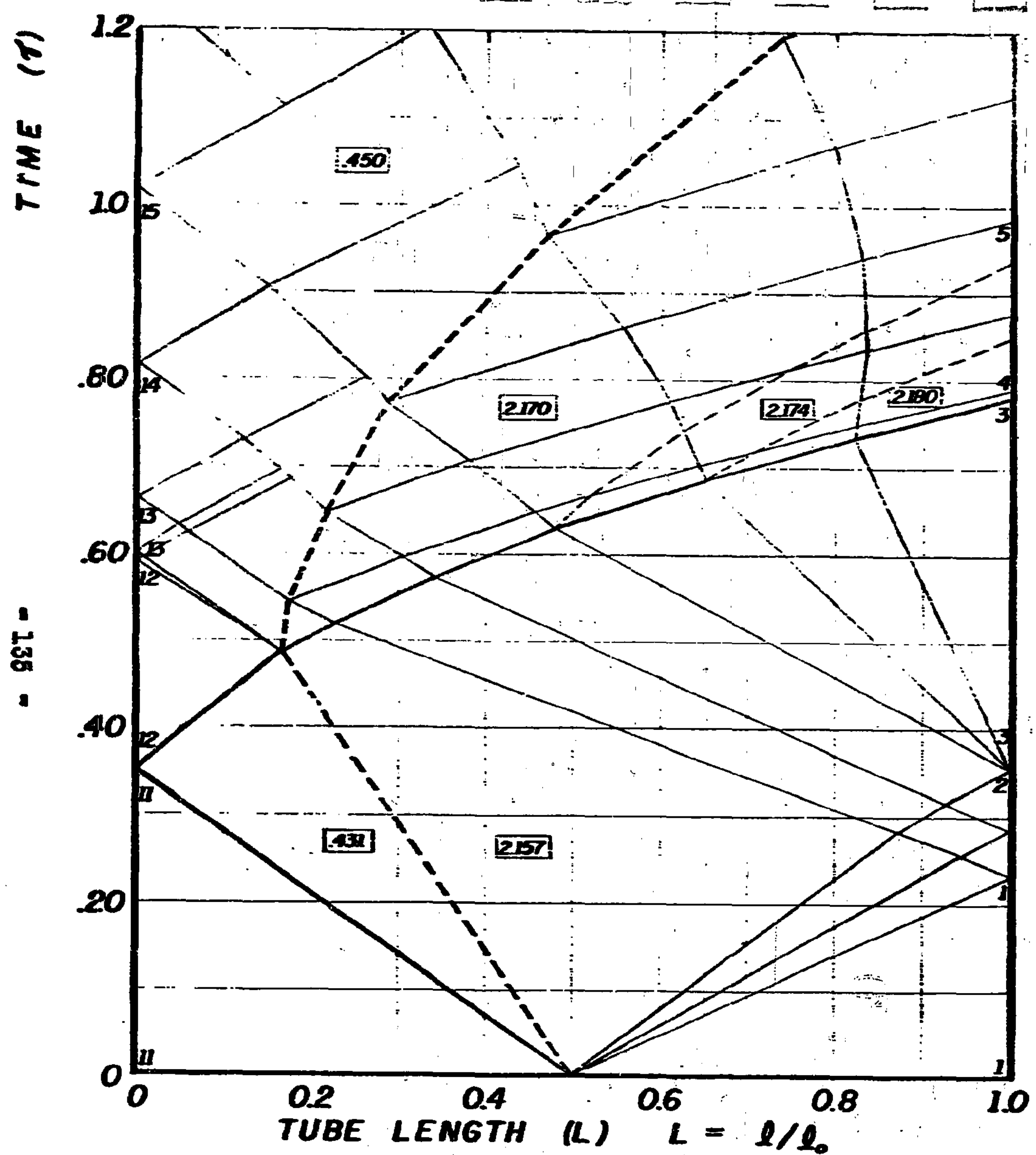

AVERAGE CONDITIONS BEFORE AND AFTER HEAT ADDITION

	BEFORE	AFTER
P =	3.290	10.299
θ =	1.474	4.614
S =	0.119	2.157

CHARACTERISTIC CYCLE PERFORMANCE

$SFC\left(\frac{LBS.\ FUEL/HR}{LBS.\ THRUST}\right) = 1.781$, $T/A\left(\frac{LBS.}{SQ.\ IN.}\right) = 12.1$

$\eta_c = 0.855$ $\eta_o = .143$

COMBUSTION CHAMBER MASS $(m/m_o) = 1.116$

FUEL-AIR RATIO – 1/56

CYCLE 1

MACH NUMBER = 0.95

WAVE ENGINE CYCLE

HEAT ADDITION MODE: CONSTANT VOLUME COMBUSTION

Fig. 16 A

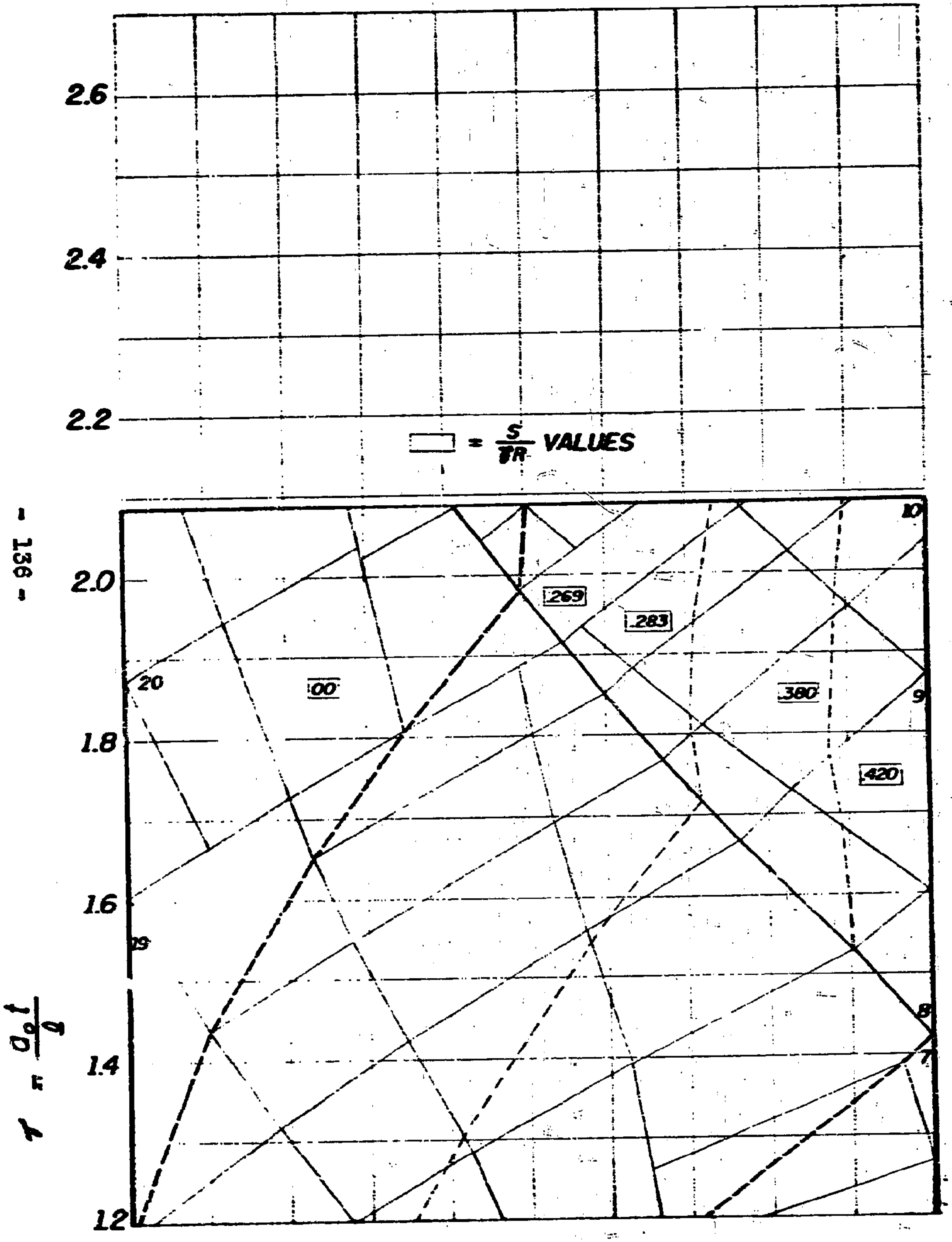

INLET AND EXIT CONDITIONS

POINT	P	u	a
EXIT			
1	6.875	0	2.171
2	6.470	0	2.152
3	3.412	0	1.964
4	1.000	1.581	1.648
5	1.021	1.653	1.653
6	1.656	2.242	1.774
7	1.000	1.123	1.650
8	3.729	0	1.316
9	1.737	0	1.180
10	2.245	0	1.224
INLET			
11	1.445	0.587	1.054
12	1.370	0.657	1.046
13	8.514	0	1.406
14	7.898	0	1.391
15	6.339	0	1.348
16	6.080	0	1.340
17	2.760	0	1.197
18	1.787	0	1.125
19	1.554	0.475	1.065
20	1.440	0.592	1.054

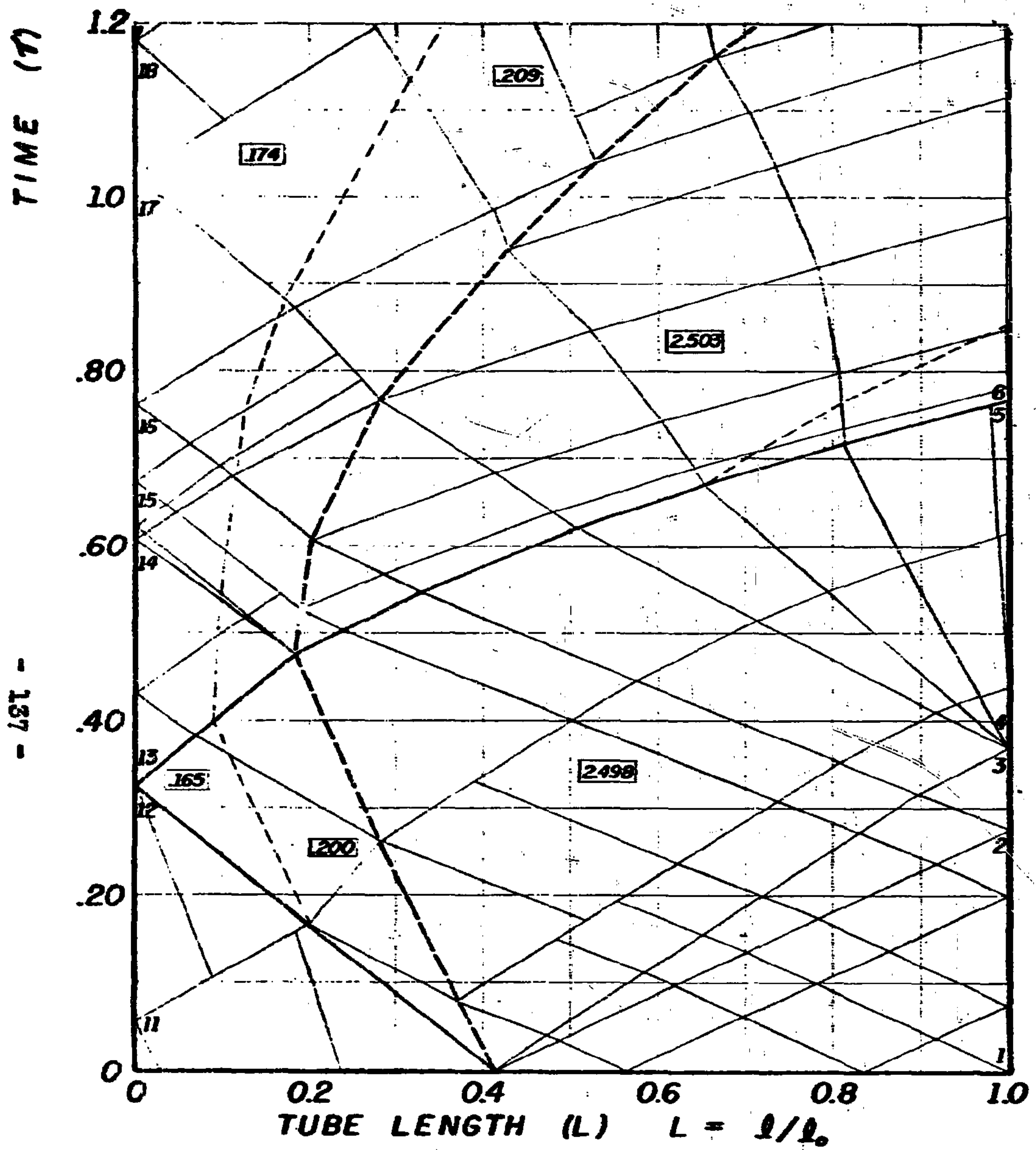

AVERAGE CONDITIONS BEFORE AND AFTER HEAT ADDITION

	BEFORE	AFTER
P =	2.315	6.875
θ =	1.587	4.712
S =	0.555	2.498

CHARACTERISTIC CYCLE PERFORMANCE

$SFC\left(\frac{LBS.\ FUEL/HR}{LBS.\ THRUST}\right) = 1.975$, $T/A\left(\frac{LBS.}{SQ.\ IN.}\right) = 7.89$

$\eta_c = 0.462$ $\eta_o = .129$

COMBUSTION CHAMBER MASS $(m/m_o) = 0.854$

FUEL*-AIR RATIO - 1/56

CYCLE 2

MACH NUMBER = 0.95

WAVE ENGINE CYCLE

HEAT ADDITION MODE: CONSTANT VOLUME COMBUSTION

Fig. 16 B

CONFIDENTIAL

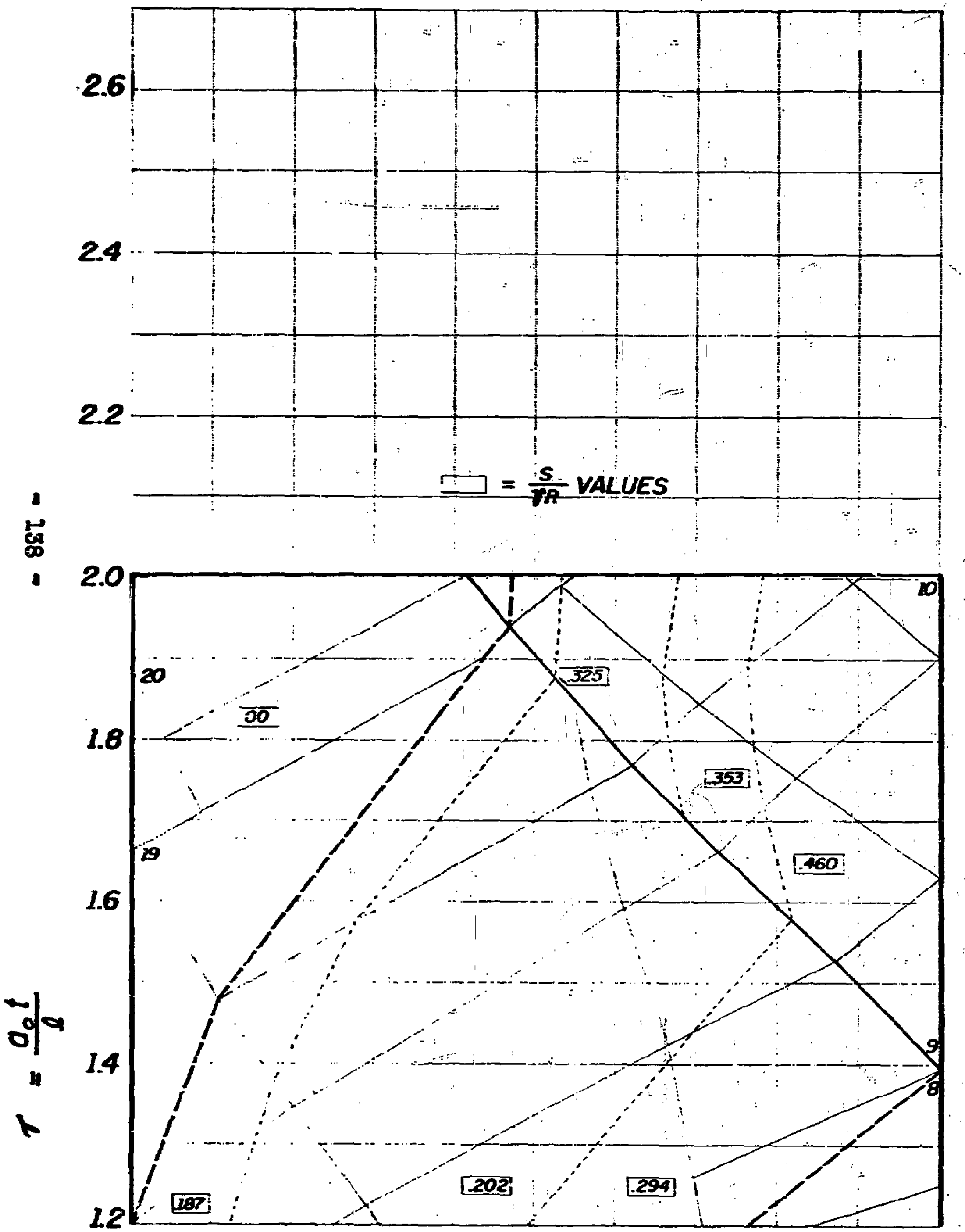

INLET AND EXIT CONDITIONS

POINT	P	u	a
EXIT			
1	7.518	0	2.142
2	7.716	0	2.150
3	4.151	0	1.923
4	1.000	1.588	1.606
5	1.055	1.642	1.618
6	1.686	2.217	1.733
7	1.494	1.752	1.702
8	1.000	1.230	1.607
9	4.079	0	1.348
10	1.926	0	1.211
INLET			
11	1.316	0.702	1.040
12	1.290	0.723	1.037
13	8.033	0	1.398
14	9.049	0	1.422
15	9.881	0	1.440
16	7.373	0	1.381
17	2.758	0	1.200
18	1.787	0	1.128
19	1.539	0.496	1.064
20	1.459	0.574	1.056

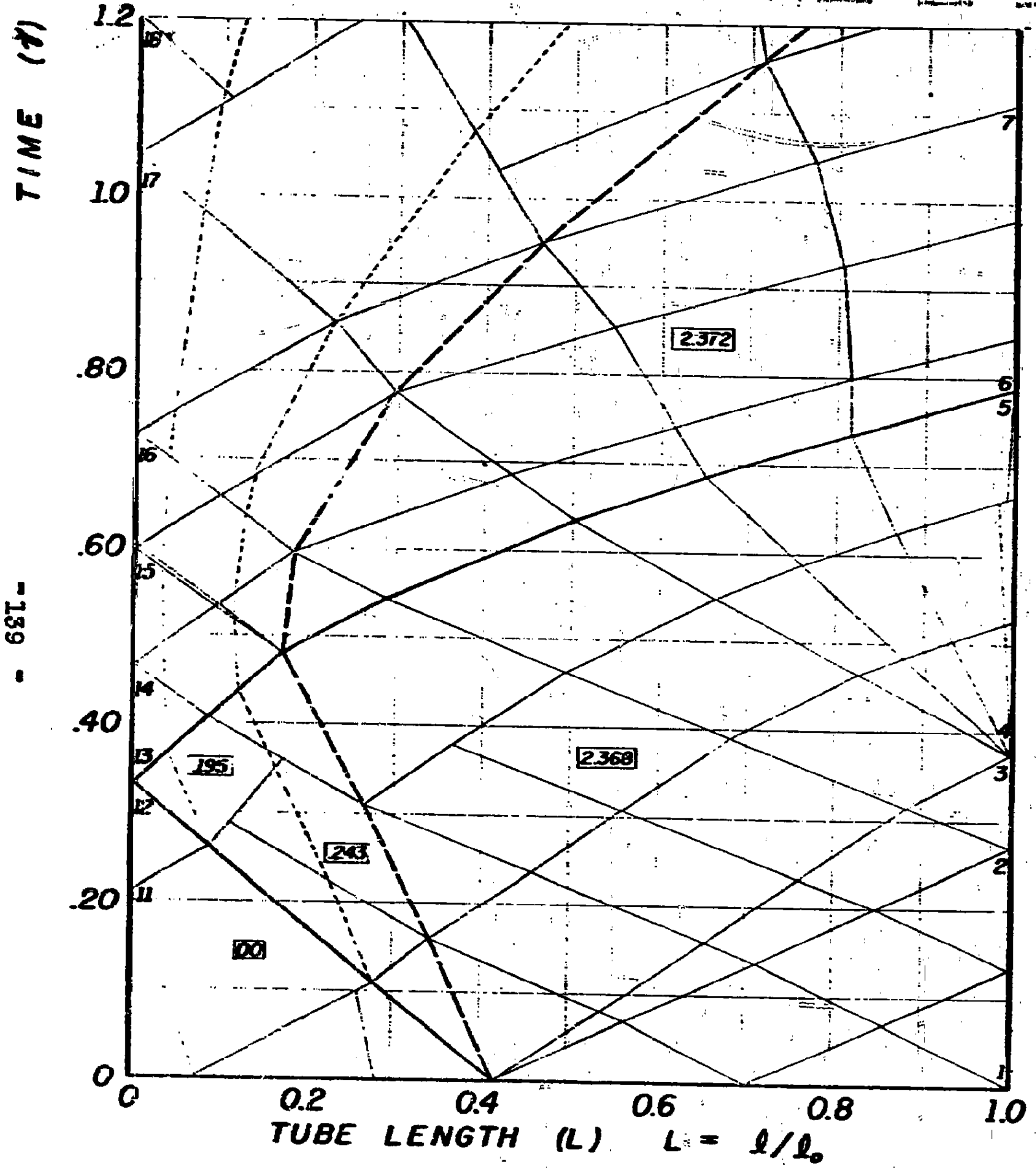

AVERAGE CONDITIONS BEFORE AND AFTER HEAT ADDITION

	BEFORE	AFTER
P =	2.397	7.518
θ =	1.463	4.588
S =	0.328	2.368

CHARACTERISTIC CYCLE PERFORMANCE

SFC $\left(\frac{\text{LBS. FUEL/HR.}}{\text{LBS. THRUST}}\right) = 1.909$, $T/A\left(\frac{\text{LBS.}}{\text{SQ. IN.}}\right) = 9.55$

$\eta_c = 0.613$ $\eta_o = 0.133$

COMBUSTION CHAMBER MASS $(m/m_o) = 0.958$

FUEL-AIR RATIO - 1/56

CYCLE 3

MACH NUMBER = 0.95

WAVE ENGINE CYCLE

HEAT ADDITION MODE: CONSTANT VOLUME COMBUSTION

Fig. 16C

CONFIDENTIAL

CONFIDENTIAL

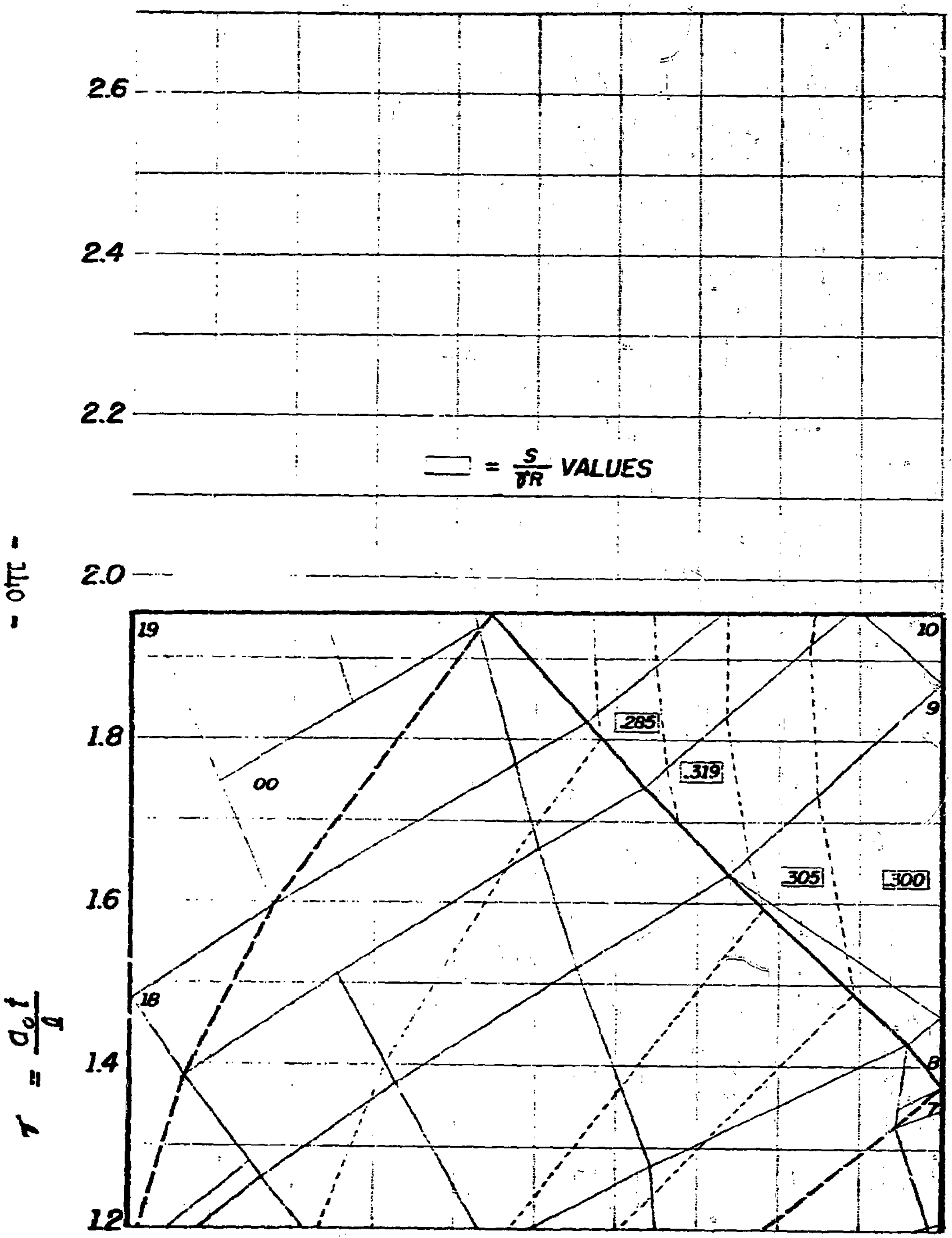

INLET AND EXIT CONDITIONS

POINT	P	u	a
	EXIT		
1	2.330	0	1.138
2	7.863	0	2.129
3	2.194	1.774	1.774
4	1.000	1.367	1.601
5	1.000	1.403	1.601
6	1.769	2.093	1.741
7	1.000	1.180	1.635
8	4.143	0	1.290
9	1.375	0	1.102
10	1.550	0	1.121
	INLET		
11	1.000	0.650	1.000
12	6.720	0	1.365
13	9.307	0	1.425
14	10.407	0	1.453
15	10.110	0	1.447
16	3.115	0	1.223
17	1.328	0	1.083
18	1.222	0.355	1.029
19	1.065	0.575	1.009
20			

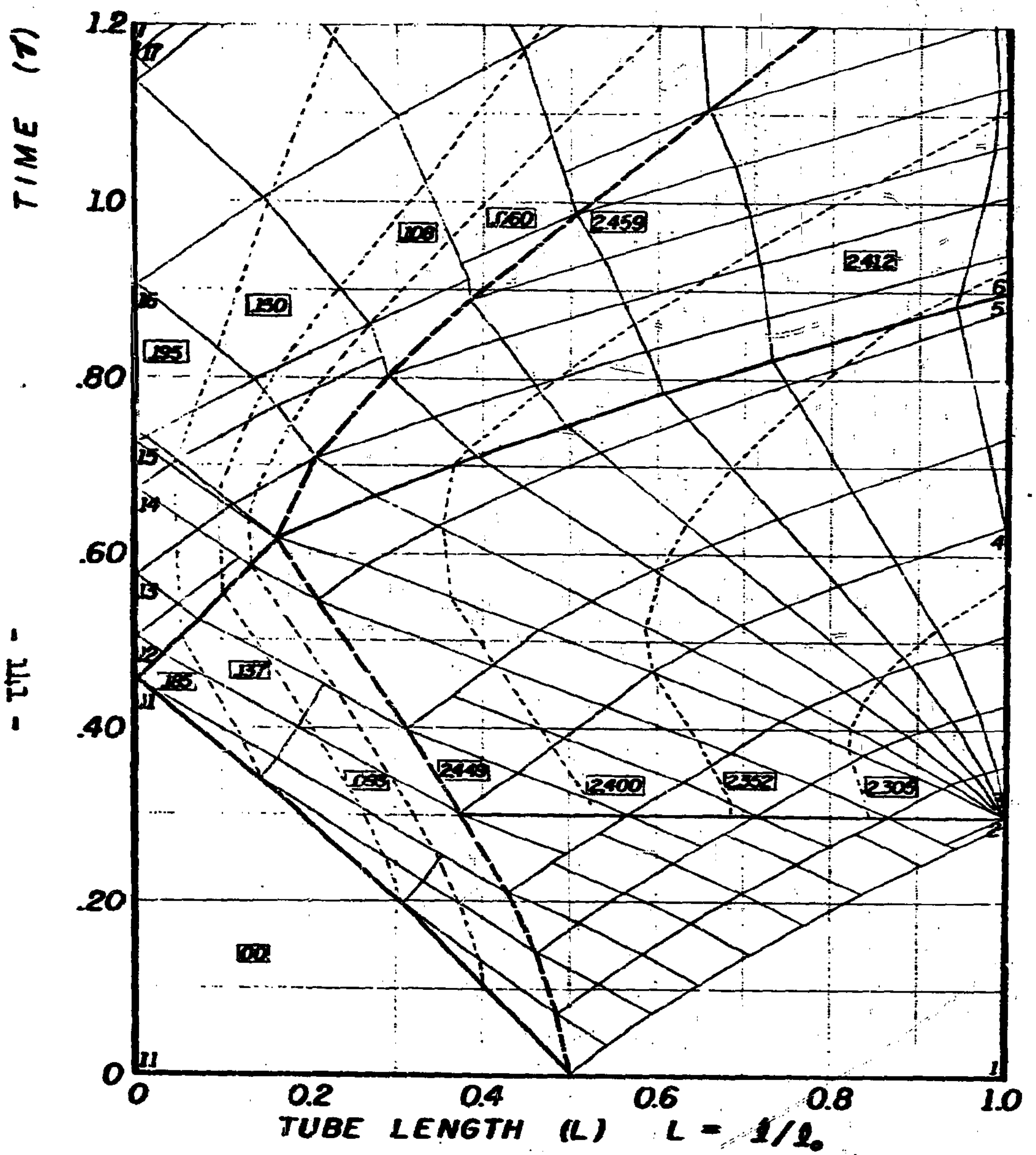

AVERAGE CONDITIONS BEFORE AND AFTER HEAT ADDITION

	BEFORE	AFTER
P =	2.330	7.863
θ =	1.295	4.533
S =	0.043	2.305

CHARACTERISTIC CYCLE PERFORMANCE

SFC $\left(\frac{\text{LBS. FUEL/HR.}}{\text{LBS. THRUST}}\right) = 1.568$, $T/A\left(\frac{\text{LBS.}}{\text{SQ. IN.}}\right) = 11.20$

$\eta_c = 0.93$ $\eta_o = 0.111$

COMBUSTION CHAMBER MASS $(m/m_o) = 0.900$

FUEL-AIR RATIO - 1/56

CYCLE I

MACH NUMBER = 0.65

WAVE ENGINE CYCLE
HEAT ADDITION MODE: GRADUAL HEAT ADDITION

Fig. 17A

CONFIDENTIAL

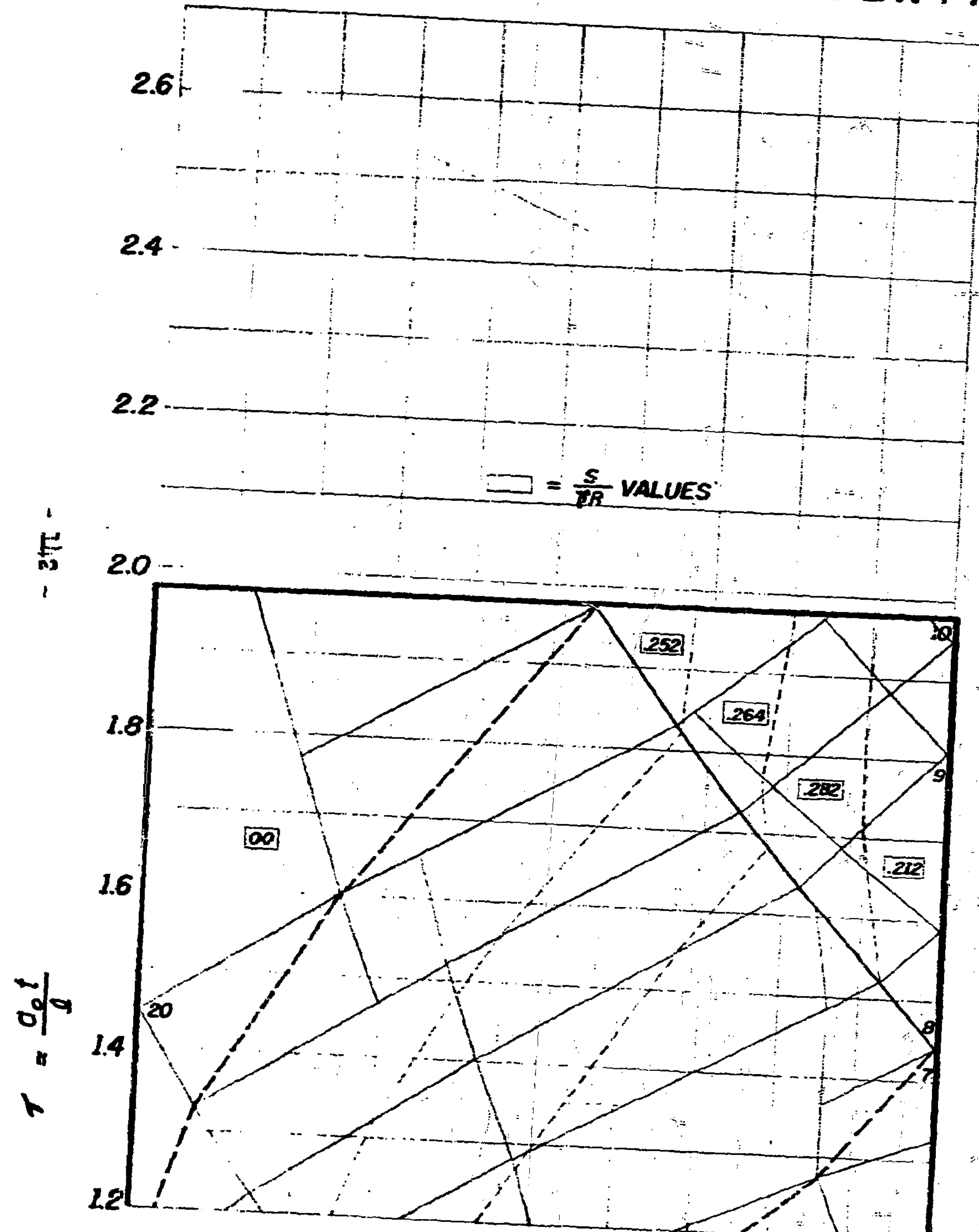

INLET AND EXIT CONDITIONS

POINT	P	u	a
EXIT			
1	1.796	0	1.156
2	6.896	0	2.172
3	1.925	1.810	1.810
4	1.000	1.434	1.672
5	1.543	1.957	1.781
6	1.076	1.715	1.715
7	1.000	0.865	1.697
8	2.955	0	1.202
9	1.275	0	1.066
10	1.640	0	1.105
INLET			
11	1.065	0.575	1.009
12	1.028	0.615	1.004
13	0.993	0.659	0.999
14	4.960	0	1.292
15	6.608	0	1.346
16	8.745	0	1.401
17	6.852	0	1.353
18	1.954	0	1.131
19	1.328	0	1.070
20	1.185	0.416	1.024

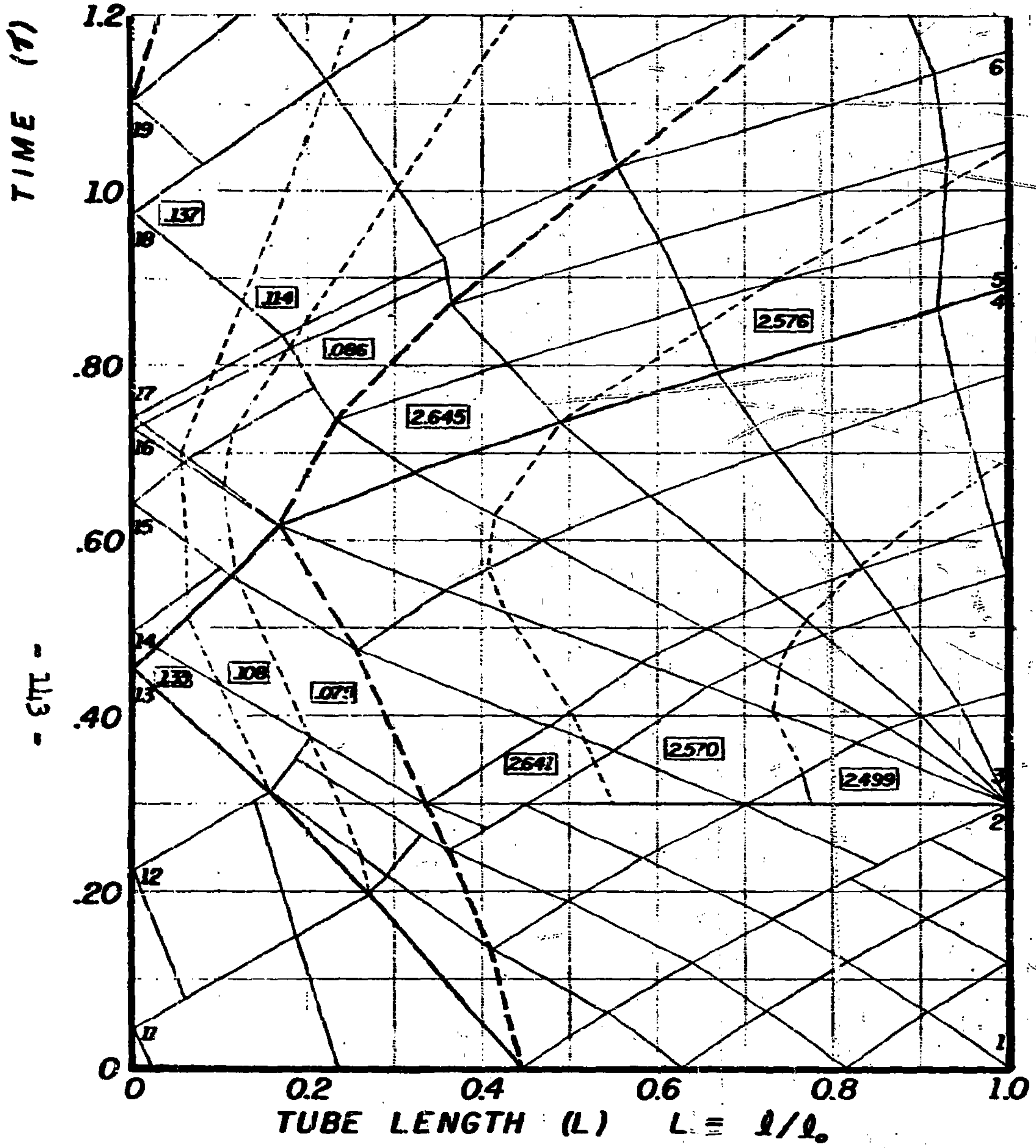

AVERAGE CONDITIONS BEFORE AND AFTER HEAT ADDITION

	BEFORE	AFTER
P =	1.796	6.896
θ =	1.335	4.718
S =	0.306	2.499

CHARACTERISTIC CYCLE PERFORMANCE

$SFC\left(\frac{LBS.\ FUEL/HR.}{LBS.\ THRUST}\right) = 1.818$, $T/A\left(\frac{LBS.}{SQ.\ IN.}\right) = 7.92$

$\tau_c = 0.540$ $l_c = 0.096$

COMBUSTION CHAMBER MASS $(m/m_0) = 0.746$

FUEL-AIR RATIO - 1/56

CYCLE 2

MACH NUMBER = 0.65

WAVE ENGINE CYCLE

HEAT ADDITION MODE: GRADUAL HEAT ADDITION

Fig. 17B

CONFIDENTIAL

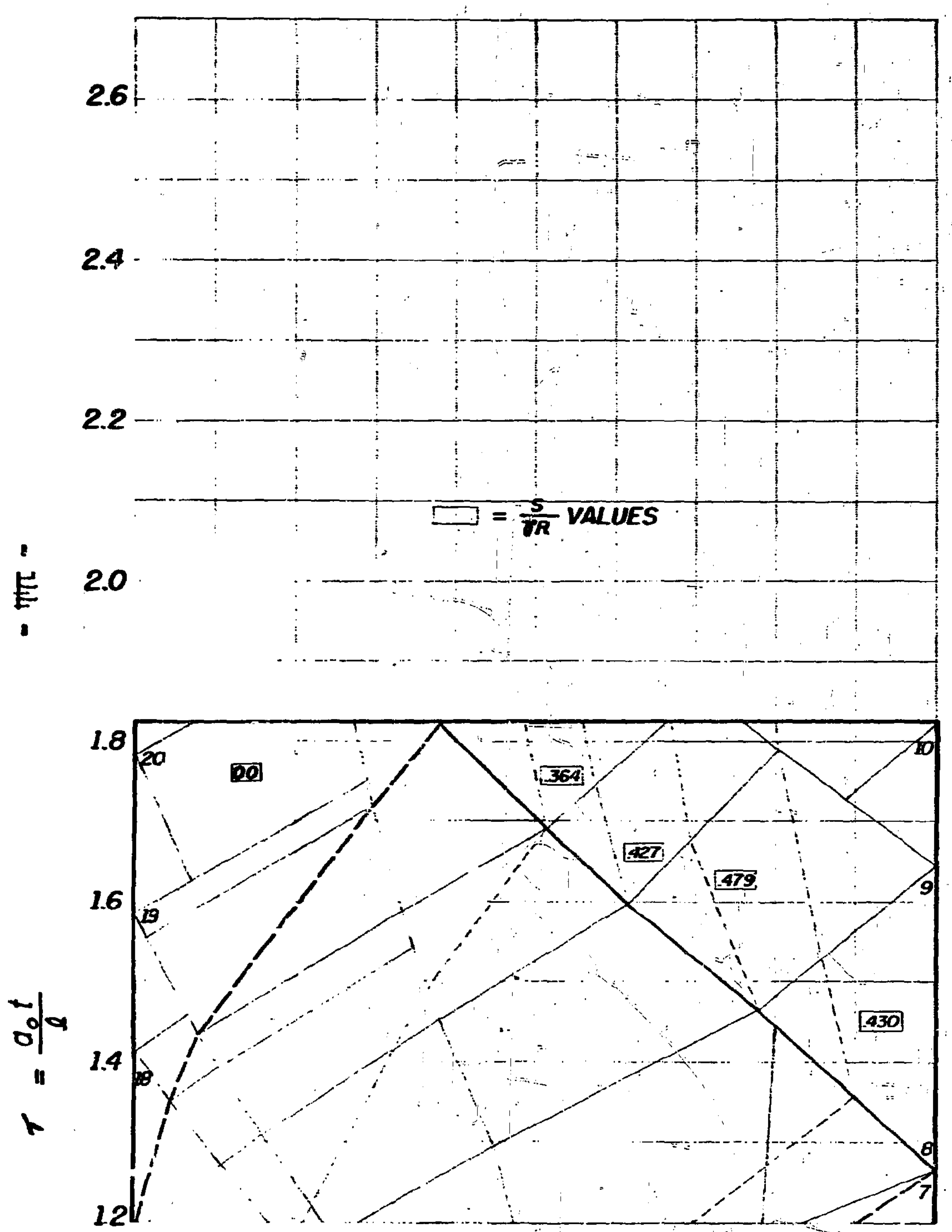

INLET AND EXIT CONDITIONS

POINT	P	u	a
EXIT			
1	1.651	0	1.135
2	6.052	0	2.134
3	1.687	1.778	1.778
4	1.000	1.354	1.676
5	1.000	0.856	1.701
6	1.211	1.751	1.751
7	1.000	1.500	1.704
8	5.639	0	1.390
9	2.015	0	1.200
10	1.552	0	1.156
INLET			
11	0.972	0.686	0.996
12	0.944	0.713	0.992
13	5.839	0	1.336
14	7.326	0	1.380
15	7.438	0	1.383
16	2.146	0	1.158
17	1.328	0	1.081
18	1.238	0.325	1.031
19	1.125	0.501	1.017
20	1.065	0.577	1.009

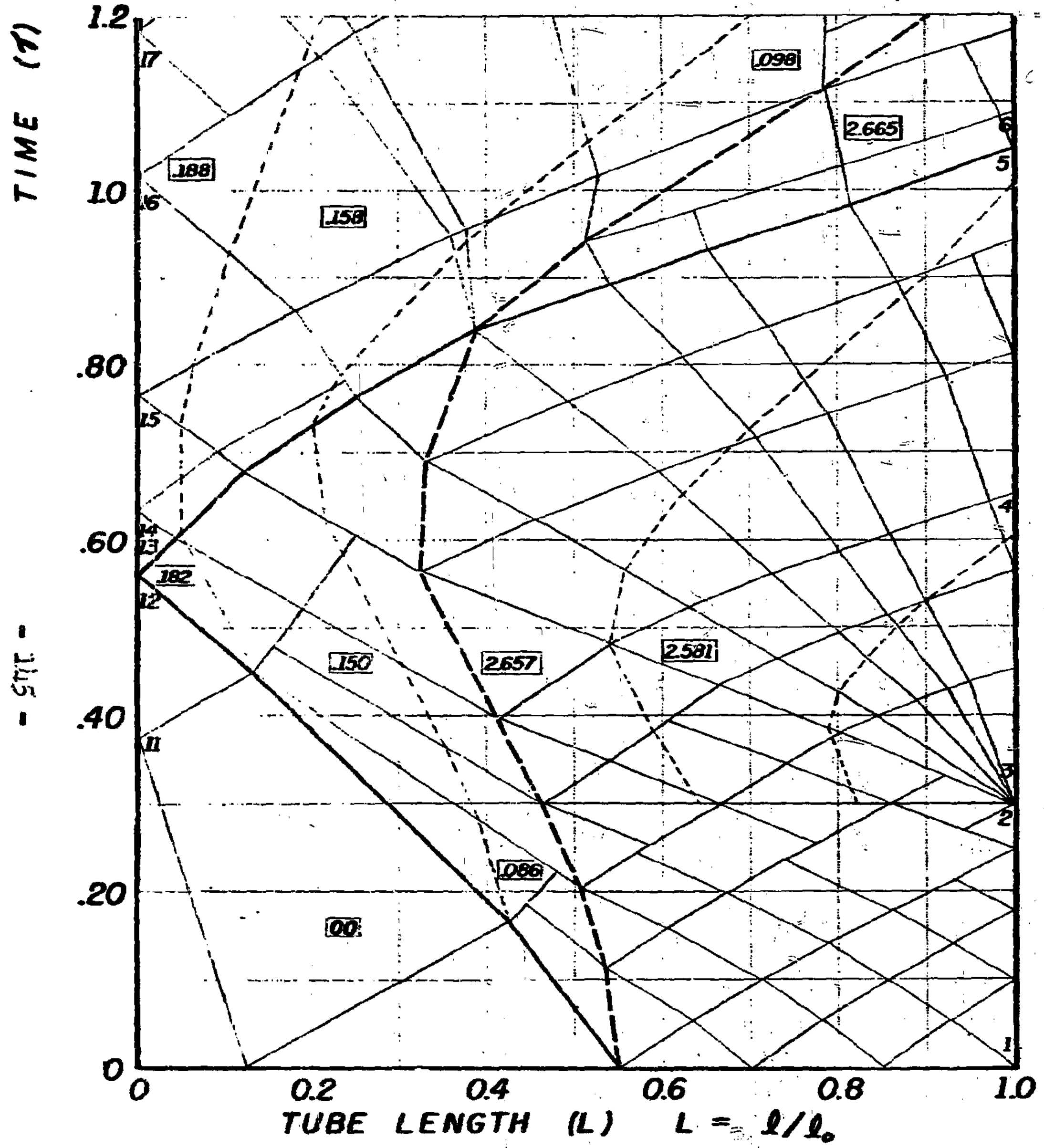

AVERAGE CONDITIONS BEFORE AND AFTER HEAT ADDITION

	BEFORE	AFTER
P =	1.651	6.052
θ =	1.228	4.554
S =	0.275	2.504

CHARACTERISTIC CYCLE PERFORMANCE

SFC $\left(\frac{\text{LBS. FUEL/HR.}}{\text{LBS. THRUST}}\right)$ = 2.130, $T/A\left(\frac{\text{LBS.}}{\text{SQ. IN.}}\right)$ = 5.66

$\eta_c = 0.530$ $\eta_o = 0.082$

COMBUSTION CHAMBER MASS $(m/m_o) = 0.577$

FUEL-AIR RATIO - 1/56

CYCLE 3

MACH NUMBER = 0.65

WAVE ENGINE CYCLE

HEAT ADDITION MODE: GRADUAL HEAT ADDITION

Fig. 17C

CONFIDENTIAL

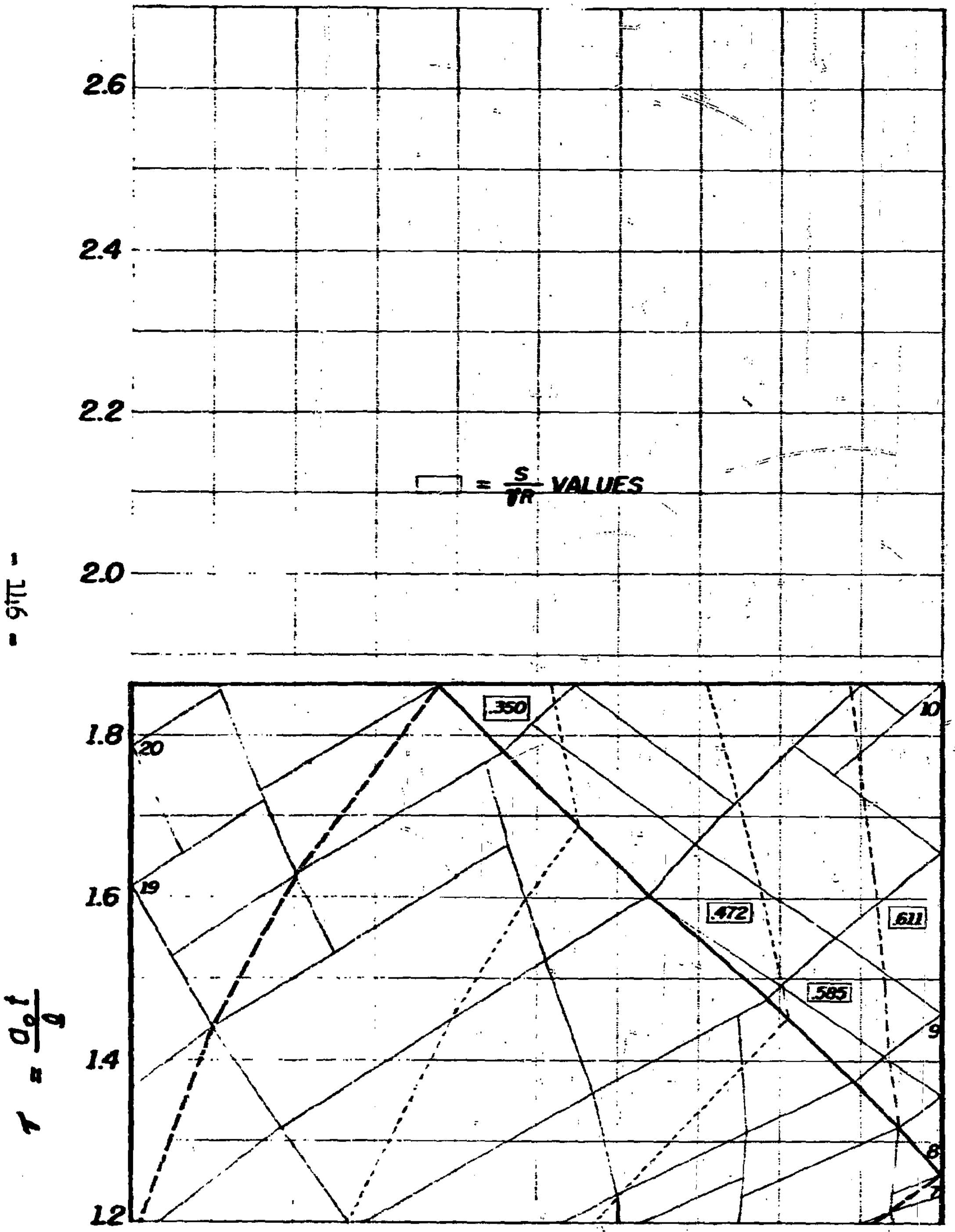

INLET AND EXIT CONDITIONS

POINT	P	u	a
EXIT			
1	5.677	0	2.108
2	2.567	0	1.882
3	1.000	1.185	1.645
4	1.000	1.199	1.645
5	1.229	1.696	1.696
6	1.179	1.686	1.686
7	1.000	1.374	1.647
8	4.617	0	1.406
9	2.682	0	1.301
10	1.437	0	1.190
INLET			
11	1.014	0.633	1.002
12	0.979	0.672	0.997
13	7.018	0	1.379
14	6.807	0	1.373
15	3.649	0	1.256
16	2.876	0	1.214
17	2.005	0	1.153
18	1.328	0	1.087
19	1.149	0.460	1.020
20	1.102	0.528	1014

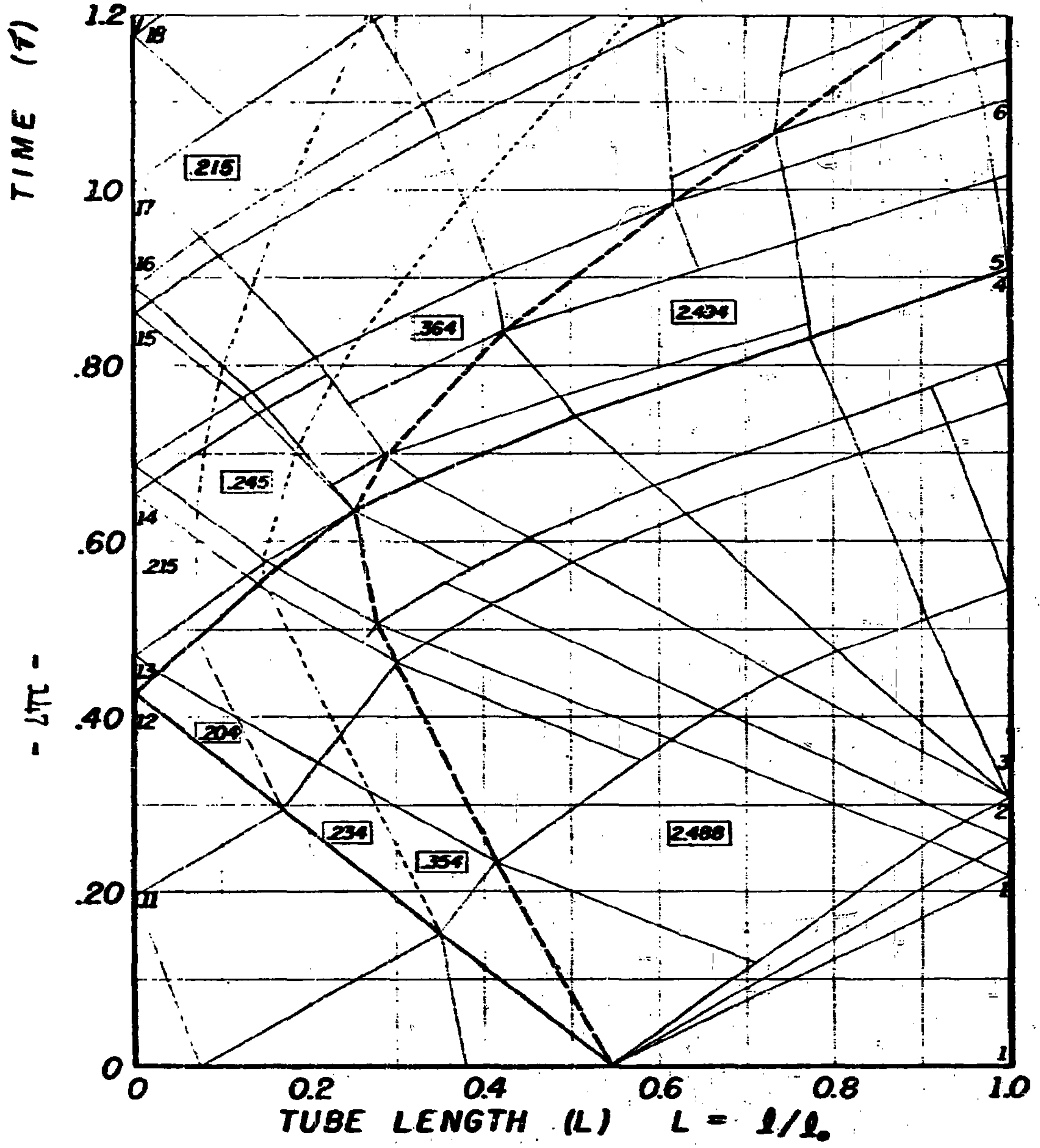

AVERAGE CONDITIONS BEFORE AND AFTER HEAT ADDITION

	BEFORE	AFTER
P =	1.683	5.677
θ =	1.317	4.442
S =	0.316	2.488

CHARACTERISTIC CYCLE PERFORMANCE

$SFC\left(\frac{LBS.\ FUEL/HR}{LBS.\ THRUST}\right) = 2.582,\ T/A\left(\frac{LBS.}{SQ.\ IN.}\right) = 4.62$

$\eta_c = 0.506 \qquad \eta_o = 0.067$

COMBUSTION CHAMBER MASS $(m/m_o) = 0.584$

FUEL-AIR RATIO – 1/56

CYCLE 3

MACH NUMBER = 0.65

WAVE ENGINE CYCLE

HEAT ADDITION MODE: CONSTANT VOLUME COMBUSTION

Fig. 18A

CONFIDENTIAL

CONFIDENTIAL

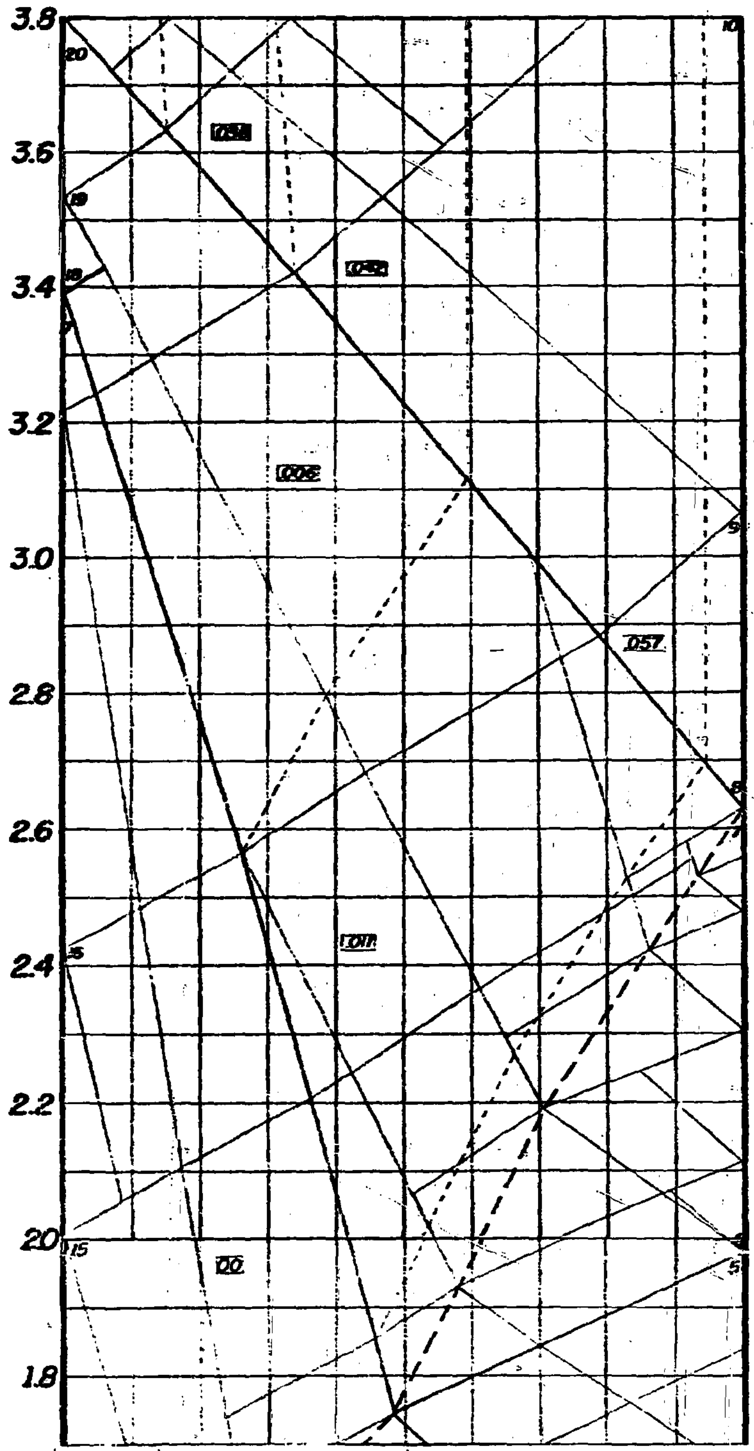

$\tau = \frac{a_0 t}{\ell}$

INLET AND EXIT CONDITIONS

POINT	P	u	a
	EXIT		
1	3.517	2.204	2.204
2	1.000	1.814	1.842
3	1.000	0.712	1.842
4	1.000	0.380	1.842
5	1.000	0.232	1.842
6	1.000	0.568	1.842
7	1.000	0.662	1.845
8	2.343	0	1.143
9	2.401	0	1.147
10	2.431	0	1.149
	INLET		
11	12.588	0	2.645
12	3.522	0	2.205
13	1.328	0	1.918
14	1.087	0.552	1.012
15	0.951	0.699	0.993
16	0.886	0.770	0.983
17	0.802	0.850	0.970
18	1.139	0.466	1.020
19	1.139	0.461	1.020
20	1.093	0.515	1.014

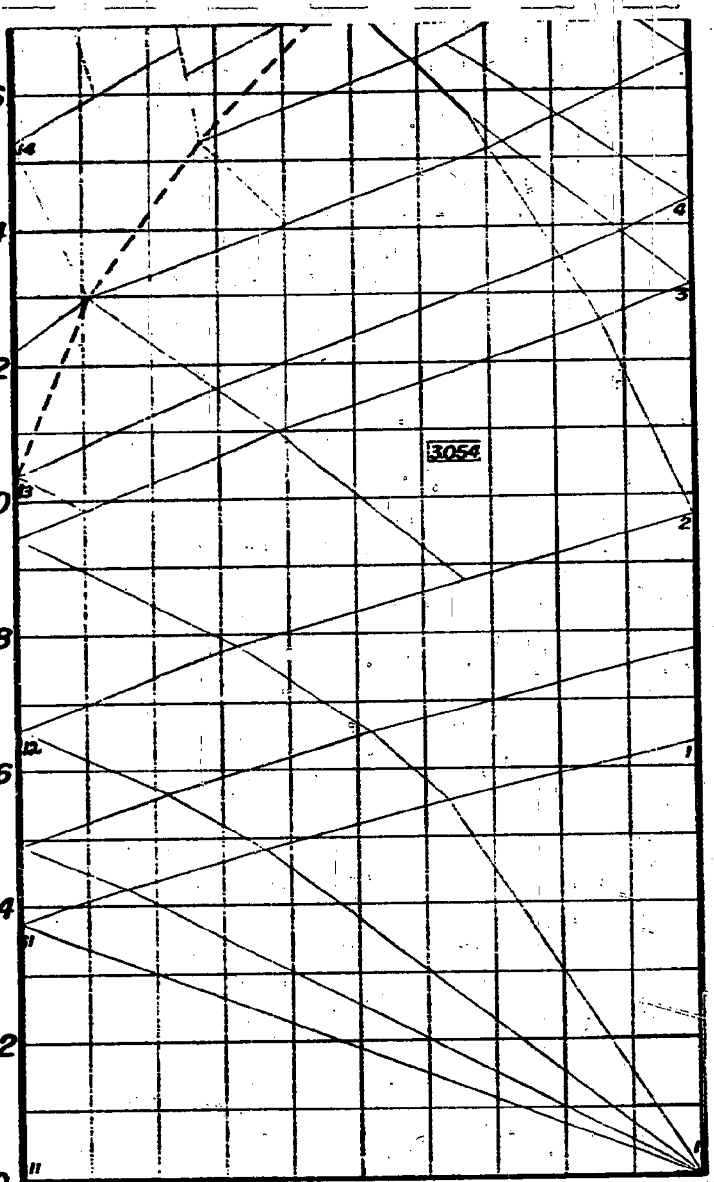

AVERAGE CONDITIONS BEFORE AND AFTER HEAT ADDITION

	BEFORE	AFTER
P =	2.334	12.588
θ =	1.296	6.996
S =	0.044	3.054

CHARACTERISTIC CYCLE PERFORMANCE

SFC $\left(\frac{\text{LBS. FUEL/HR.}}{\text{LBS. THRUST}}\right) = 1.807$, $T/A\left(\frac{\text{LBS.}}{\text{SQ. IN.}}\right) = 18.05$

$\eta_c = 0.910$ $\eta_o = 0.096$

COMBUSTION CHAMBER MASS $(m/m_o) = 1.800$

FUEL-AIR RATIO - $1/31$

CYCLE 1

MACH NUMBER = 0.65

WAVE ENGINE CYCLE

HEAT ADDITION MODE: CONSTANT VOLUME COMBUSTION

Fig. 19A

CONFIDENTIAL

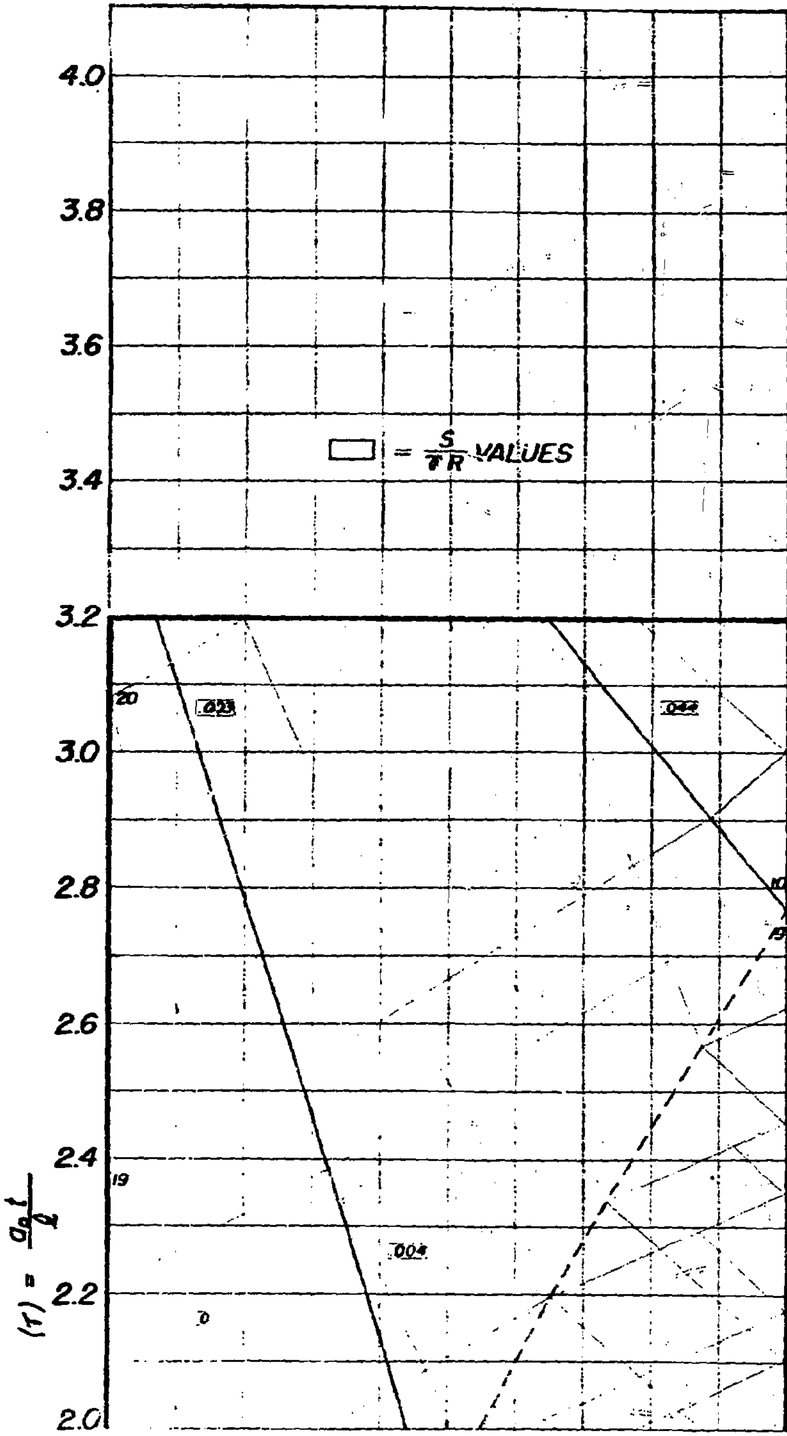

INLET AND EXIT CONDITIONS

POINT	P	u	a
	EXIT		
1	12.594	0	2.645
2	3.637	0	2.215
3	1.016	1.846	1.846
4	1.000	1.736	1.842
5	5.000	4.230	2.453
6	4.700	3.449	2.404
7	4.700	3.449	2.107
8	1.000	0.350	1.689
9	1.000	0.630	1.690
10	2.282	0	1.135
	INLET		
11	1.000	0.650	1.000
12	13.443	0	1.622
13	42.578	0	2.887
14	32.055	0	2.772
15	4.470	0	2.092
16	2.925	0	1.969
17	1.328	0	1.759
18	1.172	0.428	1.023
19	0.944	0.704	0.992
20	0.873	0.783	0.981

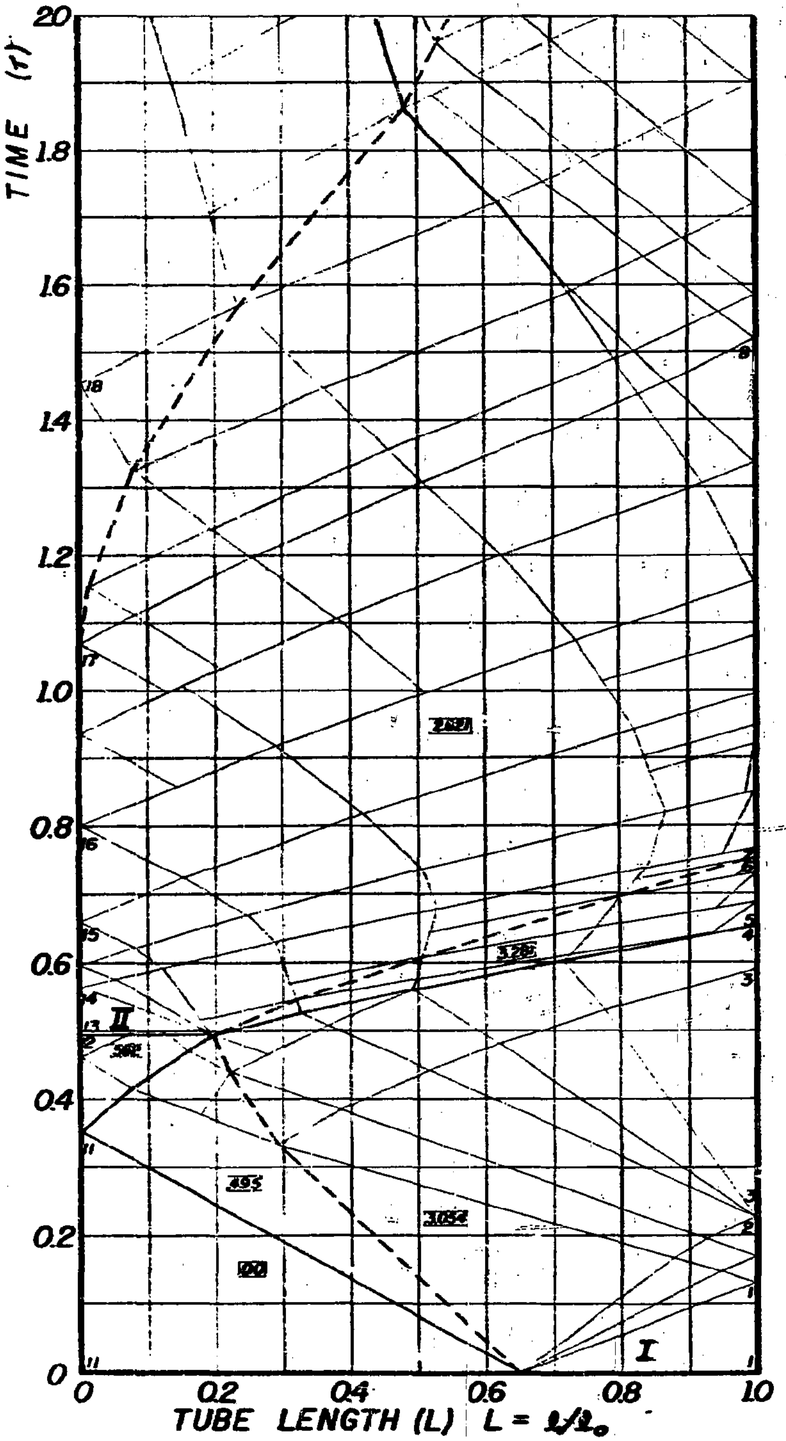

AVERAGE CONDITIONS BEFORE AND AFTER HEAT ADDITION

	I INITIAL COMBUSTION		II SECONDARY COMBUSTION	
	BEFORE	AFTER	BEFORE	AFTER
P	2.330	12.594	13.443	42.578
θ	1.295	6.996	2.631	8.332
S	0.043	3.054	0.562	2.621
η_c	0.910		0.676	
FUEL-AIR RATIO	1/31		1/31	
COMBUSTION CHAMBER MASS (m/m_o)	0.630		0.996	

CHARACTERISTIC CYCLE PERFORMANCE

$SFC\left(\frac{LBS.\ FUEL/HR.}{LBS.\ THRUST}\right) = 2.111$, $T/A\left(\frac{LBS.}{SQ.\ IN.}\right) = 16.60$

$\eta_c =$ —— $\eta_o = 0.083$

CYCLE - I MACH NUMBER = 0.65

MODIFIED WAVE ENGINE CYCLE WITH SECONDARY COMBUSTION

HEAT ADDITION MODE

CONSTANT VOLUME COMBUSTION

Fig. 20A

CONFIDENTIAL

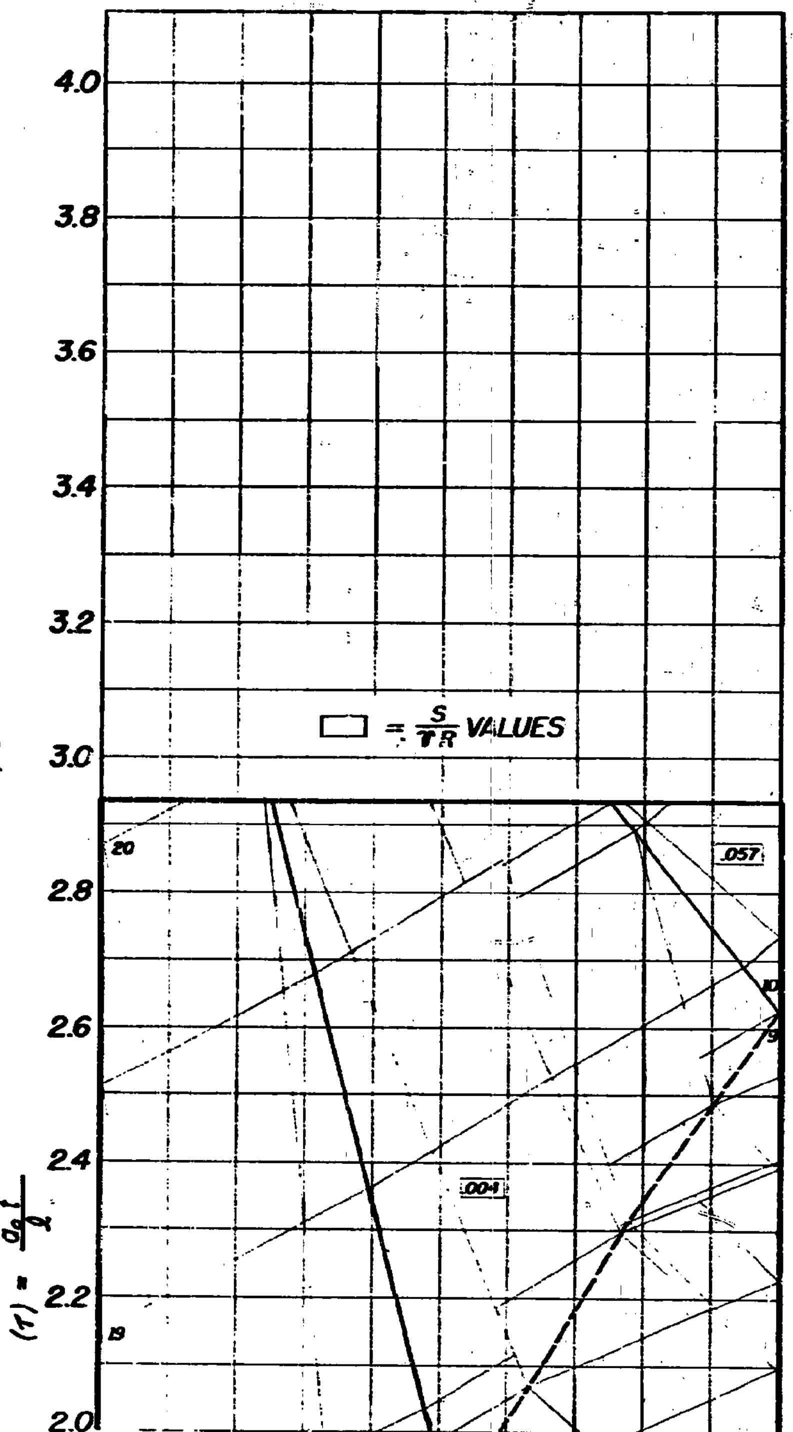

INLET AND EXIT CONDITIONS

POINT	P	u	a
EXIT			
1	12.600	0	2.645
2	3.637	0	2.215
3	1.016	1.846	1.846
4	1.000	0.998	1.842
5	4.160	3.154	2.351
6	2.431	2.832	1.365
7	1.167	1.666	1.206
8	1.000	1.397	1.683
9	1.000	0.676	1.683
10	2.410	0	1.145
INLET			
11	1.000	0.650	1.000
12	14.266	0	1.637
13	44.630	0	2.895
14	13.290	0	2.435
15	7.030	0	2.223
16	2.040	0	1.863
17	1.328	0	1.752
18	1.205	0.386	1.027
19	0.938	0.715	0.991
20	0.862	0.789	0.980

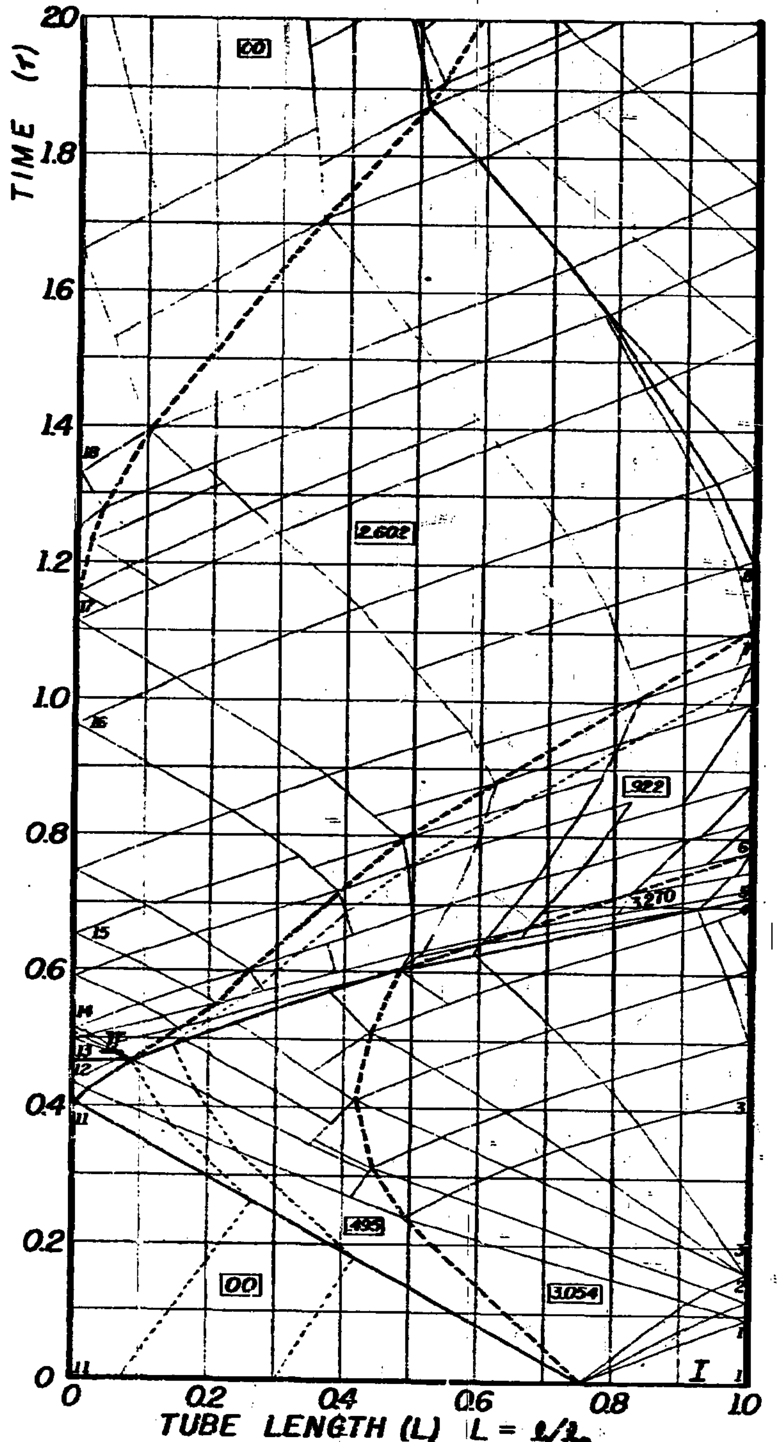

AVERAGE CONDITIONS BEFORE AND AFTER HEAT ADDITION

	I INITIAL COMBUSTION		II SECONDARY COMBUSTION	
	BEFORE	AFTER	BEFORE	AFTER
P	2.334	12.600	14.266	44.630
θ	1.295	6.996	2.679	8.381
S	0.044	3.054	0.565	2.602
η_c	0.910		0.678	
FUEL-AIR RATIO	1/31		1/31	
COMBUSTION CHAMBER MASS (m/m_o)	0.450		0.450	

CHARACTERISTIC CYCLE PERFORMANCE

$SFC\left(\frac{\text{LBS. FUEL/HR.}}{\text{LBS. THRUST}}\right) = 1.625$, $T/A\left(\frac{\text{LBS.}}{\text{SQ. IN.}}\right) = 13.00$

η_c = —— $\eta_o = 0.107$

CYCLE - I MACH NUMBER = 0.65

MODIFIED WAVE ENGINE CYCLE WITH SECONDARY COMBUSTION

HEAT ADDITION MODE

CONSTANT VOLUME COMBUSTION

Fig. 21A

CONFIDENTIAL

CONFIDENTIAL

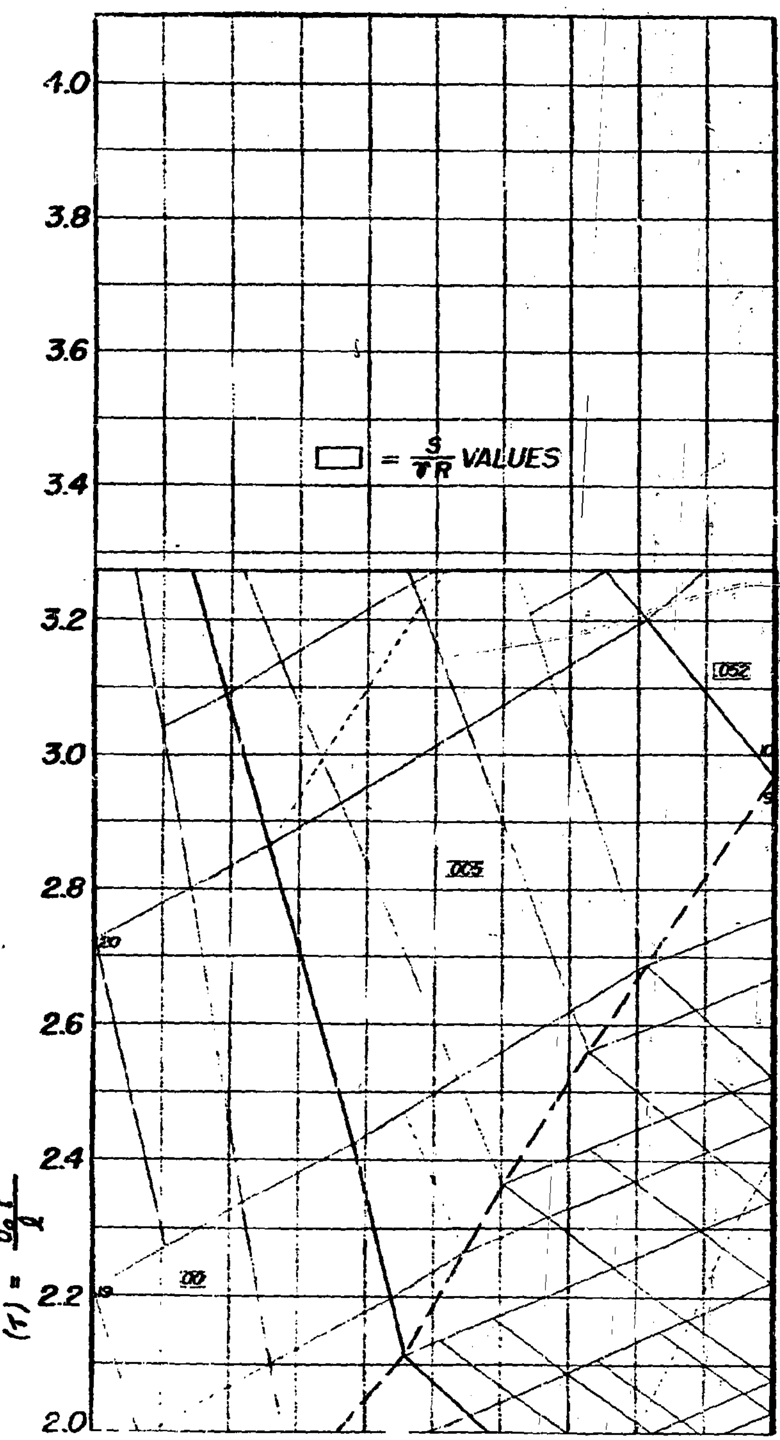

INLET AND EXIT CONDITIONS

POINT	P	u	a
	EXIT		
1	2.334	0	1.138
2	7.293	0	2.526
3	2.034	2.105	2.105
4	1.000	0.626	1.961
5	2.324	2.236	2.236
6	2.105	2.325	1.169
7	1.678	2.188	1.156
8	1.000	1.440	1.880
9	1.000	0.669	1.860
10	2.384	0	1.144
	INLET		
11	1.000	0.650	1.000
12	11.763	0	1.529
13	10.548	0	1.504
14	5.858	0	2.393
15	2.729	0	2.146
16	1.605	0	1.989
17	1.328	0	1.936
18	1.221	0.359	1.029
19	0.958	0.698	0.994
20	0.892	0.763	0.984

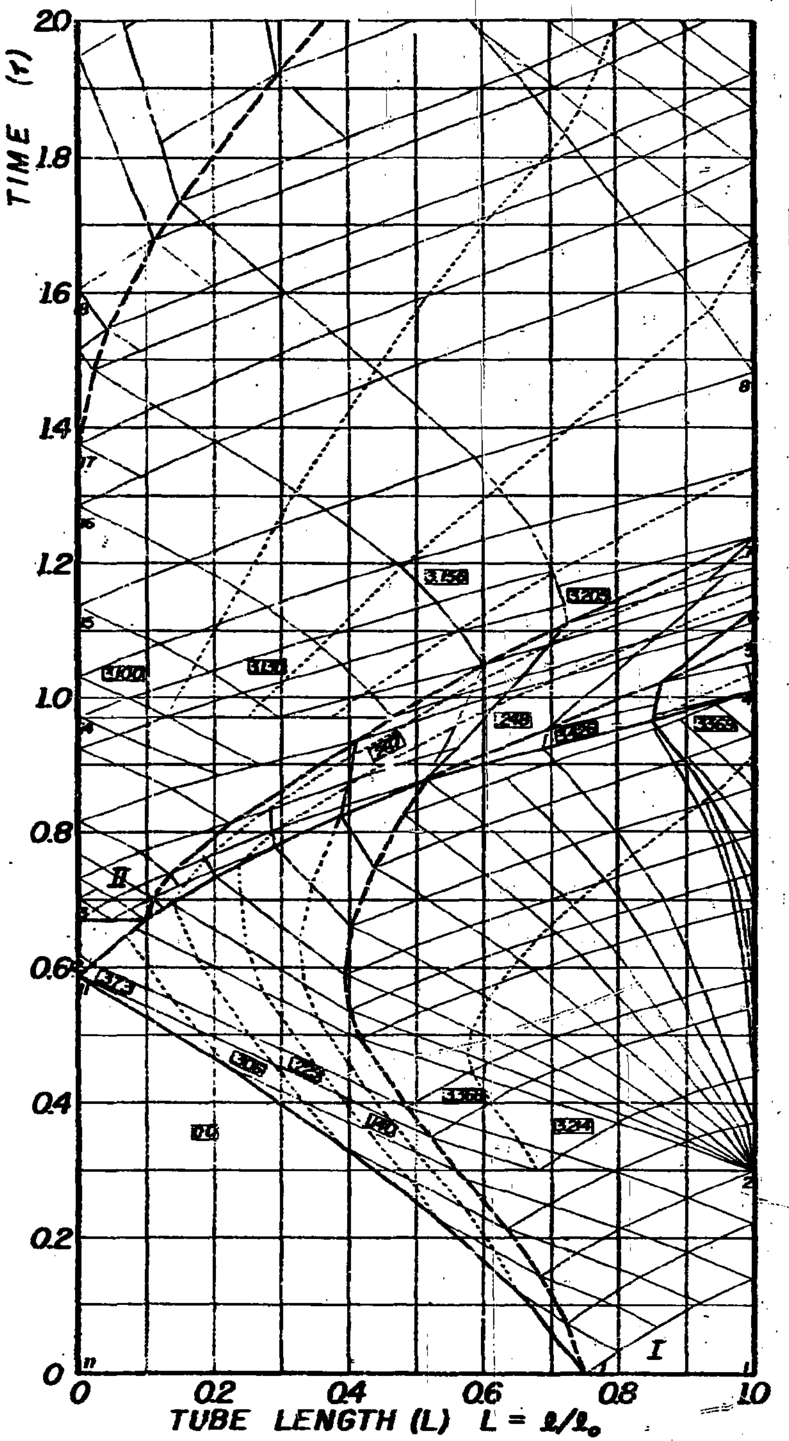

AVERAGE CONDITIONS BEFORE AND AFTER HEAT ADDITION

	I INITIAL COMBUSTION		II SECONDARY COMBUSTION	
	BEFORE	AFTER	BEFORE	AFTER
P	2.334	7.293	10.548	5.858
θ	1.296	6.408	2.262	5.726
S	0.044	3.214	0.358	3.100
η_c	0.910		0.761	
FUEL-AIR RATIO	1/31		1/31	
COMBUSTION CHAMBER MASS (m/m_o)	0.450		0.450	

CHARACTERISTIC CYCLE PERFORMANCE

SFC $\left(\frac{\text{LBS. FUEL/HR.}}{\text{LBS. THRUST}}\right)$ = 1.601 T/A $\left(\frac{\text{LBS.}}{\text{SQ. IN.}}\right)$ = 11.83

η_c = —— η_o = 0.109

CYCLE - I MACH NUMBER = 0.65

MODIFIED WAVE ENGINE CYCLE WITH SECONDARY COMBUSTION

HEAT ADDITION MODE

GRADUAL HEAT ADDITION

Fig. 22A

CONFIDENTIAL

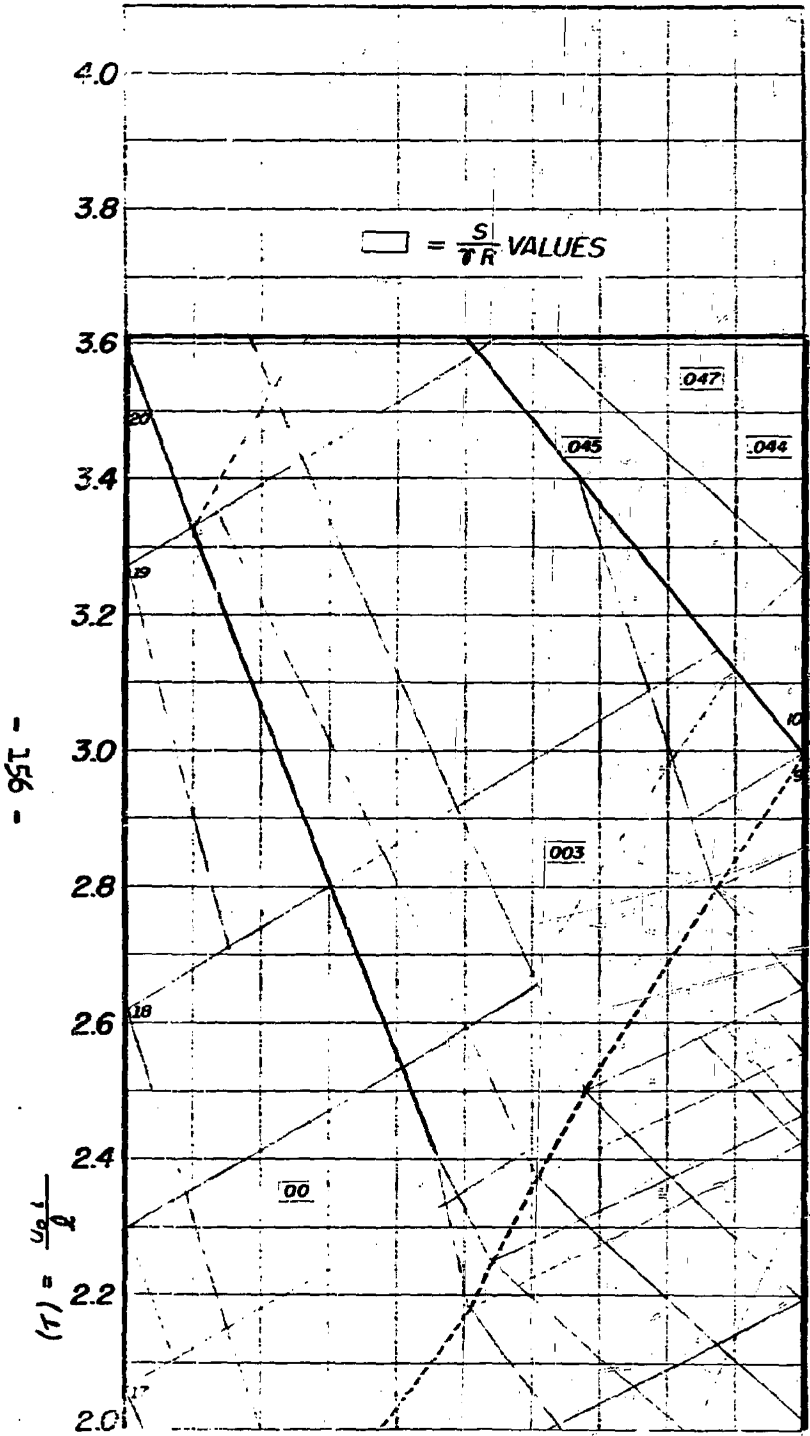

CONFIDENTIAL

INLET AND EXIT CONDITIONS

POINT	P	u	a
	EXIT		
1	2.330	0	1.138
2	7.863	0	2.129
3	2.194	1.774	1.774
4	1.000	1.401	1.601
5	1.989	2.230	1.774
6	2.159	2.045	1.825
7	2.159	2.045	1.749
8	1.000	0.382	1.543
9	1.000	0.652	1.531
10	2.336	0	1.139
	INLET		
11	1.000	0.650	1.000
12	6.720	0	1.365
13	9.630	0	1.437
14	5.830	0	1.970
15	1.328	0	1.595
16	1.157	0.453	1.021
17	1.057	0.580	1.008
18	0.955	0.698	0.994
19	0.919	0.740	0.988
20	0.900	0.755	0.985

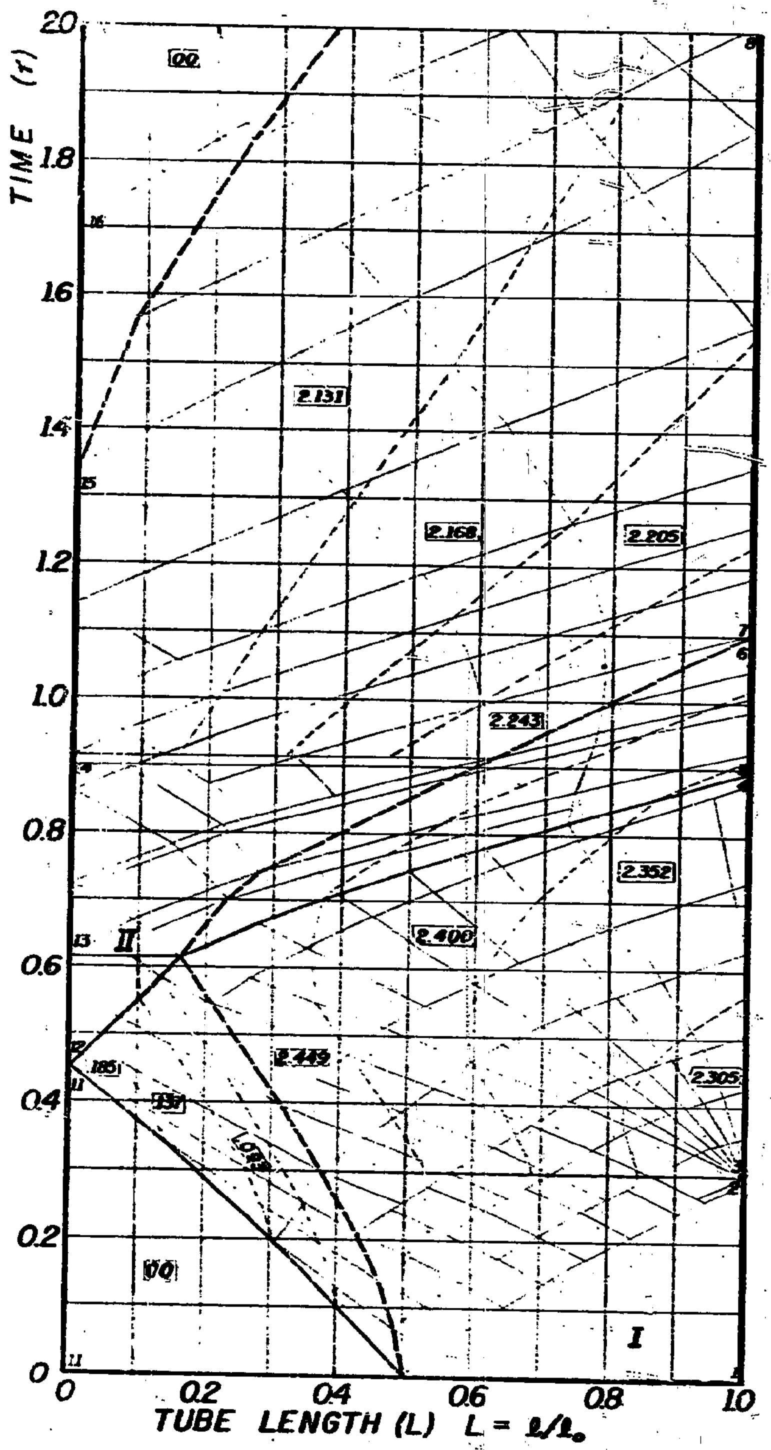

AVERAGE CONDITIONS BEFORE AND AFTER HEAT ADDITION

	I INITIAL COMBUSTION		II SECONDARY COMBUSTION	
	BEFORE	AFTER	BEFORE	AFTER
P	2.330	7.863	9.630	5.830
θ	1.295	4.533	2.065	3.881
S	0.044	2.305	0.128	2.131
η_c	0.930		0.855	
FUEL-AIR RATIO	1/56		1/56	
COMBUSTION CHAMBER MASS (m/m_o)	0.900		0.751	

CHARACTERISTIC CYCLE PERFORMANCE

SFC $\left(\frac{\text{LBS. FUEL/HR.}}{\text{LBS. THRUST}}\right)$ = 1.681 , $T/A \left(\frac{\text{LBS.}}{\text{SQ. IN.}}\right) = 10.38$

η_c = —— $\eta_o = 0.104$

CYCLE – I MACH NUMBER = 0.65

MODIFIED WAVE ENGINE CYCLE WITH SECONDARY COMBUSTION

HEAT ADDITION MODE

GRADUAL HEAT ADDITION

Fig. 23A

CONFIDENTIAL

CONFIDENTIAL

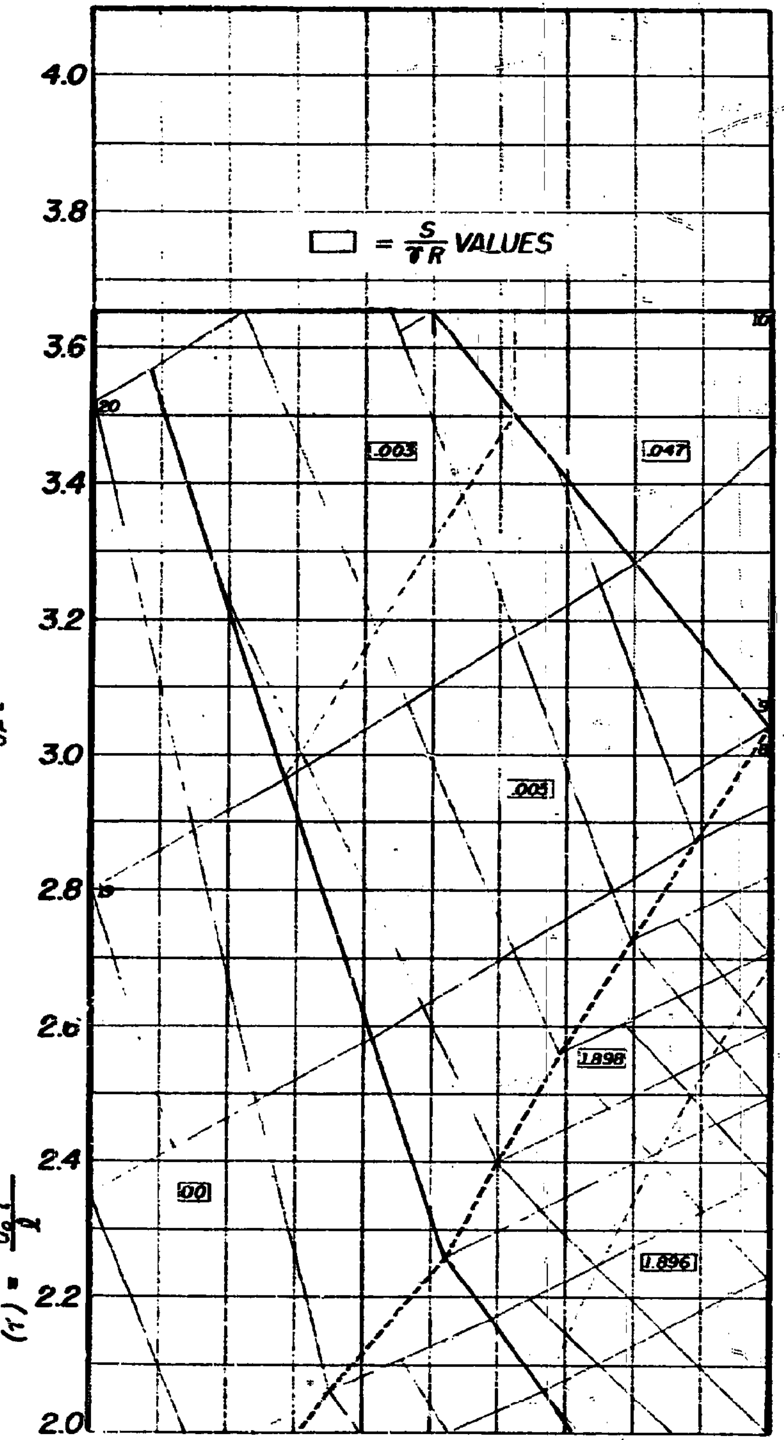

INLET AND EXIT CONDITIONS

POINT	P	u	a
EXIT			
1	7.973	0	2.102
2	2.954	0	1.824
3	1.000	1.305	1.563
4	3.578	2.902	1.930
5	1.439	1.672	1.672
6	1.439	1.672	1.539
7	1.000	0.300	1.461
8	1.000	0.641	1.462
9	2.300	0	1.137
10	2.372	0	1.142
INLET			
11	1.000	0.650	1.000
12	9.830	0	1.472
13	24.006	0	2.300
14	7.496	0	1.948
15	4.606	0	1.817
16	2.705	0	1.684
17	1.328	0	1.521
18	1.157	0.458	1.021
19	0.958	0.696	0.994
20	0.856	0.768	0.978

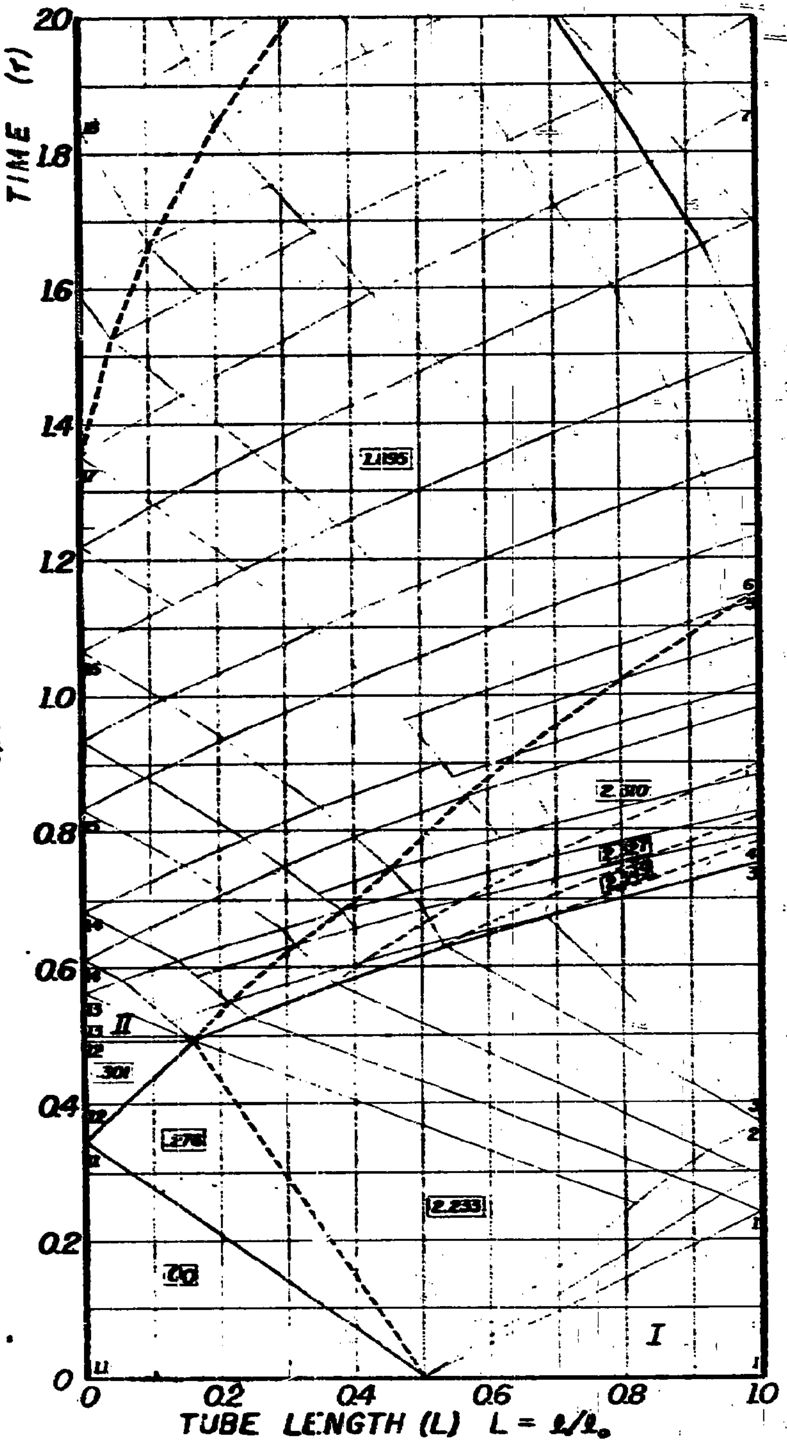

AVERAGE CONDITIONS BEFORE AND AFTER HEAT ADDITION

	I INITIAL COMBUSTION		II SECONDARY COMBUSTION	
	BEFORE	AFTER	BEFORE	AFTER
P	2.334	7.973	9.830	24.006
θ	1.295	4.418	2.167	5.292
S	0.044	2.233	0.301	1.895
η_c	0.910		0.790	
FUEL-AIR RATIO	1/56		1/56	
COMBUSTION CHAMBER MASS (m/m_o)	0.900		0.726	

CHARACTERISTIC CYCLE PERFORMANCE

$SFC \left(\frac{\text{LBS. FUEL/HR.}}{\text{LBS. THRUST}}\right) = 1513$, $T/A \left(\frac{\text{LBS.}}{\text{SQ. IN.}}\right) = 11.21$

η_c = ——— $\eta_o = 0.115$

CYCLE - I MACH NUMBER = 0.65

MODIFIED WAVE ENGINE CYCLE WITH SECONDARY COMBUSTION

HEAT ADDITION MODE

CONSTANT VOLUME COMBUSTION

Fig. 24A

CONFIDENTIAL

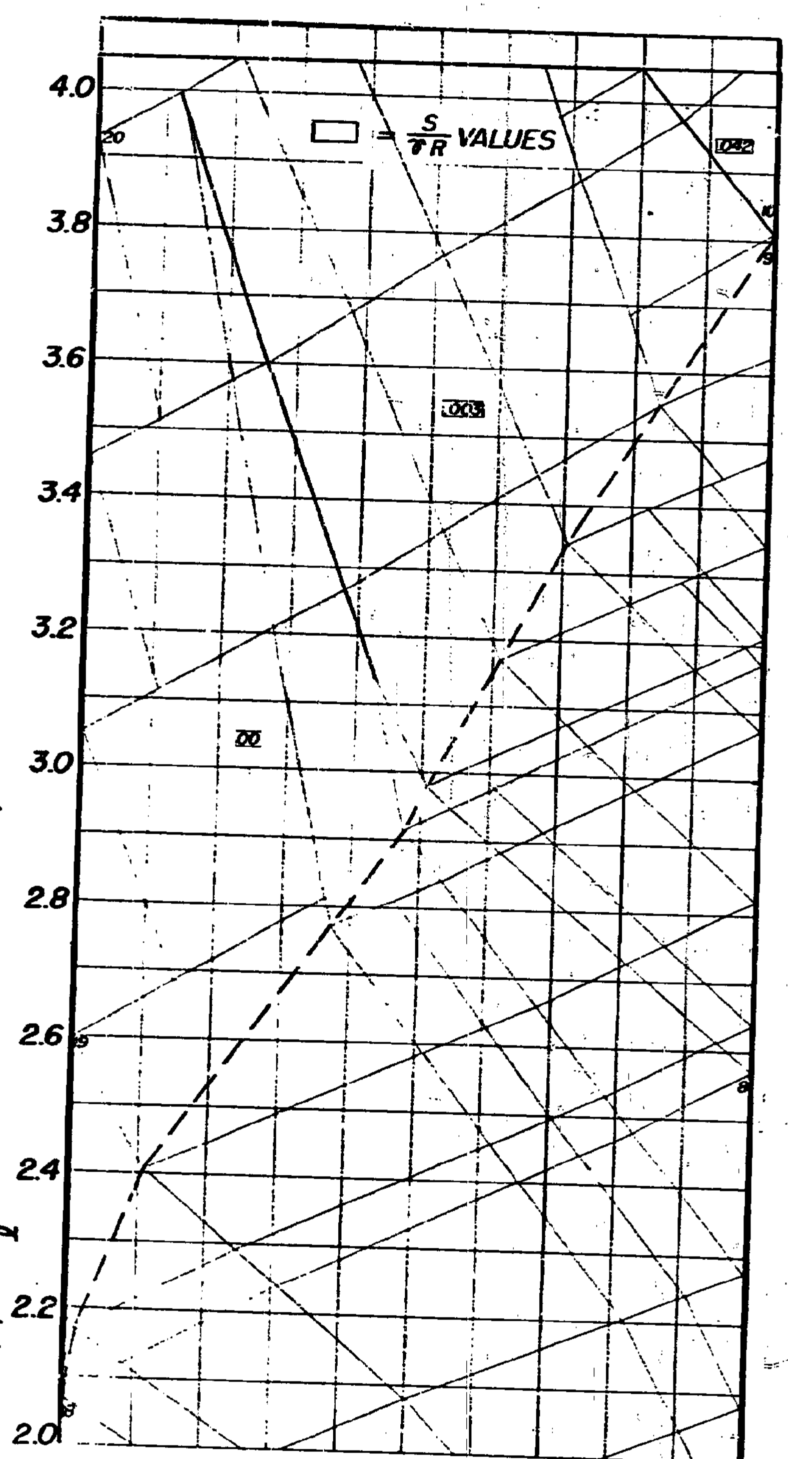

CONFIDENTIAL

INLET AND EXIT CONDITIONS

POINT	P	u	a
EXIT			
1	7.973	0	2.102
2	2.950	0	1.824
3	2.297	0	1.760
4	3.295	1.870	1.870
5	2.843	1.831	1.831
6	2.843	1.831	1.811
7	1.315	1.622	1.622
8	1.000	0.322	1.560
9	1.000	0.645	1.560
10	2.319	0	1.137
INLET			
11	1.000	0.650	1.000
12	9.784	0	1.472
13	3.539	0	1.273
14	10.364	0	2.178
15	8.798	0	2.128
16	2.366	0	1.764
17	2.292	0	1.756
18	1.328	0	1.624
19	1.139	0.475	1.019
20	0.906	0.750	0.986

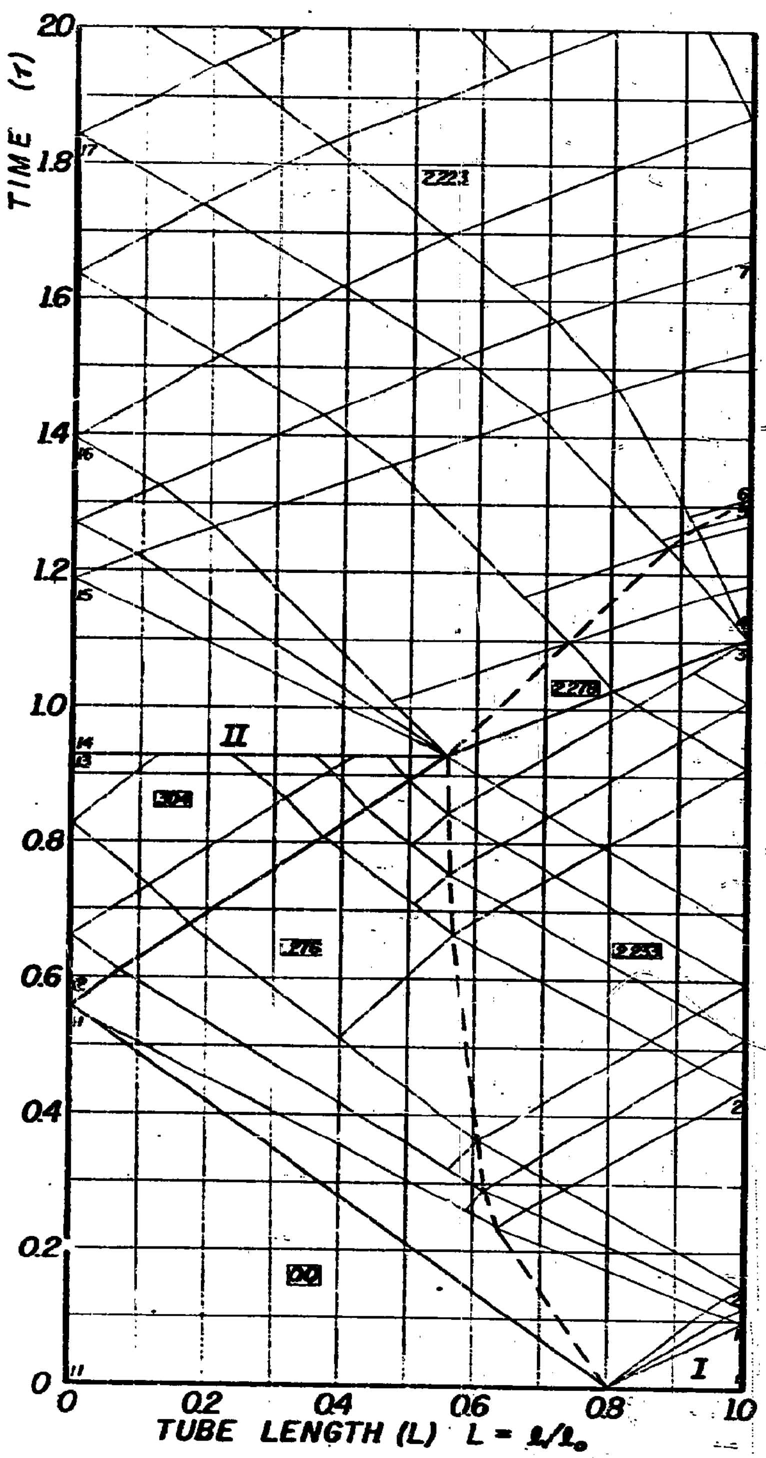

AVERAGE CONDITIONS BEFORE AND AFTER HEAT ADDITION

	I INITIAL COMBUSTION		II SECONDARY COMBUSTION	
	BEFORE	AFTER	BEFORE	AFTER
P	2.334	7.973	3.539	10.364
θ	1.295	4.418	1.620	4.745
S	0.044	2.233	0.304	2.223
η_c	0.910		0.701	
FUEL-AIR RATIO	1/56		1/56	
COMBUSTION CHAMBER MASS (m/m_o)	0.360		1.212	

CHARACTERISTIC CYCLE PERFORMANCE

$SFC\left(\frac{\text{LBS. FUEL/HR.}}{\text{LBS. THRUST}}\right) = 1.611$, $T/A\left(\frac{\text{LBS.}}{\text{SQ. IN.}}\right) = 919$

$\eta_c =$ ——— $\eta_o = 0.108$

CYCLE - I MACH NUMBER = 0.65

MODIFIED WAVE ENGINE CYCLE WITH SECONDARY COMBUSTION

HEAT ADDITION MODE

CONSTANT VOLUME COMBUSTION

Fig. 25A

CONFIDENTIAL

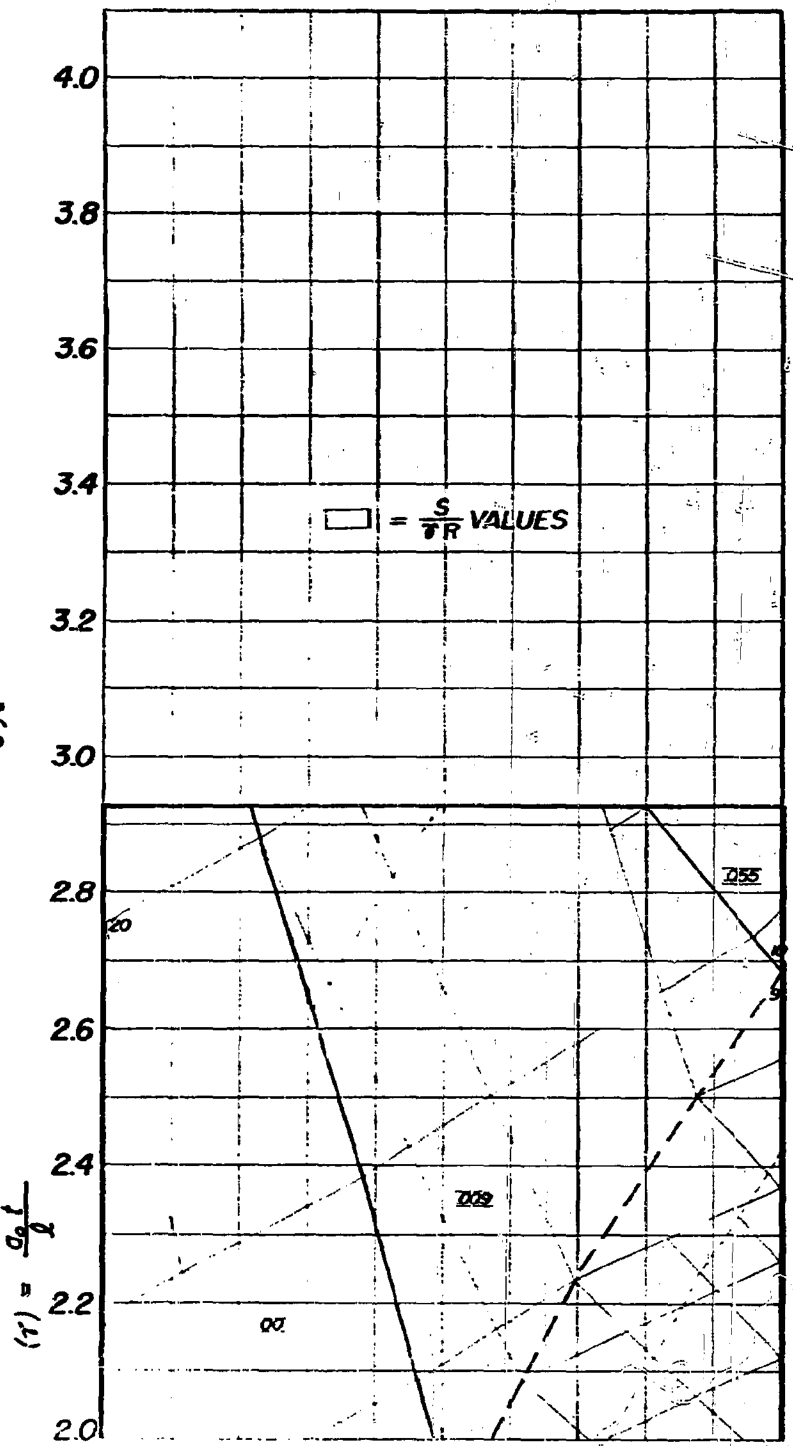

INLET AND EXIT CONDITIONS

POINT	P	u	σ
EXIT			
1	24.834	0	3.714
2	5.491	0	2.994
3	1.533	2.495	2.495
4	1.000	2.079	2.347
5	2.630	3.848	2.729
6	2.642	3.406	2.746
7	2.642	3.406	1.835
8	1.000	0.330	1.597
9	1.000	0.662	1.598
10	2.346	0	1.142
INLET			
11	1.000	0.650	1.000
12	38.917	0	2.099
13	11.187	0	1.756
14	22.525	0	2.492
15	13.503	0	2.316
16	3.490	0	1.909
17	1.642	0	1.714
18	1.328	0	1.663
19	1.141	0.482	1.019
20	0.903	0.754	0.985

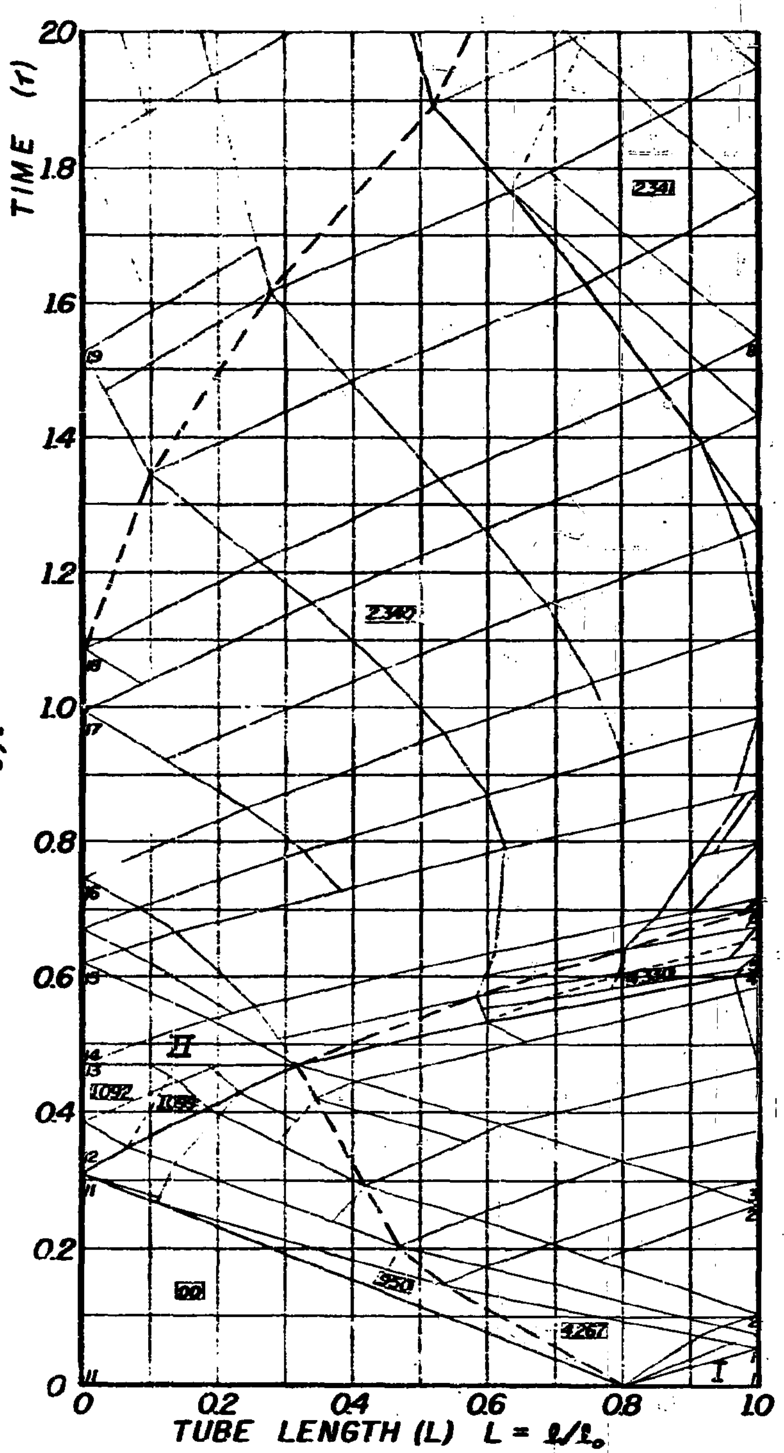

AVERAGE CONDITIONS BEFORE AND AFTER HEAT ADDITION

	I INITIAL COMBUSTION		II SECONDARY COMBUSTION	
	BEFORE	AFTER	BEFORE	AFTER
P	2.334	24.834	11.187	22.525
θ	1.296	13.796	3.084	6.208
S	0.044	4.267	1.090	2.340
η_c	0.910		0.500	
FUEL-AIR RATIO	1/14		1/56	
COMBUSTION CHAMBER MASS (m/m_o)	0.360		1.147	

CHARACTERISTIC CYCLE PERFORMANCE

SFC $\left(\frac{\text{LBS. FUEL/HR.}}{\text{LBS. THRUST}}\right)$ = 1.951 , $T/A \left(\frac{\text{LBS.}}{\text{SQ. IN.}}\right)$ = 17.32

η_c = ——— η_o = 0.089

CYCLE - 1 MACH NUMBER = 0.65

MODIFIED WAVE ENGINE CYCLE WITH SECONDARY COMBUSTION

HEAT ADDITION MODE

CONSTANT VOLUME COMBUSTION

Fig. 26A

CONFIDENTIAL

APPENDIX 2

In order to carry out the characteristics calculations, it was necessary to make a number of assumptions concerning the heat addition process, valve closing time and the flow boundary conditions. These assumptions are discussed in detail in Section 2A.

General methods for construction of the wave cycles can be found in a number of recent articles. Complete details of the method are not as yet available in print. For this reason, a brief review of the procedures is given in Section 2B and a few specific examples are worked.

The engine performance parameters such as thrust per unit area, mass flow and specific fuel consumption can be obtained from these characteristic diagrams. Details of the methods of obtaining this performance data, as well as methods of extending the performance obtained for a single altitude condition to other altitude conditions, are described in Section 2C.

A. Heat Addition Assumptions

The processes of heat addition was represented by the following modes of heat addition:

1. Constant volume combustion
2. Gradual heat addition with heat added at a constant rate.

For the latter case, the combustion time was based on the values observed in experimental intermittent engine studies about 1.2 milliseconds. In both cases, it was assumed that all the gas particles in the combustion region were ignited at the same instant and that the process of heat addition was delayed until all the gas to be burned reached approximately the same state. Since the compression occurred through a reflected shock wave, the heat-addition process was, therefore, assumed to be delayed until the shock traversed the whole combustion zone. This assumption was only made to simplify the characteristics calculations. After the shock passage, the pressure and temperature were nearly uniform in the combustion region. Average values of pressure and temperature could, therefore, be used and uniform conditions could be assumed for the whole of the combustion region.

In the studies it was found that as a result of the wave phenomena established, the maximum pressures prior to heat addition occurred at the instant of valve closure. With the delay assumed in the heat-addition process in order to bring all the gas in the combustion chamber to approximately the same state, it was observed that the pressure in the combustion region gradually decreased. This pressure drop occurred because expansion waves previously created by valve opening reached the combustion region shortly after the shock reflection and caused a drop in the pressure. Consequently, in all the cycles studied, heat addition occurred at pressures much lower than those obtained at the instant of valve closure. The assumption of the ignition delay was, therefore, conservative in that, if ignition had been assumed to occur at the instant the gas was brought to rest, the assumed heat addition process would have been initiated at much higher pressures.

The first heat addition mode, constant volume combustion, was selected primarily because of the simplicity of the calculations. Two different assumptions were made: the first, that a constant pressure rise of four atmospheres occurred during the heating process, and, the second, that a constant amount of heat, 520 BTU's per lb. of air, was added per cycle. The pressure rise of four atmospheres was initially assumed in order to study the wave pattern generated. Early wave engine tests had indicated that a pressure rise of the order of 4 atmospheres was obtained during the heat addition process. In succeeding studies, it was found to be more convenient to employ a fixed quantity of heat per lb. of air, since the engine performance for a fixed air-fuel ratio could be determined.

All of the studies made were for straight-tube configurations operating with instantaneous valve opening and closing times. The use of the instantaneously-operating valve assumption results also in an appreciable simplication of the procedures, although it probably tends to over-emphasize the shock losses. Actually, a shock is formed gradually because of a finite valve closing time and is not created instantaneously. During the early phases of the valve closing the compression is, therefore, essentially isentropic. On the other hand, this assumption tends to eliminate the actual leakage losses obtained during a finite period of closing.

As yet, very few studies have been undertaken to determine the validity of the conventional boundary conditions assumed in the nonsteady flow calculations. These are: ram pressure at the intake during inflow and ambient pressures at the exit during outflow for nonchoked flow conditions. Probably the most serious error is introduced by the assumption of ambient pressure during the exhaust-flow phase. During a large period of the nonsteady exhaust process at high flight speeds, when the velocity of the exhausting air becomes appreciably less than that of the surrounding stream, the total head of the ejected gas becomes much lower than that of the external flow. It would be expected then, that the exhaust gas would be accelerated, due to shear effects, to a velocity near that of flight. This would appreciably alter the internal flow phenomena, i.e., the rapidity of scavenging, the internal pressure, and the resultant cycle time. Since no experimental information concerning the magnitude of this effect has been obtained, the conservative assumption of constant ambient pressure during nonchoked outflow has been used.

B. The Method of Characteristics

General methods of construction of characteristic or wave cycles can be found in a number of recent articles[4,5]. Details of the methods, applicable to a specific problem, are not as yet available in print (see Reference 6). A brief review of some of the procedures is given in the following pages.* The specific example selected is a wave cycle with the conditions:

(a) Constant volume combustion

(b) $M = 0.65$

(c) Pressure rise at the end of heat addition equal to foud times the initial pressure.

The calculations for the gradual heat addition process are similar. For the gradual heat addition process, it was assumed that the heat addition process in the combustion chamber was only a function of time, and that the heat was added at a constant rate.

$$\frac{dq}{dt} = q/t_c \quad (t_c = \text{combustion time})$$

The change in the characteristic values, as defined in the following section, for the heat addition process would then be given by

$$\delta P = \delta Q = \frac{\gamma q J}{a_0^2} \frac{q}{t_c} \delta \tau_c .$$

C. Performance Calculations

The total impulse generated per cycle may be calculated either by integration of the pressure forces over the walls for the cycle, or by integration of the total momentum flow over the cycle. In the latter case

---

*see page 171

$$I_{total} = AP_o \int \left(\frac{P_e}{P_o} - 1\right) dt + A \int \frac{(\rho u)_e}{g} (u_e - u_o)\, dt$$

where

A = tube area

P = pressure

V = A ℓ_o (ℓ_o = over-all length)

and the subscript (o) refers to ambient conditions and (e) to exit conditions.

In dimensionless form this may be written

$$\frac{I_{(total)}}{VP_o/a_o} = \int \left(\frac{P_e}{P_o} - 1\right) d\tau + \int \frac{\rho_e}{\rho_o} \frac{u_e}{a_o} \left(\frac{u_e - u_o}{a_o}\right) d\tau \qquad (1)$$

where

$$\tau = a_o t / \ell \,.$$

The air specific impulse is given by

$$I_a = I\,total/_{mass(cycle)} \qquad (2)$$

where

$$\frac{mass}{\rho_o} = A L_c \left(\frac{\rho_c}{\rho_o}\right) \quad (c \text{ refers to combustion chamber}).$$

In dimensionless form, the air specific impulse is given by

$$I_a \Big/ \frac{P_o}{\rho_o a_o} = \frac{1}{\left(\frac{L_c}{L_o}\right)\left(\frac{\rho_c}{\rho_o}\right)} \int \left(\frac{P_e}{P_o} - 1\right) d\tau + \frac{1}{\frac{L}{L_o}\,\frac{\rho_c}{\rho_o}} \int \frac{\rho_e}{\rho_o} \frac{u_e}{a_o} \left(\frac{u_e - u_o}{a_o}\right) d\tau. \qquad (3)$$

The mass flow per sec. per sq.ft. may be determined from the relation

$$\frac{\text{Mass per cycle}}{\text{cycle time}} = \frac{L_c}{L_o} \frac{a_o \rho_o A}{\tau_c} \left(\frac{\rho_c}{\rho_o}\right).$$

Hence

$$\frac{\text{Mass flow per sec.}}{\text{sq.ft.}} = \left(\frac{L_c}{L_o} \frac{\rho_c}{\rho_o}\right) \frac{a_o \rho_o}{\tau_c}$$

or in dimensionless form

$$\frac{\text{Mass flow/sec}}{\text{sq.ft.}} \cdot \frac{1}{a_0 \rho_0} = \frac{1}{\tau_c}\left(\frac{L_c}{L_0}\,\frac{\rho_c}{\rho_0}\right). \tag{4}$$

Since

$$I_a = \frac{\text{lbs.thrust}}{\text{lb.air/sec}} = \frac{\text{Thrust}\cdot\tau_c}{(L_c/L_0)\,a_0\rho_0\left(\frac{\rho_c}{\rho_0}\right)A}$$

the thrust per sq. in. may be written

$$\frac{T}{A}\ \frac{\text{lbs.}}{\text{sq.in.}} = \frac{I_a\left(\frac{L_c}{L_0}\right)a_0\rho_0\left(\rho_c/\rho_0\right)}{144\,\tau_c}. \tag{5}$$

The specific fuel consumption can be determined from

$$\text{S.F.C.} = \frac{3600}{I_a/\ f/a} \tag{6}$$

since

$$I_f = \frac{I_a}{f/a}.$$

The adiabatic compression efficiency is defined by

$$\eta_{comp} = \frac{\left(\frac{P_2}{P_1}\right)^{\frac{\gamma-1}{\gamma}}-1}{\theta_2/\theta_1-1}. \tag{7}$$

The over-all efficiency is defined in the usual manner:

$$\eta_{\text{over-all}} = \eta_{\text{Prop.}}\,\eta_{\text{thermal}} \tag{8}$$

and can be written

$$\eta_{\text{over-all}} = \frac{I_f\,u_0}{15\times10^6}. \tag{9}$$

where u_0 is the flight velocity. This efficiency was calculated by integration of the momentum flow.

The performance parameters given in the Tables and Figures were determined for standard sea-level conditions. For any other altitude condition the performance parameter S.F.C., Thrust/unit area and mass flow/sec/unit area may be determined using the following relations:

$$(\text{S.F.C.})_{alt} = (\text{S.F.C.})_{S.L.}\,\frac{(a_0)_{alt.}}{(a_0)_{S.L.}} \tag{10}$$

$$(\text{Thrust/unit area})_{alt} = (\text{Thrust/unit area})_{S.L.} \frac{(a_0^2 \rho_0)_{alt.}}{(a_0^2 \rho_0)_{S.L.}} \tag{11}$$

(Mass flow per sec/unit area)$_{alt}$ =

$$(\text{Mass flow per sec/unit area})_{S.L.} \frac{(a_0 \rho_0)_{alt}}{(a_0 \rho_0)_{S.L.}} \tag{12}$$

$$(f/a)_{alt.} = (f/a)_{S.L.} \frac{(a_0^2)_{alt.}}{a_0^2{}_{S.L.}} \tag{13}$$

The ratio $\frac{\Delta s}{\gamma R}$, the entropy parameter in the characteristics calculations is also dimensionless. Consequently,

$$\left(\frac{q}{\theta}\right)_{S.L.} = \left(\frac{q}{\theta}\right)_{alt.}$$

or

$$\left(\frac{(f/a)}{a_0^2}\right)_{alt} = \left(\frac{f/a}{a_0^2}\right)_{S.L.}$$

and

$$(f/a)_{alt} = (f/a)_{SL} \frac{(a_0^2)_{alt}}{(a_0^2)_{S.L.}}$$

which is relation (13). The remaining relations (10), (11), and (12) may be obtained by direct substitution observing that

$$(I_a)_{alt.} = (I_a)_{S.L.} \frac{(a_0)_{alt}}{(a_0)_{S.L.}}$$

from (3) and

$$\frac{(I_a)_{alt}}{(f/a)_{alt}} = \left(\frac{1}{S.F.C.}\right)_{alt.}$$

GRAPHICAL PROCEDURES FOR CALCULATION OF WAVE ENGINE CYCLE

The continuity and momentum equations for one-dimensional nonsteady flow are

$$A \frac{\delta \rho}{\delta t} + \frac{\delta}{\delta x} (\rho u A) = 0$$

$$\frac{\delta u}{\delta t} + \frac{\delta u}{\delta x} + \frac{1}{\rho} \frac{\delta P}{\delta x} = 0$$

These may be transformed to yield

$$P = - \frac{ua}{u+a} \quad \delta \log A + \frac{a}{\gamma R} \delta S + \frac{a}{Cp} \frac{Ds}{dt} \delta t$$

$$Q = - \frac{ua}{u-a} \quad \delta \log A + \frac{a}{\gamma R} \delta S + \frac{a}{Cp} \frac{Ds}{dt} \delta t$$

where

A = area

ρ = density

u = velocity

a = velocity of sound

P = pressure

For a tube of constant area and isentropic flow

$$\delta Q = \quad \delta P = 0$$

$$P = \frac{2}{\gamma-1} a + u = \text{constant}$$

$$Q = \frac{2}{\gamma-1} a - u = \text{constant}$$

These quantities, P & Q are constant along characteristic lines where the characteristic velocities are u + a and u - a, respectively. With these relations we can construct a characteristic network in the x,t-plane which enables a determination of the flow parameters u,a,etc. at each point of intersection.

General Procedure for Wave Engine Characteristics Diagram with Constant Volume Combustion

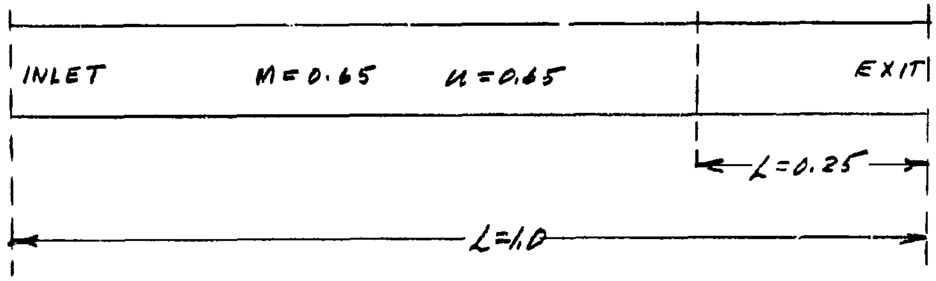

I. Initial Conditions

1. Uniform flow through the tube which is completely open, with a flow Mach Number M = 0.65.

   All quantities are dimensionless.

   Pressure, $p = p/p_o$

   Velocity of Sound, $A = a/a_o$

   Velocity, $U = u/a_o$ (where a_o and p_o are reference sound velocity and pressure)

   Time, $\tau = \frac{a_o t}{l}$

   Length of tube, $L = \frac{l}{l_o}$

   Entropy $= \frac{S}{\gamma R}$

2. At some time, τ_1 , the valve at the exit closes. The flow velocity at the closed valve equals zero and a shock wave is created which propagates into the tube.

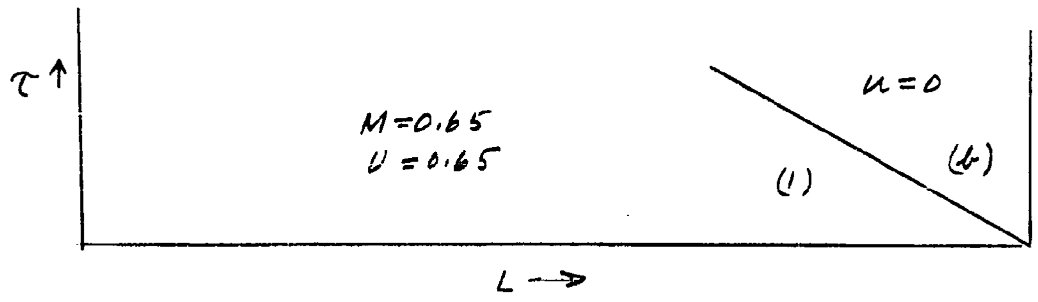

3. In order to determine conditions in (b) the change in velocity across the shock that is formed is given by the shock relations.

NOTE: Until the shock reaches the inlet we have uniform flow in the tube with a velocity U = 0.65.

To determine the ratio a_2/a_1 across the shock it is necessary to revert to the Rankine-Hugoniot relations

$$M_2^2 = \frac{2 + (\gamma-1)M_1^2}{2\gamma M_1^2 - (\gamma-1)}$$

Normal shock
M_1 | M_2

$$a_2/a_1 = \left[\frac{1 + \frac{\gamma-1}{2} M_1^2}{1 + \frac{\gamma-1}{2} M_2^2}\right]^{-1/2}$$

and obtain relations between the steady flow parameters and the velocities U_1 and U_2 in the nonsteady flow case.

$$\frac{U_1-U_2}{a_1} = \frac{\Delta U}{a_1} = M_1 - M_2 \frac{a_2}{a_1}$$

$$M_1 = \frac{U_1 + W_S}{a_1}$$

$$M_2 = \frac{U_2 + W_S}{a_2}$$

W_S = shock velocity

Since the entropy rise across the shock may be required, we also have

$$\frac{P_2}{P_1} = \frac{2\gamma M_1^2 - (\gamma-1)}{\gamma+1}$$

and

$$\frac{\Delta S}{\gamma R} = \frac{2}{\gamma-1} \ln \frac{a_2}{a_1} - \frac{1}{\gamma} \ln \frac{P_2}{P_1}$$

where

$$\frac{a_2}{a_1} = \frac{a(b)}{a_1} \text{ etc.} \qquad \left(a_2/a_1 = \frac{A_2}{A_1} \right)$$

4. When the shock reaches the position L = 0.25 we assume constant volume heat addition

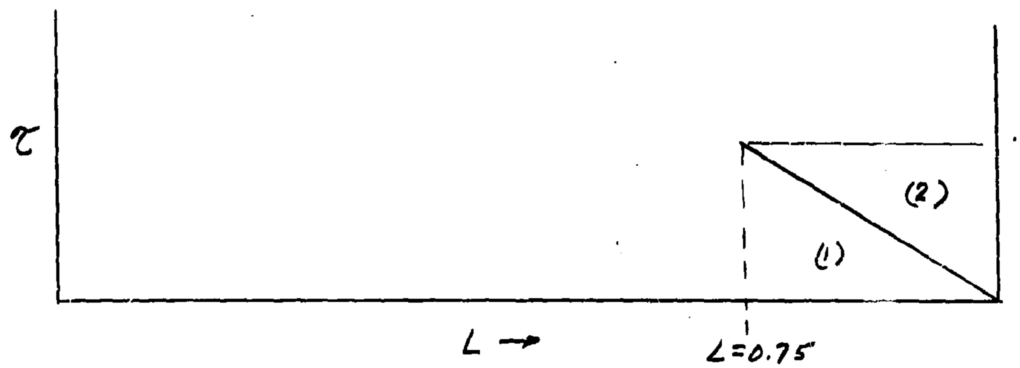

II. <u>Characteristic solution in the heating region</u>

1. Heat addition

For the heat addition $P_2/P_b = 4.0$ and $a_2/a_b = \sqrt{4}$.

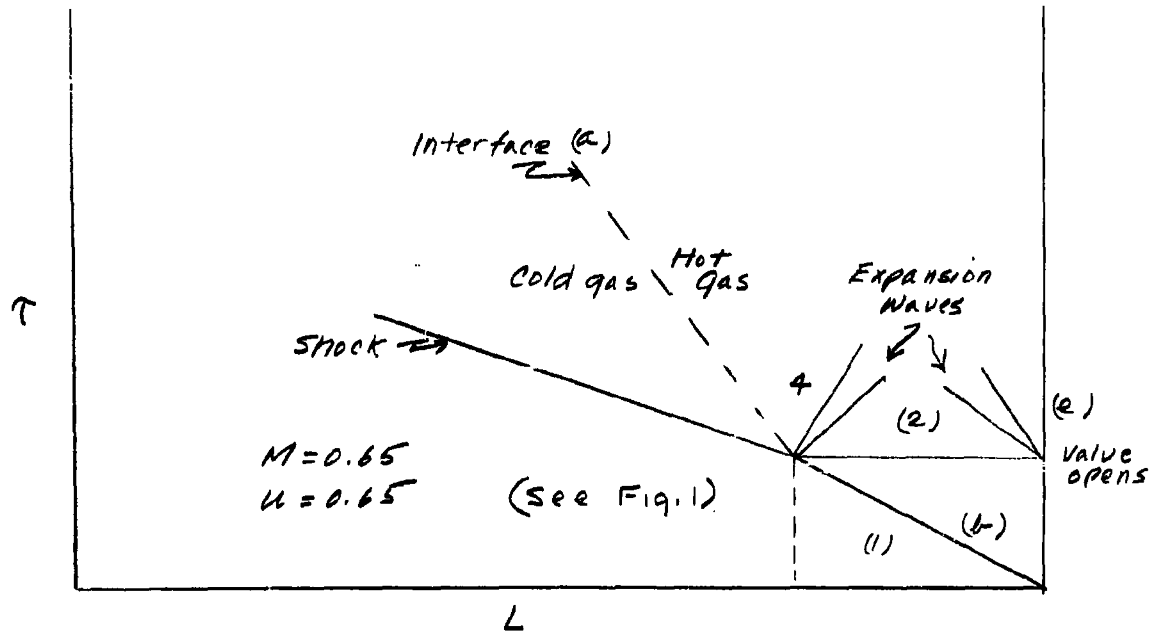

Immediately after the heat addition we assume the rear valve opens and outflow begins, while, simultaneously, a strong shock moves upstream. The interface (a) separates the hot and cold gas.

2. Boundary conditions

Exit:

(a) The general boundary condition for outflow is that the pressure at the exit is equal to the reference pressure $p_e = p_o$. This condi- exists only when $U_e < A_e$.

(b) Since U_e can never become greater than A_e, choking occurs when $U_e = A_e$, then $p_e > p_o$.

e.g.

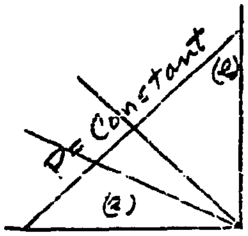

$5 A_2 = 5A_e + U_e = \text{constant}$

(a) $\frac{p_2}{p_o} = \frac{A_2}{A_e}^{\frac{2\gamma}{\gamma-1}}$

(b) $p_e/p_e = (5/6)^7$

Since $p_e = p_o = 1.0$

For U_e A_e

For $U_e = A_e$

Consequently for this particular diagram –

$5\ A_2 + U_2 = P_2 = 11.385$ Since $U_2 = 0$

$5\ A_{10} + U_{10} = P_{10} = 11.385$

$\therefore\ A_{10} = U_{10} = 1.8975$

Also $p_{10} = p_e = 2.6054$ Since $p_{10} = 1.0$ would make $U_{10} > A_{10}$

3. Solution across the interface

$p_e = p_4$

$U_e = U_4$

The strength of the expansion fan created at point No. 4, and the strength of the shock between points No. 1 and No. 3, must be selected so that $p_3 = p_4$ across the interface.

$$p_3 = \frac{2\gamma M_1^2 - (\gamma-1)}{\gamma+1} \cdot p_1$$

$$p_4 = (A_4/A_2)^7 \cdot p_2$$

$$\frac{U_3 - U_1}{A_1} = M_1 - M_3 \frac{A_3}{A_1}$$

$$U_4 = 5\ A_4 - Q_4 = 5\ A_4 - Q_2 \qquad [Q_2 = Q_4 = 11.385]$$

Solving these relations yields

$P_3 = P_4 = 5.5324$

$U_e = U_4 = -0.820$

$A_3 = 1.366$

$A_4 = 2.113$

4. Determination of Pts. 5 to 9 and 11 to 16 (*see Fig. 2*)

Q remains constant going from right to left, P remains constant going from left to right } in regions where there are no entropy changes and no change in cross-sectional area.

$\Delta P = \Delta Q = 0$

$P_2 = P_5 = P_6 = P_7 = P_8 = P_9 = P_{10} = 11.385$

$Q_2 = 11.385$ and $Q_{10} = 7.590$

Taking values of Q between 11.385 and 7.590 and using the constant value of P, solve for U and A at these points

$$5A + U = P \qquad A = \frac{P + Q}{10} \ \& \ U = \frac{P-Q}{2}$$

$$5A - U = Q$$

In a similar manner -

$$P_r = P_{11} = P_{12} = P_{13} \ldots\ldots\ldots P_{16} = P_{17} = 9.745$$

$Q_4 = Q_2$, $Q_{11} = Q_5$, $Q_{12} = Q_6$ — Since Q is constant going right to left when there is no entropy or area change.

5. Boundary point 17

$$P_{17} = P_4 = 9.745 = 5\,A_{17} + U_{17}$$

Since, $p_{17} = p_e = p_o = 1.00$, $U_{17} < A_{17}$

$$\therefore A_{17} = A_e = \frac{1.000}{p_2} A_2 = 1.655$$

This value of $A_e = 1.655$ remains constant at the exit as long as $p_e = p_o$ and $U_e < A_e$.

6. <u>All subsequent points</u> within the boundary formed by the interface, Nos. 11 to 93, the shock, Nos. 93-17, and the characteristic line Nos. 11 to 17, are determined in the same manner since here also there is no entropy change and no cross-sectional area change.

III. <u>Change in Characteristics in Crossing Large Entropy Discontinuities</u>

Solution for Point 18-19 (Fig 2).

Along the high pressure side of the shock, point 3, P is constant until the intersection of the first Q characteristic with the shock.

Therefore $P_{18} = P_3 = 6.010$.

$Q_{19} = Q_{11} = Q_5$

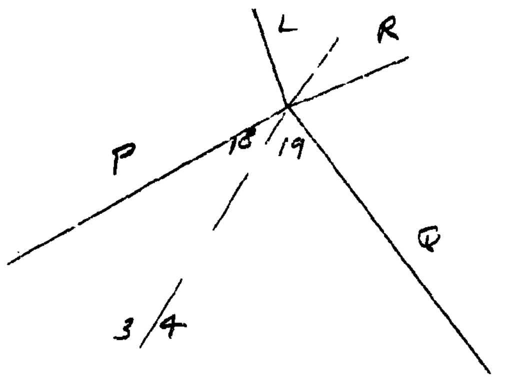

$$P_{18} = 5\,A_{18} + U_{18}$$

$$Q_{19} = 5\,A_{19} - U_{19}$$

$$U_{19} = U_{18}$$

$$P_{19} = P_{18}$$

Also A_L/A_R remains constant. It is equal to $A_3/A_4 = 0.646472$.

From the characteristics relations

$$\frac{A_L}{A_R} = \frac{A_{18}}{A_{19}} = \frac{A_3}{A_4} = 0.646472$$

$$5\,A_{18} + 5\,A_{19} = P_{18} + Q_{19}$$

or

$$A_{19} = \frac{P_{18} + Q_{19}}{5(1 + \frac{A_L}{A_R})} = \frac{P_{18} + Q_{19}}{8.232360}$$

Therefore:

$$A_{19} = 2.022$$

$$U_{19} = U_{18} = -0.525$$

$$A_{18} = 1.307$$

This procedure enables all points along the interface, Nos. 18 to 100, and Nos. 19 to 101, to be determined.

IV. <u>Procedure for determining changing shock conditions as characteristics overtake the shock</u>

1. General Procedure

In this case, we know P_1, Q_1, and Q_2

From ΔQ, $\frac{Q_2 - Q_1}{A_1}$, we can find ΔP (Fig 4)

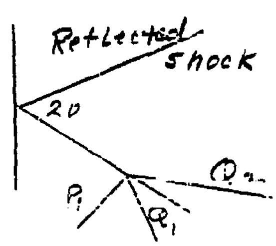

Relations across shock

$$\frac{P_2 - P_1}{A_1} = M_2 \frac{A_2}{A_1} - M_1 + \frac{2}{\gamma-1} \left(\frac{A_2}{A_1} - 1\right)$$

$$\frac{Q_2 - Q_1}{A_1} = M_2 \frac{A_2}{A_1} - M_1 - \frac{2}{\gamma-1} \left(\frac{A_2}{A_1} - 1\right)$$

Example: Solution for point No. 20

$$P_1 = 5.650, \; Q_1 = 4.350$$

A value of Q was interpolated between No. 3 and No. 18 which would reach the shock at No. 20. From $\Delta Q/A_1$ we determine $\Delta P/A_1$ which enables the determination of A_{20} and U_{20} from the usual relations, $5A + U = P$ and $5A - U = Q$. From the A ratios and pressure ratios which can be obtained in terms of the Mach number, the new value of entropy can be determined from the previously mentioned relation -

$$\frac{\Delta s}{\gamma R} = \frac{2}{\gamma-1} \ln A_2/A_1 - 1/\gamma \ln P_2/P_1$$

At No. 20 we obtain $\frac{A20}{A_1} = 1.3307$, $\frac{P20}{P1} = 4.9785$ with a new $S/\gamma R = 0.285$. Since the initial entropy change across the shock equaled 0.338, Q is no longer constant between No. 3 and No. 20. The correct value of Q_{20} can be obtained by use of the relation

$$\Delta Q = A \frac{\Delta S}{\gamma R}$$

$$\therefore Q_{20} = Q_3 + A_3 \frac{S_{20} - S_3}{\gamma R}$$

This yields a new value of Q_{20} so that a new value of P_{20}, A_{20}, U_{20} and S_{20} may be determined. In general, one iteration is sufficient to determine the value of Q_{20}. For this case, $Q_{20} = 7.355$.

V. Inlet Boundary Conditions

1. At point No. 1 the inlet valve is open. As soon as the shock reaches the inlet we assume the valve closes instantaneously and the new boundary condition at point No. 21 is that $U_{21} = 0$. The solution for point No. 21 is identical with the solution for points 1 and 2.

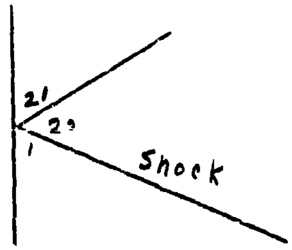

Subsequent points along the reflected shock, Nos. 23, 35, etc. are determined in the same manner as point No. 20.

2. For regions of variable entropy the changes of P and Q are determined (as previously) by the relation

$$\Delta Q = \Delta P = A \frac{\Delta S}{\gamma R}$$

Example: No. 49

$$P_{49} = P_{37} + A_{37} \left(\frac{S_{49} - S_{37}}{\gamma R}\right)$$

$$Q_{49} = Q_{48} + A_{48} \left(\frac{S_{49} - S_{48}}{\gamma R}\right)$$

Hence,

$$P_{49} = 6.478 \text{ and } Q_{49} = 5.888$$

Also, at No. 37, $U_{37} = 0$ and $P_{37} = Q_{37}$ since $Q_{37} = -U_{37} + 5A_{37}$

and $P_{37} = U_{37} + 5A_{37} \cdot \left[\frac{2}{\gamma-1} = 5\right]$

At No. 142 the pressure as determined by the relation

$$\frac{\Delta S}{\gamma R} = \frac{2}{\gamma-1} \ln \frac{A_2}{A_1} - \frac{1}{\gamma} \ln \frac{P_2}{P_1}$$

is

$$\frac{P_2}{P_1} = \left(\frac{A_2}{A_1}\right)^7 \times e^{-\gamma\left(\frac{\Delta S}{\gamma R}\right)}$$

3. Inflow occurs when the pressure at the valve becomes equal to the outside pressure. For the particular problem selected, the

surrounding stagnation pressure, $\frac{P_s}{P_o}$ equals 1.3283. We assume that when the inside pressure drops to this value the valve opens instantaneously and inflow takes place.

4. Procedure for determining inflow.

For inflow the energy equation always holds

$$U^2 + \frac{2}{\gamma-1} A^2 = \frac{2}{\gamma-1} A_s^2$$

Since U at the inlet is $\frac{P-Q}{2}$ and A at the inlet is $\frac{P+Q}{10}$ we obtain the relation between P and Q, which must hold at the inlet. On substituting in the energy equation

$$\frac{P-Q}{2}^2 + \frac{2}{\gamma-1} \frac{P\&Q}{10}^2 = \frac{2}{\gamma-1} A_s^2$$

Example: Point No. 189

We assume a velocity which gives the initial slope of the interface. $Q_{186} = Q_{143} + \Delta Q$. At the interface there is a temperature discontinuity and

$$U_{185} = U_{186}$$

$$P_{185} = P_{186}$$

The A ratio is a constant along this interface. Since $P_{185} = P_{186}$,

$$\frac{\Delta S}{\gamma R} = \frac{2}{\gamma-1} \ell n \frac{A_L}{A_R}$$

where $\frac{A_L}{A_R} = \frac{A_{185}}{A_{186}}$.

In the inflow region $S/\gamma R = 0$.

Hence, we can determine Q_{185} which equals Q_{187}. Knowing Q_{187} we can then find P_{187}, U_{187} and A_{187}. The correctness of the assumed initial inflow velocity may be checked by drawing back the characteristic P_{185}

to the inlet and comparing with the interpolated value between P_{142A} and P_{187} at this point.

VI Outflow at the Exit

When the pressure at the exit becomes equal to p_o, in general U_e is less than A_e. For subsonic outflow A_e is a constant (A_e = 1.655) for the hot gas. Since A_e is fixed, U_e can be determined since

$$5\ A_e + U_e = P_e$$

The reflected characteristic, Q_e, is immediately determined. Points 17 to 130 along the exit are determined in this manner.

VII Intersection of Shock and Interface

Characteristics from Nos. 31 to 44 overtake the characteristic from No. 17 to 93 to form a shock. Therefore at No. 101 it is necessary to solve the intersection of the shock and the interface.

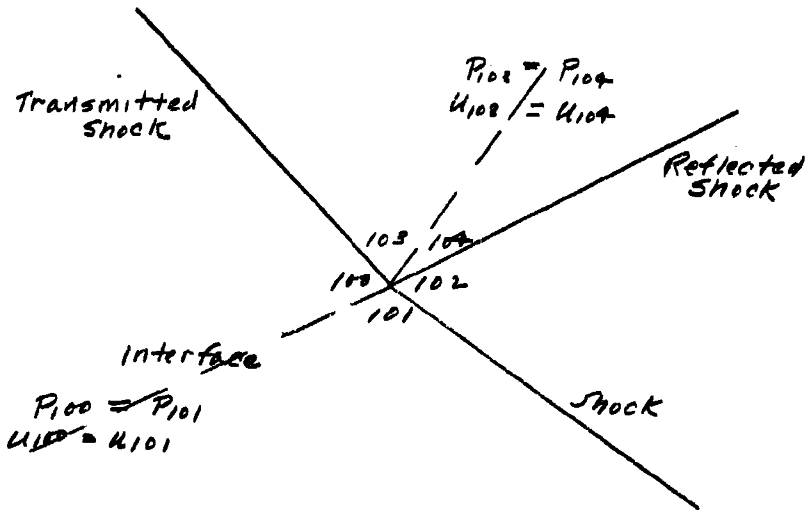

In general, the simplest method of solution is to assume a value of A_{104}. This will determine the strength of the reflected shock, A_{104}/A_{102}, which in turn yields p_{104}/p_{102} and the pressure at point No. 104. Since the pressures are equal across the interface, $p_{103} = p_{104}$. The pressure ratio, p_{103}/p_{100}, of the transmitted shock gives A_{103}/A_{100}. This, in turn, yields a new A ratio across the interface.

Knowing A_{103}/A_{100}, we find U_{103} from the shock relations. From A_{104}/A_{102} we obtain U_{104}. If the assumed value of A_{104} is correct, $U_{103} = U_{104}$.

VIII. Intersection of two shocks

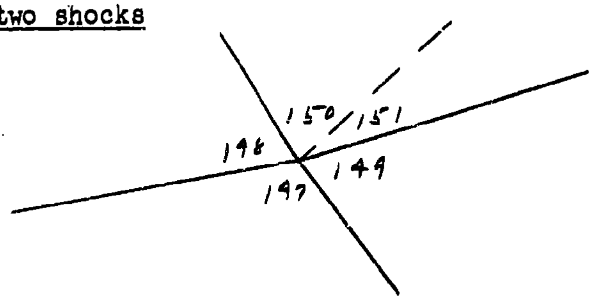

$$p_{150} = p_{151}$$

$$U_{150} = U_{151}$$

This problem may be solved by procedures similar to those used for the intersection of a shock and an interface.

Assuming a value of A_{151} determines the new strength of the shock moving to the right, the pressure ratio across the shock and the value of U_{151}. From the continuity of velocity and pressure at the interface we find p_{150}/p_{148}, the pressure ratio across the shock moving to the left. This in turn yields A_{150}/A_{148} and U_{150}. If $U_{150} = U_{151}$, the assumed value of A_{151} is correct.

IX 1. End of Scavenging Period

When the interface reaches the exit, point No. 130, it is assumed that the valve closes instantaneously.

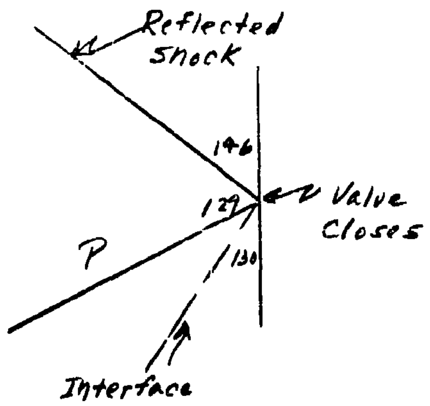

$P_{129} = P_{130} = P_o$

$U_{129} = U_{130}$

$A_{130} = A_3 = 1.655$

$U_{146} = 0$

In general, in order to determine the value of P_{129}, it may be necessary to interpolate to obtain the correct characteristic that just reaches point No. 129. For this case, however, since P does not change between the points No. 125 to the shock at No. 133, $P_{129} = 6.010$. Since $A_2/A_R = 0.646472$, $A_{129} = 1.070$ and $U_{129} = U_{130} = 0.660$.

At point No. 129 the valve closes and a shock is generated because of the sudden interruption of the flow. $U_{146} = 0$ and knowing $\frac{U_{129} - U_{146}}{A_{129}}$ the parameters behind the shock may be determined in the same manner as points No. 21 and (b) were determined previously.

2. Shock Reflection at a Closed End

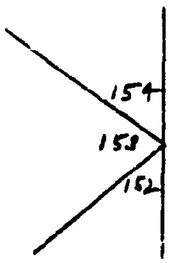

$U_{154} = 0$

$U_{152} = 0$

Since the boundary condition at point No. 154 is that $U_{154} = 0$, the solution of the reflected shock is obtained in the same manner as in the previous Section IX, 1.

3. Two Shock Coalescing

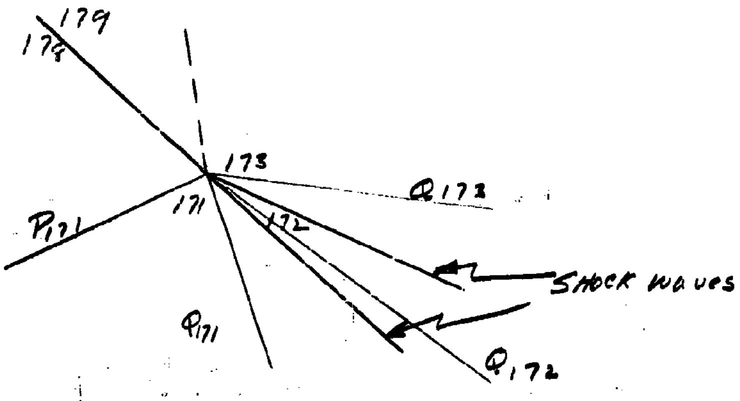

This problem may be solved by treating each shock separately. From the values of P_{171}, Q_{171}, and Q_{172}, we find $\frac{P_{172} - P_{171}}{A_{171}}$, also U_{172} and A_{172} since we know

$$\frac{Q_{172} - Q_{171}}{A_{171}}$$

In the same manner we find $\frac{P_{173} - P_{172}}{A_{172}}$ from $\frac{Q_{173} - Q_{172}}{A_{172}}$.

Hence, the A ratio across the two shocks, $\frac{A_{173}}{A_{171}}$, is simply

$$\frac{A_{173}}{A_{171}} = \frac{A_{173}}{A_{172}} \cdot \frac{A_{172}}{A_{171}}$$

For strong initial shocks this may lead to an entropy discontinuity at the junction.

X **Beginning of Second Cycle**

When the shock reflected at point No. 154 reaches the position L = 0.25, combustion occurs and the cycle is repeated.

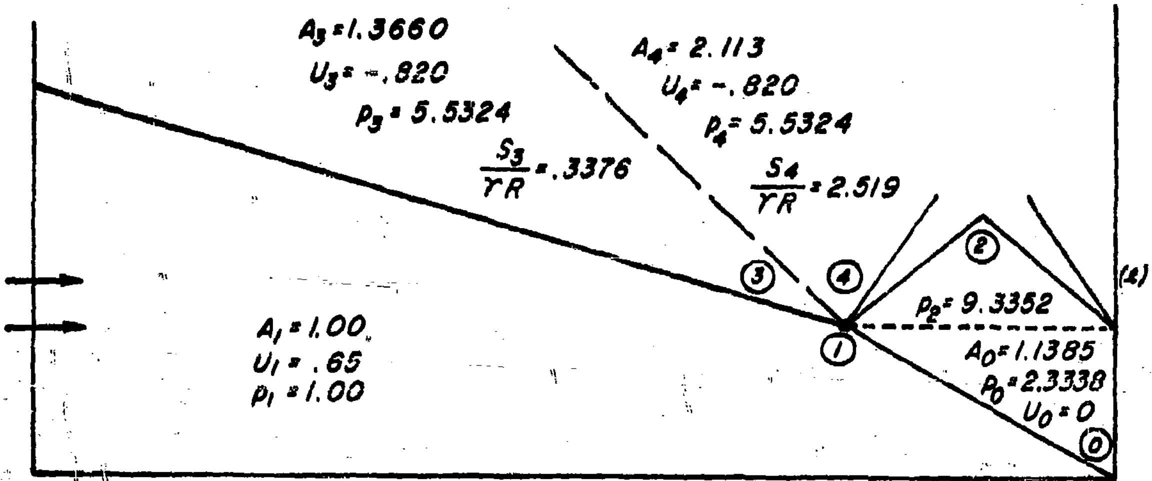

AFTER COMBUSTION } $p_2 = 4(p_0) = 9.3352$, $A_2 = 2(A_0) = 2.2770$, $U_2 = 0$

AT THE EXIT } WHEN $p_2 = 1.0$, $A_2 = 1.6549$

ACROSS THE INTERFACE } $A_L/A_R = 0.646472$, $A_R = \dfrac{p_L + Q_R}{8.232360}$ $\quad U_L = U_R$, $p_L = p_R$

INFLOW } TUBE OPENS WHEN $p_T = 1.3283$

$M_1 = .65 \rightarrow p/p_T = .75283 \rightarrow p_T = 1.3283$

$A/A_T = .96025 \rightarrow A_T = 1.0414$

$\therefore$ BOUNDARY CONDITION $= U^2 + 5A^2 = 5A_T^2 = 5.422570$

CALCULATIONS FOR STRAIGHT TUBE WAVE ENGINE

Fig. 1

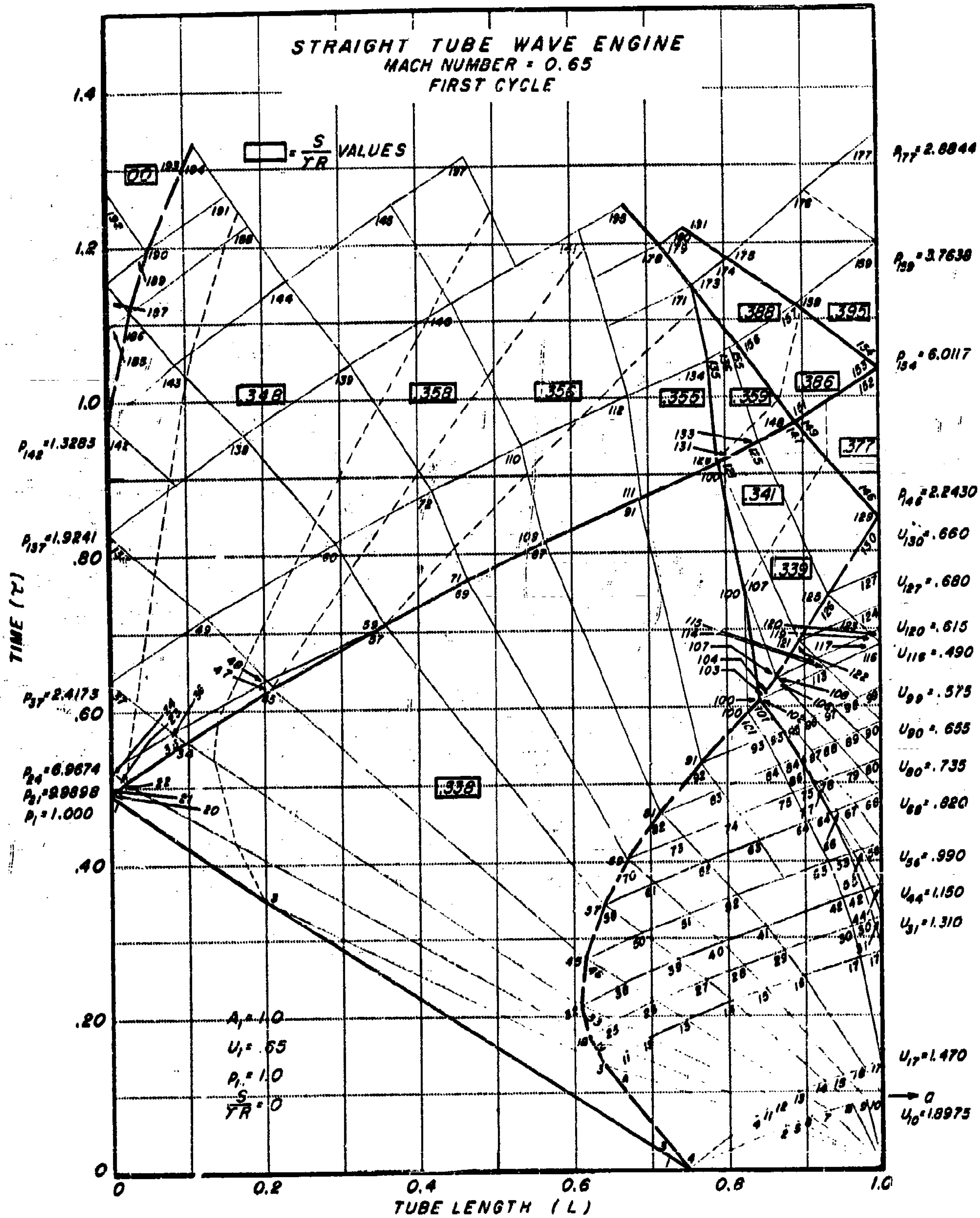
STRAIGHT TUBE WAVE ENGINE
MACH NUMBER = 0.65
FIRST CYCLE
= S/γR VALUES
TIME (τ)
TUBE LENGTH (L)
A_1 = 1.0
U_1 = .65
P_1 = 1.0
S/γR = 0
P_{177} = 2.8844
P_{159} = 3.7638
P_{154} = 6.0117
P_{146} = 2.2430
U_{130} = .660
U_{127} = .680
U_{120} = .615
U_{116} = .490
U_{99} = .575
U_{90} = .655
U_{80} = .735
U_{68} = .820
U_{56} = .990
U_{44} = 1.150
U_{31} = 1.310
U_{17} = 1.470
U_{10} = 1.8975
P_{142} = 1.3283
P_{137} = 1.9241
P_{37} = 2.4173
P_{24} = 6.9674
P_{21} = 2.9898
P_1 = 1.000

Fig. 2

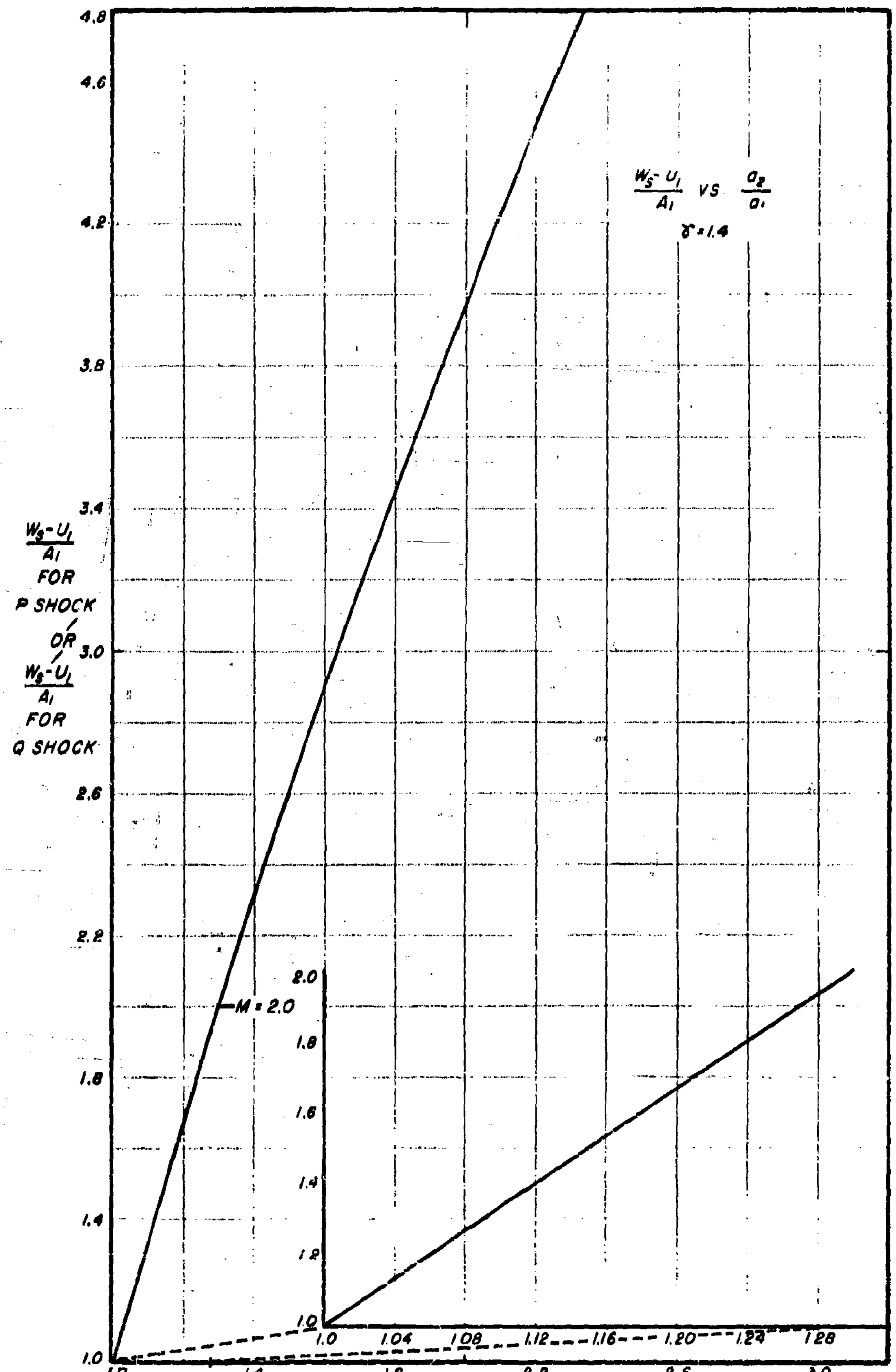

Fig. 3

CONFIDENTIAL

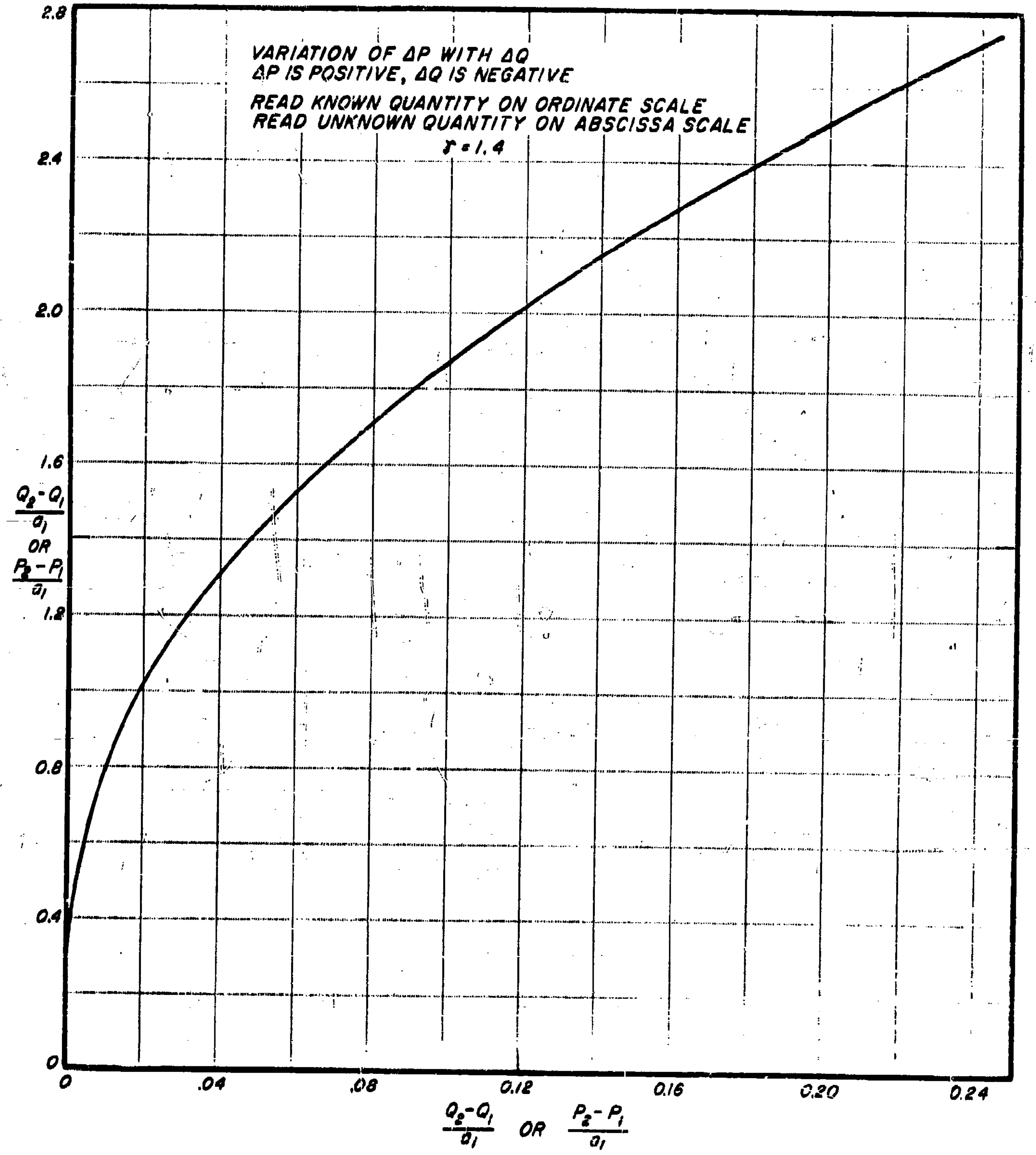
VARIATION OF ΔP WITH ΔQ
ΔP IS POSITIVE, ΔQ IS NEGATIVE
READ KNOWN QUANTITY ON ORDINATE SCALE
READ UNKNOWN QUANTITY ON ABSCISSA SCALE
γ = 1.4
2.8
2.4
2.0
1.6
1.2
0.8
0.4
0
$\frac{Q_2 - Q_1}{a_1}$ OR $\frac{P_2 - P_1}{a_1}$
0
.04
.08
0.12
0.16
0.20
0.24
$\frac{Q_2 - Q_1}{a_1}$ OR $\frac{P_2 - P_1}{a_1}$

Fig.4

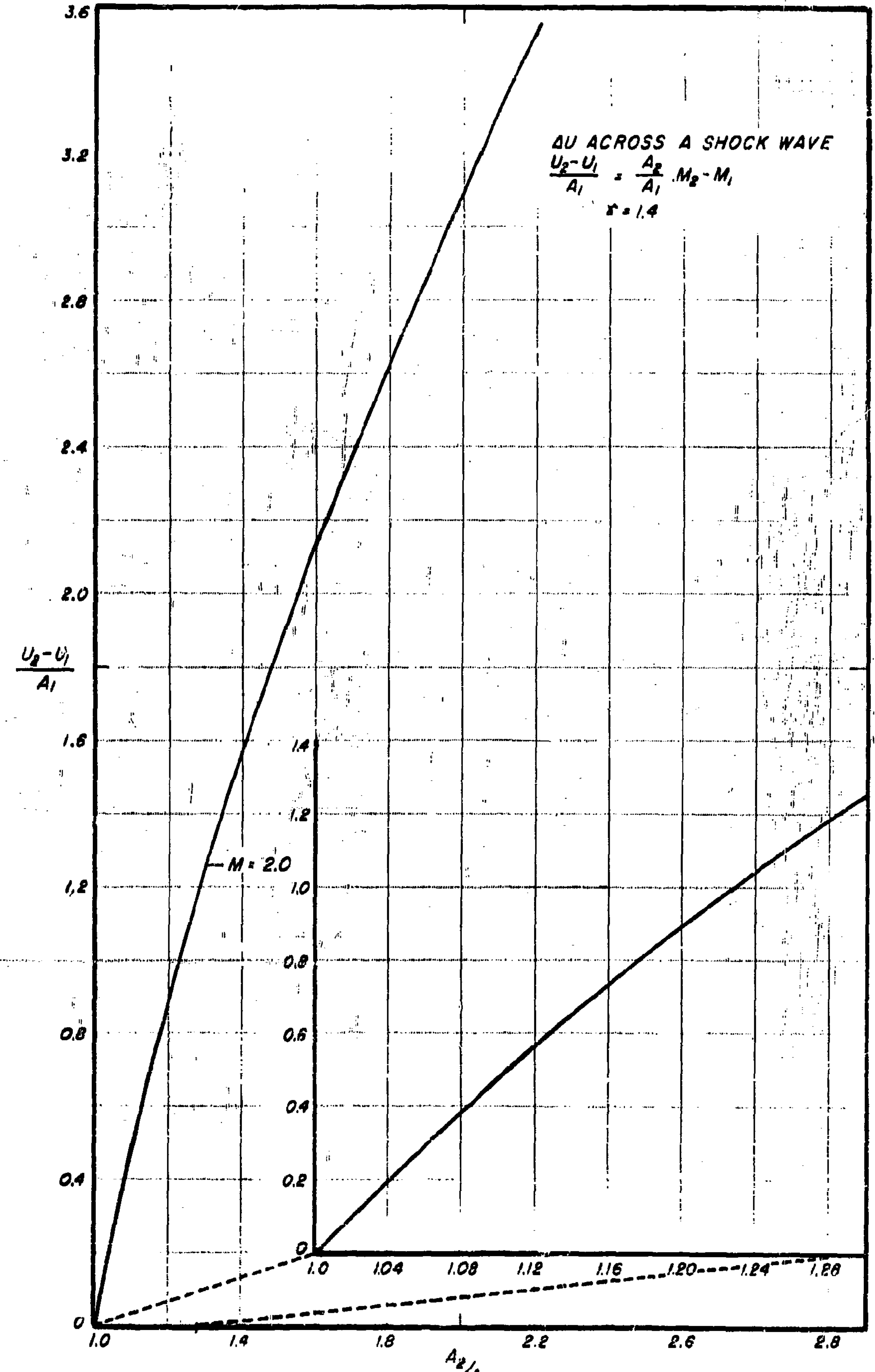
ΔU ACROSS A SHOCK WAVE
$\frac{U_2-U_1}{A_1} = \frac{A_2}{A_1} M_2 - M_1$
γ = 1.4
M = 2.0
$\frac{U_2-U_1}{A_1}$
A_2/A_1
3.6
3.2
2.8
2.4
2.0
1.6
1.2
0.8
0.4
0
1.0
1.4
1.8
2.2
2.6
2.8
1.4
1.2
1.0
0.8
0.6
0.4
0.2
0
1.0
1.04
1.08
1.12
1.16
1.20
1.24
1.28

Fig.5

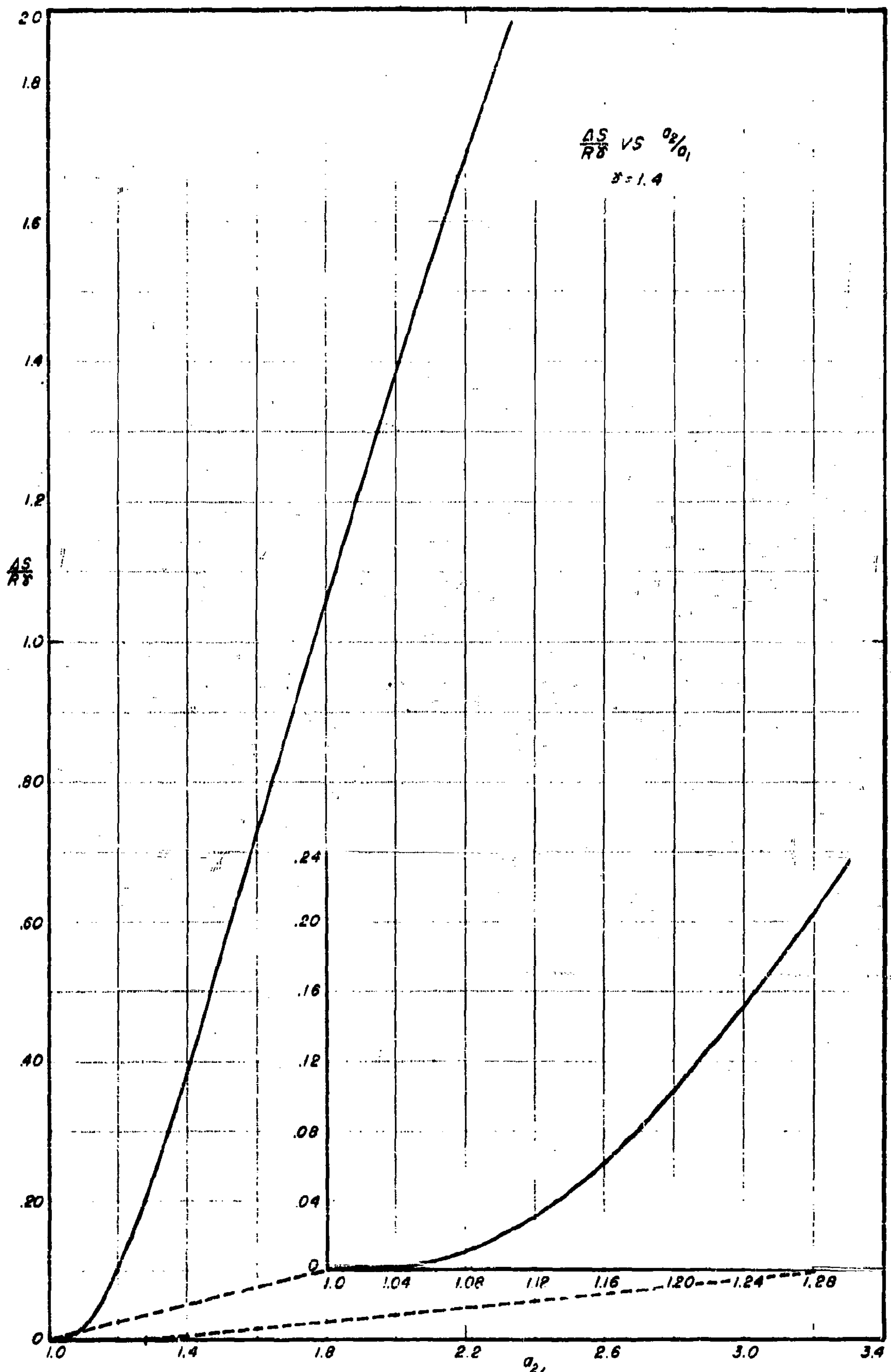

$\frac{\Delta S}{R\delta}$ VS a_2/a_1
$\gamma = 1.4$
$\frac{\Delta S}{R\delta}$
2.0
1.8
1.6
1.4
1.2
1.0
.80
.60
.40
.20
0
1.0
1.4
1.8
2.2
2.6
3.0
3.4
a_2/a_1
.24
.20
.16
.12
.08
.04
0
1.0
1.04
1.08
1.12
1.16
1.20
1.24
1.28

Fig. 6

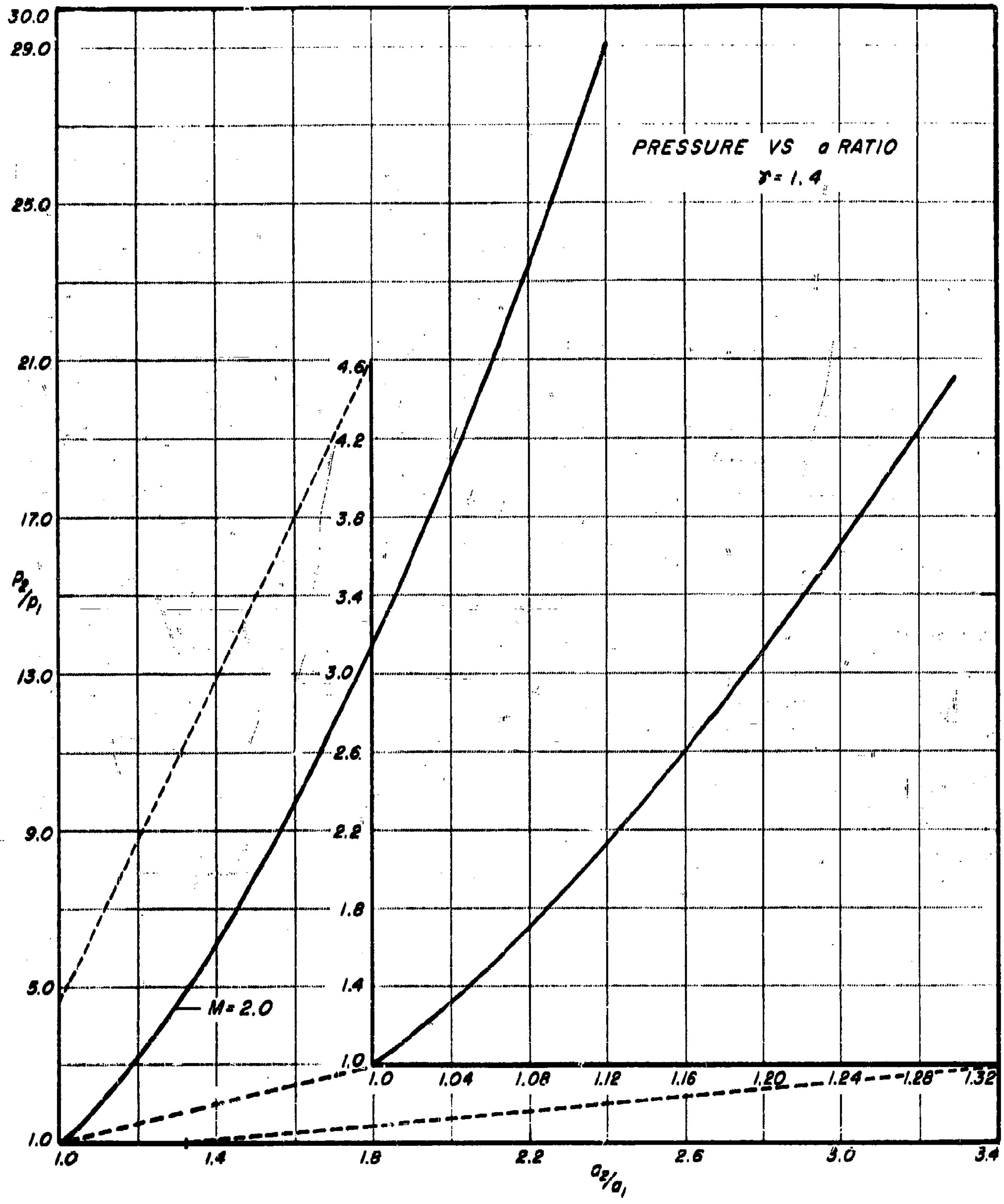
PRESSURE VS a RATIO
γ = 1.4
30.0
29.0
25.0
21.0
17.0
13.0
9.0
5.0
1.0
p_2/p_1
4.6
4.2
3.8
3.4
3.0
2.6
2.2
1.8
1.4
1.0
M = 2.0
1.0
1.04
1.08
1.12
1.16
1.20
1.24
1.28
1.32
1.0
1.4
1.8
2.2
2.6
3.0
3.4
a_2/a_1

Fig. 7

STRAIGHT TUBE WAVE ENGINE WITH RAM M = 0.65

1st Cycle

No.	P	Q	U	W	U+A	U-A	W_s	S	A_2/A_1	P/P_0	ρ/ρ_0
1	5.650	4.350	0.650	1.000	1.650	-0.350		o	1.000	1.000	1.000
2	11.385	11.385	-0	2.277	2.277	-2.277		2.519		9.3352	1.800
3	6.010	7.650	-0.820	1.366	0.446	-2.086	-1.552	0.338	1.3660	5.5324	
4	9.745	11.385	-0.820	2.113	1.293	-2.933		2.519		5.5324	
5	11.385	10.635	0.375	2.202	2.577	-1.827					
6	11.385	9.885	0.750	2.127	2.877	-1.377					
7	11.385	9.135	1.125	2.052	3.177	-0.927					
8	11.385	8.385	1.500	1.977	3.477	-0.477					
9	11.385	7.950	1.717	1.934	3.651	-0.217					
10	11.385	7.590	1.8975	1.8974	3.795	0				2.6054	
11	9.745	10.635	-0.445	2.038	1.593	-2.483					
12	9.745	9.885	-0.070	1.963	1.893	-2.033					
13	9.745	9.135	0.305	1.880	2.185	-1.575					
14	9.745	8.385	0.680	1.813	2.493	-1.133					
15	9.745	7.950	0.898	1.770	2.668	-0.872					
16	9.745	7.590	1.078	1.734	2.812	-0.656					
17	9.745	6.805	1.470	1.655	3.125	-0.185				1.000	
18	6.010	7.060	-0.525	1.307	0.782	-1.832		0.338			
19	9.585	10.635	-0.525	2.022	1.497	-2.547		2.519			
20	5.952	7.355	-0.702	1.3307	0.629	-2.033	-1.450	0.285	1.3307	4.9785	
21	7.385	7.385	0	1.4771	1.477	-1.477	+1.120	0.309	1.1100	0.9898	
22	5.955	7.008	-0.526	1.296	0.777	-1.813		0.297			
23	7.348	7.032	0.158	1.438	1.603	-1.271	+1.384	0.321	1.1100		
24	7.015	7.015	0	1.4030	1.403	-1.4033		0.309		6.9674	
25	9.585	9.885	-0.150	1.947	1.797	-2.097					
26	9.585	9.135	0.225	1.872	2.097	-1.647					
27	9.585	8.385	0.600	1.797	2.397	-1.197					
28	9.585	7.950	0.818	1.754	2.572	-0.936					
29	9.585	7.590	0.998	1.718	2.716	-0.720					
30	9.585	6.805	1.390	1.639	3.029	-0.249					
31	9.585	6.965	1.310	1.655	2.965	-0.345				1.000	
32	6.010	6.4170	-0.230	1.248	1.018	-1.478		0.338			
33	9.425	9.885	-0.230	1.931	1.701	-2.161		2.519			
34	5.994	6.456	-0.231	1.245	1.014	-1.476		0.327			
35	7.363	6.481	0.397	1.374	1.765	-0.983	+1.443	0.348	1.1036		
36	7.070	6.481	0.294	1.355	1.649	-1.061		0.348			
37	6.428	6.428	0	1.286	1.286	-1.286		0.309		2.4173	
38	9.425	9.135	0.145	1.856	2.001	-1.711					
39	9.425	8.385	0.520	1.781	2.301	-1.261					
40	9.425	7.950	0.738	1.738	2.476	-1.000					
41	9.425	7.590	0.918	1.702	2.620	-0.784					
42	9.425	6.805	1.310	1.623	2.933	-0.313					
43	9.425	6.965	1.230	1.639	2.869	-0.509					
44	9.425	7.125	1.150	1.655	2.805	-0.505					
45	6.010	5.880	0.065	1.189	1.254	-1.124		0.338			
46	9.265	9.135	0.065	1.840	1.905	-1.775		2.519			
47	7.181	5.901	0.640	1.308	1.948	-0.668	1.649	0.358	1.1001		
48	7.084	5.901	0.592	1.298	1.890	-0.706		0.358			

STRAIGHT TUBE WAVE ENGINE WITH RAM M = 0.65 (Cont.)

No.	P	Q	U	W	U+A	U-A	W_s	S	A_2/A_1	p/p_o
49	6.478	5.888	0.295	1.237	1.532	-0.942		0.348		
50	9.265	8.385	0.440	1.765	2.205	-1.325				
51	9.265	7.950	0.658	1.722	2.380	-1.064				
52	9.265	7.590	0.838	1.686	2.524	-0.848				
53	9.265	6.805	1.230	1.607	2.837	-0.377				
54	9.265	6.965	1.150	1.623	2.773	-0.473				
55	9.265	7.125	1.070	1.639	2.709	-0.569				
56	9.265	7.285	0.990	1.655	2.645	-0.665				
57	6.010	5.295	0.355	1.130	1.485	-0.775		0.338		
58	9.095	8.385	0.355	1.748	2.103	-1.393		2.519		
59	7.084	5.314	0.885	1.240	2.125	-0.355	+1.852	0.356	1.0973	
60	6.490	5.316	0.587	1.181	1.768	-0.594		0.358		
61	9.095	7.950	0.572	1.704	2.276	-1.132				
62	9.095	7.590	0.752	1.668	2.420	-0.916				
63	9.095	7.200	0.948	1.630	2.578	-0.682				
64	9.095	6.805	1.145	1.590	2.735	-0.445				
65	9.095	6.965	1.065	1.606	2.671	-0.541				
66	9.095	7.125	0.985	1.622	2.607	-0.637				
67	3.095	7.285	0.905	1.638	2.543	-0.733				
68	9.095	7.455	0.820	1.655	2.475	-0.835				
69	6.010	4.950	0.530	1.096	1.626	-0.566		0.338		
70	9.010	7.950	0.530	1.696	2.226	-1.166		2.519		
71	7.034	4.967	1.034	1.200	2.234	-0.166	+1.874	0.355	1.0949	
72	6.488	4.968	0.760	1.146	1.906	-0.386		0.356		
73	9.010	7.590	0.710	1.660	2.370	-0.950				
74	9.010	7.200	0.905	1.621	2.526	-0.716				
75	9.010	6.805	1.102	1.582	2.684	-0.480				
76	9.010	6.965	1.022	1.598	2.620	-0.576		2.519	1.0101	
77	9.010	7.125	0.942	1.614	2.556	-0.672		2.519		
78	9.010	7.285	0.862	1.630	2.492	-0.768		2.519		
79	9.010	7.455	0.778	1.646	2.424	-0.868		2.519		
80	9.010	7.540	0.735	1.655	2.390	-0.920				
81	6.010	4.670	0.670	1.068	1.738	-0.398		0.338		
82	8.930	7.590	0.670	1.652	2.322	-0.982		2.519		
83	8.930	7.200	0.865	1.613	2.478	-0.748		2.519		
84	8.930	6.805	1.062	1.574	2.636	-0.512		2.519		
85	8.930	6.980	0.975	1.591	2.566	-0.616	-0.569	2.519	1.0108	
86	8.930	7.125	0.902	1.606	2.508	-0.704		2.519	1.0203	
87	8.930	7.285	0.822	1.622	2.444	-0.800		2.519	1.0203	
88	8.930	7.455	0.739	1.638	2.376	-0.900		2.519		
89	8.930	7.540	0.695	1.647	2.342	-0.952		2.519		
90	8.930	7.620	0.655	1.655	2.310	-1.000		2.519		
91	6.010	4.360	0.825	1.038	1.862	-0.212		0.338		
92	8.850	7.200	0.825	1.605	2.430	-0.780		2.519		
93	8.850	6.805	1.022	1.566	2.588	-0.544		2.519		
94	8.850	7.140	0.855	1.599	2.454	-0.744	-0.654	2.519	1.0211	
95	8.850	7.285	0.782	1.614	2.396	-0.832				
96	8.850	7.455	0.698	1.630	2.328	-0.932				
97	8.850	7.540	0.655	1.639	2.294	-0.984				
98	8.850	7.620	0.615	1.647	2.262	-1.032				
99	8.850	7.700	0.575	1.655	2.230	-1.080				

STRAIGHT TUBE WAVE ENGINE WITH RAM M = 0.65 (Cont.)

No	P	Q	U	W	U+A	U-A	W_s	S	A_2/A_1	p/p_o
100	6.010	4.050	0.980	1.006	1.986	-0.026		0.338		0.6512
101	8.765	6.805	0.980	1.557	2.537	-0.577		2.519		0.6512
102	8.765	7.155	0.805	1.592	2.397	-0.787	-0.697	2.519	1.0225	0.7620
103	6.010	4.330	0.840	1.0338	1.874	-0.194	-0.116	0.339	1.0278	0.7870
104	8.835	7.155	0.840	1.5992	2.439	-0.759		2.519	1.0044	0.7870
105	8.765	7.455	0.655	1.622	2.277	-0.967				
106	8.835	7.455	0.690	1.629	2.319	-0.939	2.308	2.519	1.0043	
107	6.010	4.560	0.725	1.057	1.782	-0.332	-0.192	0.341	1.0506	
108	8.905	7.455	0.725	1.636	2.361	-0.911		2.519		
109	7.000	4.686	1.157	1.169	2.326	-0.012	2.075	0.355	1.0946	
110	6.488	4.687	0.900	1.118	2.018	-0.218		0.356		
111	6.975	4.376	1.300	1.135	2.435	+0.165	2.190	0.355	1.0945	
112	6.487	4.376	1.056	1.086	2.142	-0.030		0.355		
113	8.765	7.620	0.572	1.638	2.210	-1.066		2.519		
114	8.840	7.620	0.610	1.646	2.256	-1.036	2.243	2.519	1.0049	
115	8.905	7.620	0.642	1.652	2.294	-1.010		2.519		
116	8.765	7.785	0.490	1.655	2.145	-1.165		2.519		
117	8.845	7.785	0.530	1.663	2.193	-1.663	2.178	2.519	1.0048	
118	8.845	7.705	0.570	1.655	2.225	-1.085		2.519		
119	8.905	7.705	0.600	1.661	2.261	-1.061				
120	8.905	7.645	0.615	1.655	2.270	-1.040				
121	6.015	4.690	0.550	1.0705	1.730	-0.410		0.344	1.0636	0.9958
122	8.940	7.620	0.660	1.656	2.316	-0.996				
123	8.940	7.705	0.618	1.664	2.282	-1.046				
124	8.940	7.610	0.665	1.655	2.320	-0.990				
125	6.010	4.760	0.625	1.077	1.702	-0.452		0.341		
126	8.955	7.705	0.625	1.666	2.291	-1.041				
127	8.955	7.595	0.680	1.655	2.335	-0.975				
128	6.940	4.066	1.437	1.101	2.544	+0.341	2.304	0.355	1.0944	1.1966
129	6.010	4.690	0.660	1.070	1.730	-0.410		0.338		1.0004
130	8.935	7.615	0.660	1.655				2.519		1.000
131	6.950	4.710	1.120	1.166	2.286	-0.046	+0.122	0.359	1.0587	1.7735
132	6.950	4.710	1.120	1.166	2.286	-0.046	+2.049	0.359	1.0890	1.7735
133	6.950	4.780	1.085	1.173	2.258	-0.088	2.022	0.355	1.0888	
134	6.487	4.144	1.172	1.063	2.235	+0.109		0.355		
135	6.495	4.735	0.880	1.123	2.003	-0.243	-0.091	0.359	1.0564	
136	6.495	4.784	0.858	1.128	1.986	-0.270		0.359		
137	5.840	5.840	0	1.168	1.168	-1.168		0.309	1.9241	
138	5.886	5.304	0.291	1.119	1.410	-0.828		0.348		
139	5.886	4.959	0.464	1.084	1.548	-0.620		0.348		
140	5.897	4.689	0.604	1.059	1.663	-0.455		0.358		
141	5.897	4.379	0.759	1.028	1.787	-0.269		0.358		
142	5.540	5.540	0	1.1078	1.108	-1.108		0.309	1.3283	
143	5.553	5.274	0.140	1.083	1.223	-0.943		0.321		
144	5.582	4.959	0.312	1.054	1.366	-0.742		0.348		
145	5.582	4.679	0.452	1.026	1.478	-0.574		0.348		
146	6.050	6.050	0	1.210	1.210	-1.210		0.377	1.1308	2.2430
147	6.012	4.725	0.644	1.074	1.718	-0.430		0.341		1.0225
148	6.940	4.738	1.101	1.168	2.269	-0.067	+2.029	0.355	1.0875	1.8055
149	6.048	6.050	-0.001	1.210	1.209	-1.211		0.376	1.1266	2.2448
150	6.971	6.059	0.456	1.303				0.383	1.1160	3.7439
151	6.976	-6.064	0.456	1.304				0.386	1.0779	3.7439

STRAIGHT TUBE WAVE ENGINE WITH RAM M = 0.65 (Cont)

No.	P	Q	U	A	U+A	U−A	W_s	S	A_2/A_1	p/p_o	
152	6.049	6.049	0	1.2098	1.210	−1.210		0.377		2.2430	
153	6.976	6.058	0.459	1.3034	1.762	−0.844	+1.518	0.387	1.0768	3.7171	
154	6.990	6.990	0	1.398	1.398	−1.398	−1.159	0.395	1.0728	6.0117	
155	6.495	4.770	0.862	1.126	1.996	−0.242		0.359			
156	6.526	6.062	0.232	1.259	1.491	−1.027	−0.709	0.388	1.1181	2.9126	
157	6.526	6.060	0.233	1.259	1.492	−1.026		0.388		2.9126	
158	6.540	6.970	−0.215	1.351	1.136	−1.566	−1.331	0.396	1.0731	4.7190	
159	6.539	6.539	0	1.3078	1.3078	−1.308		0.395		3.7638	2.2006
171	6.251	4.180	1.035	1.043	2.074	−0.008		0.356			
172	6.255	4.760	0.748	1.102	1.850	−0.354	−0.205	0.360	1.0566		
173	6.288	6.062	0.113	1.235	1.348	−1.122	− .799	0.390	1.1207		
174	6.286	6.060	0.113	1.235	1.348	−1.122		0.388	1.1841		
175	6.295	6.930	−0.318	1.322	1.004	−1.640	−1.410	0.395	1.0704		
176	6.295	6.539	−0.122	1.283	1.161	−1.405		0.395			
177	6.295	6.295	0	1.259	1.259	−1.259		0.395		2.8844	
178	6.074	4.240	0.917	1.031	1.948	−0.114		0.356			
179	6.172	6.138	0.017	1.231	1.248	−1.248	−0.784	0.452	1.1940		
180	6.158	6.125	0.016	1.228	1.244	−1.212		0.441		2.2712	
181	6.166	6.977	−0.406	1.314	0.908	−1.720	−1.497	0.448	1.0700	3.6114	2.0916
182			−0.222	1.303				0.395		3.6679	2.1604
183			−0.037	1.3005				0.395		3.6192	2.1399
184			0	1.299				0.395		3.5901	2.1276
185	5.340	4.930	0.205	1.027	1.232	−0.822		0			
186	5.670	5.260	0.205	1.093	1.298	−0.888		0.309			
187	5.420	4.930	0.245	1.035	1.280	−0.790		0			
188	5.713	4.959	0.377	1.067	1.444	−0.690		0.348			
189	5.420	4.810	0.305	1.023	1.328	−0.718		0			
190	5.750	5.140	0.305	1.089	1.394	−0.784		0.309			
191	5.763	4.930	0.416	1.069	1.485	−0.653		0.321			
192	5.490	4.810	0.340	1.030	1.370	−0.690		0			
193	5.480	4.660	0.440	1.008	1.458	−0.558		0			
194	5.800	4.917	0.440	1.072	1.523	−0.623		0.309			
195	5.895	4.280	0.808	1.018	1.827	−0.207		0.356			
196	5.990	6.138	−0.074	1.213			−0.862	0.449	1.1916		
197	5.582	4.524	0.529	1.011	1.540	−0.482		0.348			

ACKNOWLEDGMENT

This project was sponsored by the Office of Naval Research, Contract No. Nonr-665-(00) under the technical supervision of Commander R. L. Duncan of the United States Navy. The writer wishes to express his appreciation to Commander Duncan for his continued encouragement and valuable suggestions during the course of the project. He also wishes to thank Messrs. H. R. Lawrence, G. Rudinger, and A. Hertzberg for helpful suggestions of many problems, and Mmes. A. Dowd and M. Johnson for constructing the wave diagrams.

UNCLASSIFIED

AD 56235

CLASSIFICATION CHANGED FROM CONFIDENTIAL

TO UNCLASSIFIED AUTHORITY LISTED IN

ASTIA TAB NO. U60-1-4 DATE 15 Feb. 60

Armed Services Technical Information Agency

ARLINGTON HALL STATION; ARLINGTON 12 VIRGINIA

UNCLASSIFIED